Master's Thesis

Stereoscopic method for characterization of concrete surfaces

submitted in satisfaction of the requirements for the academic degree of
Diplom-Ingenieur
of the Vienna University of Technology, Faculty of Civil Engineering

---

Diplomarbeit

Stereoskopische Methode zur Charakterisierung von Betonoberflächen

ausgeführt zum Zwecke der Erlangung des akademischen Grades eines
Diplom-Ingenieurs
eingerichtet an der Technischen Universität Wien, Fakultät für Bauingenieurwesen

von

Blerim Morina, BSc
Matrikelnummer: 01425264

unter der Anleitung von
Univ.Prof. PhD **Agathe Robisson**
Ass.Prof. Dipl.-Ing. Dr.techn. **Karl Deix**

Institut für Werkstofftechnologie, Bauphysik und Bauökologie
Forschungsbereich Baustofflehre und Werkstofftechnologie
Technische Universität Wien,
Karlsplatz 13/207-01, A-1040 Wien

Wien, im Januar 2023

Acknowledgements

From the first moments of our lives and continuously, almost throughout our life's journey, we have a constant need for care, help, support, encouragement, advice, guidance, lectures, motivation, but also for positive criticism that helps us to improve both in human terms and in academic and professional terms.

Of course, throughout my life's journey, I have also felt the need for all mentioned above. Therefore, I feel blessed by God that I have managed to complete the master's degree through this diploma thesis despite the various challenges, starting from being far away from the children and family to living abroad, up to health problems.

I dedicate my most profound and most significant thanks and gratitude to Heavenly Father, who gave me strength, confidence, and the will to move forward in all the challenges and difficulties of my life!

A special thanks go to Mr. Ass. Prof. Dipl.-Ing. Dr. tech. Karl Deix, who, from the beginning of our first conversation about working on the thesis of the diploma until its successful conclusion, showed unconditional mentoring, cooperation, and support for me, both in the field of scientific theoretical advice, up to perform experimental research and software calculations. Therefore, my gratitude to him will be eternal!

Expressing my endless gratitude, I also apologize to my children and my wife, who, for most of these years of study abroad, have been deprived of my presence! I also warmly thank my parents, brother, and sisters for their continued material and moral support! I love you all very much, and I pray to God that one day I can reward you with the best!

Abstract

The stereoscopic method's basic working principle consists of creating the impression of 3-Dimensional images obtained by capturing 2-Dimensional planar images from small tilting angles on the left and right side of tilt angle, although even these are 2-Dimensional images. So, the primary purpose of this method is, through different measuring methods, to interpret the content of the image, respectively, of the object we are investigating, which in our case are the concrete surfaces.

The suitability of this method for the characterization of concrete surfaces, lies in the accuracy of the measurements and the economic aspect of its use, compared to alternative methods, such as the laser scanning method. Various research has concluded that photogrammetric methods have a geometric accuracy of more than 95% in estimating the surfaces and volumes of the examined objects.

All that is needed to realize this method is a digital SLR camera for capturing the photographic images, a stable device for positioning the SLR camera, and a computer with good performance, which serves to transfer captured images and the evaluation and extraction of software data. In the framework of my Master' Thesis, I mainly deal with the parameters of roughness, profile, and volume of concrete surfaces. So, if we wanted to define the work of this method in phases, then we would divide it in the first phase, as mechanical-experimental work, and in the second phase, as automated software work.

In the framework of this thesis, I will elaborate in detail on both phases of this method, starting with the basic knowledge and including the various factors that influence its best realization. I have tried to present this elaboration according to a meaningful scientific order, starting with the formulation of the thesis, then with the fundamental theoretical bases for the characterization of concrete surfaces in civil engineering, with the essential theoretical bases of the function of the stereoscopic method. In the following chapters, continue with experimental laboratory research, assessment, and evaluation of obtained software results, comparison with obtained laboratory results and concluding with the conclusions of all this work.

Kurzfassung

Das grundlegende Funktionsprinzip der stereoskopischen Methode besteht darin, den Eindruck dreidimensionaler Bilder zu erwecken, die durch die Aufnahme zweidimensionaler ebener Bilder aus kleinen Kippwinkeln auf der linken und rechten Seite des Neigungswinkels gewonnen werden, obwohl es sich auch hier um zweidimensionale Bilder handelt. Der Hauptzweck dieser Methode besteht also darin, durch verschiedene Messmethoden den Inhalt des Bildes bzw. des zu untersuchenden Objekts, in unserem Fall der Betonoberfläche, zu interpretieren.

Die Eignung dieser Methode für die Charakterisierung von Betonoberflächen liegt in der Genauigkeit der Messungen und dem wirtschaftlichen Aspekt ihres Einsatzes im Vergleich zu alternativen Methoden, wie z. B. der Laserscanmethode. Verschiedene Untersuchungen haben ergeben, dass photogrammetrische Methoden eine geometrische Genauigkeit von mehr als 95 % bei der Schätzung der Oberflächen und Volumina der untersuchten Objekte aufweisen.

Alles, was zur Realisierung dieser Methode benötigt wird, sind eine digitale Spiegelreflexkamera zur Aufnahme der fotografischen Bilder, eine stabile Vorrichtung zur Positionierung der Spiegelreflexkamera und ein leistungsfähiger Computer, der zur Übertragung der aufgenommenen Bilder und zur Auswertung und Extraktion der Softwaredaten dient. Im Rahmen meiner Diplomarbeit haben wir es hauptsächlich mit den Parametern Rauheit, Profil und Volumen von Betonoberflächen zu tun. Wenn wir also die Arbeit mit dieser Methode in Phasen definieren wollten, dann würden wir sie in der ersten Phase als mechanisch-experimentelle Arbeit und in der zweiten Phase als automatisierte Softwarearbeit unterteilen.

Im Rahmen dieser Arbeit werde ich diese beiden Phasen dieser Methode, beginnend mit den Grundkenntnissen und unter Einbeziehung der verschiedenen Faktoren, die ihre bestmögliche Umsetzung beeinflussen, detailliert ausarbeiten. Ich habe versucht, diese Ausarbeitung nach einer sinnvollen wissenschaftlichen Reihenfolge darzustellen, beginnend mit der Formulierung der These, dann mit den grundlegenden theoretischen Grundlagen für die Charakterisierung von Betonoberflächen im Bauwesen, mit den wesentlichen theoretischen Grundlagen der Funktion der stereoskopischen Methode. In den folgenden Kapiteln geht es weiter mit der experimentellen Laborforschung, der Bewertung und Auswertung der erzielten Softwareergebnisse, dem Vergleich mit den erzielten Laborergebnissen und abschließend mit den Schlussfolgerungen dieser Arbeit.

List of abbreviations

BAC	Bearing Area Curve
CEN	European Committee for Standardization
cm	Centimeter
cm^2	square centimeters
cm^3	Cubic centimeter
c	section height
c0	reference section height
c1	upper section line
c2	lower section line
C_{ref}	reference line
d	diameter
DEM	Digital Elevation Model
DIN	Deutsches Institut für Normung
DPI	Dots per Inch
DSM	Digital Surface Model
e.g.	Example
EN	European Standard
Eq.	Equation
etc.	Etcetera
Fig.	Figure
g	Gram
HSC	high spot count
ISO	International Organization for Standardization
L	specific/certain length
l	Liter
ln	Evaluation length
lp	Sampling length of the Profile
lr	Sampling length of the Roughness
lro	Run-off length
lsu	Start-up length
lt	Traverse length
lw	Sampling length of the Waviness
m	Meter
mm	Millimeter
mm^2	square millimeters
mm^3	Cubic millimeter
Ml (c)	Material of the profile's elements
Mr1	smallest percentage of the material ratio
Mr2	Greatest material ratio
P	Primary profile

Pa	Arithmetic mean value of the P-profile ordinates
Pc	Mean height of the P-profile elements
pix.	Pixels
Pku	Kurtosis of the P-profile
Pp	Height of the largest P-profile peak
PPI	Pixels per Inch
Pq	Quadratic mean value of the P-profile coordinates
Psk	Skewness of the P-profile
Psm	Mean groove width of the P-profile elements
Pt	Profile depth - Total height of the P-profile
Pv	Depth of the largest P-profile valley
Pz	Greatest height of the P-profile
R	Roughness profile
Ra	arithmetical mean deviation of the assessed profile
Rc	Mean Height of the profile elements
Rk	core roughness depth
Rku	Kurtosis of roughness profile
Rmq	relative Material ratio
Rmr	relative material ratio
Rmr(c)	material ratio of the profile
ROI	Region of interest
Rp	Height of the highest profile peak
RPc	standardized number of peaks (peak count)
Rpk	reduced peak height
Rpq	
Rq	root mean square value of profile coordinates
Rsk	Skewness of roughness profile
Rsm	mean width of the profile elements
Rt	Total height of profile
Rv	Depth of the largest profile valley
Rvk	reduced valley depth
Rvq	
Rz	maximum height of profile - Average depth of roughness
Rz1max	Maximum roughness depth
RΔq	mean profile slope
Rδc	section line-height
Sa	Average height of selected area
Sdq	Root mean square gradient
Sdr	Developed interfacial area ratio
SEM	Scanning Electron Microscope
Sk	Core roughness depth
Sku	Kurtosis of selected area
SLR	Single lense reflex
Sp	Maximum peak height of selected area

ix

Spk	Reduced peak height
Srm1	Functional parameter
Srm2	Functional parameter
Sq	Root-mean-square height of selected area
Ssk	Skewness of the selected area
Sv	Maximum valley depth of selected area
Svk	Reduced valley height
Sz	Maximum height of selected area
S10z	Maximum height of 10 peaks/valleys of selected area
t	thickness
Tab.	Table
V	Volume
Vmc	Core material volume of the topographic surface
Vmp	Peak material volume of the topographic surface
Vvc	Core void volume of the surface
Vvv	Valley void volume of the surface
W	Waviness profile
Wa	Arithmetic mean value of the W-profile ordinates
Wc	Mean height of the W-profile elements
Wku	Kurtosis of the W-profile
Wp	Height of the largest W-profile peak
Wq	Quadratic mean value of the W-profile coordinates
Wsk	Skewness of the W-profile
Wsm	Mean groove width of the W-profile elements
Wt	Wave depth - Total height of the W-profile
Wv	Depth of the largest W-profile valley
Wz	Greatest height of the W-profile
Xs	Width of the profile element
Zp	Height of the profile peak
Zt	Depth of the profile valley
Zw	Height difference of the profile element
ΔX	Digitization distance
λc	Long wavelength cut-off
λf	Short wavelength of waviness
λs	Short wavelength cut-off
µm	Micrometer
nm	Nanometer

Keywords

Concrete surface

Stereoscopic Method

Photogrammetric Method

Characterization

Roughness

Waviness

Volume

Surface profile

Profile measurement

Parameters

Table of Contents

1. Structure of the work

Concrete surfaces in the field of civil engineering are numerous, diverse, and have different uses. In concrete surfaces executed outdoors, it is much more important to know the level of their roughness, to reduce the risk of slipping, given the humidity created on them, especially in autumn and winter, which could also cause injury to people while moving. For this reason, especially at the entrances, exits and terraces of private and public buildings, the squares and sidewalks of cities today use concrete tiles with different grooves and roughness.

1.1 Problem statement and objective of this work Thesis

The main purpose of this diploma thesis is, through 3-Dimensional analysis, or microscopic technologies, to characterize concrete surfaces, more specifically the determination of profile parameters, such as roughness, waviness, shape, surface parameters, and the determination of the volume of the examined surfaces. My focus throughout this thesis was on the applicability of photogrammetry in measuring the roughness of surfaces treated in different forms and defining their volume.

So, the essential issues that I have addressed in this thesis are as follows:

1.) Concrete surfaces, including their variety, technical requirements, and functions
2.) The use of the stereoscopic method, which is based on the comparison of stereo images, obtained experimentally through a high-resolution digital SLR camera, from different tilt angles, and with different scaling, to measure and calculate different parameters, which serve to characterize these surfaces.
3.) The impact of the tilt angle, of the size of the selected area, of illumination, magnification, projection distance, sampling distance, cut-off wavelength, etc., in the determination of the roughness profile parameters, surface roughness parameters, and of the volume in the characterization of the concrete surfaces.
4.) The results comparison of the earlier mentioned analysis for different types of concretes, which includes roughness parameters, Bearing Area Curve (BAC), etc. as like as the comparison of the results between the stereoscopic and the sand area method for the determination of the volume of the treated surfaces, with the intention to define the process of calibration during image capturing.

1.2 Structure of the thesis

As can be understood from the above explanation, the entire work of this thesis is divided into two phases, i.e., practical, and analytical, or numerical, where for the realization of these calculations, we have used software from the company Alicona, known as MeX, version 6.2.1. This program is based on scanning electron microscope images (SEM images), a process during which the projection of 3-Dimensional surfaces occurs by overlapping two 2-Dimensional planar images. This process results in the loss of information about the depth of field. However, by applying the eucentric tilt of objects for a slight angle, we obtain such images, which seem to be from slightly different directions, but contain the correct information for the third dimension. At the same time, such a differently created image is also known as an anaglyph image.

2. Technical basics of concrete surfaces and their characterization

2.1 Elaboration of concrete surfaces in civil engineering

The structural composition of concrete as a construction material produced artificially at first glance seems very simple because it consists of standard components, such as aggregate, water, cement, and in exceptional cases, various additives. However, a more accurate and correct understanding of this is possible only by defining the properties of the material.

From general knowledge, we know that concrete is an inorganic mineral material with high compressive strength and lower tensile strength. Therefore, its use as a material in construction engineering is extensive and varied, both in vertical and horizontal elements, including surfaces, depending on the purpose. For this reason, in the framework of this study, it is crucial to define the characterization of concrete surfaces, at the macro, meso, and micro level, based on European norms and standards, which are in the application and to which I will refer in the following.

While at the macro and meso levels, the characteristic features of concrete surfaces can be seen with the free eyes, at the micro-level, they are made possible by the electron microscope test method.

Concrete surfaces must perform certain functions depending on the various technical applications. To fulfill the intended function optimally, surface properties must be precisely defined. Below I have given an example of the relationship between function and the required properties:

Function: *Adhesive strength* ↔ **Required properties:** *Defined minimum roughness, special profile*

2.2 Technical requirements for the definition of surface roughness

"The surface roughness of the concrete shall:

➤ *Provide a sufficient skid resistance by securing concrete road surfaces even in wet conditions, while causing only low rolling resistance and rolling noise,*
➤ *Make concrete pavements sufficiently slip-resistant,*
➤ *Give a special appearance to factory-finished exposed concrete surfaces and regulate water runoff and the tendency to soil,*
➤ *Ensure a sufficient contact surface (adhesion surface) and interlocking possibility for coatings and bonding, while causing only low material consumption ".* [1]

The conditions in which concrete is produced and applied make it an inhomogeneous material, so its quality can only be controlled with the naked eye. However, since there is no standardized comparison system for characterizing concrete surfaces, definitions of

roughness parameters and texture features should be taken as analogous to those of almost homogeneous materials such as metals or plastics. [2]

One of the main reasons we are interested in examining the roughness of concrete surfaces is that it is the decisive factor in the anti-slip effect. In short, as the roughness increases, the slip decreases.

Since part of the investigation of this thesis on the characterization of concrete surfaces were their roughness, waviness and volume, the following progression of the topic results. Regarding the structure of concrete surfaces, the technical requirements for their characterization are usually defined only briefly and refer to the roughness suitable for use or the removal of impurities from the surface. More precisely, it is necessary to determine the roughness of concrete surfaces by the sand surface method according to the author N. Kaufmann, which, despite its suitability in the evaluation, does not provide us with sufficient information about the surface structure. [3] Therefore, in this work it became necessary to use the method of photogrammetry in the following research steps.

2.3 Definition and elaboration of terms of surface parameters

The characterization of surfaces, including the definition of surface parameters, the definition of surface characteristics and the methods to achieve this goal, can be based on certain European EN, German DIN and international ISO standards. Depending on the parameters studied in the following, starting from shape deviations, surface texture, surface formation definitions up to roughness and waviness profile and surface parameters, reference is therefore also made to the relevant applicable standards.

"Although the definitions of terms to which we refer in the following mainly refer to homogeneous materials such as metal or plastic, they can be applied with fewer adaptations and certain limitations to concrete surfaces", [4] which for us means the foundation of this thesis.

To make an analysis and elaboration of the surface parameters as understandable as possible, based on the above-mentioned norms and standards, we have used this work progress:

2.3.1 Surface shape and shape deviations

Given that for certain concrete surfaces, such as industrial floors, for which it is more than necessary to meet specific technical requirements, because their topographical characterization is not precise, it is essential to use understandable and measurable criteria to evaluate their design. [4]

Since no suitable texture criteria or parameters are currently known or identified for concrete surfaces, the definitions, and terms we use for the most detailed characterization of the surface are specified in the standard DIN 4760:1982, which simultaneously distinguishes different shape deviations of the surface through a classification system as given below: [4]

> **Real surface**

„The real surface is the surface that separates the object from the medium surrounding it. It does not include the inner surface of porous materials." [5]

> **Actual surface**

„The actual surface is the measured, approximated image of the real surface of a form element. Depending on the measuring method, different actual surfaces can result." [5]

> **Geometric surface**

„The geometric surface is an ideal surface whose nominal shape is defined by the drawing and/or other technical documents." [5]

These different deviations of the surface shapes according to the DIN 4762 standard, which were later used to define the surface profile, are to be visually represented by the following Figure 1:
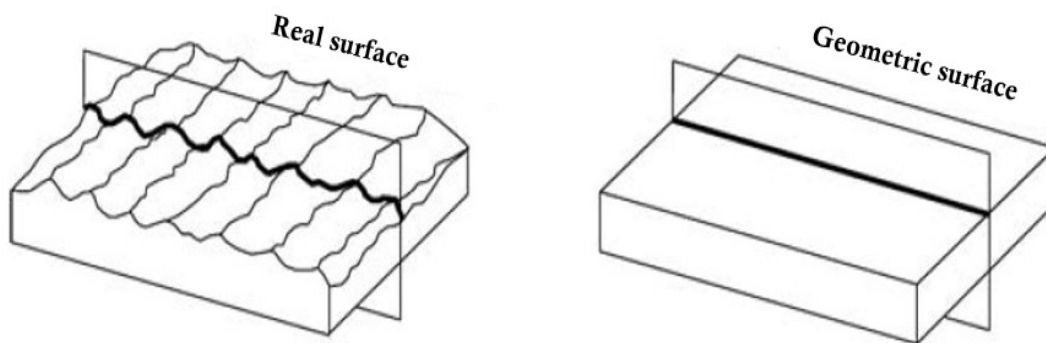
Figure 1: Terms of surface formation according to DIN 4762 [6]

> **Shape deviations**

If from the geometric surface occurs a large number of deviations in the actual surface, then the total of all these deviations constitutes the shape deviation, which according to the norm DIN 4760:1982 can be of different orders, i.e. from the order of 1st to the 6th and can be determined only within the sampling length *lr*, in which case those of the 1st order has to do with the shape and can be recognized by looking at the whole surface, those of the 2nd order have to do with the waviness and are mainly periodic surface deviations with different wave periods, while those of the 3rd to the 5th order have to do with roughness and are regular or irregular deviations of the current surface, where the ratio distance-depth ranges from 100:1 to 5:1. Shape deviations of the 6th order are less important because the structure of the Materia causes them.

Order system for shape deviations with corresponding types of deviation:

- 1st Order: Shape deviations – Straightness, flatness, roundness deviations, etc.
- 2nd Order: Waviness – Waves
- 3rd Order: Roughness – Grooves
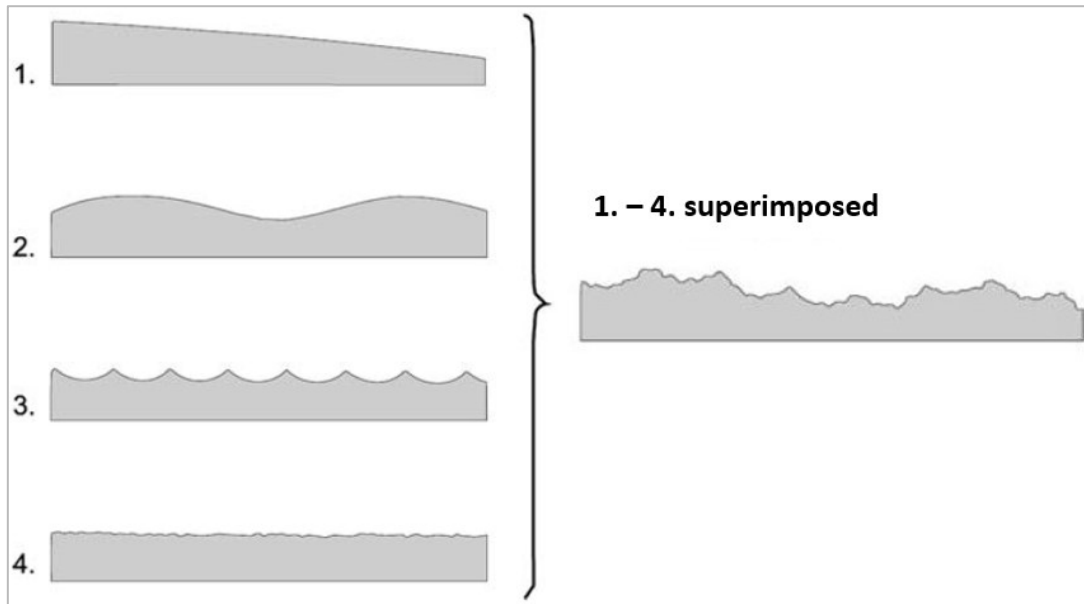- 4th Order: Roughness – Grooves, scales, crests. [5]

Figure 2: Classification system for shape deviations according to DIN 4760 [7]

„*The represented shape deviations of 1st to 4th order usually overlap to the actual surface."* [7]

2.3.2 Surface imperfections

With the intention to define the terms and parameters related to surface imperfection, or for the determination of the permissible degree of surface imperfection and the methods of measuring this imperfection, we refer to the international standard EN ISO 8785:1999, which not only does not take into account the roughness or waviness of the surface but also does not specify intended or unintended exact surface imperfections and differ significantly from the irregularities that form a rough surface..

The international standard EN ISO 8785:1999 defines the imperfection of the surface as follows: *"Element or irregularity or group of elements and irregularities of the real surface, unintentionally or accidentally caused by machining, storage or function of the surface."* [8]

In the context of this international standard, the reference surface is defined as follows: *"Surface, which has the form of a geometric surface and from which the characteristics of surface imperfections are determined."* [9]

Aiming, that despite the presence of surface imperfections it does not become unsuitable in the context of the application, from which we could avoid the term surface defect, it is important that the number, type, or amount of these imperfections in each unit of surface be as tolerable as possible. [10]

According to EN ISO 8785:1999 we distinguish these types of surface imperfections, which are presented in the tables below:

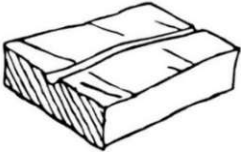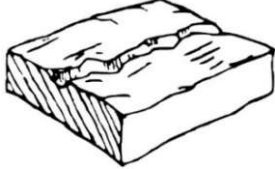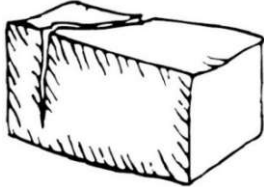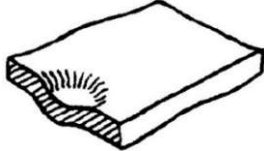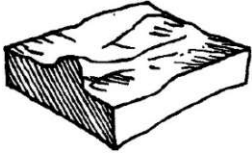*Table 1: Type 1 of surface imperfection according to EN ISO 8785:1999 – Deepening [11]*

Type and description	Subtype	Imperfection	Subtype description
Deepening: *Surface imperfection directed inward.*	**Groove**		*Linear depression with irregular shape or surface imperfection*
	Scratches		*A depression of irregular shape in an unspecified direction causes surface imperfection.*
	Crack		*Linear indentation with a sharp bottom, caused by the destruction of the uniformity of the surface*
	Dent		*Indentation, without raised portion, often caused by plastic deformation due to the impact*

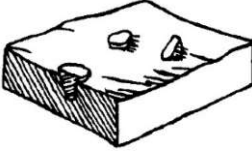*Table 2: Type 2 of surface imperfection according to EN ISO 8775:1999 – Hump [11]*

Type and description	Subtype	Imperfection	Subtype description
Hump: *Surface imperfection directed outward*	**Outgrowth**		*Wave- or hill-shaped elevation of small size and small height*
	Bubble		*Localized bulge caused by gas or liquid inclusions beneath the surface.*
	Inclusion		*Material of the workpiece containing foreign particle causes Surface imperfection.*
	Burr		*Sharp-edged elevation of the surface, often with a rounding on the opposite side*

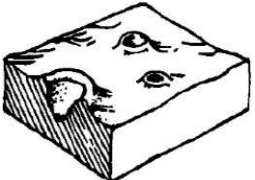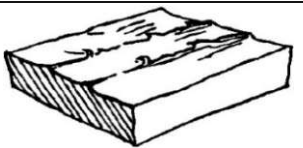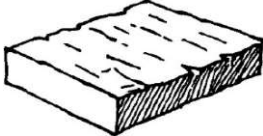*Table 3: Type 3 of surface imperfection according to EN ISO 8785:1999 – Combined [11]*
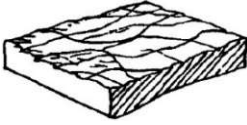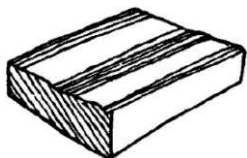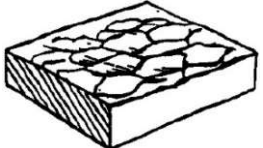
Type and description	Subtype	Imperfection	Subtype description
Combined: Partly inward and partly outward surface imperfection.	**Craters**		*Depression in the form of a volcanic crater, with a circular contour and raised edges, higher than the reference surface*
	Overlap		*Tongue-shaped elevation of small thickness, usually in the form of a seam caused by a fold on the material*
	Notch cut		*Successive depressions, craters, and elevations caused by the material's detachment from the surface of the workpiece which forms the surface imperfection.*
	Rips		*band-shaped elevations caused by poor machining.*

Table 4: Type 4 of surface imperfection according to EN ISO 8785:1999 – Appearance imperfections [11]

Type and description	Subtype	Imperfection	Subtype description
Appearance imperfections: The outermost layer of the surface associated with scattered imperfections whose height and depth are not measured in practice.	**Erosion**		*Surface, damaged by physical destruction or its wear.*
	Microcracks		*A network of cracks on the surface that form a surface imperfection*
	Stripe		*A recessed area on the surface is usually shallow depth and ribbon shaped.*
	Layered surface		*caused by the flaking of a partial surface of the surface layer of a workpiece*

2.3.3 Surface texture

The international standard EN ISO 8785 provides the general conditions for the definition of surface texture, which states: "*Repeated or random deviations from the geometric surface in three-dimensional topography of the surface which includes roughness, waviness, form, surface character, surface imperfections and shape deviations within a subarea of the surface.*" [9]
While the roughness indicates the surface structure in small intervals and the waviness indicates the structure with longer intervals, the shape represents the surface structure with subsequently even longer intervals. All three of these surface structures, which we will discuss in more detail below, form the palpated surface.
An example of such a tactile (palpated) surface is shown in the Figure 3 below:
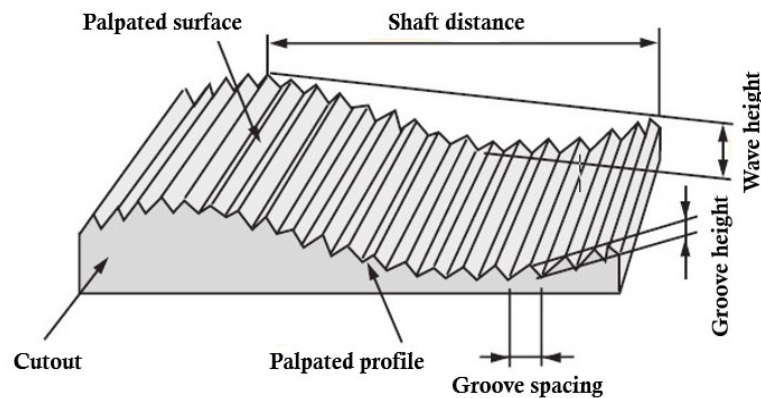

Figure 3: Cutout of a palpated surface [12]

The most detailed elaboration of the surface structure is given in the international standard DIN EN ISO 4287:1998, which is based on the profile method to define the terms, definitions, and parameters that make it up. Although the profile method of primary profiles, of roughness and waviness consists, however, for the description of this surface texture, the norm mentioned above at its foundation has mainly the roughness profile and the parameters that characterize it, for the sole fact that they are better and more precisely defined. For this reason, my focus on the characterization of concrete surfaces is the roughness of the profile and the roughness of the surface, which we have dealt with in detail in the following subchapter.
„*Profile method is a metrological method for the two-dimensional detection of a surface: A feed device moves a probe system horizontally over the surface at a constant speed.*" [13]
So, within this standard, the characteristic parameters of the surface profile can be considered vertical, horizontal components, or as both together, including the definition of certain profiles or sections.

2.3.3.1 Surface Profile

Within the framework of the elaboration of the surface structure with the profile method, the international standard DIN EN ISO 4287:2010 gives the highest priority to the surface

profile, which is defined as follows: *"Profile resulting from the intersection of a workpiece surface with a given plane."* [14]

In the Figure 4 and Figure 5 we represent the surface profile as well as the profile planes, which can be selected as longitudinal or transverse (cross) profile depending on the case under consideration:
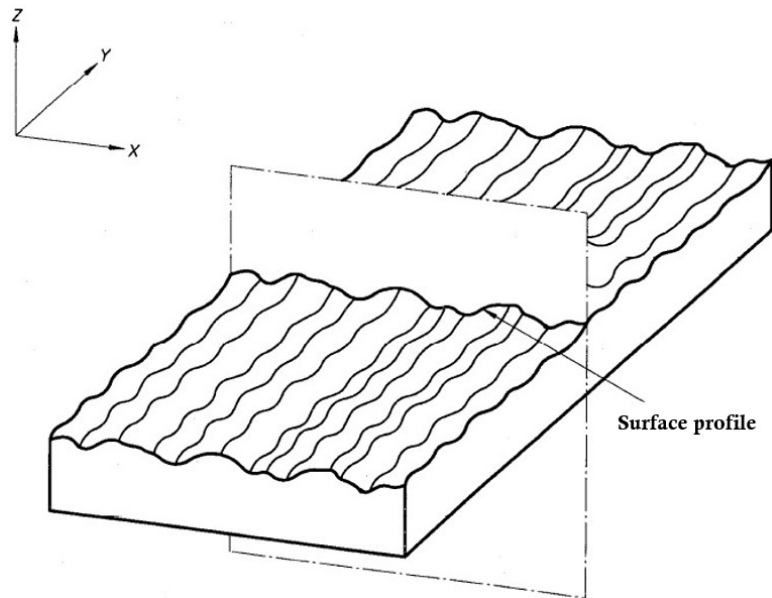

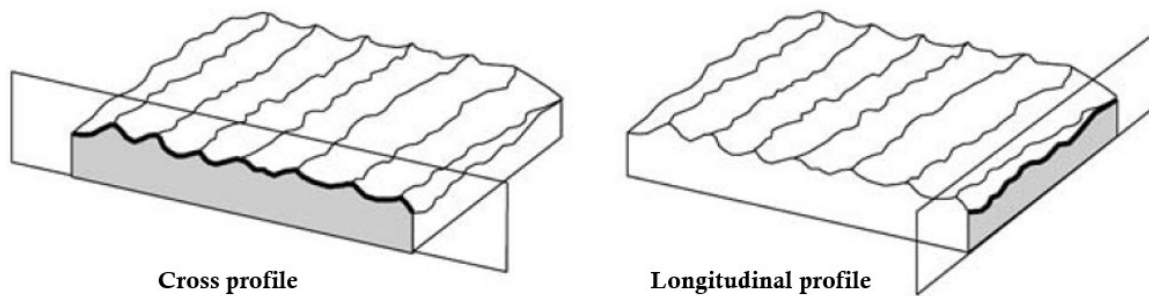*Figure 4: Surface profile according to DIN EN ISO 4287:2010 [15]*

Figure 5: Longitudinal and cross profile (Vertical cut) according to DIN EN ISO 4287:2010 [6]

„So, transverse profiles are those cut lines that are perpendicular to the direction of the groove, while longitudinal profiles are created by cuts parallel to the direction of the groove." [10]

As shown in Figure 5 above, the intersection of the real surface with a perpendicular plane in practice gives rise to the roughness as either a longitudinal or transverse profile, which means that these profile lines are examined and measured in the following steps, represent it.

To adequately assess the surface profile, the international standard DIN EN ISO 4287:2010, also based on the normative EN ISO 11562, has introduced a flow chart of divisions and subdivisions of profiles and profile filters in its Annex B, which must be

understood and analyzed in advance. Therefore, as a first step, this standard gives the definitions of general terms as follows:

- **_Profile filter_** – *„Filter that separates profiles into long-wave and short-wave components. Profile filters are characterized by the numerical value of their cutoff wavelength."* [12] Within the filter profile, there are three filters, λs, λc, and λf, for limiting the transmission of short wavelengths that have the same transmission characteristics but due to the different cutoff wavelengths, they can be used by various devices to measure primary profile, roughness, and waviness.

  - ✓ **λs-Profile filter:** Through this filter, it is possible that the roughness with short wavelengths transitioning into components of even shorter wavelengths within a profile or surface. [16]
  - ✓ **λc-Profile filter:** *„Filter that defines the transition from roughness to waviness."* [16]
  - ✓ **λf-Profile filter:** Through this filter, it is possible that the waviness with long wavelengths transitioning into components of even longer wavelengths within a profile or surface. [16]

- **Gaussian filter** – Represents a digital phase-correct or phase compensation filter with the sinusoidal waveform of the profile and of the cut-off wavelength λc, in which case its reduced amplitude continues to be transmitted at 50% in the roughness profile. [12]

- **Cut-off wavelength λc** – This wavelength of a profile filter determines the wavelengths to be removed from the primary profile to create the roughness and waviness profile. Thus, if we remove the component with long-wavelength, i.e., that which belongs to the waviness, then only the short wavelength remains, and thus the roughness profile is obtained. In contrast, if we remove the component with a short wavelength, i.e., that which belongs to the roughness, then only the long wavelength remains, and thus the waviness profile is obtained. In this way, Cut-off wavelength forms the boundary between the roughness and the waviness of a profile.

- **Transmission band** – The ratio λc to λs which is explained presented through the Figure 6 below:
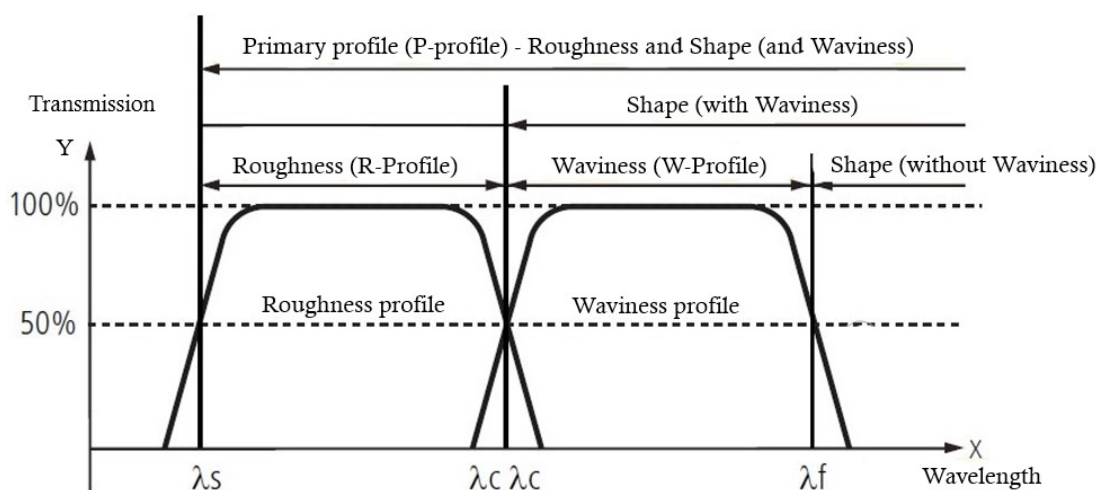

Figure 6: Transmission band for characterization of the roughness and waviness profile [12]

- **Coordinate system** – It is a rectangular coordinate system in which the profile parameters are defined, and its axes (X, Y, and Z) form a right-hand Cartesian system. In the framework of this system, concerning the X-axis the traverse length *lt* and the central line are corresponding. Then we have the workpiece surface, which nominally corresponds to the Y-axis, and finally, concerning the Z-axis, we have the examined material and the surrounding medium. [16]

- *Workpiece surface* – „*Surface that delimits the body and separates it from the surrounding medium.*" [14]

- **Center lines** – The compensation line, which serves as a reference for the surface parameters, is formed in a phase-corrected filter by forming a weighted average for each location of the profile. We distinguish three types of centerlines:

   - ✓ **Centerline for the primary profile** – Indicates the determined line, which specifies the nominal shape by fitting the method of the least squares of deviation applied into the primary profile. [17]
   - ✓ **Centerline for the roughness profile** – Also known as the reference line, which according to DIN EN ISO 11562:1996 means the line obtained by using the method of the least squares and corresponds to those components of the profile, which are long-wavelength but short-frequency, which is determined and suppressed by the low-pass Gaussian filter λc. [15]
   - ✓ **Centerline for the waviness profile** – Based on the standard EN ISO 11562:1996, 3.2, this is a profile line, in which the components are presented with a long wavelength, but with low frequency and which is suppressed by the low-pass profile filter λf. [17]

- **Sampling length (lp, lr, lw)** – means a certain length of the profile, which is used in cases of its evaluation through the detection of shape deviations and extends along the central line in the direction of the X-axis. [17] Since in the framework of the examined profile, we distinguish the primary profile, the roughness, and the waviness, we consequently distinguish different sampling lengths, respectively for the roughness lr = λc, for the waviness lw = λf and for the primary profile lp = ln.

- **Evaluation length (ln)** – Indicates a section of the traverse length (lt) during the scanning process for the profile evaluation, which extends in the centerline along the X-axis and corresponds to the sum of two to five sampling lengths (lp, lr). It must include at least one sampling length, in which case, based on ISO 4288: 1998, the test sections of the W parameters cannot be specified. [17]

- **Traverse length (lt)** – Indicates what distance is traversed by the movement of the touch probe during the measurement process to capture the scanned profile and that, in addition to the evaluation length ln, it also consists of the start-up length and run-off length, to form the roughness profile. [18] Mathematically it derives from the Figure 7 shown below and is expressed as follows:

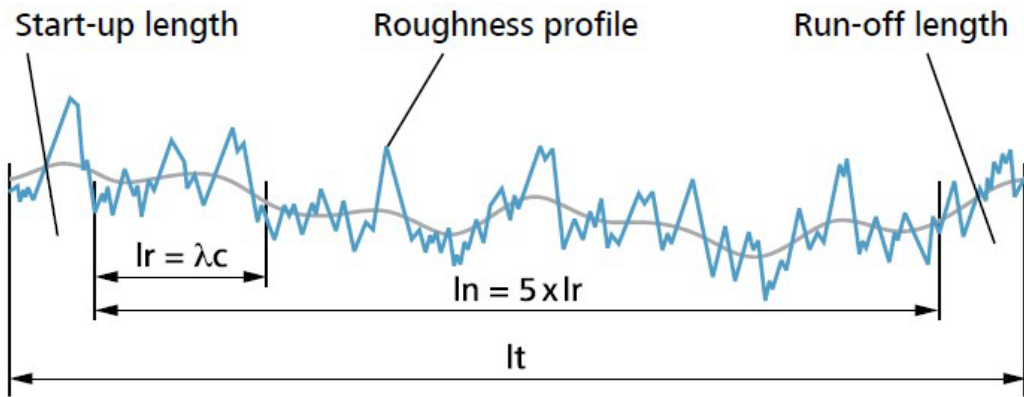$$lt = lsu + ln + lro \quad \text{with} \quad ln = 5 \text{ x } lr \qquad (2.1)$$

Another important and necessary specification for processing the surface profile according to the standard DIN EN ISO 4287: 1998 is the definition of the necessary geometrical parameters such as:

- ❖ **P-Parameter:** *„Parameter calculated from the primary profile."* [17]
- ❖ **R-Parameter:** *„Parameter calculated from the roughness profile."* [17]
- ❖ **W-Parameter:** *„Parameter calculated from the waviness profile."* [17]
- ❖ **Profile peak**: Means the protruding part from the measured profile concerning the X-axis, respectively the center line of the profile, which corresponds to the protruding profile of the material in the surrounding medium, in which the junction of two points adjacent it. [17]
- ❖ **Profile valley**: Means the protruding part into the measured profile concerning the X-axis, respectively the center line of the profile, which corresponds to the protruding part from the surrounding medium into the material, in which the junction of two points adjacent it. [17]
- ❖ **Profile element:** *„Means the profile peak and the adjacent profile valley."* [19]
- ❖ **Height of the profile peak (Zp):** *„Distance from the X axis (center line) to the highest point of the profile peak."* [19]
- ❖ **Depth of the profile valley (Zv):** *„Distance from the X-axis (center line) to the lowest point of the profile valley."* [19]
- ❖ **Height difference of the profile element (Zt)**: Represent the *„Sum of the height of the peak and the depth of the valley in a profile element."* [19]
- ❖ **Width of the profile element (Xs):** *„Section on the X axis (center line) bounded by the profile element."* [20]

Figure 8 shows a visual representation of the profile element and all its components (dimensions):
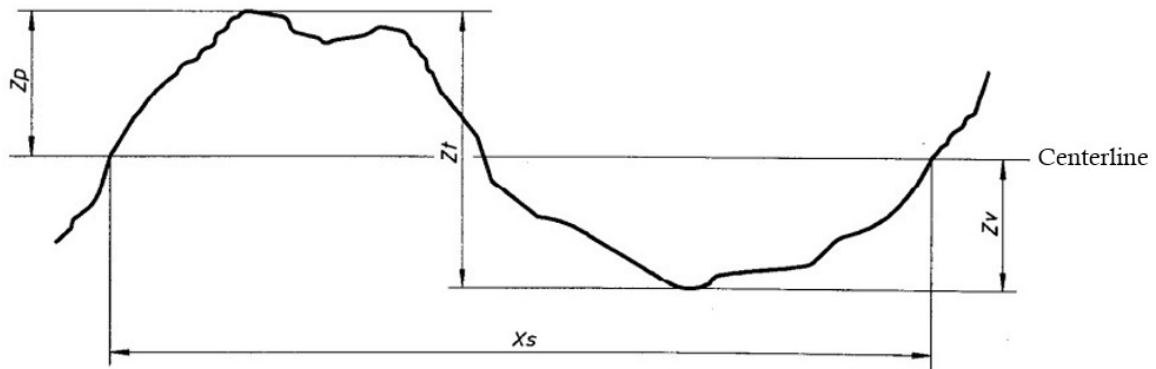
Figure 8: Profile element and all its components according to DIN EN ISO 4287:2010 [20]

To get a complete picture of the surface profile, we must also break it down into profiles and lines of which it consists, which the standards DIN EN ISO 4287:1998 and DIN EN ISO 3274:1998 have defined as follows:

- ***Palpated profile*** – *„The unaligned line of the center of a probe tip as it was sampled."* [12] It contains as the most important shape deviations: Form deviations, waviness, and roughness.
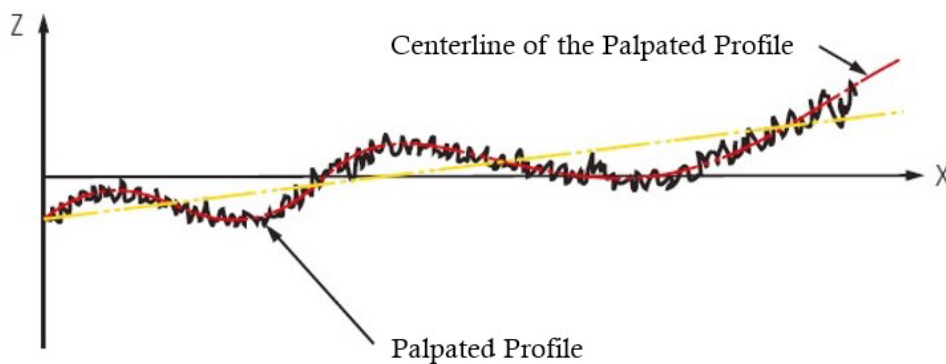

Figure 9: Palpated profile [12]

- **Primary profile (P)** – *„Means the total profile after the application of the short wavelength filter, λs"* [13] a filter, which is not included in the evaluation. This Profile is created if, before applying these filters, through a regression line, which corresponds to the least sum of squares of deviations on the line of the given shape, we eliminate the nominal form.
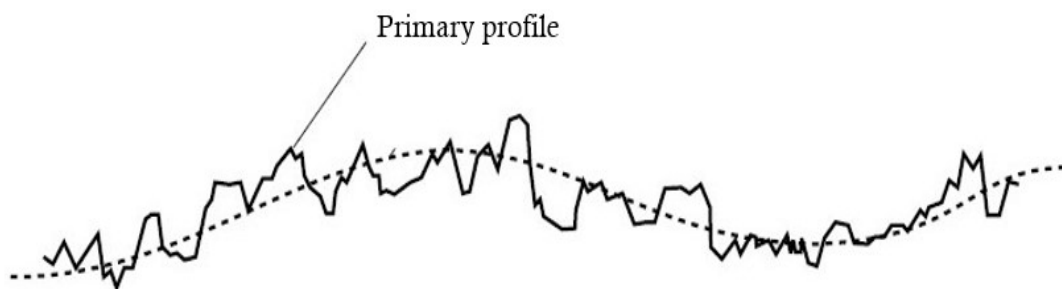

Figure 10: Unfiltered P-profile display [21]

14

- **Waviness profile (W)** – *"Profile created by applying the λf and λc profile filters to the primary profile one after the other."* [15] So, this intentional modification of the total profile with the profile filters λf and λc, which also constitute the transmission band and realize the separation of long and short-wave components, to create the waviness profile, is realized according to this procedure: Before applying the profile filter λf, the least squares method, which is otherwise known as the "best-fit" method is used for eliminating the nominal shape.
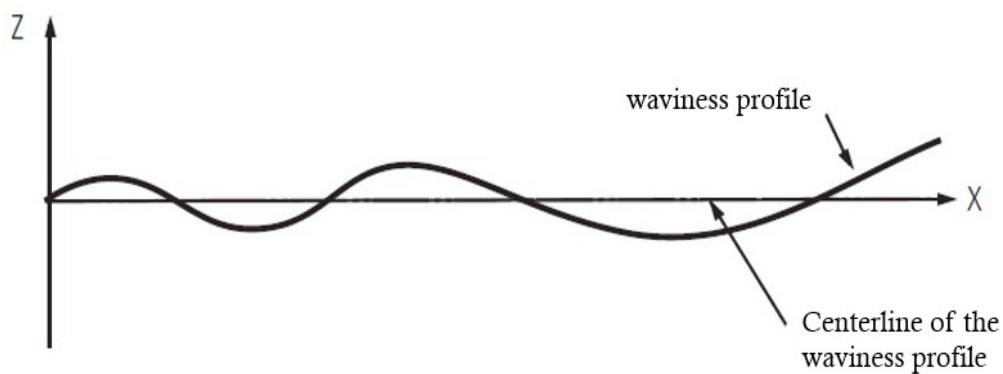
Figure 11: Unfiltered W-profile display [12]

- **Roughness profile (R)** – *„The roughness profile derives from the primary profile. It is created by separating the long-wave profile components with the profile filter λc respectively generated by intentional profile modification."* [14] If we have abstracted the waviness profile, it can be understood as the primary profile, which mathematically expresses (R = P-W) and has a transmission band obtained from the area between the λs filter and the λc filter of the profile. As we can see from Figure 12 below, the centerline of the roughness profile has shifted from the centerline of the primary profile after the waviness profile has been removed and now corresponds to the zero line, respectively the x-axis.
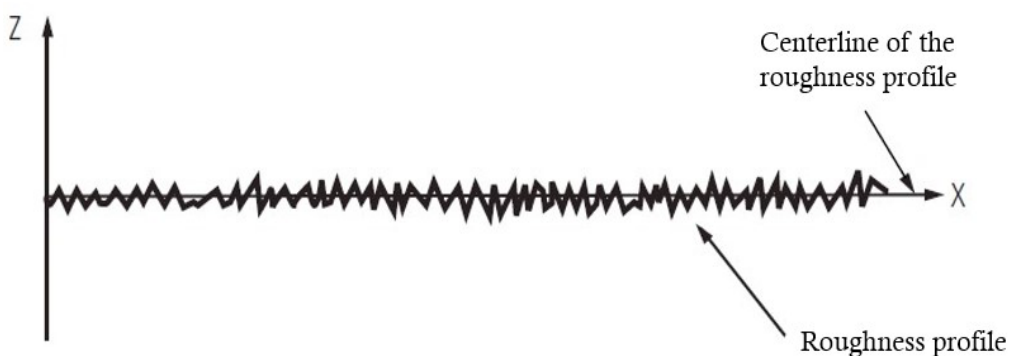

Figure 12: Filtered R-profile display [12]

2.3.3.2 Definition of the parameters of the surface profile

The surface profile parameters defined on a sampling length lr, are mathematically describable. Their results are calculated as an average value from several, usually five sampling lengths lr.

With the help of these parameters, we can define the properties of surfaces, first by a selected profile of this surface as profile analysis, then as a group of profiles arranged in a plane as surface analysis, and finally between different planes of this surface as volume analysis. [22]

Since most of the surface parameters can be obtained from profile analysis, for this reason, the standard DIN EN ISO 4287:1998 has put the main emphasis on their elaboration for each category of surface profile, such as primary profile, waviness profile, and roughness profile. However, my most significant focus will be mainly on the roughness parameters, as this is also the main topic of this diploma thesis.

In the following, we give some important terms, definitions, formulas, and graphical representations of the surface parameters for the primary profile and the waviness profile, based on the above standard, while the roughness parameters are elaborated below in a separate subchapter. Nevertheless, some of the parameters, which have the same definitions, formulas or graphical representations and differ only in the respective letters P, W or R, will not be discussed here, because the same parameters will be elaborated in detail in the subchapter of the roughness parameters.

While for the calculation of the primary profile parameters, denoted by the letter P, the basis is the primary profile. The base of the waviness profile parameters, which are denoted by the letter W, is the waviness profile. [14]

Common amplitude and distance characteristics (parameters) from the primary and waviness profile:

a. **Height of the largest profile peak (Pp, Wp)**: are defined analogously to Rp, as in the following subchapter it is described. Mathematiclly it can be expressed as follow:

$$Pp \equiv Wp = |maxZp| \tag{2.2}$$

b. **Depth of the largest profile valley (Pv, Wv)**: are defined analogously to Rv, as in the following subchapter it is described. Mathematiclly expression as in the following:

$$Pv \equiv Wv = |maxZv| \tag{2.3}$$

c. **Greatest height of the profile (Pz, Wz)**: are defined analogously to Rz and will be calculated through the formula below:

$$Pz \equiv Wz = (|maxZp| + |maxZv|) \tag{2.4}$$

d. **Mean height of profile elements (Pc, Wc)**: are defined analogously to Rc.

e. **Profile depth (Pt) (Total height of the P-profile)** is the vertical distance between two parallel lines that enclose the unfiltered surface profile. *„It corresponds to the sum of the height of the largest profile peak and the depth of the largest profile valley of the*

P profile within the evaluation length ln." [23] In the Figure 13 we have represented Profile depth Pt visually:

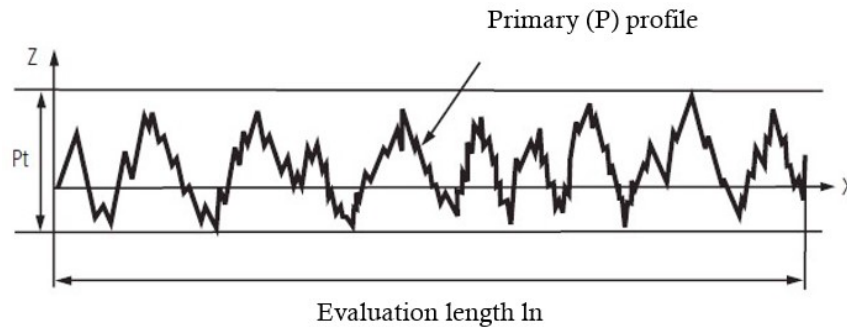*Figure 13: Graphical representation of profile depth Pt according to DIN EN ISO 4287:2010 [12]*

f. **Total height of the W-profile (Wt)** known also as **Wave depth** is *„the sum of the height of the largest profile peak and the depth of the largest profile valley of the W profile within the evaluation length ln* [23] by specifying it after the roughness has been filtered out. Figure 14 shows how the wave depth Wt will visually represented:
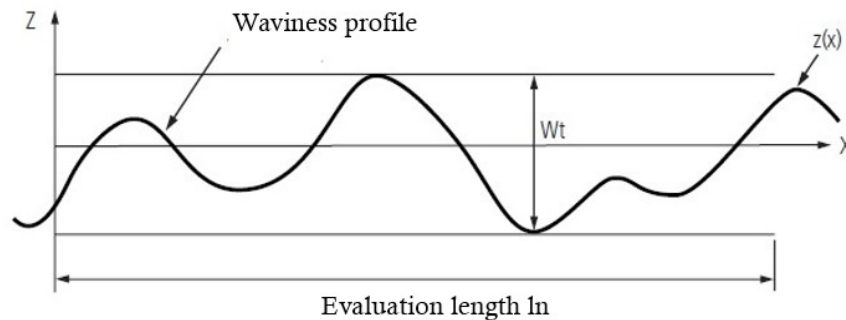
Figure 14: Graphical representation of wave depth Wt according to DIN EN ISO 4287:2010 [12]

g. **Arithmetic mean value of the profile ordinates (Pa, Wa):** Analogue definition as Ra parameter with the only difference to the sampling length marking, so instead of lr should be lp or lw.

h. **Quadratic mean value of the profile coordinates (Pq, Wq):** Analogous definition to the Rq parameter with the changes mentioned above.

i. **Skewness of the profile (Psk, Wsk):** Analogue to the definition of the Rsk parameter, available for lp and lw sampling length.

j. **Kurtosis of the profile (Pku, Wku):** Is defined identically to the Rku parameter as in the following elaboration. Here is the lr sampling length substituted to the lp and lw marking.

k. **Mean groove width of the profile elements (PSm, WSm):** The definition of these two parameters has the same meaning with the Rsm parameter below. The sampling length corresponds to lp and lw designations.

2.3.4 Definition and elaboration of roughness parameters

Before elaborating on the parameters of roughness through definitions, formulas, and graphs, based on the relevant norms in force, it is indispensable first to mention some notions, which are not mentioned above, but crucial for treating roughness as a characteristic of the surface in general, and of the concrete surfaces more specifically in our case.

By the term roughness, which extends over a range of wavelengths from a few micrometers to a few decimeters, we mean the deviation of a surface from an ideally geometrically smooth surface. [24] To better understand how the structure of the surface affects the properties of its service, these wavelengths of surface textures must be divided into ranges of micro-, macro-, and mega-roughness.

Since the microroughness in a lateral extent, λ to 0.5 mm affect, and the macro roughness with wavelengths λ between 0.5 to 50 mm is authoritative, are considered in the context of this Diploma thesis. In contrast, the mega roughness, which has a λ between 50 to 500 mm, remains unconsidered. A subdivision of the roughness according to wavelength ranges is shown in the following Figure 15:
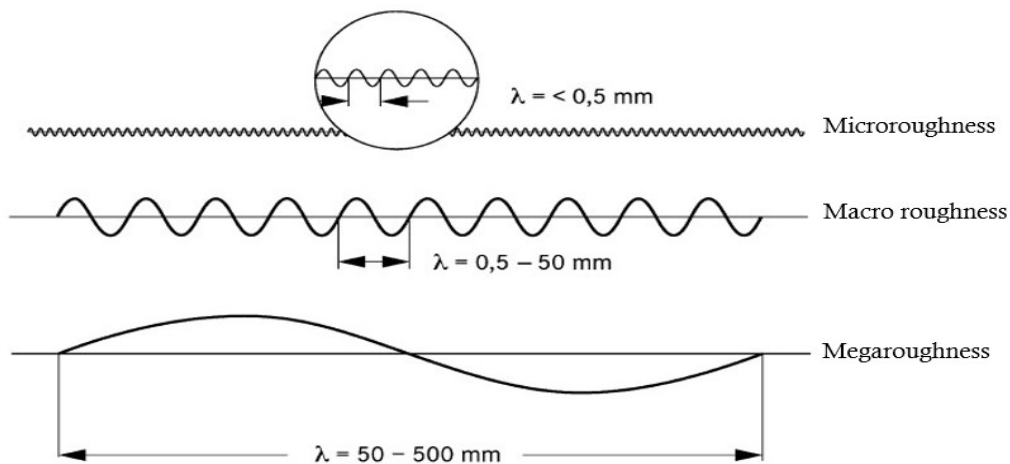

Figure 15: Subdivision of the roughness of road surfaces according to wavelength ranges [25]

Having such a wide range of wavelengths and to measure the roughness parameters, the standards DIN EN ISO 4288:1997 and DIN EN ISO 3274:1998, depending on the periodicity of the profile, respectively periodic and aperiodic, have given through Table 5 the selection of the cut-off wavelength λc, depending on the ratio of the sampling length lr and the evaluation length ln, respectively through (lr / ln).

Table 5: Selection of the cut-off (profile filter) according to DIN EN ISO 4288:1998 [26]

Periodic profiles	Measuring conditions				Aperiodic profiles	
e.g. turning, milling	Cut-off	evaluation length	traverse length	sampling/ evaluation length	e.g. grinding, eroding	
RSm (mm)	λc = lr (mm)	ln (mm)	lt (mm)	lr/ln (mm)	Ra (µm)	Rz (µm)
> 0.013 …0.04	0.08	0.4	0.48	0.08/0.4	> (0.006) …0.02	> (0.025) …0.1
> 0.04 …0.13	0.25	1.25	1.5	0.25/1.25	> 0.02 …0.1	> 0.1 …0.5
> 0.13 …0.4	0.8	4	4.8	0.8/4.0	> 0.1 …2	> 0.5 …10
> 0.4 …1.3	2.5	12.5	15	2.5/12.5	> 2 …10	> 10 …50
> 1.3 …4	8	40	48	8.0/40	> 10 …80	> 50 …200

So, from the table above we can conclude that, depending on the expected values of the roughness parameters such as mean width of the profile elements – RSm for periodic profiles and arithmetical mean deviation of the assessed profile – Ra, or maximum height of profile – Rz for aperiodic profiles, or the space of the groove on the workpiece surface we can choose the Cut-off wavelength. As a result, the amplitude of the filtered roughness profile decreases as a function of the cutoff wavelength, and we will measure smaller values of roughness parameters. To make the above table even more understandable, in the following we are graphically presenting the periodic and aperiodic profile:
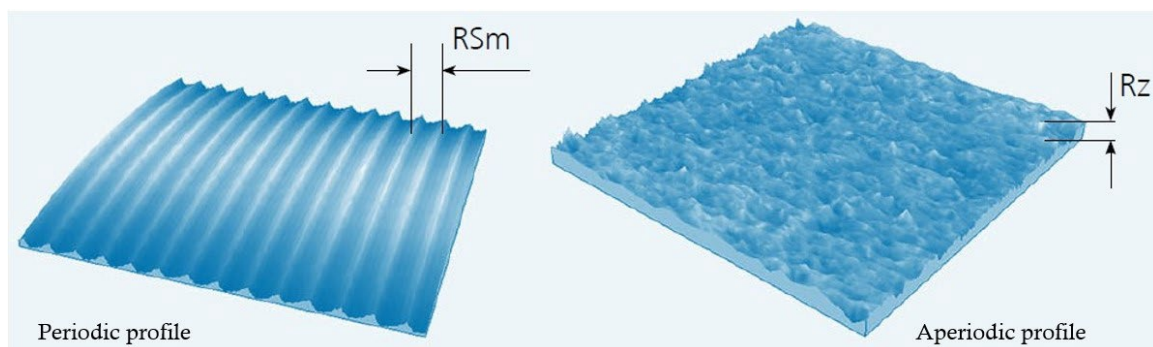
Figure 16: Periodic and Aperiodic profile according to DIN EN ISO 3274:1998 [18]

Another important term is the surface roughness, which indicates the appearance of continuous surface irregularities, in the form of peaks or valleys at relatively shorter distances compared to their height, respectively their depth.

Before we start with the step-by-step elaboration of all roughness parameters according to the standard DIN EN ISO 3274:1998, it is important to tabulate the relationship of the

19

roughness transmission bands with the phase-correct Gauss filter for the stylus instruments. Table 6 presents the above correlation:

Table 6: Relationship of the roughness transmission bands with the phase-correct Gauss filter for the stylus instruments according to DIN EN ISO 3274:1998 [12] & [18]

Long wavelength cut-off	Short wavelength cut-off	Transmission band	Stylus tip radius	Digitization distance
λc (mm)	λs (µm)	$\lambda c : \lambda s$	r^{tip} [µm]	ΔX
0.08	2.5	30	2	0.5
0.25	2.5	100	2	0.5
0.8	2.5	300	2 or 5	0.5
2.5	8	300	5	1.5
8	25	300	10	5

To define and evaluate the roughness profile and its parameters, it is necessary that the evaluation length ln include at last one or an average five of sampling lengths lr, which in this case corresponds to the cut-off λc, so it should be ln = 5 x lr.

According to DIN EN ISO 4287:2010, the basis for the determination, explanation and calculation of roughness parameters and their differences, which are defined except for Rt, Rmr(c) and RPc parameters within an evaluation length ln and are determined as the average of five sampling lengths lr, is the filtered roughness profile.

Nevertheless, not all surface imperfections are considered when measuring roughness parameters. Some examples are cracks and pores, which are described in the standard DIN EN ISO 8785:1999.

Even though with the use of modern surface measuring instruments, many surface parameters with their significance are output, in the following list we have only dealt with the most important roughness parameters according to DIN EN ISO 4287:2010, DIN EN ISO 13565:1998 and DIN EN 10049.

2.3.4.1 Parameters of roughness profile (Profile parameters)

The list of roughness profile parameters will be done by dividing it into several groups, respectively according to the normative that defines and measured them, as follows:

- **DIN EN ISO 4287:2010** – Within this standard, the roughness parameters that have been discussed here are divided into 3 major subdivisions, namely:
  - **Vertical parameters (Amplitude parameters)**, which takes into consideration the peak heights, valley depths and mean values of ordinates and do not allow the distinguish between profiles with many peaks and profiles with many grooves, are:
    - ✓ **Rp – Height of the largest profile peak** corresponds to *„the height of the largest profile peak Zp within the single sampling length lr."* [27] Rp is shown graphically following in Figure 17:
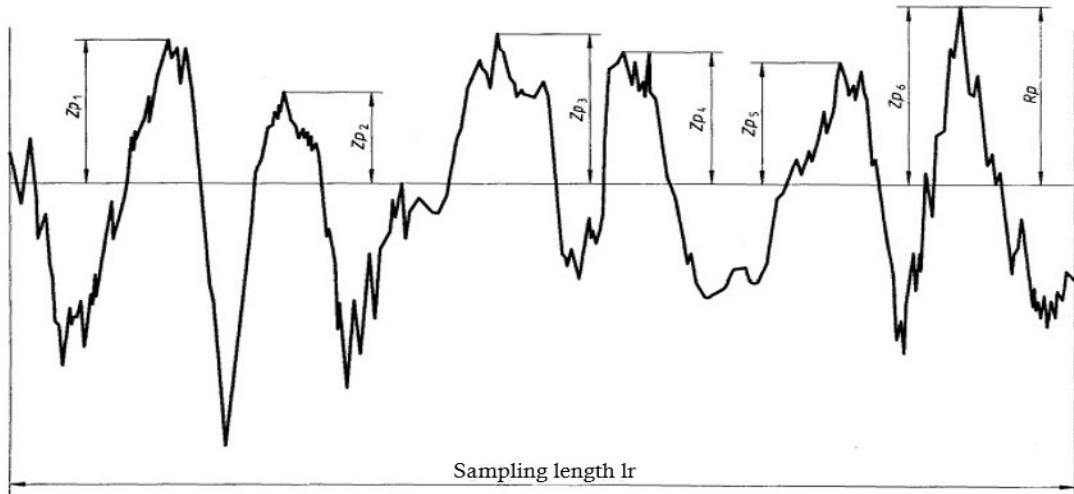
Figure 17: Rp – Height of the largest profile peak according to DIN EN ISO 4287:2010 [28]

✓ **Rv – Depth of the largest profile valley** corresponds to the *„depth of the largest profile valley Zv within the single sampling length lr"* [27] and is visually represented in the Figure 18:
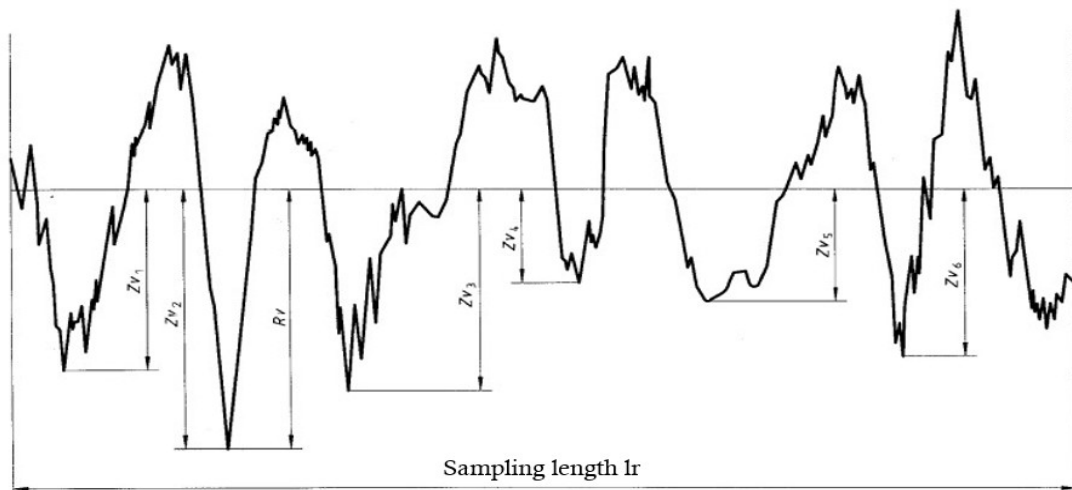

Figure 18: Rv – Depth of the largest profile valley according to DIN EN ISO 4287:2010 [28]

✓ **Rz – The average depth of roughness,** which depending on the measured length (lr or ln) is also known as **maximum height of profile** calculates as *"Sum of the height of the largest profile peak Zp and the depth of the largest profile valley Zv within a single sampling length lr"* [27] is defined as the arithmetic mean value of all five roughness depths Rz (i=1-5) for the entire evaluation length ln, measured within the sampling lengths lr separately. It helps us to measure the bearing and sliding surfaces. This parameter can be measured using the following mathematical expressions:

$$\mathrm{Rz} = \frac{1}{n}(Rz1 + Rz2 + \cdots + Rzn) \tag{2.5}$$

21

$$Rz = \frac{1}{5} \sum_{i=1}^{5} R_z(i) \qquad (2.6)$$

✓ **Rz1max – Maximum roughness depth** is the largest individual roughness depth measured from all five sampling lengths lr within the evaluation length ln. Following we will visually define the maximum height of the roughness profile Rz according to DIN EN ISO 4287 through the Figure 19 below:
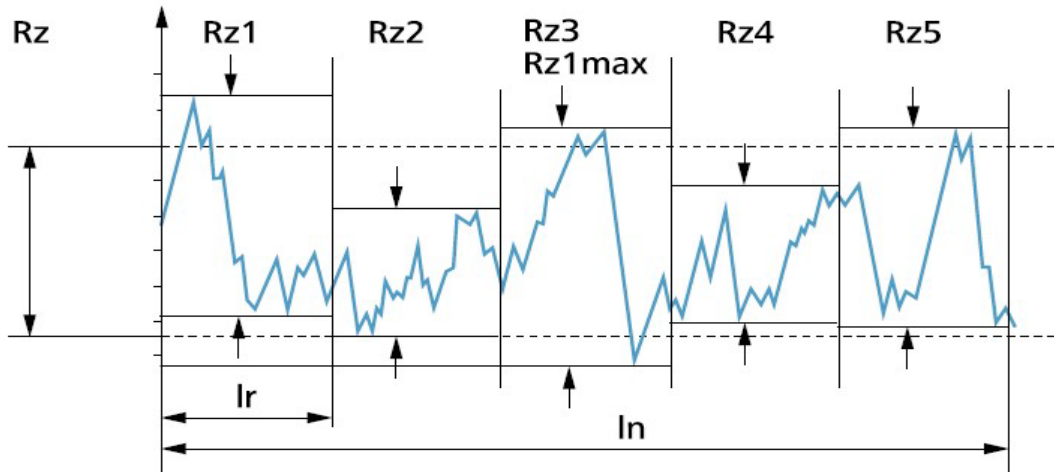
Figure 19: Definition of the maximum height of the roughness profile Rz according to DIN EN ISO 4287:2010 [18]

✓ **Rt – Total height of profile** *„is the sum or the vertical distance between the highest peak Zp and the deepest valley Zv of the profile of the total evaluation length ln."* [23] A concrete example what Rt-Parameter determine, is presented in the Figure 20:
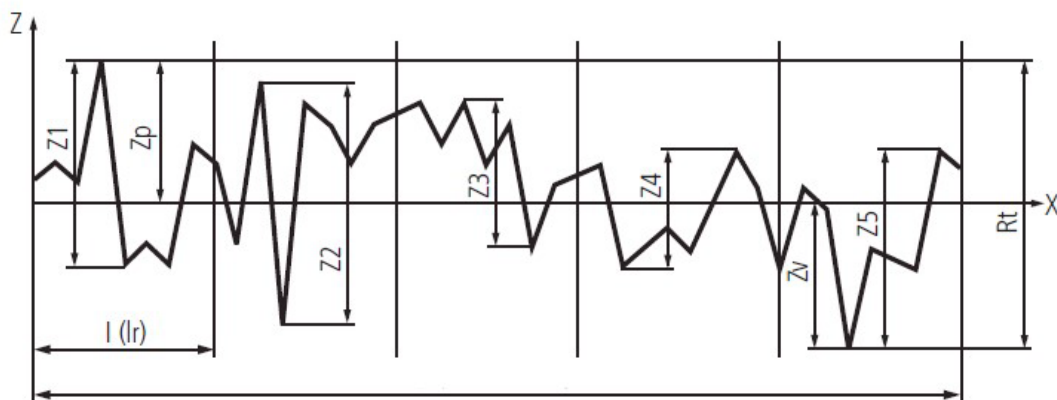
Figure 20: Definition of the total height of profile Rt according to DIN EN ISO 4287:2010 [12]

✓ **Rc – Mean height of profile elements (irregularities)** *„is the mean value of the heights of profile elements Zt within a sampling length lr."* [27] Visual representation of this parameter shown in the figure below helps us to determine the mathematical expression for its calculation:

$$Rc = \frac{1}{m} \sum_{i=1}^{m} Zt_i \qquad (2.7)$$
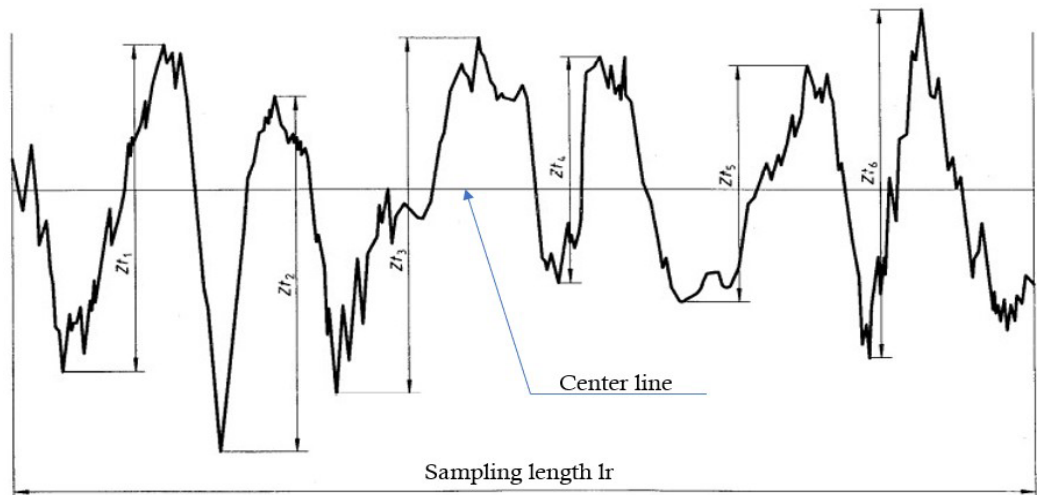
Figure 21: Height of profile elements Zti for definition of Rc according to DIN EN ISO 4287:2010 [29]

✓ **Ra – arithmetical mean deviation of the assessed profile** is the first parameter measured in the context of surface characterization and *"corresponds to the arithmetic mean value of the amounts of all ordinate values Z(x) of the roughness profile within the sampling length lr."* [23] It also correlates to the designations AA (Arithmetic Average) and CLA (Center Line Average). [12]

Nevertheless, the Ra value is usually determined within an evaluation length ln, which is the projected length on the centerline of the part of the roughness profile used directly for the evaluation and includes one or more individual sampling lengths lr, which neglects the extreme values of the profile ultimately, be they peaks or even valleys. In connection with the definition, the above standard also specified the diagram for determining the parameter Ra, through which the mathematical expressions for determining its numerical value are obtained.
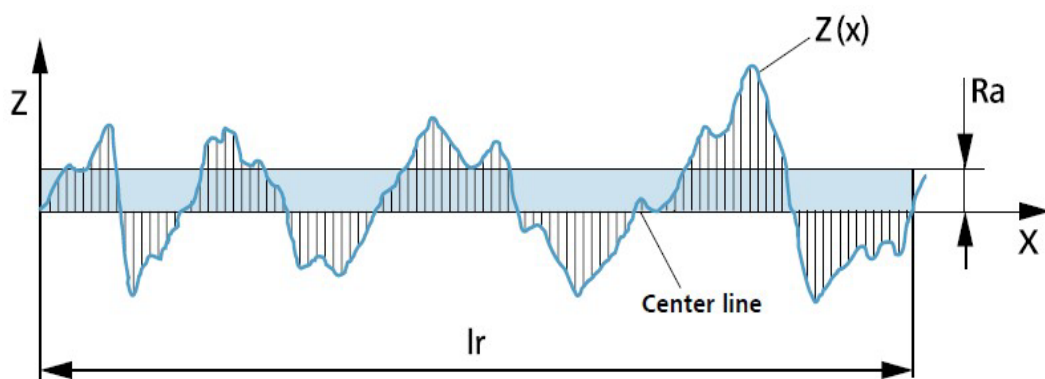
Figure 22: Definition of the arithmetic mean Ra of the profile ordinates Z(x) within a sampling length according to DIN EN ISO 4287:2010 [18]

$$\text{Ra} = \frac{1}{l_r} \int_0^{l_r} |z(x)| dx \tag{2.8}$$

$$\text{Ra} = \frac{1}{l_n} \int_0^{l_n} |z(x)| dx \quad \text{for ln = lr} \tag{2.9}$$

23

Being completely negligent of the extreme values of the profile, such as peaks and grooves, respectively valleys, and having a relatively weak information character, it turns out that the center-line roughness value Ra cannot even recognize their various forms. This happens, *"because its definition is based on a strong averaging, the values scatter only slightly and are easily reproducible."* [21] This statement can be confirmed by Figure 23, which shows different profiles with equal mean roughness value Ra.
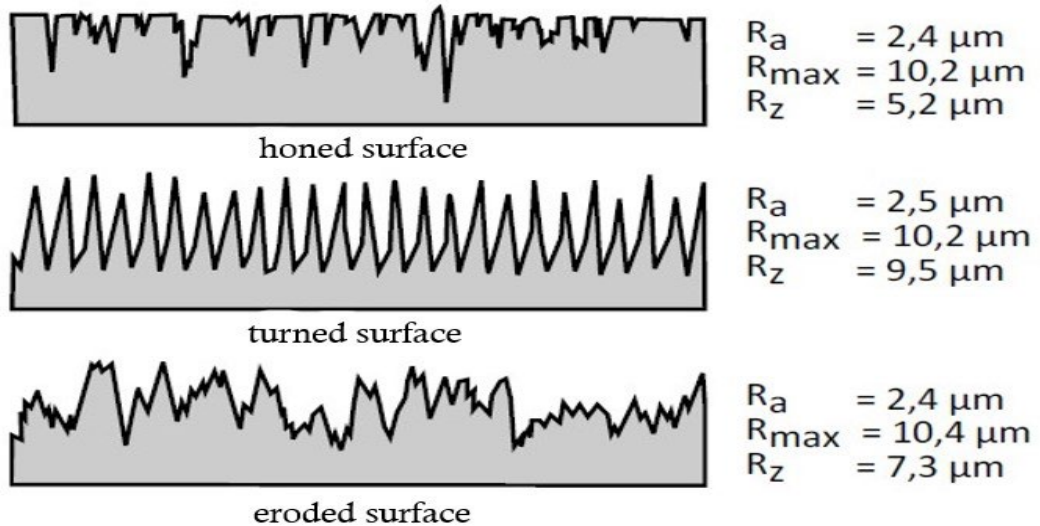
Figure 23: Different profiles with equal mean roughness value Ra [21]

✓ **Rq – root mean square value of profile coordinates** is defined as *"the root mean square of the ordinate values Z(x) within the sampling length lr"* [23] and correspond to the standard deviation of these coordinates of the profile showing a higher sensitivity of individual peaks and valleys comparing to the Ra parameter. The relevant standard ISO 4287 also specifies the graphical representation of the parameter Rq, from which the mathematical expression for calculating the specific numerical value is derived:
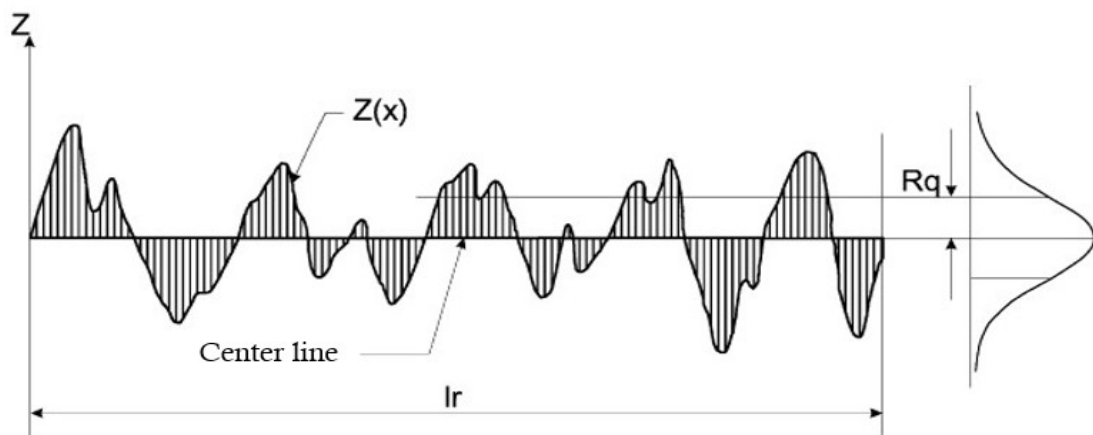
Figure 24: Definition of the Rq of the profile ordinates Z(x) within a sampling length lr according to DIN 4287:2010 [30]

$$R_q = \sqrt{\frac{1}{l_r} \int_0^{l_r} z^2\,(x) dx} \qquad\qquad (2.10)$$

$$R_q = \sqrt{\frac{1}{l_n} \int_0^{l_n} z^2\,(x) dx} \qquad \text{for} \quad \text{ln} = \text{lr} \qquad (2.11)$$

✓ **Rsk – Skewness of roughness profile,** which is strongly influenced by isolated peaks and valleys, *"is a measure of the asymmetry of the amplitude density curve of the ordinate values and corresponds to the quotient of the averaged third power of the ordinate values (x) and the third power of Rq within a Sampling length lr."* [23] The Rsk parameter is determined using the Eq. 2.12 given below, through which certain values are obtained, from positive to neutral and to negative.

$$R_{sk} = \frac{1}{Rq^3} \left[\frac{1}{l_r} \int_0^{l_r} z^3\,(x) dx \right] \qquad (2.12)$$
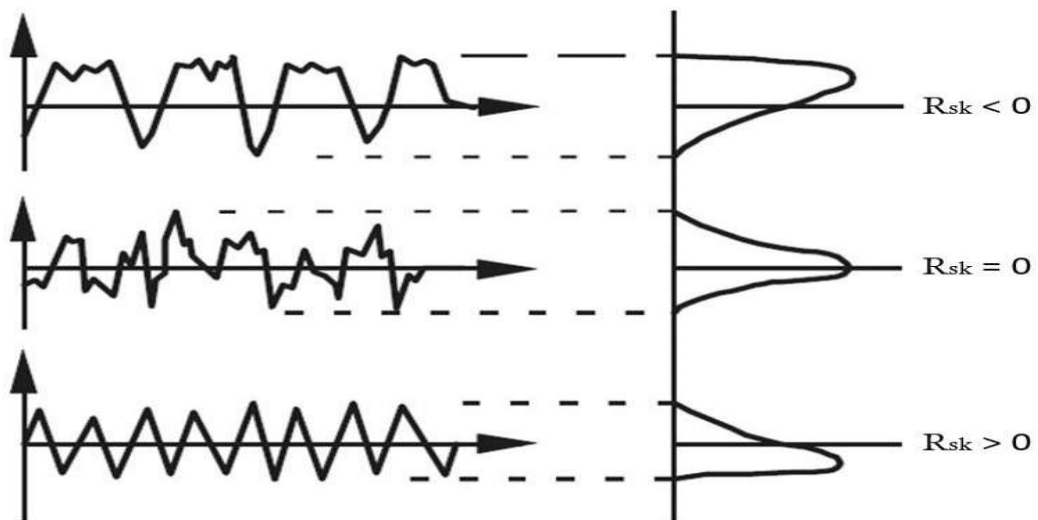
Figure 25: Skewness of roughness profile definition vor different Rsk values [31]

The conclusions drawn from the analysis of Figure 25 are as follows: if the value of Rsk=0, then the profile ordinates are distributed normally if the value of Rsk < 0, then the profile ordinates are distributed asymmetrically, and the surface shows good bearing properties, and if the value of Rsk > 0, then we are dealing with profiles, which contain a high percentage of peaks.

✓ **Rku – Kurtosis of roughness profile** is a profile with flattened peaks and valleys when it has small values, thus reducing their practical importance. *"Rku is a measure of the kurtosis of the amplitude density curve of the ordinate values and corresponds to the quotient of the averaged fourth power of the ordinate values (x) and the fourth power of Rq within the sampling length lr."* [32] This parameter is defined by Eq. 2.13 given below:

25

$$\text{Rku} = \frac{1}{Rq^4} \left[\frac{1}{l_r} \int_0^{l_r} z^4 (x) dx \right] \qquad (2.13)$$
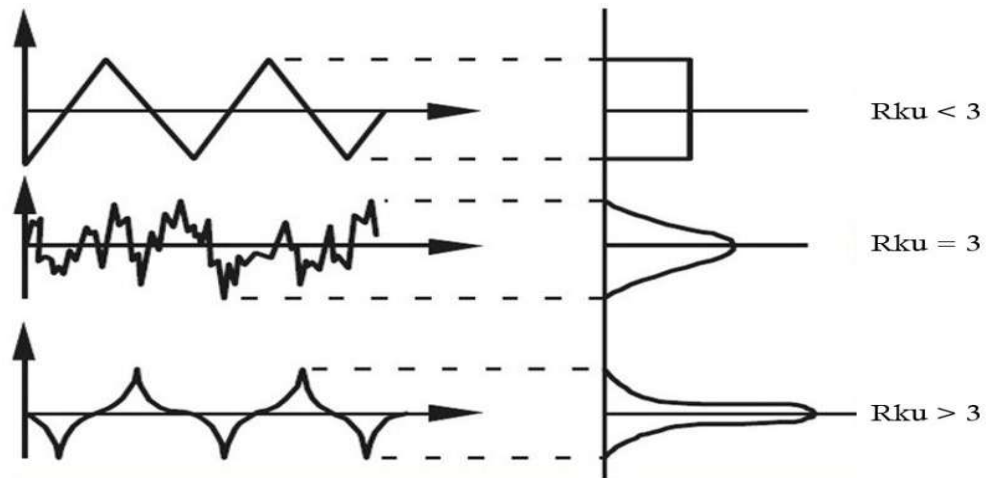
Figure 26: Kurtosis of roughness profile definition for different Rku values [31]

From the above Figure 26, we can conclude as follow: when Rku = 3, then the profile values are normally distributed, when Rku <3, the profile values are characterized by flat peaks and valleys, while when Rku> 3, then the profile is characterized by sharp peaks and valleys.

- **Horizontal parameter (Distance parameters)** can be considered only the mean groove width, which is:
  - ✓ **Rsm – mean width of the profile elements** also known as **mean groove spacing** is *„the arithmetic mean value of the widths of the profile elements Xs of the roughness profile within the sampling length lr"* [32], where the profile element means its height and an adjacent valley, which must meet the standards of minimum height and length. So, more specifically, it is obtained, when from 5 different sampling lengths, lr we derive the average value of Xs, and through it, we select the wavelength of the filter λc.

    Regarding the surface function, the Rsm parameter requires that the height discrimations (c1 and c2), the sum of which does not exceed the 10% threshold of the Rz value, be defined accordingly and is determined with Eq. (2.14) according to Figure 27

$$\text{RSm} = \frac{1}{m} \sum_{i=1}^{m} Xs_i \qquad (2.14)$$
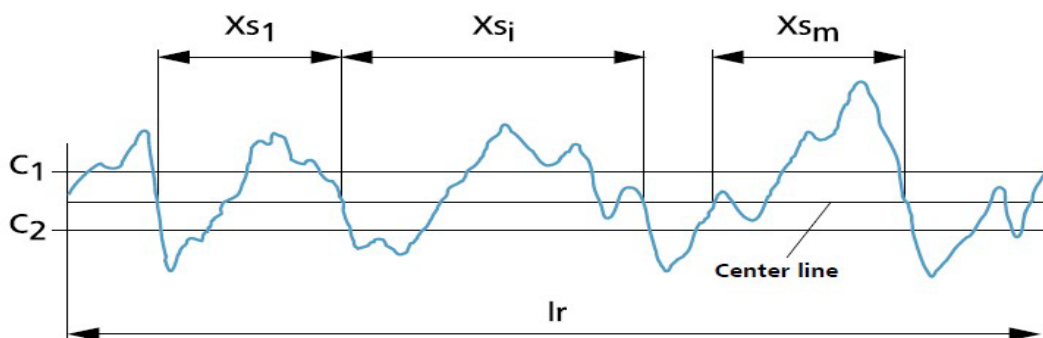
Figure 27: Definition of the mean value RSm of the groove widths of the profile elements Xs within a sampling length lr according to DIN EN ISO 4287:2010 [18]

26

✓ **RPc – standardized number of peaks (peak count)** This parameter indicates the number of local peaks, which corresponds to the mean widths of the profile elements (RSm), usually calculated within the limits of ± 0.5 µm. [32] A characteristic of these peaks is that they exceed the upper section line c1 and the lower section line c2 against the centerline and can also be found within a specific length L, a length which in most cases has the value of 10 mm and corresponds to the evaluation length ln. Sometimes it happens that at a certain length L=10 mm of the roughness profile, the number of profile peaks is exceeded only on the upper section line c1 and not on the lower section line c2, and this condition we describe as the high spot count (HSC). A good example of the visual representation of the RPc (Peak Count) is given in the following Figure 28:
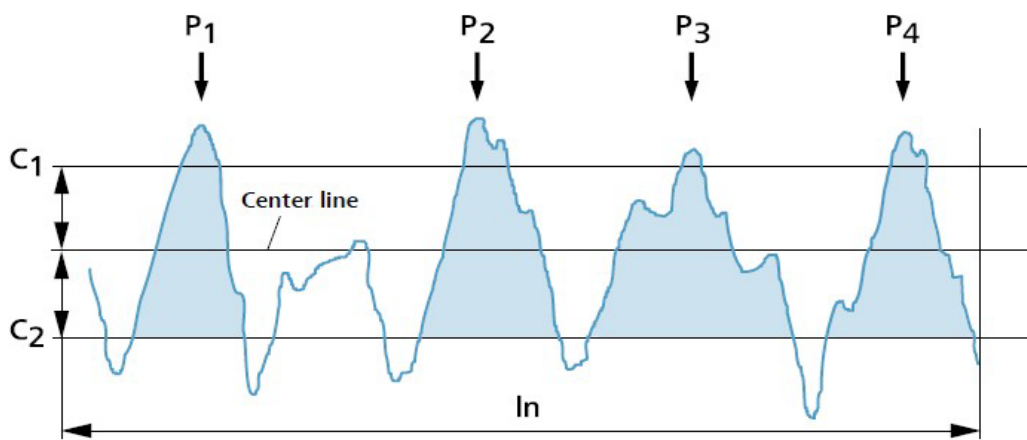
Figure 28: Definition of RPc - Peak Count parameter [18]

Mathematical expression for calculating the RPc parameter is as below:

$$RPc = \frac{L}{RSm}$$ (2.15)

- **Mixed parameters**, such as:
  ✓ **RΔq – root-mean-square slope of the profile** also known as **mean profile slope** *„is the root mean square value of the local profile slopes dZ/dX of the roughness profile within the sampling length lr.“* [33] In the context of the function and evaluation of surfaces, this parameter together with local profile gradient seem to play an important role, either in reducing the impact of noise, or in capturing the reflection of light, due to the standard deviation of angles of profile. We can calculate RΔq value with help of mathematical expression represented in Eq. (2.16), which derives from the Figure 29:
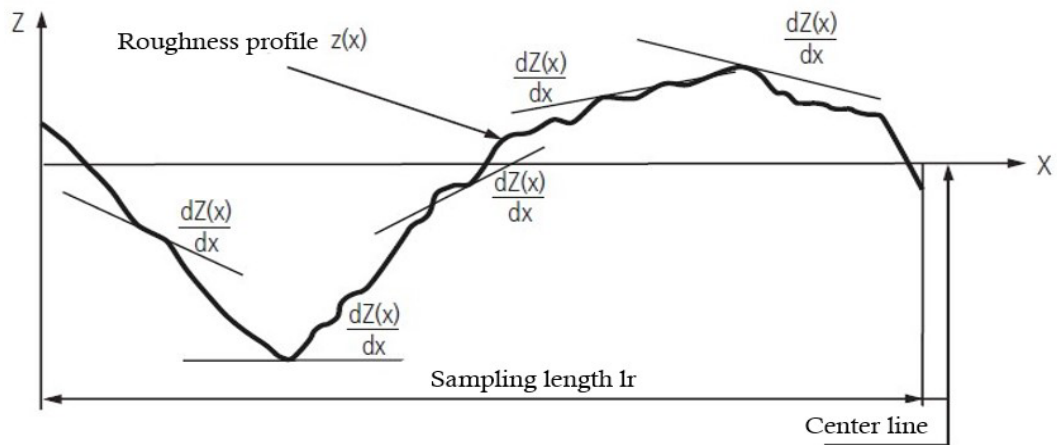
Figure 29: Definition of the root-mean-square slope of the profile RΔq [12]

$$R\Delta_q = \sqrt{\frac{1}{l} \int_0^l \left(\frac{dz}{dx}\right)^2 dx} \tag{2.16}$$

- **Characteristic curves and characteristic values derived from them**: The Abbott curve, also known as the material proportion curve, is used to characterize the vertical distribution of material of a surface.
  - ✓ **Rmr(c) – material ratio of the profile** shows, in what ratio lies the sum of all lengths filled with material Ml (c) of the profile's elements, defined at a section height c in the material ratio curve, compared to the total evaluation length ln, expressed in%. Initially, the material's content is determined by the reference line, which in this case corresponds to the highest peak of the profile, which by moving it in the profile, we obtain the reference section height c0. This newly obtained line differs from the final section height c by one section line height Rδc.

    The selection of the section height c is made in two different methods:
    I.   Method, I expressed in% and shows that if c is selected at the peak height of the profile, it has the value 0, while if the selection is made at the deepest point of the valley, it has the value 100,
    II. Method II expressed in mm shows how deep the profile is in mm compared to its highest peak. [12]

    The Rmr(c) value will be determined through the following mathematical expression shown in Eq. 2.17, which is also available for the Abbot curve:

$$\text{Rmr(c)} = \frac{100}{l_n} \sum_{i=1}^{n} Ml_i(c) \tag{2.17}$$

  - ✓ **Material ratio curve of the profile,** also known as **Abbot-Curve** or **(BAC – Bearing Area Curve)** *„is the cumulative frequency curve of the ordinate values Z(x) within the evaluation length ln and represents the material ratio of the profile Rmr(c) as a function of the section height c.*" [34]

    To understand more precisely the function of this curve and the interdependence that the section height c and the evaluation length ln have on it, at the first point, we divide the roughness profile at a specific height

28

Z(x) with any particular line. In this case, several material-cutting distances li are created (at least 5 of them), which cut the peaks of the profile roughness. Then, we add up these distances li and put their sum concerning the evaluation length ln. As a reference line of the material ratio curve, we have the highest peak of the profile at 0% of material ratio Rmr(c), which in practice moves vertically downwards for an $R\delta c=5\%$ and in this case creates the reference section height c0, which simultaneously represents the consumption of the individual peaks of the profile, which in this case lose their importance slightly. In the next Figure 30, we have shown the relationship of the Abbot-Curve and the roughness profile:
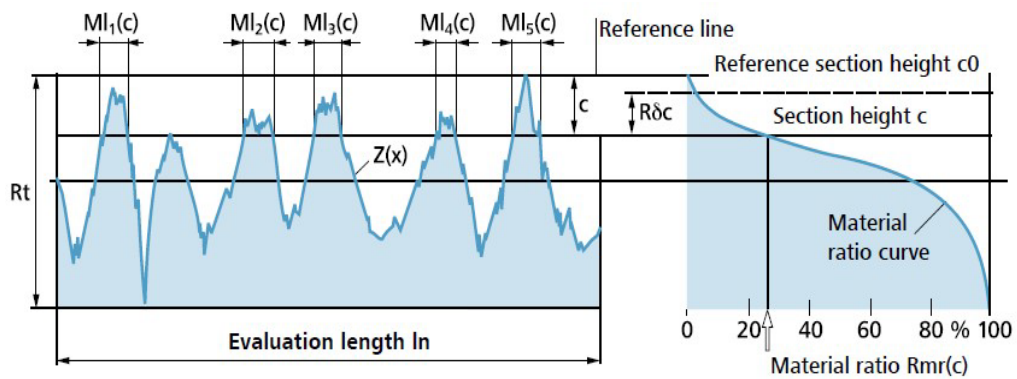
Figure 30: Relationship between roughness profile and Abbott curve [18]

We distinguish different corresponding Abbot curves for different roughness profiles, and such a relationship is shown in
Figure 31 below:

Roughness profile shapes   BAC shapes
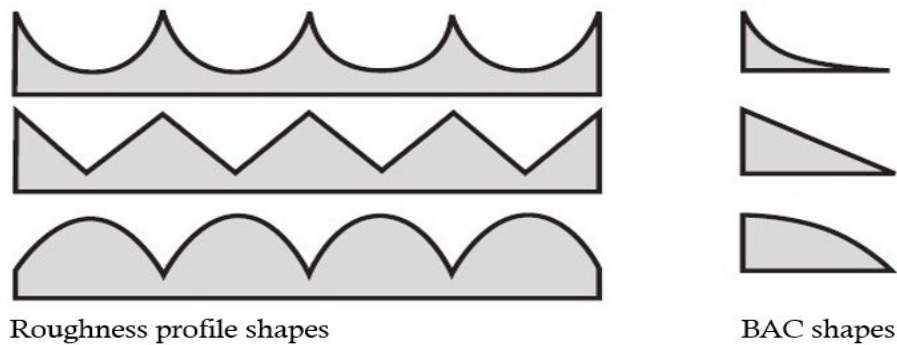
Figure 31: Different roughness profiles and their Abbott curves [12]

✓ **Rmr – relative material ratio** „*is the material ratio in a section line-height $R\delta c$ relative to the reference section line-height c0.*" [34] It corresponds to the ratio of material filled length to the evaluation length ln in section level c given in %, where section level c is defined as the distance of the evaluated section line to the selected reference line c_{ref}." A good way to graphically represent this

parameter is with the help of the height of the cutting line that is shown in the following Figure 32:
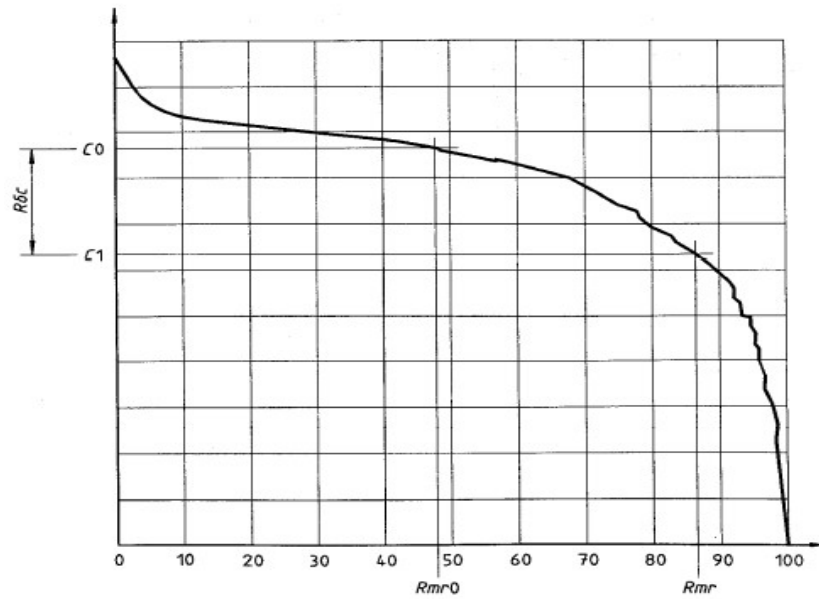
Figure 32: Height of the cutting line Rmr_Rmr0 according to DIN EN ISO 4287:2010 [33]

To calculate the parameter Rmr we need to use this Eq. 2.18 below:

$$R_{mr} = \frac{1}{l_n}(L_1 + L_2 + \dots + L_n)\, 100\ [\%] \qquad (2.18)$$

✓ **Amplitude density curve** *„is defined as the function of the amplitude density curve of the ordinate values Z(x) within the evaluation length ln."* [34] It is represented through the Figure 33:
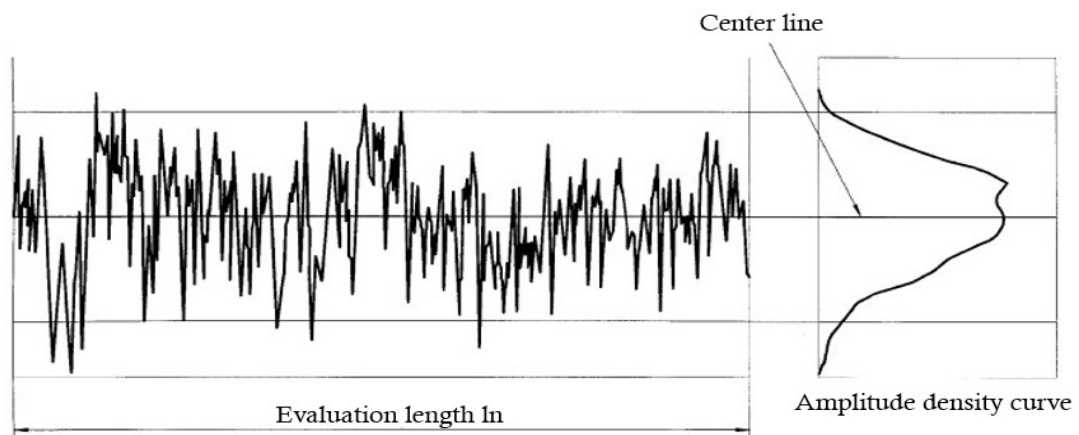
Figure 33: Amplitude density curve according to DIN EN ISO 4287:2010 [33]

➢ **DIN EN ISO 13565-2:1998** – In the framework of this second part of the DIN EN ISO 13565 standard in particular focus are the parameters of the roughness profile and their interdependence against the linear representation of the material ratio curve, now known as the Abbott-Curve in terms of definition and their assessment at all three surface levels, namely that of peaks, cores, and valleys. From this

interdependence of the roughness profile parameters with the Abbott curve, it results that the greater the depth of the roughness profile, the greater will be the material ratio of the surface. Applying this part of the above standard, we come across some definitions as well as the parameters of the material ratio curve derived from them, which we will elaborate, define, and calculate below:

- **Roughness core profile:** *„Roughness profile without prominent peaks and deep valleys”* [35] , which arises on the following parameters:

  - ✓ **„Rk – core roughness depth**: This parameter serves to measure the nominal roughness of the profile core from its highest peak to the deepest valley. [35]
  - ✓ **Mr1 – material ratio:** Represents the smallest percentage of the material ratio at the limits of the roughness core area and is determined by separating the roughness core profile from the highest peaks with an interference line, which corresponds to a line parallel to the x-axis, from the intersection of the secant/abscissa (at 0%) to the intersection with the Abbott-Curve.
  - ✓ **Mr2 – material ratio:** Greatest material ratio (in %) at the limits of the roughness core area and is determined by the separating the roughness core profile from the deepest valleys with an interference line, which corresponds to a parallel line to the x-axis from the secant/abscissa intersection (at 100%) to the intersection with the Abbott-Curve.

- **Rpk – reduced peak height:** *„Mean height of the protruding peaks above the roughness core profile”,* [36] represents the height of the triangle A1 with base length Mr1, equal in area to ridge surfaces with high peaks and small initial contact area.

- **Rvk – reduced valley depth:** *„Mean depth of the profile valleys below the core roughness profile”,* [36] which is created to determine the reduced valley depth and corresponds to a triangle A2 with the same area as the valley surfaces with the base length from Mr2 to 100%.

In the following, based on Figure 34, the relationship of the material ratio curve, also called the Abbott curve, with the profile roughness parameters derived from it is shown. Then their calculation is worked out both theoretically and visually.
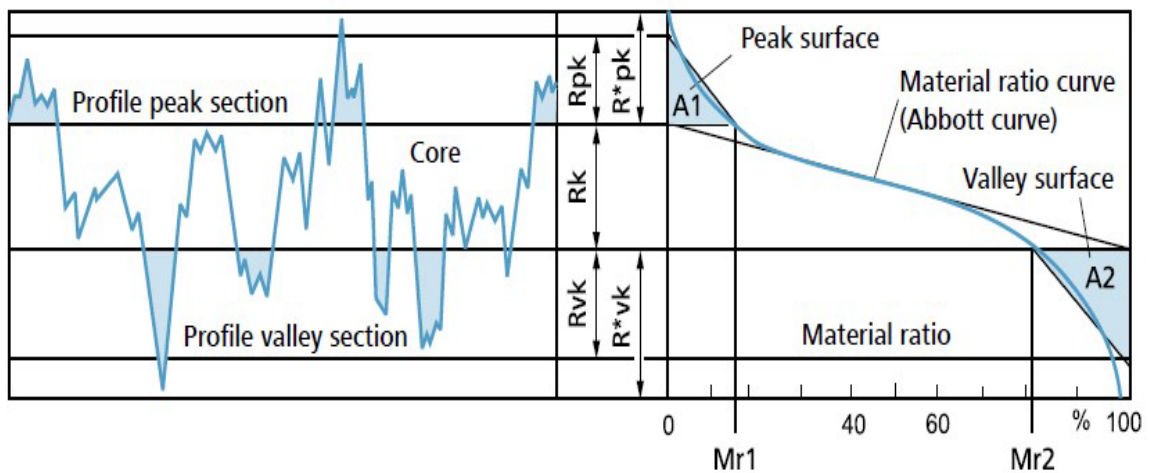
Figure 34: Derivation of the parameters Rk, Rpk, Rvk, Mr1 and Mr2 from the Abbot curve [18]

As a prerequisite for calculating the characteristic values of these roughness profile parameters from the above figure, the Abbott curve, determined from the filtered profile, must have an S-shaped course and only one inflection point. So here we can mostly talk about lapped, honed, and ground surfaces.

To be able to calculate the best compensation line, it is necessary to first define and clarify where it lies and what the "central area" of the material ratio curve includes. So, this area represents that part of the curve in which the increase of the secant is the smallest and which usually comprises at least 40% of the total length of the x-axis. This smaller rise of the secant is obtained if we move it along the material ratio curve for a value $\Delta Mr = 40\%$ from the initial value $Mr = 0\%$. This obtains the "central area" for calculating the compensation line in the middle of the material ratio curve and corresponds to the secant with the smallest increase. If during the movement of the secant along this curve we have more than one area with a slight rise, then the first area displayed should be taken as representative. Care should be taken to avoid deviations from the profile coordinates when calculating the compensation line. [36]

The Figure 35 below shows how the best fit (compensation) line is determined:
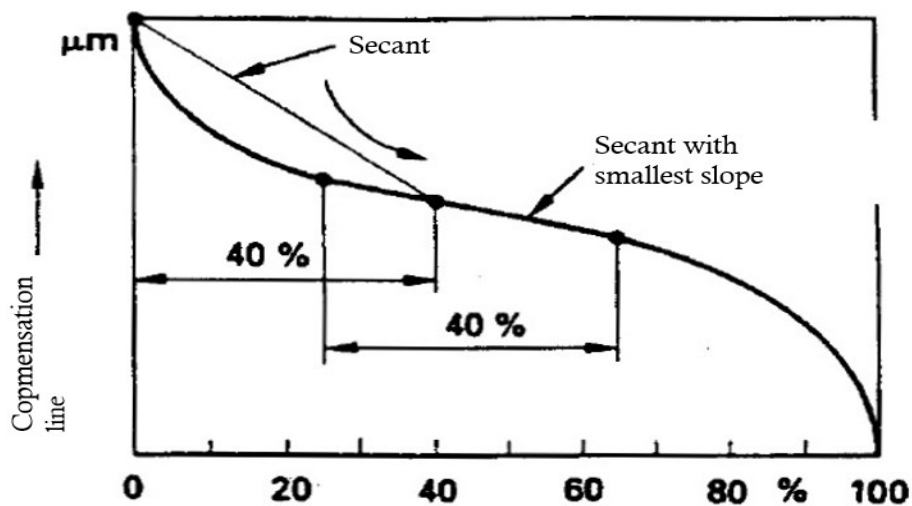
Figure 35: Compensation line according to DIN EN ISO 13565-2:1998 [36]

For the calculation of the parameters Rpk and Rvk we are based on the two right triangles A1 and A2, which have the same surface area as the "peak area" respectively the "valley area", in which case the height of the triangles correspond to the value of each of the parameters, whereas the base length Mr1 belongs to the triangle A1 or the "peak area" and the base length Mr2=100% corresponds to the triangle A2 or the "valley area". [37]

Since our main goal remains to have low Rpk values and higher Rvk values, then this affects the description of a plateau-like surface with deep grooves. So, to summarize, the Abbott curve and its parameters help to define certain surface structures. [37] In the following Figure will be represent the conversion of the "peak area" and the "valley area" into equal area right triangles:
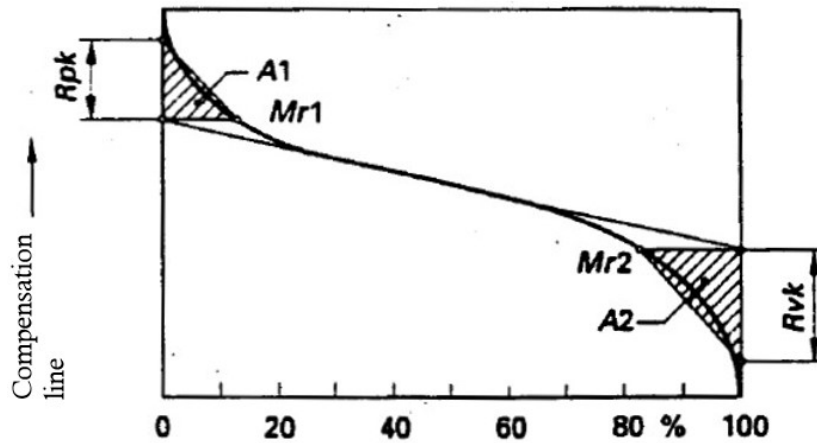
Figure 36: Conversion of the "peak area" and the "valley area" into equal area right triangles [37]

➢ **DIN EN ISO 13565-3:1998** – The main essence of the treatment of this normative is the characterization of the height of surfaces with stratified functional properties using the material probability curve. More specifically, within this part of the normative DIN EN ISO 13565, the focus is the numerical evaluation of surfaces with superimposed vertical components, respectively a relatively coarse "valley" texture and a finer "plateau" texture, which is realized by determining the parameters Rpq, Rvq, and Rmq, which then describe these two constituent components of the surface, and which are not available for surfaces that do not meet this prerequisite. To determine these parameters, it is necessary to generate the probability density curve, to determine its linear regions as well as to perform linear regression in those regions, which means the Gaussian representation of the curve of the material ratio curve, which is necessary for the evaluation procedure for obtaining them. [38] To enable the implementation of this part of the ISO 13565 norm as well as for the determination of the above parameters and the probability density curve of the material, in the following we will have to go back to the supplementary norms such as ISO 3274, ISO 4287, ISO 13565 -2. [39]

- **Material Probability Density Curve** – Based on the Gaussian probability, this curve shows the ratio of the length of the material to the length of the profile within the material ratio curve against the linear divisions of the horizons into multiples of the standard deviation. [39]
- *„Rpq parameter – Corresponds to the rise (increase) of the best fit (compensation) line through the plateau region.”* [39]
- *„Rvq parameter – Corresponds to the rise (increase) of the best fit (compensation) line through the valley section.”* [40]
- *„Rmq parameter – Is defined as the relative Material ratio at the intersection of the plateau and valley.”* [40]

The

Figure 37 below shows the relationship between the material probability density curve and the respective sections of the determination of the above-mentioned parameters in the context of the roughness profile:
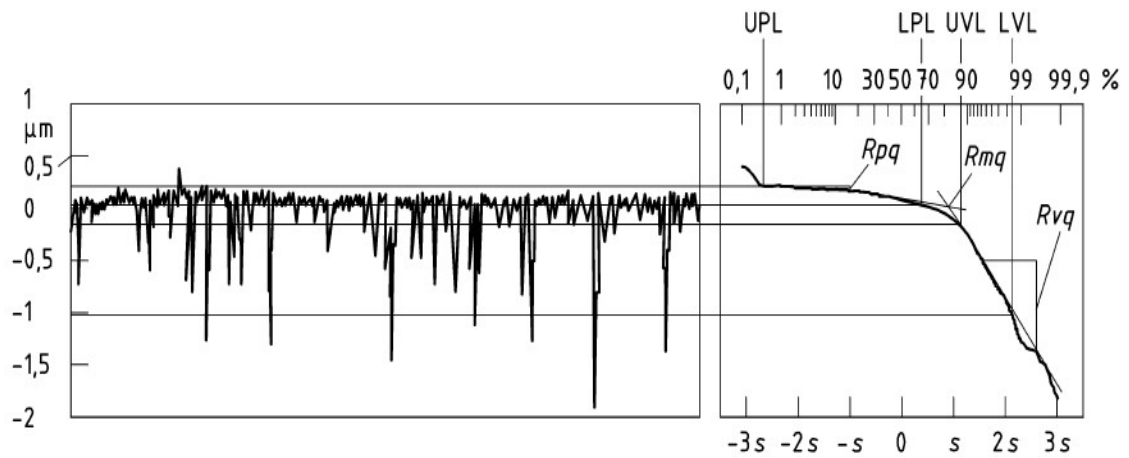
Figure 37: Roughness profile & Material probability density curve for determination of Rpq_Rmq_Rvq Parameters [40]

From the Figure 37 above, it can be seen, that we need to rely on the primary profile to define the parameters as mentioned above. In this case, the roughness profile must be calculated according to the first part of the ISO 13565 standard, regardless of the visible covering it has since this does not affect its parameters Rpq, Pvq, and Rmq, in the determination of which the lower parts of the scratches, which are deeper and which due to the significant variation depending on the measurement place on the surface are entirely neglected. [40]

Within the measurement process in relation to the roughness profile of a surface to determine the relevant parameters, it is required to meet specific criteria, which enable full compliance of the profile with the surface through an adequate measurement process, which serves, that the material probability density curve be calculated correctly. All this then enables us, that the values of the parameters Rpq, Rvq and Rmq are reliable.

In the following, we are mentioning some of the criteria that must be met concerning the above process:

- Measuring device with optical surface Rq < 30% of the nom. value of Rpq,
- Very high vertical resolution of Material probability density curve $\geq$ 40 classes,
- Very high density of digital data $\geq$ 100 profile coordinates,
- Ratio Rvq:Rpq $\geq$ 5. [40]

2.3.4.2 Surface Texture parameters of Roughness

The main task in determining these surface texture parameters, which are based on profile parameters, whether of primary, roughness, or even waviness, is to characterize the surface properties as best as possible in the context of an area analysis. [41] Therefore, the parameters derived from this surface analysis, which are analogous to the above-mentioned profile parameters, with the help of MeX software, which we will later elaborate in detail, will be categorized, and described as follows: [42]

- ➢ **Main Surface Texture Parameters of Roughness:**
    - ✓ **Sa: Average height of selected area** – It can be understood as an extension parameter of the line roughness parameter Ra, but at the same time as very simple for describing the surface roughness although not accurately and functionally. However, through the value of this parameter can also be detected deviations in the surface structure. [43]
    - ✓ **Sq: Root-mean-square height of selected area** – It has the same meanings and will be used for the same reason as the Sa parameter and mathematically can be calculated through the Formula 2.19 below:

$$Sq = \sqrt{\frac{1}{A} \int \int_A Z^2(x,y) dx dy} \qquad (2.19)$$

    - ✓ **Sp: Maximum peak height of selected area** (max_z-mean_line) – It serves to describe the relation between the height of the highest peak and the reference level of the surface area, selected during the measurement and therefore depends on a single measure point. [43]
    - ✓ **Sv: Maximun valley depth of selected area** (mean_line-min_z) – Since it serves similar measurements as the parameter Sp, but with an inverse function, this value is calculated similarly to the value Sp and corresponds to the strongest depth of the valley.
    - ✓ **Sz: Maximum height of selected area** (max_z-min_z) – This height parameter is obtained from the sum of the parameters Sp and Pv within the treated area and is used to measure surfaces with grooves and valleys, despite being determined only by a single value. The usefulness of the value of this parameter is emphasized when in the selected area of the surface are expected peaks and depths, even for the known fact that through it, the scratches are filtered. [44]
    - ✓ **S10z: Maximum height of 10 peaks/valleys of selected area** – It is an essential parameter for the structure of the surface, which is obtained from the average value of the ten most considerable heights of the peaks and represents a more robust version of the Sz value. [42]
    - ✓ **Ssk: Skewness of the selected area** – This height parameter is used to define the degree of roughness slope and corresponds to the average of all values from all points of a 3D surface, above or below the zero level, which usually are less than zero, zero, or greater than zero. [44] It will be determined with help of the following Eq. 2.20:

$$\text{Ssk} = \frac{1}{Sq^3}\left[\frac{1}{A}\int\int_A Z^3(x,y)dxdy\right] \qquad (2.20)$$

✓ **Sku: Kurtosis of selected area** – It serves to understand the irregularities in the uniformity of the profile through the description of the accumulation of heights and through a measure of the sharpness of the roughness, which means their expansion and distribution. In this case when most of them are in a small range, then its value turns out to be small, so Sku<3 and when most of them are in big range, then its value turns out to be big, so Sku>3. This paramter will be calculated through the following formula 2.21:

$$\text{Sku} = \frac{1}{Sq^4}\left[\frac{1}{A}\int\int_A Z^4(x,y)dxdy\right] \qquad (2.21)$$

✓ **Sdq: Root mean square gradient** – It is a hybrid parameter that affects the composition of the surface and describes its average slope depending on its value. That means if parts of the surface are flat, we will have low values of the parameter Sdq. Still, if the parts of the surface are sloping, respectively, if the surface slope arrives 45 degrees, then the value of the Sdq parameter is high, respectively is 1.

✓ **Sdr: Developed interfacial area ratio** – This hybrid parameter expresses in% the remainder of the ratio developed between the excess of the real surface versus the projected interface. [42] The Sdr value varies and is dependent on the slope of the surfaces, so the flatter the surface is, the more the Sdr value tends to zero, the steeper a surface is, the greater the Sdr value is.

➤ **Bearing (SMR) Parameters:** For a better understanding and better description of the bearing parameters, we must base on the bearing ratio curve, which is given during the measurements with the MeX software and is shown in the following Figure 38.
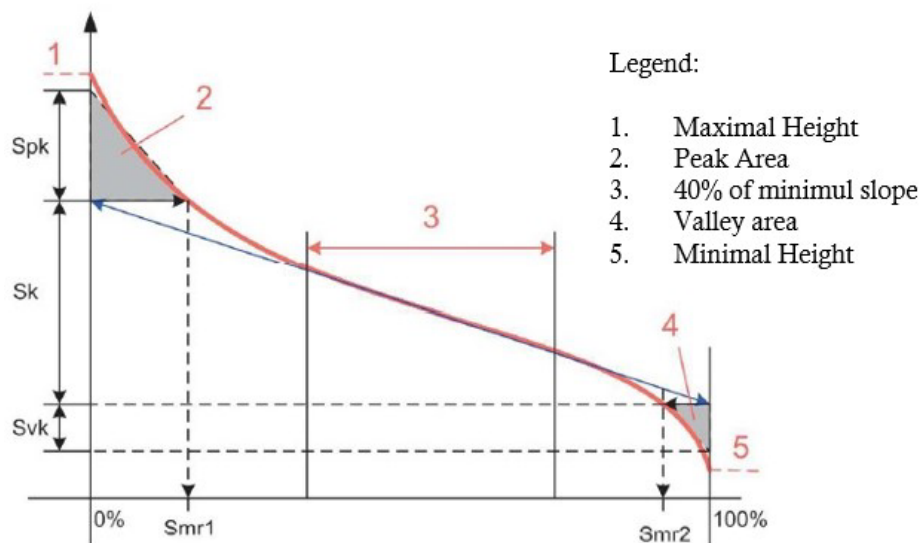
Figure 38: Bearing Area/Firestone-Abbott Curve of Roughness [45]

✓ **Sk: Core roughness depth** – This parameter corresponds to the analogue value of the Rk roughness profile parameter and represents the difference between the peak area and the valley area along the bearing ratio curve from 0% to 100%.

✓ **Spk: Reduced peak height** – It is a Parameter derived from the grey bearing area curve representing a stable value of the peak height obtained from the average height peaks with much more reliability in a description of the roughness of the surface.

✓ **Svk: Reduced valley height** – This parameter like as Spk parameter derived from the bearing ratio curve representing the gray area (4) of the surface roughness valleys up to the minimal height.

✓ **Srm1: Peak material component** – From the Figure 38 given above, we understand that the functional parameter Smr1 represented in % value is obtained from the intersection of the maximum height of the core surface Sk with the bearing ratio curve, thus determining the areal component of the material located above this intersection.

✓ **Srm2: Peak material component** – The functional parameter Smr2 represented in % value is obtained from the intersection of the minimum height of the core surface Sk with the bearing ratio curve, thus determining the areal component of the material located below this intersection.

A visual example of defining the above parameters, we are giving through the following Figure 39:
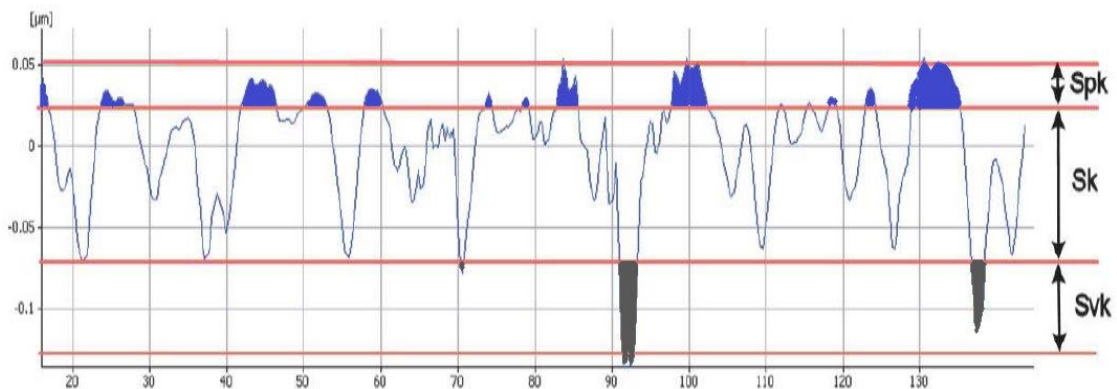
Figure 39: Bearing Parameters of surface roughness [46]

➢ **Volume Parameters:** All four below listed and visually represented volume parameters can be determined and calculated depending on the constituent components of the material within certain areas of the roughness surface, respectively as the volume of the reduced peak material, as the volume of the core material, as the volume of the core void and as the void volume of the reduced valley material. Reference values for calculating volumetric divisions of surfaces are set within the margin of 10-80% of the bearing ratio curve.
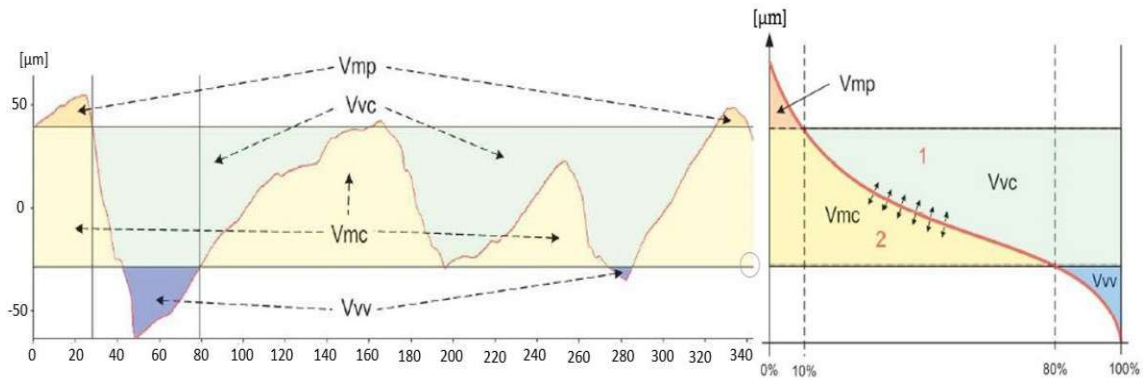
Figure 40: Volume parameters of surface roughness [46] & [47]

- ✓ **Vmp: Peak material volume of the topographic surface** – This parameter quantifies the volume of material created at the top peak over the surface core area.
- ✓ **Vmc: Core material volume of the topographic surface** – This parameter quantifies the volume of the material created within the core area of the surface roughness.
- ✓ **Vvc: Core void volume of the surface** – This parameter quantifies the void volume created within the core area of the surface roughness but outside the bearing ratio curve.
- ✓ **Vvv: Valley void volume of the surface** – This parameter quantifies the void volume created within the valley depth.

2.3.5 Rules and procedures for the assessment of surface texture according to the profile method

Intending to elaborate as completely as possible the surface texture, in the above part, within the profile method, we have treated in general the parameters of the primary profile and those of the waviness, while on the other hand, the parameters of roughness in addition to the profile method, we have treated them also for the three-dimensional method, through the surface parameters. We have elaborated all roughness parameters in terms of theoretical definition, or through mathematical expressions for their calculation, and up to the graphical representations from which proven their derivation. However, in order to better understand these parameters and their role concerning the surface texture, we must first know precisely the rules and procedures for its evaluation, which are best sanctioned in the international standard DIN EN ISO 4288:1997, according to which *"measurements on the examined surface, after visual inspection should be performed only in those areas where maximum or extreme values are to be expected"* [6] and that the realization of the measurement procedure must pass through these eight steps:

(1) Workpiece after cleaning stably positioning.

(2) The correct probe arm must be attached to the calibrated measuring system.

(3) The workpiece must be so set up, in order that the surface is perpendicular to the axis of the wand and the groove direction of the surface structure is perpendicular to the direction of measurement.

(4) In case of non-specifying of the profile filter λc and the evaluation length ln, then for the measurement of roughness parameters settings are to be selected according to Table 5.

(5) For roughness, we must set the required profile filters λc and λs

(6) The required surface parameters must be selected

(7) Measure

(8) The comparison between measurement results and the specified numerical values permitted in the technical documentation. [12]

So, for the assessment of surface texture according to the profile method, the international standard DIN EN ISO 4288:1997 as its final goal has the definition of the rules for the comparison of the results set up from the measurement with tolerance limits for surface parameters. This entire process of assessment is thrown up through these four major steps, treated in the following units:

2.3.5.1 Determination of parameters

During the determination of the roughness parameters, they are divided into two groups, in the grouping of parameters, the values of which are defined within the sampling length lr from the data obtained from its measurement, in which case to determine the average value of the value of these parameters, they must be calculated as an arithmetic means of each individual value measured in it and in the other grouping, where the parameters are defined in terms of the evaluation length ln, this length numerically standardized and equal to five sampling lengths lr and where their defined values are derived from the data obtained from the measurement.

Extracting measured data and calculating the value of the parameters becomes almost impossible without using two significant curves, such as the material ratio curve and the amplitude density curve, which are based on the evaluation length ln.

Finally, we cannot leave without mentioning the measuring distance, which specifies the evaluation length ln for the parameters of roughness R, those of profile P, and other parameters.

2.3.5.2 Evaluation of measurement results

As we explained earlier, the evaluation process of measurement results has in its core of the treatment the determination of the rules to be able to compare the measured values with the tolerance limits. According to the international standard EN ISO 4288:1997, this process should accomplish five significant rules, and we will discuss them in the following:

  i. **Maximum value rule** – The validity of this rule is said to be accomplished, then and only then, when within the entire surface which will be tested the requirement has been completed, that of all the measured values of the parameter, none of them exceeds the highest or the maximum specified value, in accordance with the international standard ISO 1302:1992, 6.2.2.

Therefore, such a parameter is denoted by the abbreviation "max" (e.g., $Rz1_{max}$)

ii. **16 % rule** – In the framework of this rule and according to the standard ISO 1302:1992, 6.2.3, if the maximum value of the parameter is not specified and with the intention that a surface to be considered acceptable or "good," then it must meet two requirements basic regarding the definition of measured parameter values. The first request is also known as the request of the upper limit of the parameter, in which case of all its measured values, less than 16% of them exceed the specified value, while the second request is that of the lower limit of the surface parameters, in which case of all the measured values of the roughness parameter, less than 16% of them are below the specified value. The abbreviation "max" must be removed when marking the parameters in both cases. To express the interdependence between the average value of the roughness measurements and the upper limit specified of a parameter, we use the Figure 41 presented below:
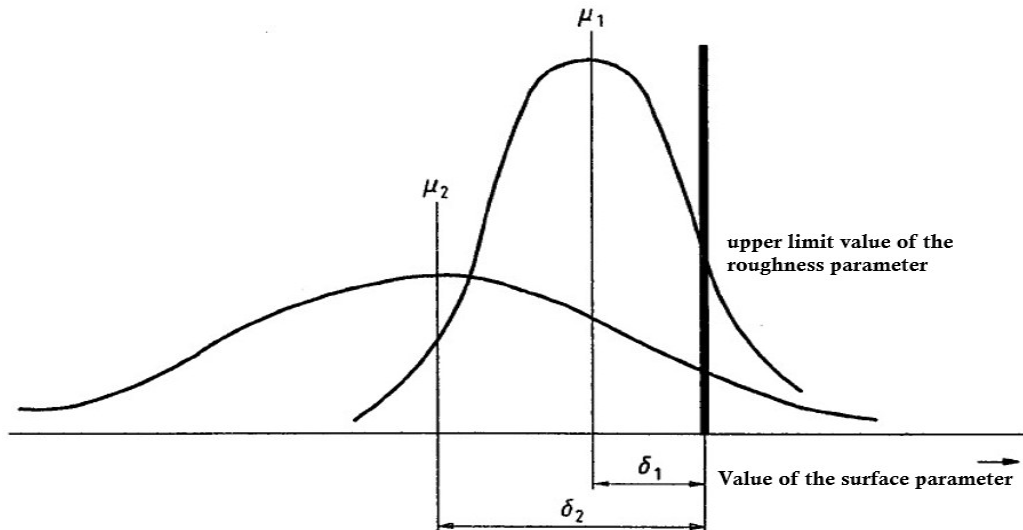
Figure 41: The 16% rule of the roughness measured values of the surface according to DIN EN ISO 4288 [48]

iii. **Special rule VDA** – Based on the assumption that the distribution of parameters should be considered in determining the limit values, it neglects the above 16% rule while applying the maximum value rule, despite not specifying the index "max" in the definition. Also, in the framework of implementing this rule, the use of the λs filter is prohibited. [18]

iv. **Areas to be inspected on a geometry element** – The reason for inspecting an element of geometry has to do with the uniformity or with the areal variability of the surface texture for the tested workpiece, an inspection performed visually on that surface. In this way, we compare the values of the roughness parameters distributed throughout the surface with the specified requirements for the first case. In contrast, for the second case, we make a separate comparison of the values of the roughness parameters determined for each area separately with the specified requirements. We should also note that there is a correlation between the requirements defined by the upper limit of the surface texture parameters and the areas with the highest roughness. [49]

v. **Measurement uncertainty** – First of all, it should be noted that the specified limit values serve to make it possible to compare the measured values of the parameters with the values specified in the ISO 14253-1 standard to verify whether they correspond to each other. Suppose despite the inhomogeneity of the surface, we have an approximation of the results from the values measured with these limit values, whether upper or lower. In that case, it must be determined how much this measurement uncertainty is after its inclusion in 16 % tolerance of overrun allowance. [48]

2.3.5.3 Assessment of the parameters

The entire process for the assessment of the parameters of the surface texture according to the international standard DIN EN ISO 4288:1997 is separated into the framework of two main parts, which are:

a) **General criterions** – The surface texture test corresponds to the fulfillment of special requirements, therefore in the absence of complete suitability by the surface parameters for the description of its imperfection, some of these imperfections such as scratches or pores should be left out of the testing process. To create the reliability of meeting the testing requirements of the workpiece surface, as well as of the accuracy of the average value of measured values, it is necessary that the number of measurements performed on this surface, respectively the number of sampling lengths lr within the evaluation length ln, as like as the number of evaluation lengths ln itself, within which each measured value of the parameter must be determined, to be as higher as possible. [48] & [50]

b) **Roughness parameters** – The number of sampling lengths lr within the evaluation length ln, for the roughness parameters R according to the international standard ISO 4287:2010 must be at least five and that its upper and lower limit values must be recalculated and referred to that length ln. Knowing on the one hand that many measurements across the surface has a direct impact on the reliability of the surface testing process, but on the other hand, knowing that this also affects the time and costs of testing, then it is necessary that between these three preconditions, we should find an acceptable compromise. [50]

2.3.5.4 Rules and procedures for testing using stylus instruments

Using stylus instruments for testing of the surface, we distinguish different rules and procedures, which the international standard EN ISO 4288:1997 has divided into two main categories as follows:

➢ **Basic rules for the determination of the cut-off wavelength for the measurement of roughness profile parameters** – The selection of the cut-off wavelength λc seems to be a complex procedure, and its determination depends on its or the roughness specification in the technical product specification. So, when it is specificized, it is equal to sampling length lr; if not, it needs another selecting procedure. [50]

➢ **Measurement of roughness profile parameters** – During the process of measuring the roughness profile parameters, the direction of the scan must correspond to the direction of the grooves; however, in the opposite case, it should be chosen according to the desire of the examiner of the respective surface. However, suppose we want the measurement results to be independent of each other. In that case, they must not only be evenly distributed in that part of the surface but also that through a visual inspection, they must be obtained at that point on the surface, which is expected to have critical measurement values of the roughness parameters, so that we can then decide whether we are dealing with a periodic or aperiodic roughness profile. [50] As can be seen from Table 5 and Figure 16, which correspond to the values of the roughness parameters, the procedure of this measurement is divided into two sub-procedures, namely:

✓ **Procedure for aperiodic roughness profiles** – It is used for surfaces with an aperiodic roughness profile, and it develops itself through these following steps:

- The estimation of the unknown value of the roughness parameters Ra, Rz, $Rz1_{max}$ and Rsm by using different means,
- The selection of the sampling length lr from the estimated values of the roughness parameters in the Table 5,
- Determination of the representative measurement result of Ra, Rz, $Rz1_{max}$ or Rsm parameters using a roughness measuring instrument,
- Comparison of the measured values of Ra, Rz, $Rz1_{max}$ or Rsm parameters with the range values of Ra, Rz, $Rz1_{max}$ or Rsm parameters form the Table 5, according to the determined sampling length lr,
- Determination of a representative value of Ra, Rz, $Rz1_{max}$ or Rsm parameters for shorter sampling length lr not determined before,
- This representative values of Ra, Rz, $Rz1_{max}$ or Rsm parameters for shorter sampling length lr are correct, if they are in the combination of the values form the Table 5,
- The performance of a representative measurement of parameters by using the cut-off wavelength. [26] & [50]

✓ **Procedure for periodic roughness profiles** – It is used for surfaces with a periodic roughness profile. It elaborates only the Rsm value parameter, and it develops itself through these following steps:

- Graphical estimation of the value of the Rsm parameter for the surface with unknown roughness,
- Determination of the recommended cut-off wavelength for the estimated value of the RSm parameter corresponding to the Table 5,
- Measuring the RSm value in accordance with the determined sampling length lr from above,
- The use of the RSm value in complete connection with the value of the cut-off wavelength,
- The performance of a representative measurement of the parameter Rsm by using the cut-off wavelength (sampling length lr) determined earlier. [51]

2.4 Roughness measuring methods for the characterization of the surfaces

For the characterization of the surfaces through the analysis and evaluation of the roughness parameters, numerous practical measuring methods and instruments with different accuracy and measurement efforts exist. These measuring methods distinguish each other based on different physical principles, characteristics, and properties, treated in the framework of the direct quantitative profile measurement methods and the direct quantitative topographic measurement methods. However, despite this large number of measuring methods, we have focused only on some of them, which we have considered as the most important for the elaboration of the surface roughness and as the most suitable with this diploma thesis and which are listed as follows:

2.4.1 Sand patch method (volumetric)

It is a simple, fast, and practical volumetric method developed and presented for the first time by the author N. Kaufmann, which determines the depth of roughness Rt within the texture of concrete surfaces by measuring the amount of volume, whether through sand or glass beads. As we have illustrated in the following figures, the process of applying this method requires the appropriate equipment to make the necessary measurements, such as:
- ✓ a dry, clean concrete surface and with surface depressions,
- ✓ fine material (dry quartz sand) with a grain size of 0.1 to 0.3 mm and an amount on volume of 25-50 cm^3. In the case of pavement surfaces by replacement of dry sand with glass beads, we should consider the standard DIN ISO 10844, which determines that 90 wt.% of the beads must be retained between the 0.25 mm and 0.18 mm hole width of a sieve,
- ✓ a container with volumetric scaling for measuring fine filling material,
- ✓ a wooden distribution disk in round shape and with a central grip pin on the upper side, which has a diameter Ø = 5 cm and a thickness of t = 1 cm.
- ✓ a scale for measuring the diameter of the sand distributed on the concrete surface
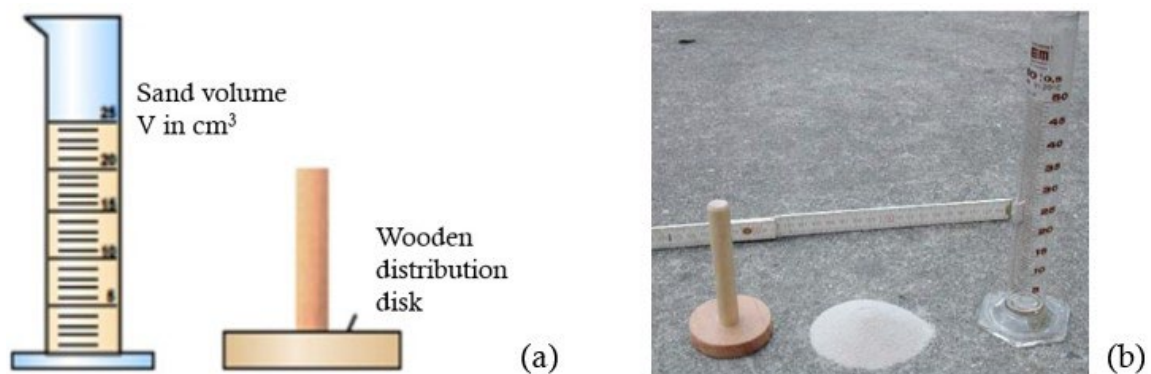
Figure 42: Sand area method equipment [52]

Since the essence of this experimental method is to determine the depth of roughness Rt through the volume of cavities filled with quartz sand on the concrete surface, then as we can understand from Figure 42 and Figure 43, the experiment is performed according to the performance in the following steps:

(1) The concrete surface must first be cleaned and dried,
(2) Fill the container with dry quartz sand, then pour conically on the concrete surface,
(3) Distribute the poured sand without pressure with the help of a wooden distribution disk so that through its rotation, we obtain a circular surface with a specific diameter
(4) Measure the diameter d of this circular surface of the sand, where the accuracy should be up to 1 mm,
(5) In total, we must perform 3-4 randomly distributed measuring points, from which we then derive the average diameter of the spread sand.
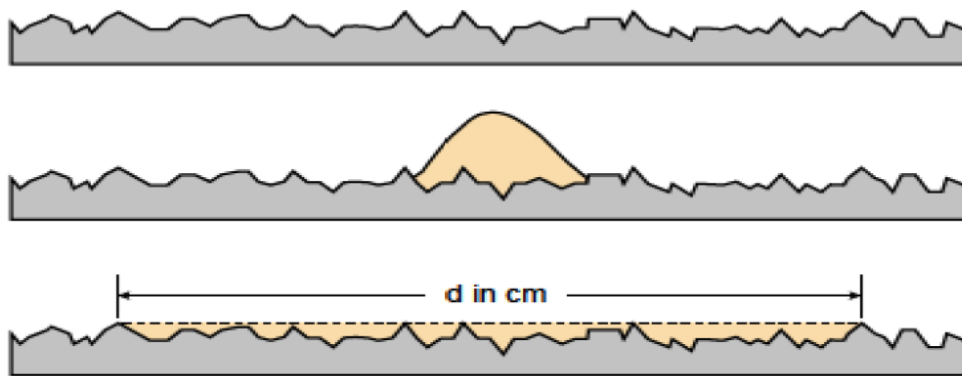
Figure 43: Sand area method experiment Steps 1 to 3 [52]
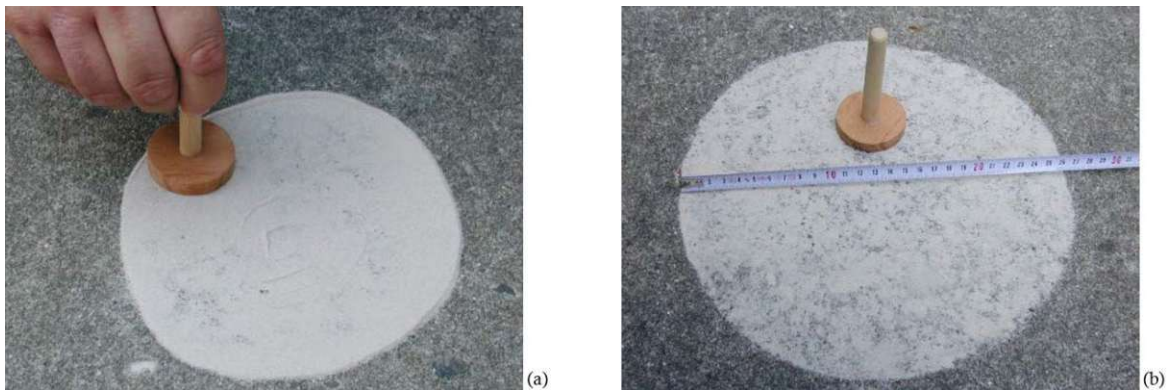
Figure 44: Sand area method (volumetric method) - (a) Step (3) (b) step (4) [53]

„The roughness depth Rt is defined as the height of the imaginary cylindrical body with the circular diameter d and the sand volume V." [54] It derives from the following figure and will be calculated with help of the mathematical expression 2.23 below:
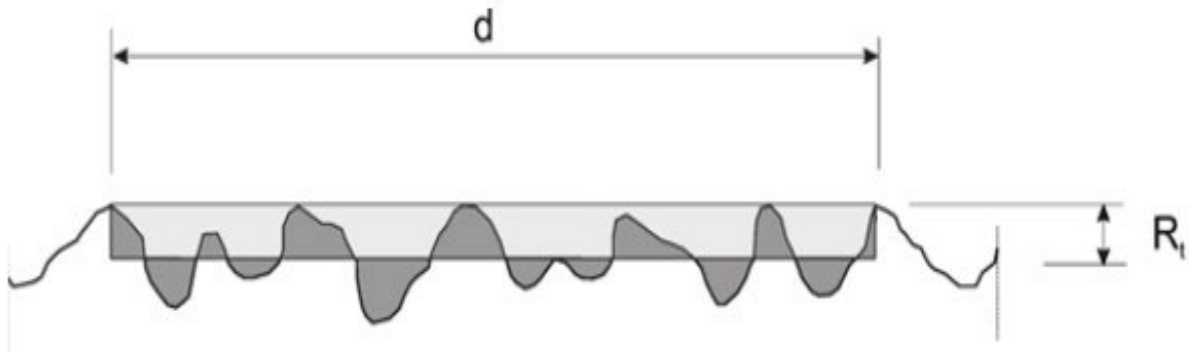
Figure 45: Definition of the roughness depth Rt in the sand surface method according to N. KAUFMANN [53]

$$R_t = \frac{4 \cdot V}{\pi \cdot d^2}$$ (2.23)

whereby: Rt – height of the imaginary cylindrical body in mm
  d – circular diameter in cm
  V – sand volume in cm^3

With the help of the Table 7 presented below, when the depth of roughness Rt reaches the maximum value of 1.5 mm, the minimum value of the diameter of the sand distribution d must correspond to its volume quantity V.

Table 7: Minimum diameter (d_min) of the sand spot as a function of the sand volume V for a maximum roughness depth of 1.5 mm [55]

Volume in cm^3	25	30	35	40	45	50
Diameter in cm	15	16	17	18	20	21

Despite the simplicity and the extraordinary practical advantages in the realization of this method, it certainly has specific limitations and disadvantages, which we will try to mention briefly:

- it is successfully carried out only for the horizontal surfaces,
- it can record only the macrotexture depth,
- it cannot capture texture details below the grain size of the sand,
- it needs more than one attempt to obtain the diameter of the distributed sand.

2.4.2 Profile or Stylus method

This mechanical method for determining surface roughness or surface profiles is realized by using a hard stylus made of diamond or hard metal and a slightly flexible measuring tongue, which pulls the hard stylus over the surface to be measured. Through this drag of the measuring tongue, the profile of the measured surface and its deformation can be precisely recorded in two different ways: either inductively or through a change in

45

resistance and in very high resolution, in which case, along a line a profile surface is scanned and created and for its evaluation, we will use the profile parameters determined and mentioned in the earlier subchapters.

Within the scope of this measuring method, three different measuring systems are distinguished, which are used for various purposes. The common skid probe systems, shown in Figure 46 (a) and (b), are used to determine the filtered roughness parameters Ra and Rz by on-site and laboratory measurements. The movements of the stylus are recorded according to the skids. In contrast, the reference surface probe system, shown in Figure 46 (c), is used only to determine the unfiltered measured values or in case of caused defects.
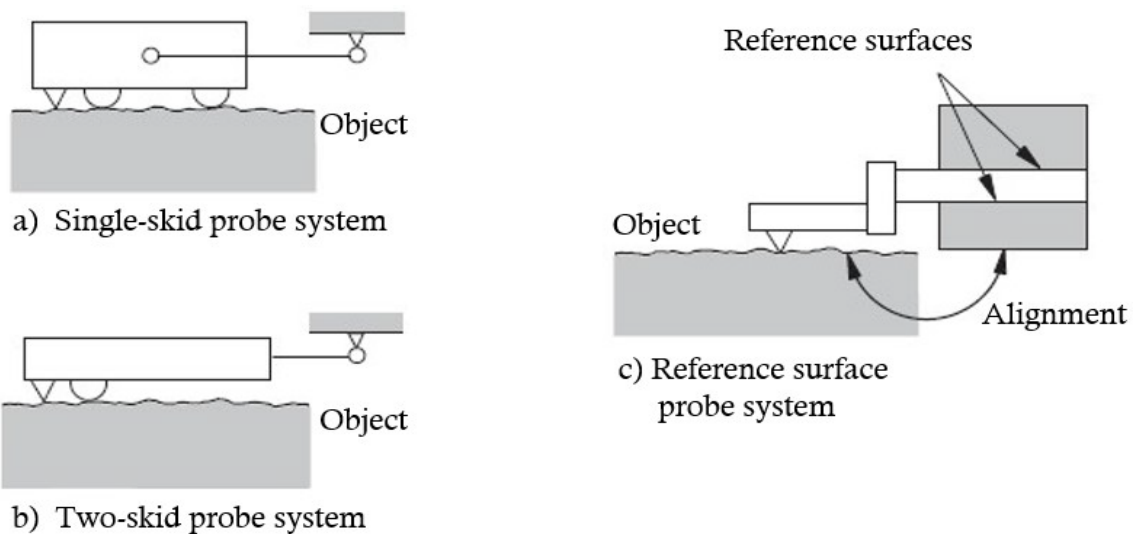
Figure 46: Representation of the different touch probes [56]

One of the authors who has described the use of this stylus method in the function of the texture analysis of concrete is Deelmann. According to him, this method should allow the difference between the individual concrete constituents and etched surfaces and therefore it is considered a very accurate method. [57]

The high scanning accuracy of this measuring system comes because of the probe tip dimensions and the constant speed of needle movement over the examined relief. This process we have shown in the Figure 47 below:
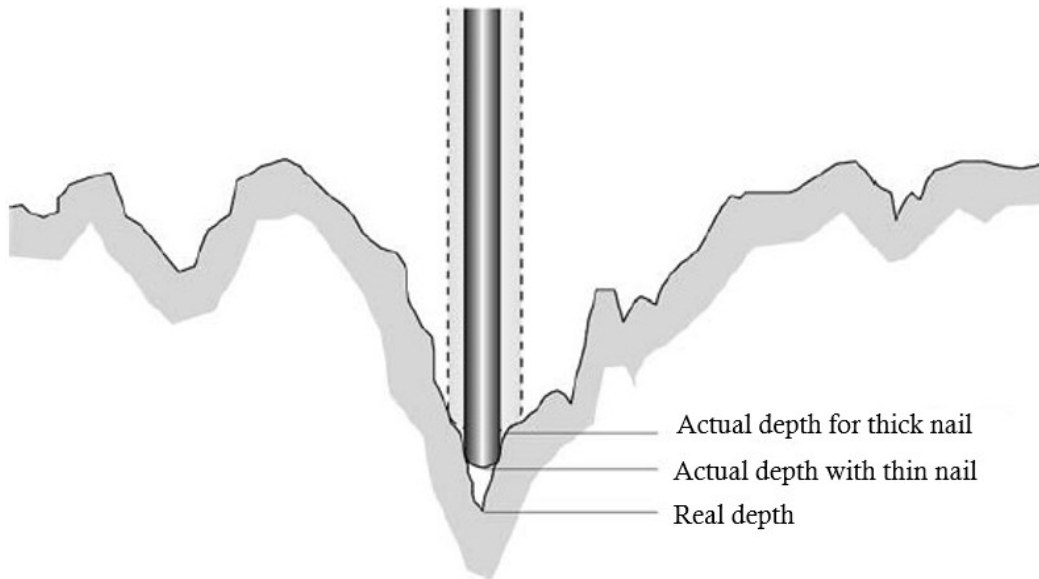
Figure 47: Scanning accuracy as a function of the radius of the probe tip (needle) [58]

So, as we can see from the Figure 47 above, depending on the thickness of the needle, the measurements can be continuous and intermittent. Continuous measurements are performed with a thicker and stiffer needle, while very thin needles, due to the possibility of their breaking, perform only intermittent measurements, which negatively affects the accurate reproduction of the current profile. A more concrete elaboration is made possible through Figure 48:
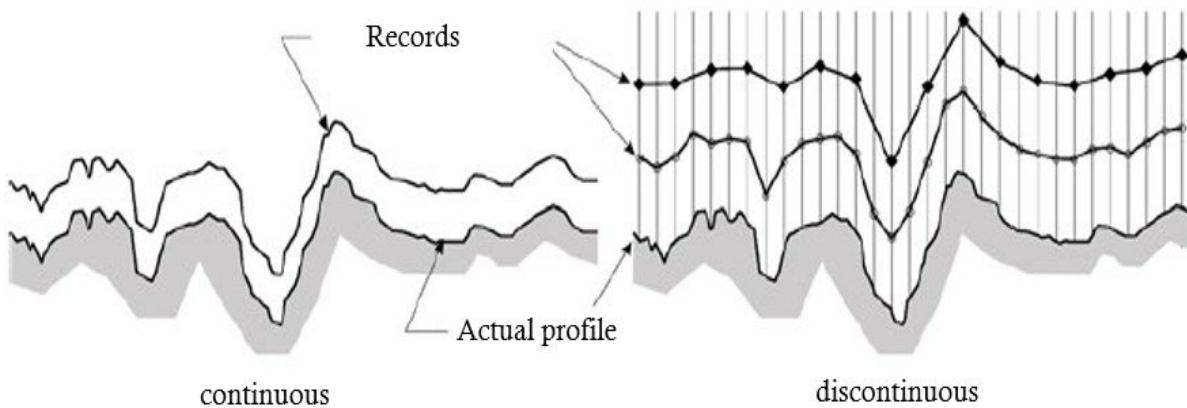
Figure 48: Differences between continuously and discontinuously determined roughness profiles [57]

Despite the many advantages of this method of measuring the surface profile, it undoubtedly shows some shortcomings, among which we can mention:

➢ Unsuitability of this process for very rough surfaces,
➢ No detection of very deep cracks,
➢ Evidence of the recorded signal from the current topography due to exceeding the maximum value of vertical deflections,
➢ Very complex recording on large surface roughness etc.

47

2.4.3 Stereoscopic method

The detailed theoretical elaboration and practical implementation of this measuring method for the characterization of the surfaces are given in Chapter 3. Therefore, any explanation here could be considered a non-scientific useless repetition below.

3. Theoretical Basics of the stereoscopic method and its application

3.1 History, definition, and application of photogrammetry

„The German civil engineer Albrecht Meydenbauer is known as the first man to use the term Photogrammetry. Since the middle of the 19th century, he has promoted the further development of this method in Germany ". [59]

The photogrammetric method, which we have used for the characterization of surfaces through measurements of roughness, waviness, volume, etc., has to do with a precise record and measurement analysis of the 3-Dimensional shape of an object in the accuracy of millimeters, respectfully of micrometers, where it is initially necessary to capture images of the specific object in different proportions and sizes, with special digital measuring cameras from at least 2 to 6 different eucentric tilting angles.

A more specific definition of photogrammetry states: *" Photogrammetry is the science and art of reconstructing the position and shape of objects from images, especially photographs. The images are usually recorded photoelectrically (digital photography). "* [60]

So, Photogrammetry enables us to build a 3-Dimensional object without having contact with it, but only from the reflection recorded during the photography process, making it a distance measurement method.

"The results of a photogrammetric evaluation can be:

- *Measurements, namely digital point determination,*
- *Drawings (analog), namely maps and plans in plan,*
- *Geometric models (digital), which are used in information systems,*
- *Images (digital or analog)."* [60]

Photogrammetric research focuses on the acquisition of surfaces themselves, their evaluation, and modeling, with particular emphasis on accuracy, efficient design, and automation of the process. [60] Through this we can conclude that Photogrammetry is currently the only method through which we can generate not only the geometry and texture, but also the volume of the object.

To know and explain the photogrammetric method as wholly as possible, it is essential to emphasize that this method is divided into three main stages due to the different procedures of acquisition the objects and automatic or manual evaluation of the results, which are:

- ➢ Stage 1: Analog Photogrammetry
- ➢ Stage 2: Analytical Photogrammetry and
- ➢ Stage 3: Digital Photogrammetry

In analog photogrammetry, the acquisition begins with photochemical images and the evaluation continues with optical-mechanical devices. Unlike the first stage, analytical photogrammetry is also based on photochemical images, but the entire evaluation process

is computerized. In the last stage, which is also called digital photogrammetry, we can say that it is completely electronic, because not only the photo taking is digital, where *"incident light in the image plane of the camera is electronically detected and digitally stored"*, but also the evaluation process is completely computerized. [61]

The application of photogrammetry in civil engineering using its techniques is large, diverse and of particular importance, because in addition to our diploma thesis topic, it is also applied to the detection of cracks, distortion measurements and structural deviations. [62]

Also worth mentioning is close-range photogrammetry, which involves recording objects with cameras at close distances and is used for the following tasks, such as:

- ✓ Precision surveying of buildings and other engineering objects,
- ✓ Construction monitoring measurements and construction damage documentation
- ✓ Deformation measurements
- ✓ Measurement of engineering models [63]

Although within the photogrammetric method a variety of acquisition and evaluation methods are included, such as microscopic methods, laser scanning or photographic documentation, we have placed our focus on the stereoscopic method.

The photogrammetric method, like any other method in practice, also has its advantages and disadvantages, which we list below:

- Advantages of photogrammetry:

  - Edges and corners are precisely detected
  - Amounts of data are relatively small,
  - Color of an object is exactly detected,
  - Recording of objects in short times,
  - The suitability of the photos whether for archiving or for use at any time.

- Disadvantages of photogrammetry:

  - At least two images with a visible point are required to obtain the 3D coordinates,
  - Orientation of the recordings usually takes place only during data processing,
  - external lighting conditions and texture of the object as decisive influencing factors. [64]

3.2 Stereoscopic method and the capture of stereo images

The essence of the stereoscopic method lies in the non-physical reconstruction of three-dimensional objects together with their component information from the acquisition of two or more digital images. To achieve this goal, and especially to obtain information about the depth of the three-dimensional surface model, it is necessary to take the image from at least two different angles of the camera with respect to the studied object, and in this way obtain at least two images with different projections.

The implementation of this method requires certain conditions and appropriate equipment for the qualitative and precise acquisition of digital images of the objects under study. We will discuss these two necessary factors in more detail below.

3.3 The principle of capturing stereoscopic images

In practice, there are several alternatives for creating a stereoscopic image pair, either by eucentric tilting of the specimen while the microscope remains in a stationary position, or by two other alternatives with a fixed base, where one measurement method, also known as standard configuration, uses two cameras and consists of receiving images from parallel optical axes, one from the left camera and one from the right camera. A visualization of these measurement methods can be seen in Figure 49. [65]
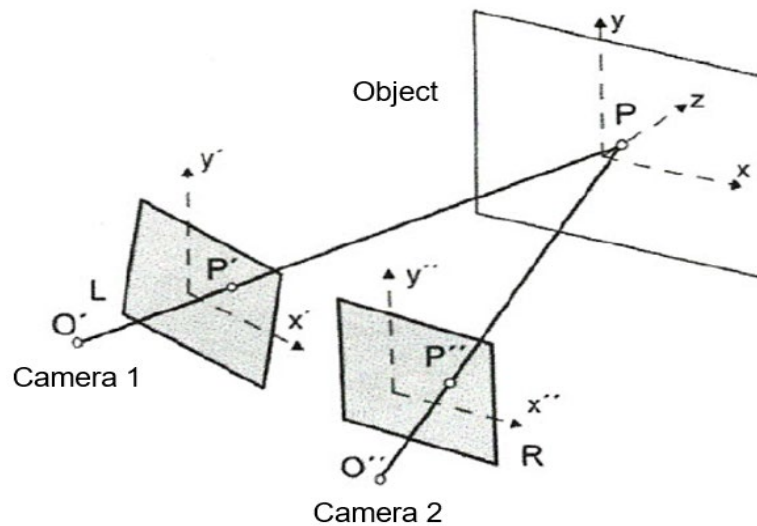
Figure 49: Standard configuration - Measurement configuration for generating a stereoscopic image pair [66]

The third alternative is based on the left-right shift of the camera position for the selected tilt angle perpendicular to the tilt axis in the image plane from a certain projection distance. Since the last alternative is fully compatible with the readout of the data from the MeX software, is also inexpensive, fast, and easily performed by anyone, I have also adopted it for the creation of a stereo image pair for my thesis and present it with the help of Figure 50.
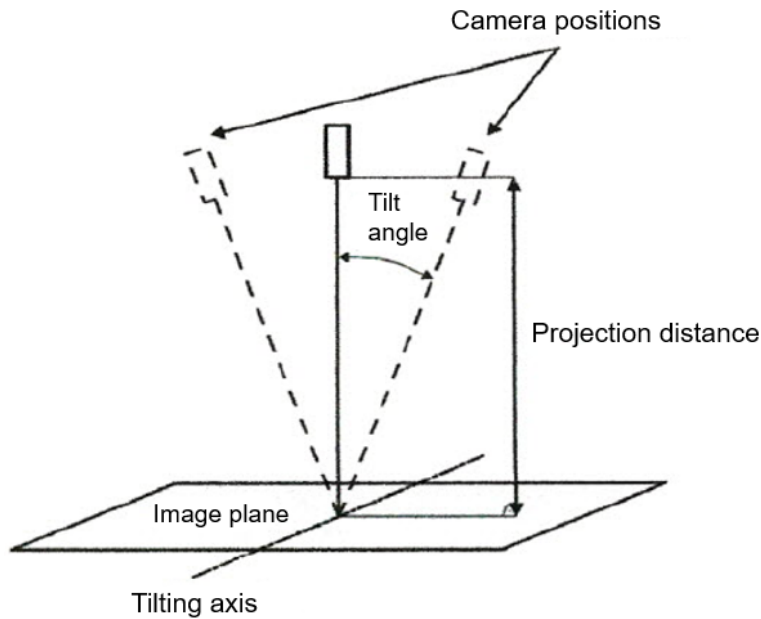
Figure 50: Selected measuring configuration with tilting axis in the image plane [66]

A very important task that we should focus on maximally when taking digital images is their quality, which is crucial, first in creating the digital surface model and then in calculating the 3-dimensional data as accurately as possible by the MeX software. However, it should be noted that there are many factors and conditions that can positively or negatively affect the quality of the images created. In the following, we have treated all possible known factors, which affect the quality of stereo images and are consequently determinants in evaluating the software measurements of the required data for the characterization of the examined surfaces.

3.3.1 Illumination sources and their impact

Depending on the indoor or outdoor environment, atmospheric conditions (cloudy or clear), the type of surface material and the position of taking photographic images in relation to the angle of the sunshine or artificial light, we will notice its reflection from the object to the digital camera, its intensity, and the increase of shading on the examined surface. These factors can significantly affect the quality of the captured images, which then impact the reading process and software calculations. Therefore, optimal illumination evenly distributed over the entire surface of the specimen is a crucial and necessary factor when capturing images.

It goes without saying that we do not need additional lighting when taking pictures outdoors, as the sunlight is more than sufficient. On sunny, bright summer days, we may need to provide shade with an umbrella or other aid to reduce the brightness of the examined object due to the strong sunlight or to avoid uneven lighting conditions or even contrasts, especially if the surface of the specimen is painted in color. [67] We will deal with a similar specimen surface case in the next chapter.

We use artificial lighting in three specific cases: first, when we are forced to record digital images indoors due to the location of the object or for atmospheric reasons; second, when the illumination of the object is insufficient and the images are therefore taken somewhat darker; and third, because it is mainly used for small objects. The problem we most often encounter with artificial lighting is the appearance of partial shading in the object under study, which leads to inaccurate calculations in software measurements.

The reflected natural or artificial lighting as well as the shading of the captured surface are essential for the next steps of the software process, because if an image is darker or lighter than it should be, either from the left or from the right side, it will not provide correct three-dimensional information. Consequently, the results may not be accurate.

Thus, in terms of illumination, we can state that to carry out an accurate and precise process of taking digital images for the necessary steps of the photogrammetric method, it is essential that the illumination of the studied surface is not only sufficient, but also uniform for both images from which three-dimensional information is generated.

3.3.2 Sharpness

It is now well known that the successful application of the stereoscopic method requires, in addition to the acquisition of stereo image pairs, a software application to create the three-dimensional digital surface model and calculate the surface parameters, which we intend to study and analyze. Therefore, it is essential that the left and right stereo images of the same pair not only necessarily correspond to each other, but they must also be of maximum quality, respectively they must provide clarity, especially in terms of sharpness theirs. The clarity and sharpness of the stereo images are critical to the measurement process, as any slight deviation from these criteria will result in inaccurate measurements of the generated surface.

When capturing stereo images outdoors, where the sun shines very strongly, it often happens that some areas of the examined object are brighter than others. It is therefore recommended to reduce this illumination, as it also has a positive effect on the sharpness of the images. [68]

An example of optimal sharpness of stereo images is illustrated in Figure 51:
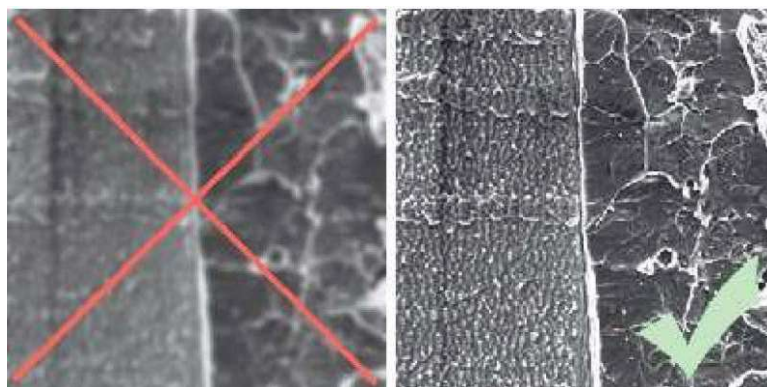
Figure 51: Optimal sharpness of the captured stereo images [69]

3.3.3 Size of the image section

The size of the image section taken during the analysis of surfaces with the aim of applying the stereoscopic method is a very important indicator for the three-dimensional digital reconstruction of the desired object, as well as for obtaining the correct parameters resulting from the creation of the surface model and the performed software calculations. With particular emphasis, the size of the image section has the greatest influence on the reading of the roughness parameters, whether of the profile or especially on the surface texture. A lower correlation between it and the depth of the three-dimensional model is also observed in the volume measurements of the studied specimen.

Because of the possible non-uniformity of the surface of the object under study, the section of the acquired image should generally be as large as possible, since in this way we have better maneuverability in selecting the region of interest for software analysis when creating a low-density stereo dataset. Principally, the size of the captured image depends on the interest of the person performing the measurements, but also on the scaling of the image by the lens.

3.3.4 Magnification (image scaling)

Above we elaborated in an exhaustive manner how important the size of the image section is for obtaining the most accurate results from the software calculation. However, the use of lenses in the digital camera when capturing stereo images allows for a magnification or image scale that is directly related to the resolution of those images. More precisely, the more the surface of the examined object is magnified, the higher the quality and the resolution of the images, but the smaller the size of the image section.

It is estimated, that the larger the image magnification of the surface through the focal length, the higher is the resolution of the image. This means that the images are crisper and more detailed, because the number of pixels for a given surface in cm^2, dm^2 or m^2 is greater. In cases of low image resolution, which depends on the sensor of the SLR camera they will blur into their edges and will be less colorful. Therefore, in this work, in the context of characterization of concrete surfaces with the stereoscopic method, special attention was paid to the quality of the images and, in particular to the changes that occur in the final results of the calculation of the parameters of roughness, waviness and volume for the images of different qualities, then the magnifications taken by the camera lenses are also different. However, regardless of the lens and magnification used to capture images with digital cameras, it should be remembered that there are two types of resolutions, print and screen.

Since the purpose of our research work with surfaces has to do with the image of the screen, the print resolution will not be considered in the following. Just to make clear the difference between them, we must point out that while the print resolution is measured by the number of dots per inch (DPI) and it is preferable that the dpi value is as high as possible, since the printed image should be of maximum quality, the screen resolution is measured by the number of pixels per inch (PPI). In this case based on the help of the "**Fast Stone Image Viewer**", https://www.faststone.org/ , software we can read and understand that the ideal

54

number of dots per inch (DPI) for this type of resolution, regardless of the image scaling or type of lens, it is preferred to always be 72.

Another factor that affects the scaling of the image during acquisition, in addition to the magnification provided by the lens, is the working distance.

We must be very careful not to have even small changes in the magnifications or in the working distances for the left and right images when taking the images, because the inaccuracies in the measurement, even if they are sometimes completely negligible at first glance, can be so crucial that it can happen that the software does not create the digital surface model, nor extract the results of the parameters for the analyzed object. [70] In Figure 52, we show how a very small difference caused by either the magnification or the working distance of the object can look for left-right stereo images.
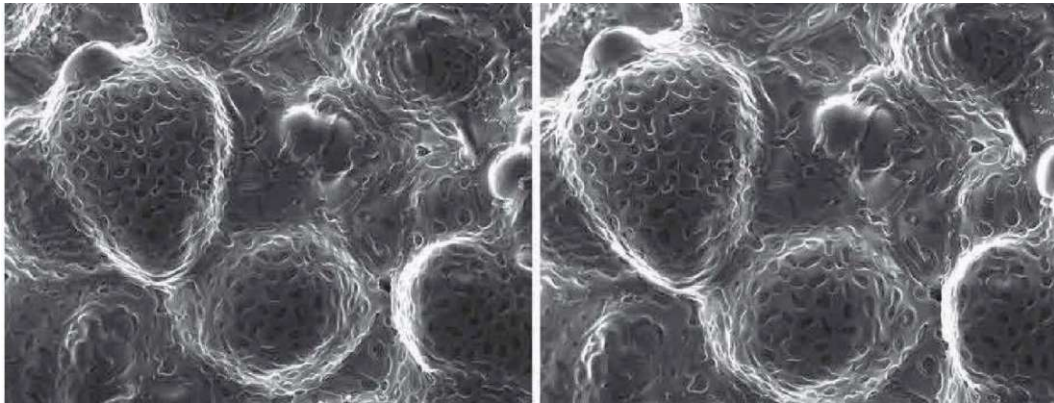
Figure 52: Stereo pair images with different magnification or working distance [70]

3.3.6 Sources of errors when capturing stereo images

When capturing object surfaces, there may be sources of errors or obstacles that significantly reduce the quality of the software scan or make it difficult to further process the data in the program for the photogrammetric method. The most common sources of errors we may encounter are listed below:

1. an unsuitable camera with too small sensor or unsuitable lenses
2. too few shots or too few perspectives
3. environmental and lighting conditions
4. material properties of the object, which can be:
    a. very smooth, transparent, or shiny surface
    b. very filigree objects such as hair or fur
    c. Objects with holes and cavities

These errors or hurdles can cause the software to make an erroneous recognition and calculation of the object and consequently the created 3-Dimensional model to be inaccurate and erroneous.

3.4 Processing of the captured stereo images

After the stereo image pairs have been successfully captured, these images should be processed for quality, if necessary, especially if the captured image is brighter than it should be, and for file format.

It is necessary that all captured images have the same file format, so that they can then be imported and read successfully by the software. Even in cases where the digital camera used to capture stereo images automatically saves them in a lossy file format, i.e., JPEG, which can lead to distorted results, we should be able to convert these images to one of the lossless formats such as: TIFF, BMP or PNG through various programs or software applications of graphic design. [71]

The processing of images in terms of their quality after saving them in the above-mentioned desired file formats can also be done by intervening in these applications, i.e., by reducing the level of brightness or saturation, then by improving the level of contrast and eliminating their possible blurring, the presence of which makes depth-based measurements impossible. Nowadays, there are an infinite number of programs on the market for graphic editing or designing images. However, in the context of this thesis, with the recommendation of my supervisor, I chose the software "**Fast Stone Image Viewer"**, https://www.faststone.org/ , software, which is very practical to work with.

There is another option for processing captured images in cases where the tilt angle for the left and right sides is not identical, called rectification. However, since this option can have an unfavorable effect on the accuracy of the digital surface model and on the software calculations, it is recommended to repeat the acquisition of the stereo image pair rather than applying it yourself. [72]

3.5 Scanning of images and measurements in MeX software

MeX software, version 6.2.1, produced by the Austrian company Alicona Imagining, located in Graz, which was used throughout my work for the digital reconstruction of concrete surfaces taken by recording pairs of stereo images with a digital camera of the SLR system from different tilting angles, as the basis of its work has the three-dimensional analysis of the studied surfaces by the scanning electron microscope (SEM) and the generation of the digital surface model (DSM), which has a lot of information about the studied object, including its depth. The working scale of this software ranges from a few meters in the macro range to a few nanometers in the micro range, which makes it also suitable for civil engineering.

3.5.1 Aim and method of measurements by MeX

In this analysis, this software performs measurements and calculations of the surface of the object depending on the parameters desired by the researcher, thus creating a database of these surfaces. This program generates the digital surface model (DSM), first by superimposing the recorded stereo images and then by comparing the geometric points in the three-dimensional coordinate system, otherwise known as pixels, for each of these images.

3.5.2 Explanation of the calibration data

For this software application to perform the measurements required to generate the digital surface model (DSM), some measurement values must be defined beforehand, also known as calibration data, which are as follows:

a. **Projection distance:** Must necessarily be the same for both images and is set during the acquisition of the images. The projection distance (pd) for automatic calibration of measurements for stereo images is composed of the EM working distance (wd) and the value ε, which, if it is taken to be around 10 mm, leads to good measurement results. Under no circumstances should you forget to enter the ε value, as this will be interpreted as a poor or incorrect value of the projection distance, which will then result in a curved appearance of the elevation model. [73] A better overview of the correlation between projection distance, EM working distance and value ε is given in Figure 53:
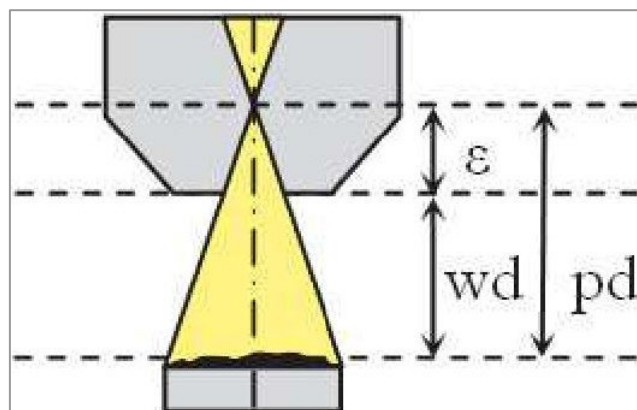
Figure 53: Projection Distance [73]

b. **Tilting angle:** A very subtle factor that must be considered when capturing the stereo image pair is the tilting angle, since any inaccuracy in this factor can become a sure source of deformation in the results of the digital surface model, and in this way, points used for the measurement will not be visible for both the left and right images. It must be completely correct or unchanged for both the left and the right captured image and means the difference between these two angles. It is also worth

57

noting that the tilt angle depends on the magnification of the recorded object with typical values ranging from 1 to 7 degrees. [74] Depending on whether the examined surface is completely flat, or with a slope, then the tilt angle must also be adapted to these circumstances. More precisely, it is preferable that for a surface with a greater slope the tilt angle is chosen smaller, although such an angle leads to greater inaccuracies in the results, until for a flat sample we choose a larger angle and therefore we will get more accurate results. Therefore, when examining surfaces with the stereoscopic method, it is recommended in general to avoid objects with a slope and especially with a large slope. Normally, an angle of 5-15 degrees is preferred for capturing stereo images [66], but even if it is a few degrees larger, this does not cause any problems with the results.

c. **Sampling distance:** Sampling distance represents in MeX software the metric size from the point of measurement of the image and is used to measure the sampling distance in the stereo import wizard before generating a digital surface model. To precisely know this value for the selected metric unit, a scale bar is very helpful when capturing stereo images, as it also appears in this stereo import wizard. Its values do not necessarily have to be the same in different directions or axes (x or y). [73]

3.6 Generation and evaluation of a 3-dimensional digital surface model

Before proceeding to the selection and uploading of captured stereo image pairs of certain concrete surfaces during experimental reviews, we must emphasize the first necessary steps of the operation of the software after its installation on the computer, which is as follows:

1) Creating a new Database
2) Creating new Folder
3) Creating new Project
4) Generating new Creator Dataset

The working principle of the MeX 6.2.1 software is to create a new surface database by importing a stereo image pair. Before the process of stereo creation can begin, we need to know the calibration data, such as projection distance, sampling distance, and tilt angle, that we used and specified when capturing these images.

To begin, we load the stereo image pair with the same properties into the software by choosing the image on the left first, then the image on the right, just as they have been recorded with the digital camera. As a result, they are superimposed on each other and initially there is a blurred image in the global offset that appears in the center of this wizard. The next step is to set the parameters of the stereo image pair and the calibration data. Then the images are aligned using a manual horizontal and vertical offset, either manually via the cursor or numerically, until the new surface created under the images of this wizard is completely clear in its central part with respect to the vertical axis of the image.

There is also the possibility of automatic offset, but its use requires exceptional rigor of the images in terms of eventual rotation of one of the loaded images, otherwise the process is interrupted, then the capacity and very high speed of the computer used for these calculations, on the contrary, it may take a long time to complete the compensation.

However, if the program detects a small rotation of the images, it also offers the possibility to correct these errors by reopening the window. To understand the creation of the database in a practical way, a visual representation of the stereo creator according to Figure 54 is given below.
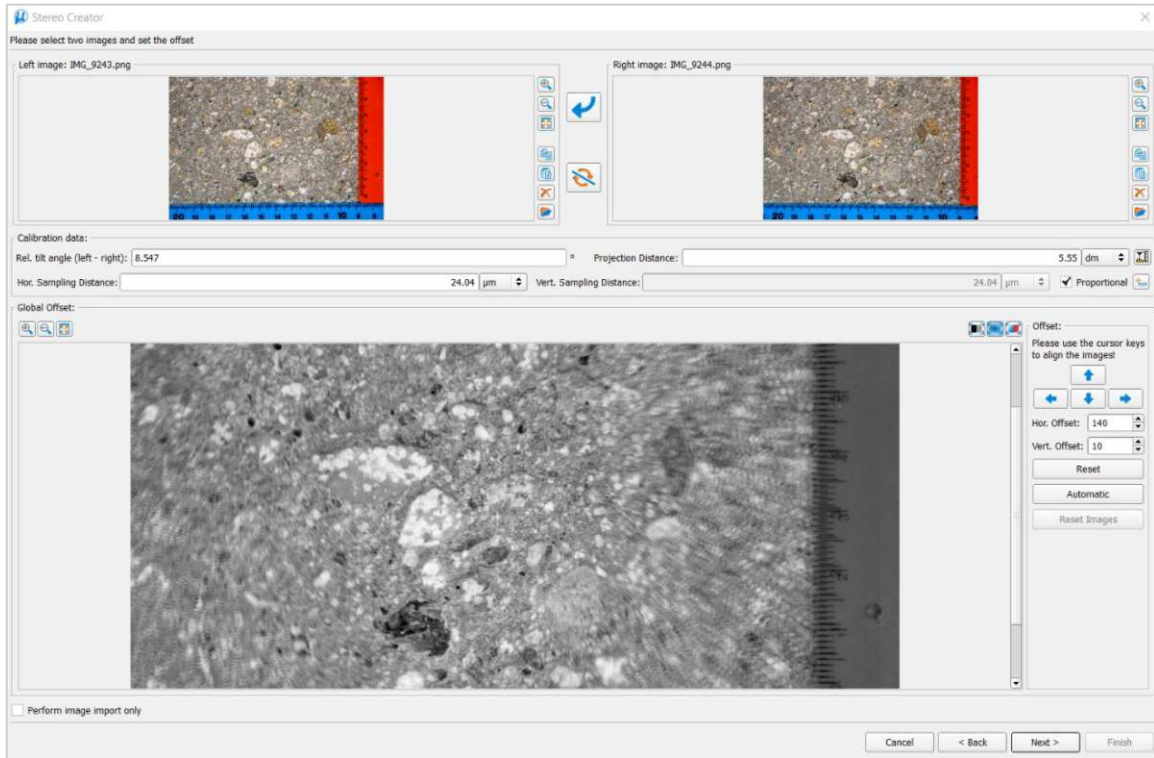
Figure 54: Stereo Creator of pair images ©

In the next step, we specify the Region of Interest (ROI) for the required measurements, which can include the center of the image or one of its four edges, necessarily extending to the center, since not including the center will not allow us to create a low-density surface dataset, which can be controlled to identify and eliminate unreasonable surface datasets. From various previous studies, it is strongly recommended that the selected Region of Interest should not be smaller than 10 cm^2, on the contrary, the larger it is, the more representative the results will be for the measured parameters. An example of the specification of the Region of Interest is visualized in the Figure 55:
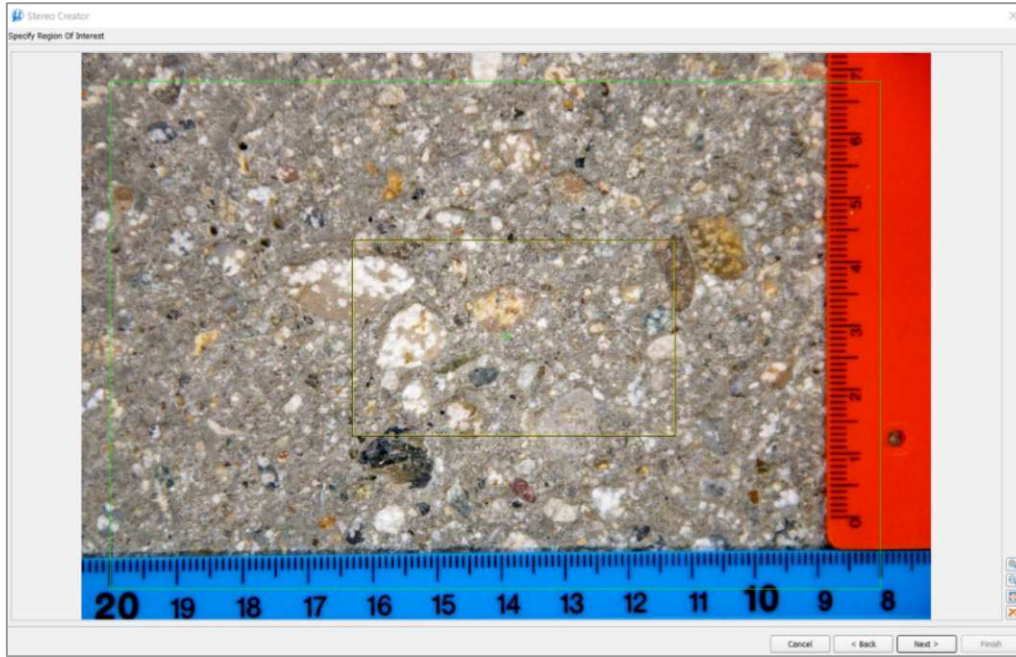
Figure 55: Specification of the region of Interest (ROI) ©

As the last step, the software creates the final surface dataset once the initial (low density) surface dataset has been approved form us. After the calculation process, which takes several minutes depending of the performance of the computer, is finished, the 3-dimensional digital surface model is successfully generated, and its view is in Figure 56 below visually illustrated.
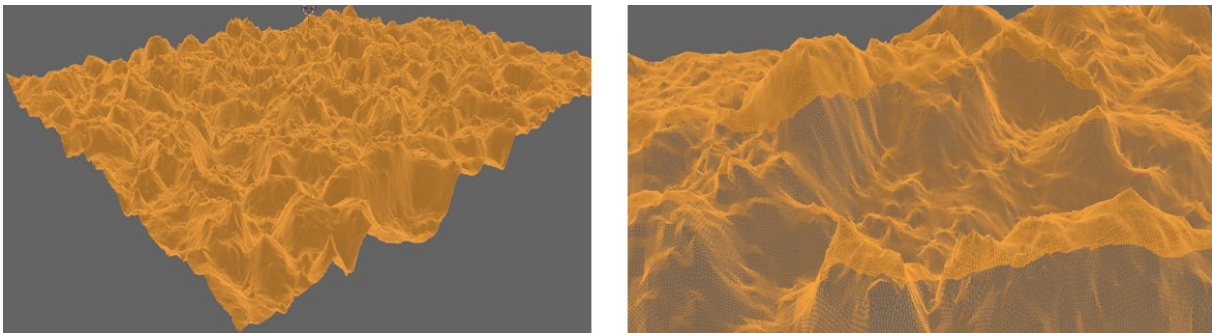
Figure 56: 3-dimensional digital surface model with net cloud points

3.6.1 3D Viewer / 3D-File

This digital surface model, shown in 3D in the figure above, will be the starting point and basis for characterizing the surfaces of selected objects of study in the continuation of our work, through measurements of profile roughness or waviness, surface texture roughness or waviness, calculation of their relevant parameters, and analysis of their volumes. It is now clear that the focus of this work is on the characterization of the surfaces. However, before we perform the measurements of profile roughness, surface texture and volume, to obtain the most accurate and precise results possible, it is necessary that after the final

60

surface dataset is created, we first look at the created three-dimensional model by selecting 3D Form Measurements to see if it is necessary for future analyses to intervene in the shape of the created three-dimensional model.

3.6.2 Profile Analysis and its Workflow

To make the profile analysis as clear as possible, it should be elaborated by a certain workflow. On the first page of the analysis, the measured surface is first displayed. Then, through quality filtering and leveling, the leveled reference surface is determined, from which the primary profile, the roughness profile or waviness profile, is then extracted. Along a line presented in the middle of the surface, which can be horizontal, vertical, or diagonal, a surface profile with a certain Path length l [in cm] and Depth z [in µm or nm] is created by a Histogram. This profile can change depending on the filtering, i.e., if it is the primary profile, the roughness, or the waviness, as it can also change depending on the value of the cut-off wavelength λc (Lc). In the context of profile roughness measurements, we can observe that the shorter the cut-off wavelength λc (Lc), the denser the surface profile, but also the less accurate the results of the parameters we obtain. Continuing the workflow of the profile analysis, on the second page the software gives the profile parameters, with special importance given to the Ra, Rq and Rz parameters. On the third page follow the advanced parameters of the profile and on the fourth page the bearing ratio curve in accordance with the EN 4287 standard. Below through the Figure 57 we will illustrate the Workflow of Profile Analysis.
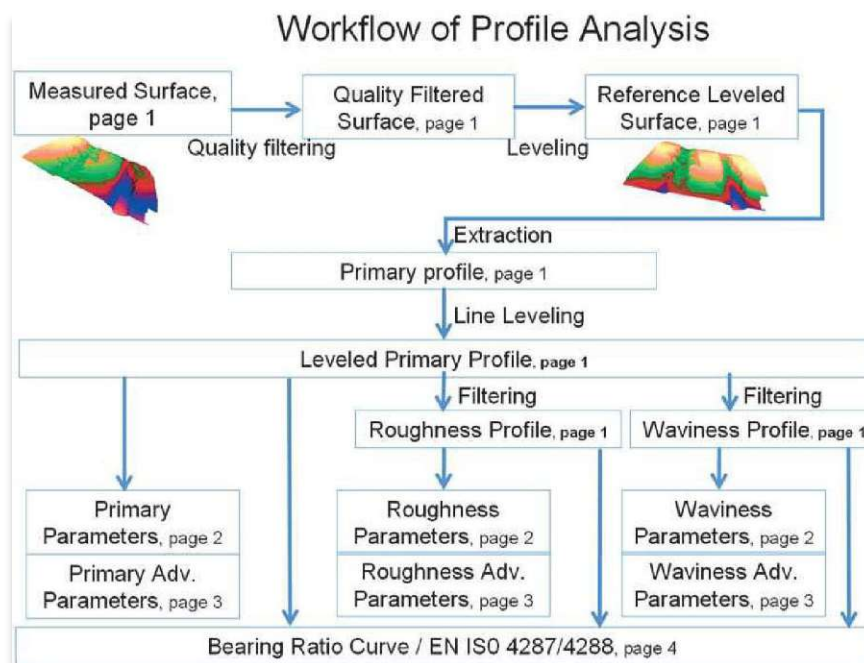
Figure 57: Workflow of Profile Analysis [75]

3.6.3 Area Analysis and its Workflow

In an almost analogous way, the work progress is also developed for the surface texture analysis. After generating the digital surface model, the measured surface is displayed on the first page, which is converted into a leveled reference surface after quality filtering and leveling, and after its selection and after further filtering, the filtered surface is obtained. This filtered surface can also be understood as a set of individual profiles, finely distributed and in the form of a network on the surface. [76] Here we select the dataset type we want to analyze, i.e., roughness or waviness. Again, before proceeding to the calculation and reading of the parameters of the surface texture, we can vary the value of the cut-off wavelength Lc, but unlike the analysis of the profile, the selection of the value of Lc must be done carefully and should be neither too small nor too large, because in both cases the value of the parameters of roughness or waviness can get on the wrong side. On the third page, the program deals with a variety of factors and parameters during the analysis, but for the purposes of this work we have focused only on Surface Texture Parameters and Bearing Area Parameters. In Figure 58 it is represented the Workflow of Area Analysis.
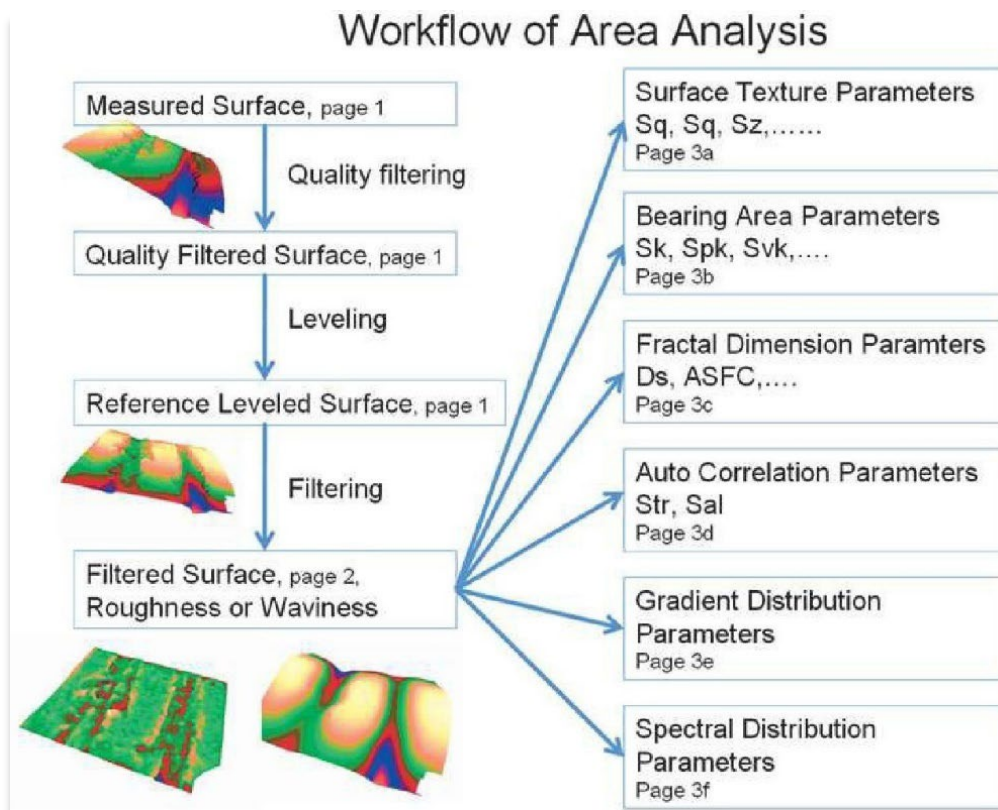
Figure 58: Workflow of Area Analysis [77]

3.6.4 Volume Analysis and Determination

For various reasons, such as illumination, shading, tilt angle, projection distance etc. during image acquisition, the shape of the digital surface model may often not be flat but slanted or even curved, which is an extremely big problem in deforming the results for volumetric measurements. However, even for such cases, the software offers the possibility of correction through the **Form Removal** tool. When selecting this tool, depending on the shape of the surface, which is displayed in the **3DFormMeasurement** module after selecting the surface, you have the possibility to choose the correction method through the offered tools, i.e., planar, spherical, parabolic, or conical. To better understand the influence of the deformed plane, namely not the reference plane, in generating data in volume measurements, in Chapter 5, as part of the evaluation of the results, we will examine the same surface once with a flat reference plane, corrected after using the Form Removal tool, and the next time with a slanted or curved reference plane.

Another significant factor in the characterization of concrete surfaces besides the primary profile and waviness is the determination of the volume of the surface, which is directly related to the roughness of the profile of that surface, and, more specifically, to the depth of roughness Rt. Currently, there are no relevant regulations or standards that specifically respond to the analysis of volume determination for the examined structure of concrete surfaces. Therefore, all that remains is to perform this type of analysis with the methods and possibilities that we can have available. A good opportunity is created for us during the surface analysis through the digital surface model (DSM), obtained from the software calculations, in which case the real volume parameters of the selected section of the Figure are determined through the projected surface, which as a prerequisite should be limited. However, before reading the values obtained, we must be careful in the dataset for calculation.

It is sometimes possible, when calculating the volumes with any of the suitable mode such as soap film or top cover, to calculate the depth of roughness Rt according to the formula given below [78]

$$\text{Rt} = \frac{V}{A_p} \qquad (3.1)$$

Since digital surface models are created by superimposing a pair of stereo images, the three-dimensional data of the generated surface, regardless of the depth represented in the model, are also not real volumes, which is a significant disadvantage for the volume measurements and the determination of their parameters. This is because the data set of the generated three-dimensional model is an open surface on one side, which must necessarily be covered with a section plane, regardless of certain disadvantages that this option may have. [75]

4. Conducting experimental investigations and software calculations

4.1 Examined concrete surfaces

Below I have listed by name all concrete surfaces as well as other objects made of non-concrete materials, which were used as aids for optimal calibration of data during the process of capturing images as well as during the software calculation of the necessary parameters for the elaboration of my thesis:

1) S_1; S_1a & S_2 Shot-blasted concrete surface
2) S_1.II short resin primed (epoxy resin) and sanded with quartz sand 0-4 to 0-8 mm
3) S_5 Foamed concrete
4) S_7 precast concrete outdoor staircase
5) S_8 In-situ concrete subtracted
6) S_9 Concrete broom finish
7) S_10 Precast smooth concrete (stone pavement)
8) S_11 Precast concrete exterior staircase (rough-grained)
9) S_12 Concrete sanded outside
10) S_13 Plinth in-situ concrete, smoothed
11) S_14a; S_14b Synthetic resin coating OS11B (surface system with Quartz sand scattering different greetings 11B for garages)
12) S_15 Synthetic resin coating OS11B (surface system with Quartz sand scattering different greetings 11B for garages)
13) S_16 Concrete terrace slabs
14) S_18 Wooden floorboards grooved
15) S_20 LEGO plastic studded board above and below

4.2 Required measuring devices for the acquisition of stereo image pair

For the acquisition of stereo image pairs in the examination of all concrete and non-concrete surfaces for their characterization in practice, I have used numerous devices and tools, which are listed below:

4.2.1 Aluminum measuring frame

The aluminum measuring frame constituted one of the main devices for capturing one or more pairs of images, depending on the surface being analyzed. Its purpose was to allow the digital camera (SLR) mounted inside it to capture pairs of images by left-right eucentric

tilt, depending on the desired angle, which varied between 8 and 16 degrees. While the height of this measuring frame was approximately 88 cm, the pivot point of the camera fixation necessarily had to be closer to the analyzed surface and located at a height of 56 cm from the contact point. Due to incomplete stability, it had to be constantly reinforced with pliers or small concrete cubes. The Figure 59 below shows the equipment, its pivot point, and the above-mentioned reinforcements:

(a)   (b)   (c)
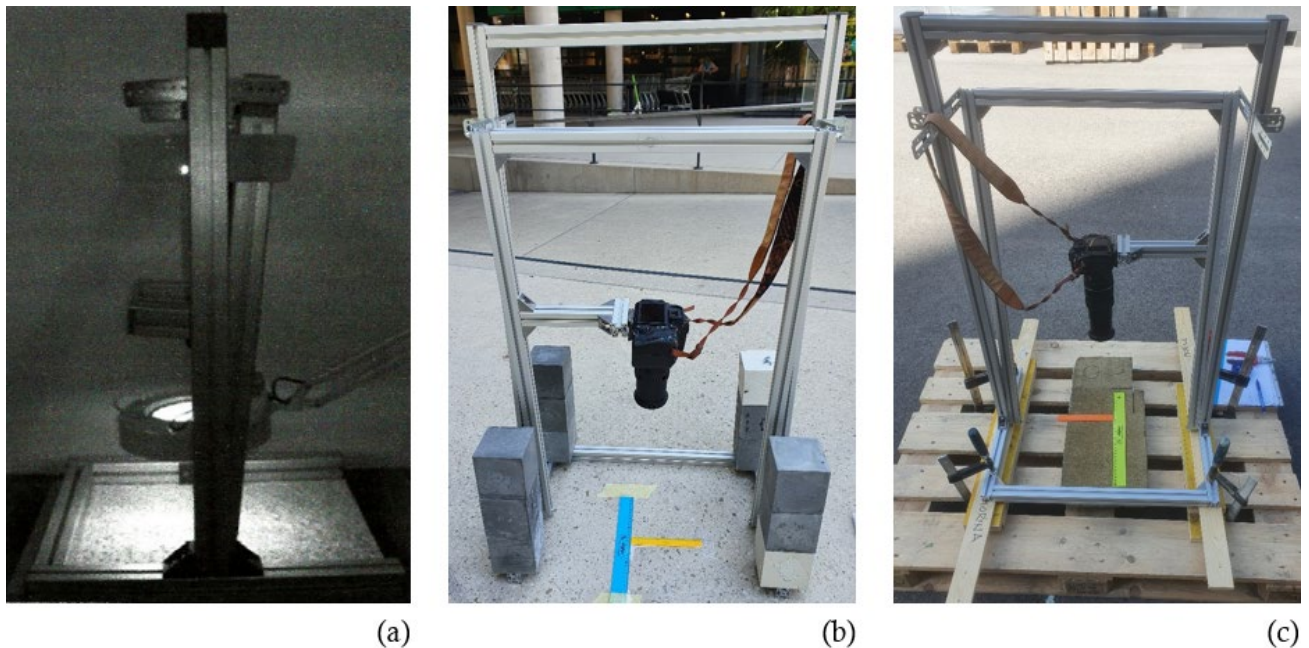
Figure 59: Aluminum measure frame, (a) pivot point [79], (b) reinforced with concrete cubes, (c) reinforced with pliers

4.2.2 Single-Lens Reflex (SLR) camera

As mentioned earlier, the quality of the recorded digital images must be as good as possible so that the data can be read and processed as accurately as possible to create the three-dimensional file of the MeX calculation software. For this purpose, for the process of obtaining pairs of images, regardless of the highest price, we have chosen the best model on the market of the camera system, that is, the SLR camera, namely the model EOS 70D of the company Canon, because this model, compared to other camera systems, has a larger sensor and a full frame, which is very important when the lighting, whether natural or artificial, is not optimal while capturing images.

Capturing of images was done almost all the time using the automatic option, which was also due to my lack of experience with such camera systems, although the camera also worked with the manual option.

In addition, the lens should be part of the digital camera during the experimental studies. For the photogrammetric method, it would be ideal if they had a fixed focal length, because any change in the focal length of the lens, no matter how small, would lead to unfavorable results when creating the digital surface model (DSM). Among the wide range of lens manufacturers, I used lenses from Sigma with different focal lengths from 50 to 300 mm

and Tamora with different focal lengths from 100 to 150 mm, which allow different image resolutions.

So, in summary, the larger the high-resolution image sensor, the more surface area is offered to the light and vice versa, which directly affects the efficiency of the light and consequently the quality of the captured digital images. [80]

Figure 60 shows the model of digital camera and the above lenses that were used in the acquisition of the digital images.

Figure 60: Single-Lens Reflex (SLR) digital Camera and Lens with large sensor

4.2.3 Rulers, Wrenches, and Pocket tape measure

Other tools and devices needed to capture digital images explained below:

- ➤ **Rulers** used to define the desired surface of the object during photographic capture and to allow vertical or horizontal offset of the stereo images after loading and overlaying into Stereo Creator. They also helped me determine the Region of Interest (ROI) as accurately as possible when selecting it for the creation of the low-density dataset.
- ➤ With the help of **wrenches**, the aluminum measuring frame was fixed at the desired angle after its eucentric tilting.
- ➤ **Pocket tape measure** made of strip steel was more than necessary to accurately measure the tilt angle of the frame and the projection distance with the intention to determine the sampling distance.

4.3 The procedure of measurements in practice

4.3.1 Selection and examination of the surfaces of the specimens

First, in consultation with the supervisor of the topic of my thesis, we made the selection of the above surfaces to characterize them in terms of roughness and waviness of the profile and surface, as well as their volume. It should also be noted that almost all the surfaces of the studied objects, except for surfaces S_14a, S_14b and S_15, which were worked on by colleague Arazli in the interest of her studies, were ready, so it was not necessary to create them for this study in the first place. Then, using the equipment described above, the stereoscopic method was applied to characterize these surfaces.

In first step stereo image pairs were acquired for each of the upper concrete surfaces at a minimum of one and a maximum of three tilt angles and for different magnifications and sizes of the image section using different lenses. During the acquisition of stereo image pairs, to facilitate the work with the computer software MeX 6.2.1 from the manufacturer Alicona, regarding the calibration of the data, it was necessary to first perform some necessary measurements related to the definition of the projection distance, sampling distance, tilt angle, etc.

To calculate the tilt angles as accurately as possible, it is first necessary to measure the projection distance on the aluminum measuring frame, from the contact with the surface under examination to the position of the exposure point, which is located on the top of the digital camera, moving to the left and right, but in the initial position is 0 degrees in each case. Then we chose the horizontal distances of the frame movement for one to three different measurements, depending on the surface of the studied object. After tilting the aluminum frame in the sliding system for each of the desired angles, it was always necessary to fix it on both sides with two screws and washers for the purpose of qualitative reception of the images.

The process for obtaining stereo image pairs as a function of the examined concrete surface was developed in various environments inside and outside the laboratory of the Institute of Building Materials, Materials Technology and Fire Safety within the framework of the Vienna University of Technology at Lilenthalgasse 14, 1030 Vienna, as well as at Fred-Zinnemann-Platz, 1030 Vienna.

4.3.2 Examination of the measurements and calculations with MeX

After the successful acquisition of stereo image pairs for each of the surfaces of the studied objects to complete the application of the stereoscopic method, the next step is to perform measurements and calculations using MeX software version 6.2.1. Thus, the main objective was to create digital surface models, to determine the required parameters under the influence of various factors, and to compare the results obtained within a surface, but influenced by various factors. After creating the digital surface model (DSM) explained in Chapter 3 respectively in point 3.6, which means the creation of the final surface dataset in three-dimensional form, I performed the analysis of profile, surface, and volume for each of the above objects. Since some of the studied objects have almost the same characteristics,

and with the aim of a more appropriate elaboration of this work, the characterization of some of these surfaces in tabular and visual form can be found in the Appendix, while in the following subsections we will deal in more detail with the surfaces of other objects.

4.3.2.1 Measurements and Calculations of Profile Parameters

As we emphasized during the profile analysis workflow, primary profile measurements, profile roughness measurements, and profile waviness measurements can be made as part of this process for the digital surface model generated by overlaying the two stereo images. To start the profile analysis, first, from the database, we mark the object we want to analyze and then click on Analysis → Profile Roughness Measurement. After opening the Profile Roughness Measurement Wizard, the first page displays the image of the examined surface, through which passes the profile center line with a width automatically determined by the program, which is used for measurement and calculation of the desired parameters. During the analysis I noticed that this width of the profile line, which usually varies in several micrometers, can be changed manually by the user, but if the change from the original width is large, then the impact on the results of the roughness parameters will be considerable. Otherwise, for the waviness parameters, the width of the profile line has almost no effect. On the bottom of the first page, we see the diagram of the profile with depth z and path length ln.

When we activate the Show measurement information tool, a moving red cross appears in the image, which together with the green cross we set can serve us as a reference point for measuring the parameters, such as: Cut-off wavelength Lc, total height of the profile Rt, sampling length lr, but also other parameters. Regarding the cut-off wavelength, the program offers two options: an automatic option is based on the DIN EN ISO 4287 standard and offers a selection range of 50-8000 micrometers, while the second option is manual and allows the user to choose the sampling length lr himself, which can be much larger than 8 mm, but in these cases the profile length l must also be very large.

To experiment in as many ways as possible when calculating the parameters of the profile, in addition to the horizontal line shown in the center of the image, for **one** of the surfaces I also examined the results of the parameters from the vertical lines selected in three different positions.

In the following, the values of the obtained parameters of roughness or waviness of the profile and their histogram are read, which consists of individual elements in the form of a bar, which has a certain width, the change of which changes the shape and number of elements. Then the advanced parameters of the profile were treated and at the very end I also evaluated them by the Bearing Ratio/Firestone-Abbott Curve together with the parameters of the material ratio. Next, Figure 61 shows the working analysis module of the roughness measurement profile of an object.
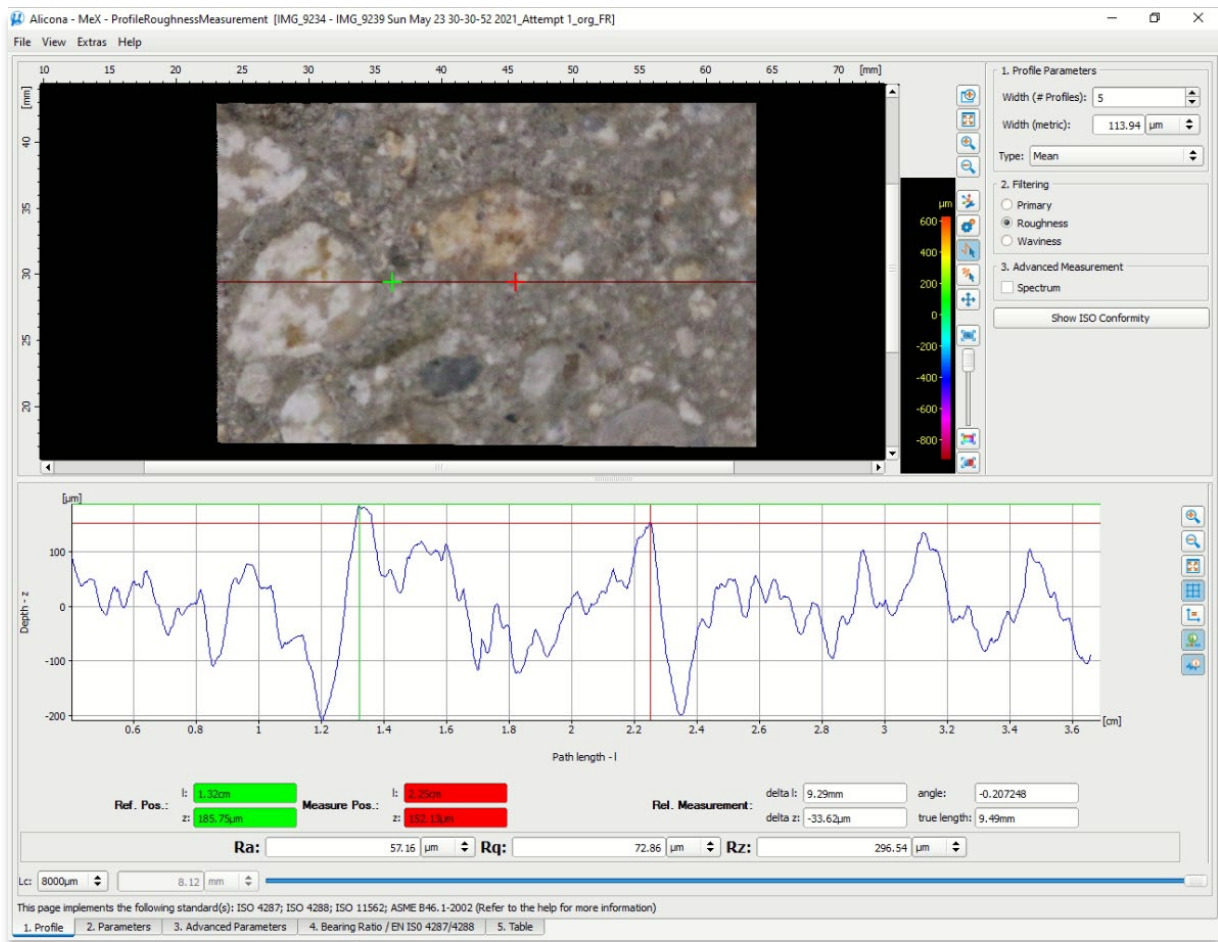
Figure 61: Roughness Profile Measurements Module

We will elaborate all the obtained results of the parameters of roughness or waviness of the profile, for all surfaces of the studied objects, separately in Chapter 5 of this Thesis.
It should be noted that the analysis based on the horizontal or vertical profile line of the image is not entirely representative when characterizing the surfaces for objects or samples with large dimensions. Therefore, to determine the parameters of a surface very accurately, it is important to analyze the texture of the surface, which we will discuss below.

4.3.2.2 Measurements and Calculations of Area Parameters

During the process of surface analysis after the selection of surface texture measurements, the first page shows the surface that was measured during the creation of the digital surface model. Then, on the right side of the first page of the tools available to us for selecting the surface image we want to analyze, which means an over the analyzed surface, we worked with the rectangle tool. After making the selection, we clicked on the second page of the progress of the analysis, located in the lower part of the page. The program automatically performed the filtering and leveling of the surface, so we got the filtered surface. In the next step, we adjusted the coordinate system of the sample in the frame of the primary profile and then selected the dataset type, namely the roughness or waviness one. Finally, we

varied the cutoff wavelength Lc in the filter parameters window, and the software again automatically performed the necessary calculations to measure the parameters.

On the third page we have read the values of the obtained parameters, respectively their qualities and statistics, numerically and in the histogram shown above, and at the very end we have examined the Bearing Area/firestone-Abbott curve in relation to the value of the SMR parameters (peak material ratio), as well as checking if the criterion of 40% of the minimum slope, also provided for in the relevant standards given above, is met.

So, each of the surfaces of the examined objects has been analyzed for several values of the cut-off wavelength Lc, to understand which value is more acceptable for concrete surfaces, because in the current standards, the given values of Lc are conditionally valid only for metal surfaces. A visual representation of the process of the Surface Texture Measurements is given in the Figure 62:
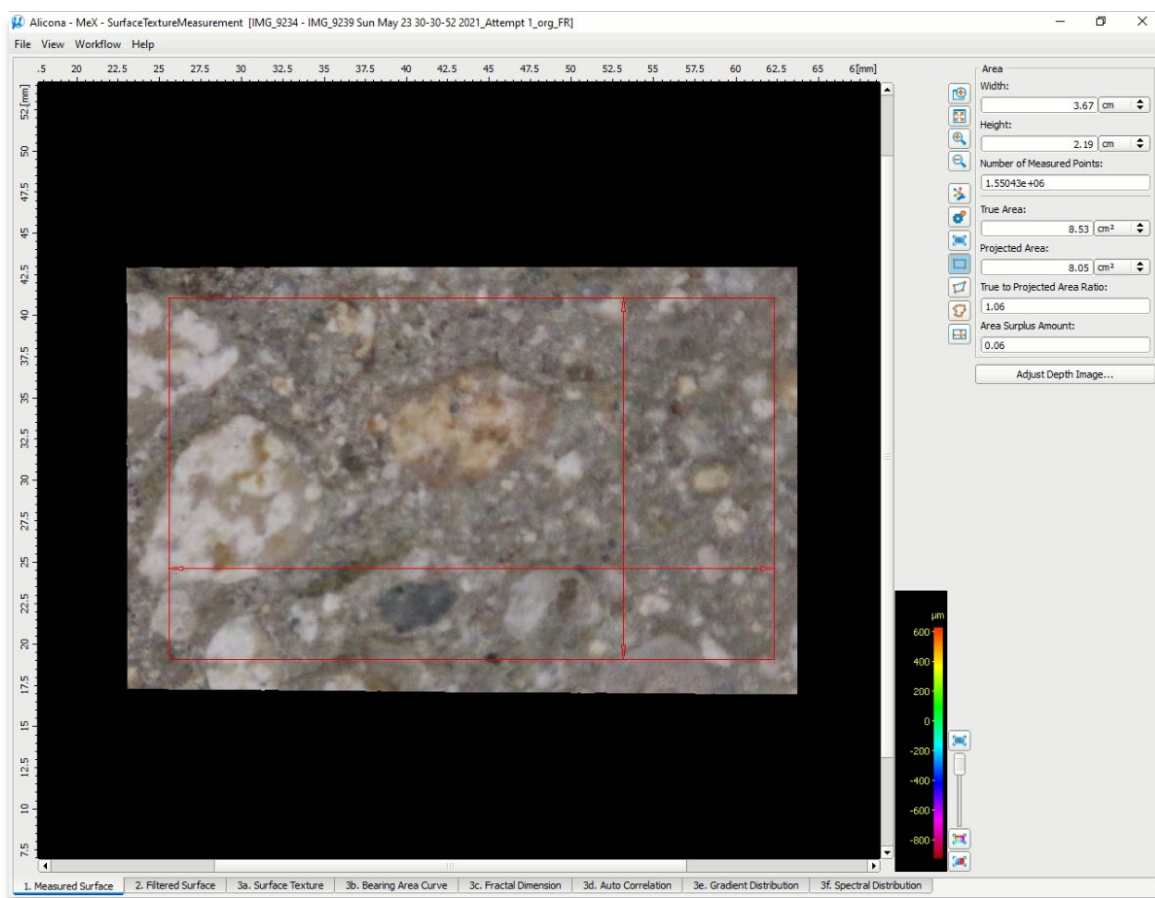
Figure 62: Surface Texture Measurements Module

Then, the elaboration of the parameters of the concrete surfaces is also done for different selected sections of the image, either within the same image, or through images taken from different tilt angles, and the obtained results and their comparison is also elaborated in Chapter 5.

4.3.2.3 Measurements and Calculations of Volume Analysis

During the elaboration of my master's thesis, in the framework of the volume measurements I've used the following steps for calculation method of MeX software:

a) First, we select the desired part through the Draw Polygon tool for volume measurement analysis from the digital surface model (DSM) displayed as an image view in the upper side of the screen view,

b) After selecting that surface area, the software automatically starts calculating the volume for the selected part according to the soap film mode,

c) Here, the surface of the structure is covered with a soap film; however, its large edges penetrate it,

d) The software after the calculation gives us through the volume view in the lower side of the screen view the following data: the extracted volume above and below the soap film in cm^3, as well as the size of the selected area, which is also known as Calculated ISO area, in cm^2,

e) If after the calculation we do not do the data processing, the software gives us inaccurate results, while after its processing, the results are better, but still not all areas are included.

However, since the software, in addition to the soap film mode, offers three other Calculation data sets, then I have chosen one of them for measuring the volume, which are:

✓ **Top Cover mode** – In this mode the selected ISO area will be cover from above including all maximums protruding.

✓ **Bottom Cover mode** – Represents the opposite of the top cover mode and includes all minima below the examined surface. This mode is not preferred for surfaces with positive textures. In contrast, it is very accurate and preferable for surfaces with negative textures.

✓ **Cutting Plane mode** – It is the simplest and most accurate mode of all four, because it makes it possible for the reference plane, respectively the ISO area, to be removeable by the hand depending on our desire. [77]

4.3.3 Practical examination of the Roughness Depth Rt and the Volumes

In order to achieve the most accurate calibration possible when capturing stereo images using the stereoscopic method, I examined not only concrete surfaces, but also other surfaces made of different materials such as wood and plastic. My main goal was to determine how rough these surfaces were or what their volume was. Then I measured these surfaces experimentally in the lab to see if the results fully matched those obtained by the software calculations for the three-dimensional surface dataset.

4.3.3.1 Roughness Depth Measurement in practice

We measured the depth of roughness Rt on the surface of the object made of plastic, on the LEGO plate with nubs, by first measuring the diameter d and then the height of the nubs t with a caliper. According to the measurements, the following dimensions were obtained: the diameter of the upper studs d_u= 4.80 mm, the diameter of the lower studs d_l= 3.05 mm, their depth together with the plate t_1= 2.44 mm, while their depth alone t_2= 1.85 mm. We will compare these data obtained by practical measurements with the results of the measurements of the digital surface model generated by the software calculations of MeX 6.2.1 to see if the results agree or if the calibration process was successful.

4.3.3.2 Volume determination in practice

To calculate the volume of these non-concrete surfaces practically or experimentally, we first examined a grooved Wooden floorboard and then a LEGO plastic studded panel from below. Before starting the calculations, I fixed these objects with tape on a given surface. In the next step, I measured this limited area by its length l and its width w, and then I filled it with sand. Following I threw a quantity of sand into a test tube, the volume and mass of which I measured beforehand when it was empty, and then I measured the test tube filled with sand again, and by the mathematical calculations given below, first for LEGO Board and then and then analogously for Wooden floorboard, I determined the volume of this area:

L=14.2 cm; W=13.3 cm; *A=188.86 cm²*; M_{tube}=56.624 gr; M_{full}=182.263 gr; V_{sand}=79.3 ml; $M_{sand,full}$=M_{full}-M_{tube}= 125.64 gr; → *M_{sand}=9.33 gr*

γ_{sand}= 125.64 gr / 79.3 ml =1.5844 gr / ml → *Vs_{sand}=9.33gr / 1.5844 gr / ml=5.889 ml*

V_{sand} / A=5889 mm³ / 188.86 cm² → *V_{sand} / A=31.18 mm³ / cm² for LEGO plastic Board*

analogously → *V_{sand} / A=50.67 mm³ / cm² for Wooden floorboard*

The entire visual illustration of the experiment is presented in Figure 63:
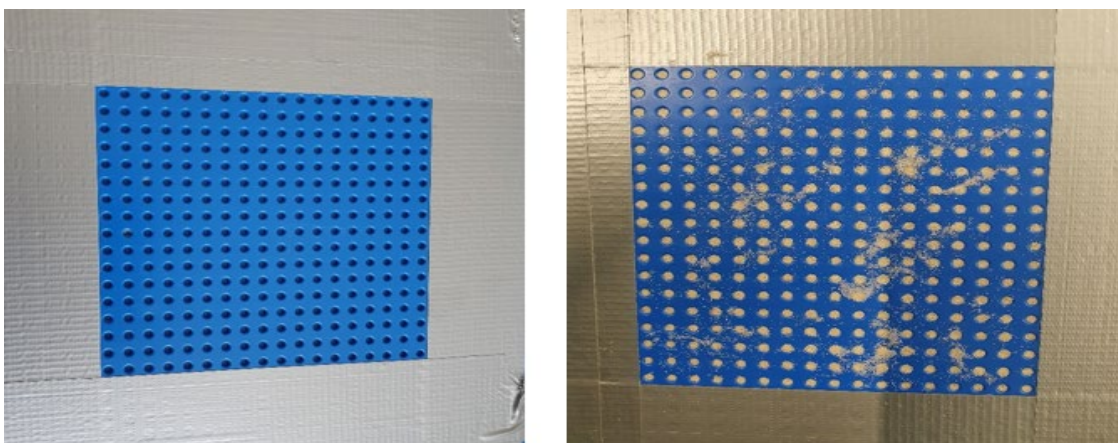
Figure 63: Practical volume measurement with grinding sand over a LEGO plate turned knobs

72

5. Processing, evaluation, and comparation of the results

In this chapter, through processing and comparison of the results, I will numerically, graphically, and tabularly elaborate on how the above factors related to stereo image quality, such as illumination, shading, magnification, size of the image section, and tilt angle, affected the calibration definition process during image acquisition. Then on the generating of the digital surface model (DSM), and primarily to the final result of the calculated values of parameters for the profile analysis, surface analysis, and volume analysis for each of the concrete surfaces listed above.

5.1 Results of the Profile Roughness Measurement Module

Aiming for the most complete, detailed, and versatile evaluation of the parameters characterizing the roughness of the profile, I have laid it out the processing and comparison of the results in several directions, depending on the influencing factors in the generating and calculation of the digital surface model from the software MeX 6.2.1. More specifically, I analyzed the obtained results of the profile parameters for the surfaces of the respective objects for different values of the tilt angle, different focal lengths of the lenses during image acquisition, for vertical or horizontal shapes as well as the position of the profile line, then for different selected sizes of the Region of Interest, for the cut-off wavelength λc, etc.

To first get a somewhat more straightforward overview of the results to be expected within the Profile Roughness Measurements module, it is necessary first to point out that this profile is designed as a measurement of individual roughness lines or a part of the object and, therefore often has distortions in the results, especially if the surface to be examined is huge or is not uniform within the scope of its illumination or if shadows occur, which is a weakness of these measurements. For this reason, depending on the analysis of profile roughness, it is necessary to define the length in the profile measurements.

It should be noted that the program for determining the profile roughness parameters usually performs measurements in the middle of the width of the generated model in the form of a horizontal line. However, this line that appears after the digital surface model is created can be a vertical, diagonal or any linear line, whether it is open or closed.

The comparison and analysis of the roughness of the profile are made in the context of the surface of the same object by some of the relevant parameters of the profile, then by the ordinate axis, also known as the z-l diagram, the histogram settings and in some instances by the BAC holding curve.

In the following subchapters, the results for some of the objects studied in this scientific work are presented graphically using the following figures.

5.1.1 Surface 1: Shot-blasted concrete surface

For this studied sample of the concrete surface, the results I will process, and compare come from two experiments with different focal lengths of the lens, taken from three different tilting angles $\alpha = 16.12°$, $\beta = 12.39°$, and $\gamma = 8.55°$, in the original and modified states, and for different sizes of the Region of Interest within the same attempt. After creating the digital surface model through the horizontal line displayed along the surface of the concrete, as part of the profile roughness measurements, the software gives us these parameter values as in the figures below:
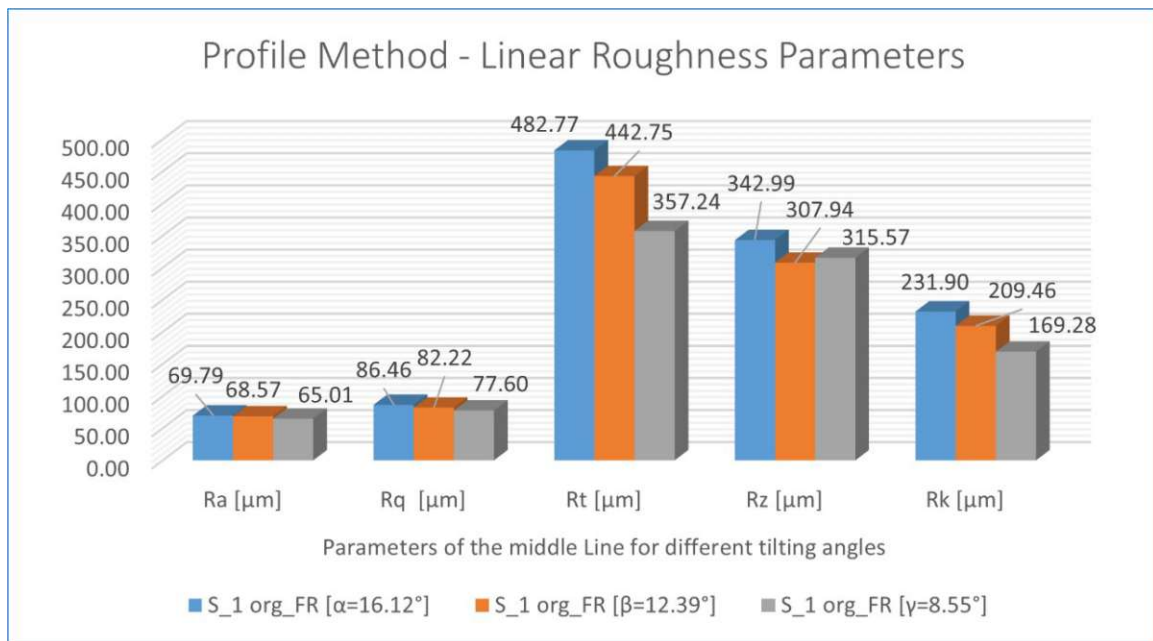
Figure 64: S_1 - Profile Roughness Parameters for different tilting angles

From the above values of the profile roughness parameters, we notice that for different tilt angles α, β or γ, there is a significant difference in the results only for the parameters Rt and Rk, while the parameters Ra, Rq and Rz give very similar results. However, using examples from other samples of concrete surfaces, I will show that this rule does not apply to all cases. This change in the results of the above parameters derives from the changes in the diagram of depth z and path length l, as can be seen in the following Figure 65:
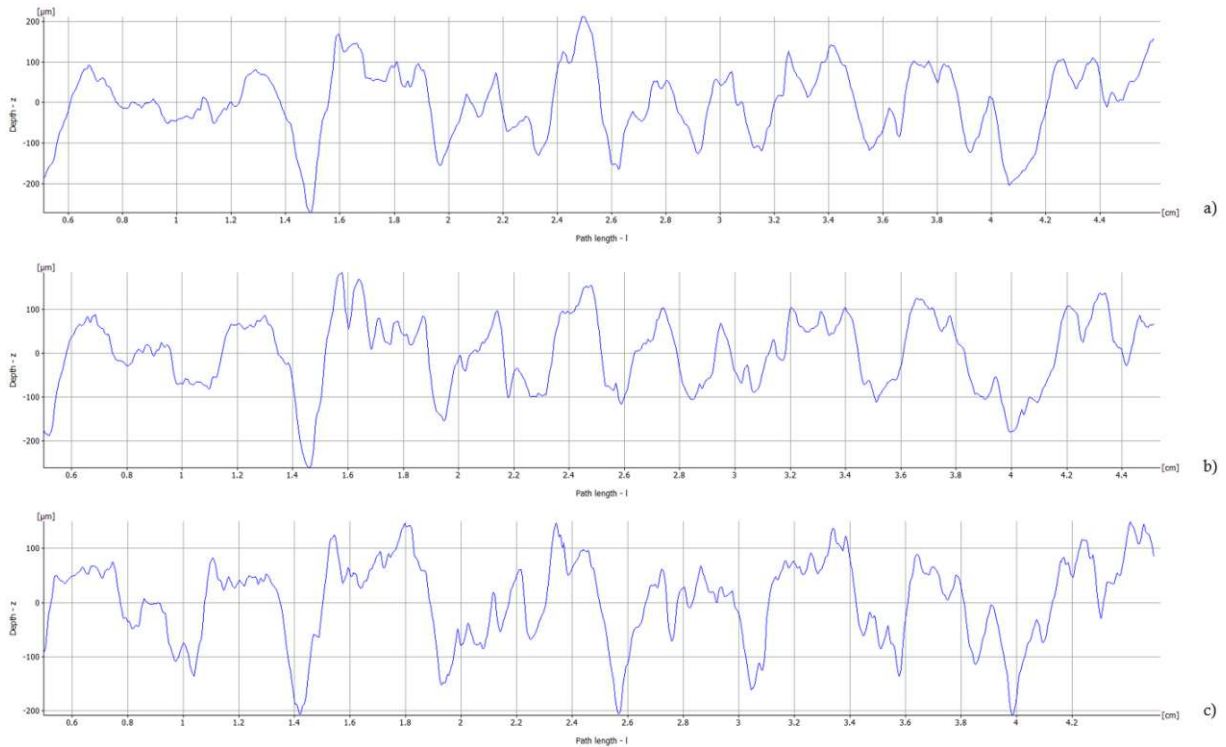
Figure 65: Surface_1 - Comparison of the Diagram z-l for different Tilting Angle
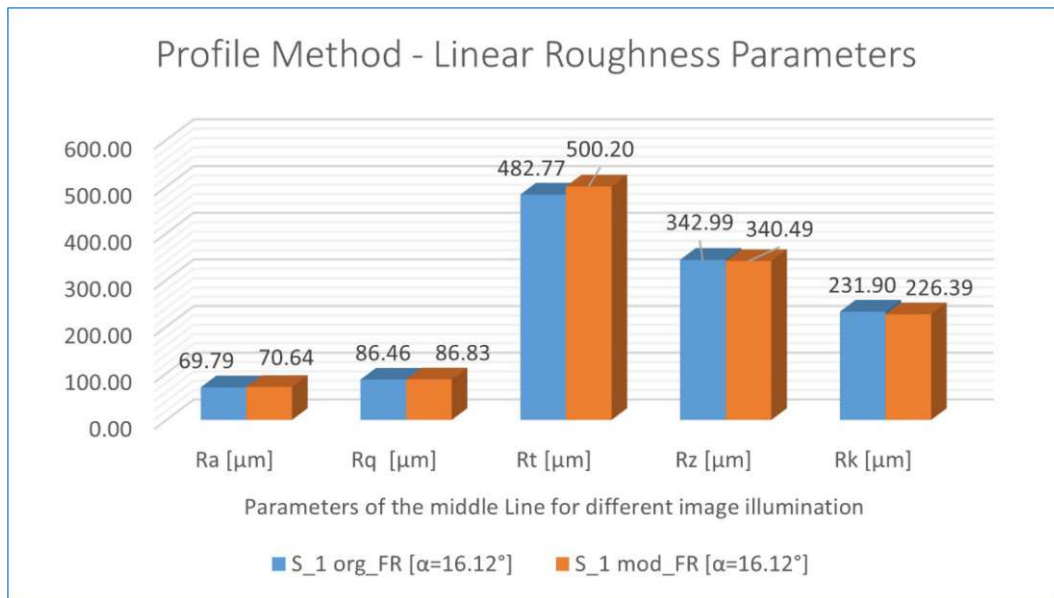
Figure 66: Surface_1 - Profile Roughness Parameters for different image illumination

With unchanged illumination, shading and contrast from the original state compared with the captured images with changed illumination, shading and contrast, the results of the values of almost all studied parameters are almost unchanged, except for some surface concrete samples, which we will discuss below. If the researcher implements and follows the basic instructions of the software, the results will be almost identical. In addition to the numerical data, we can also demonstrate this graphically using the values and positions of the depth of roughness parameters Rt of the **z-l diagram**, which are summarized and shown in the following Figure 67:

75
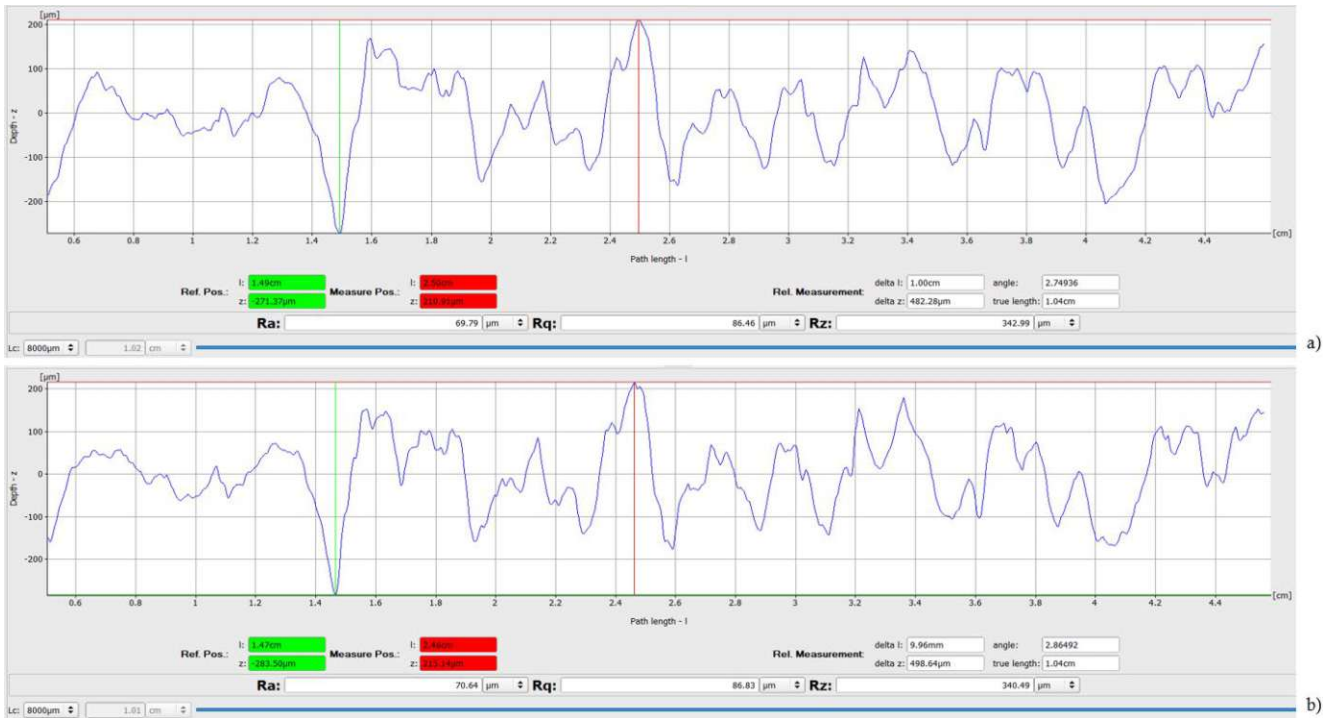
Figure 67: S_1 - Comparison of the Roughness depth Rt within the Diagram z-l for different image illumination
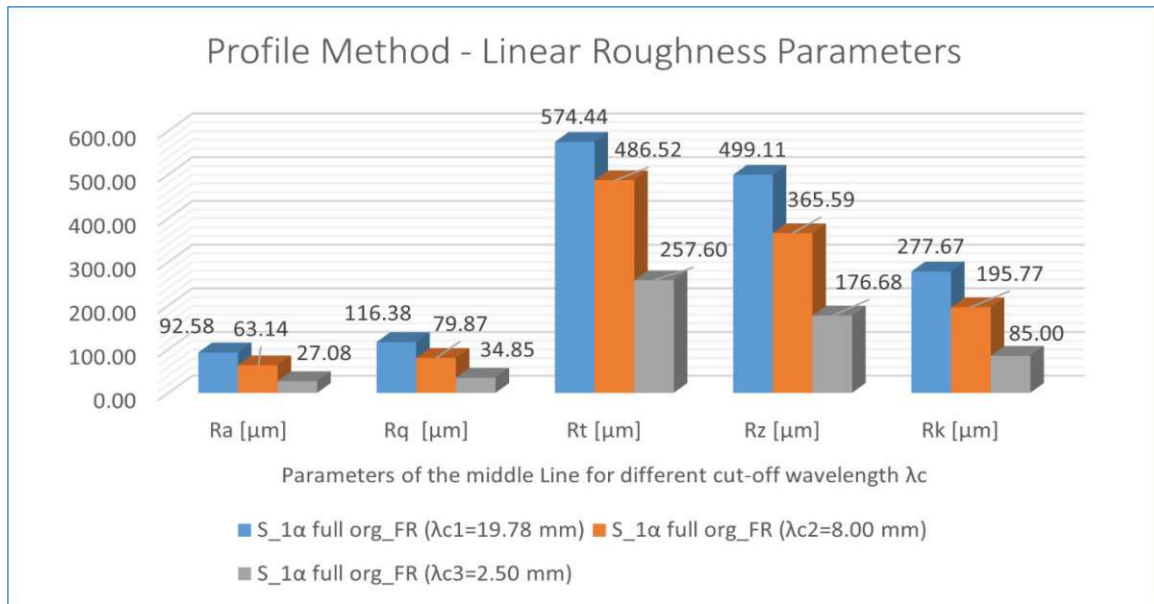
Figure 68: S_1 - Profile Roughness Parameters for different cutoff wavelength λc

From the obtained values, shown in the Figure 68 above, it is evident that for different values of the cutoff wavelength λc, all parameters of the roughness profile undergo drastic changes, ranging from 123% to 242% depending on the parameter. This type of change in the results of the profile parameters is encountered in almost all the samples of concrete surfaces studied, except for those that are porous or very flat, where the difference in the results ranges from 15 to 30%. Therefore, it should be emphasized that the selection of the cutoff wavelength λc depends on the size of the object under study, otherwise, the results may be unfavorable for the survey. By analyzing the sampling length **lr** in the framework

76

of the z-l diagram shown in the following Figure 69, we will show what is the difference in the shape of the diagram and in the size of this length, which for the cases of the largest objects studied, the small value of λc does not even satisfy the condition given by the standards, respectively **lr=λc**.
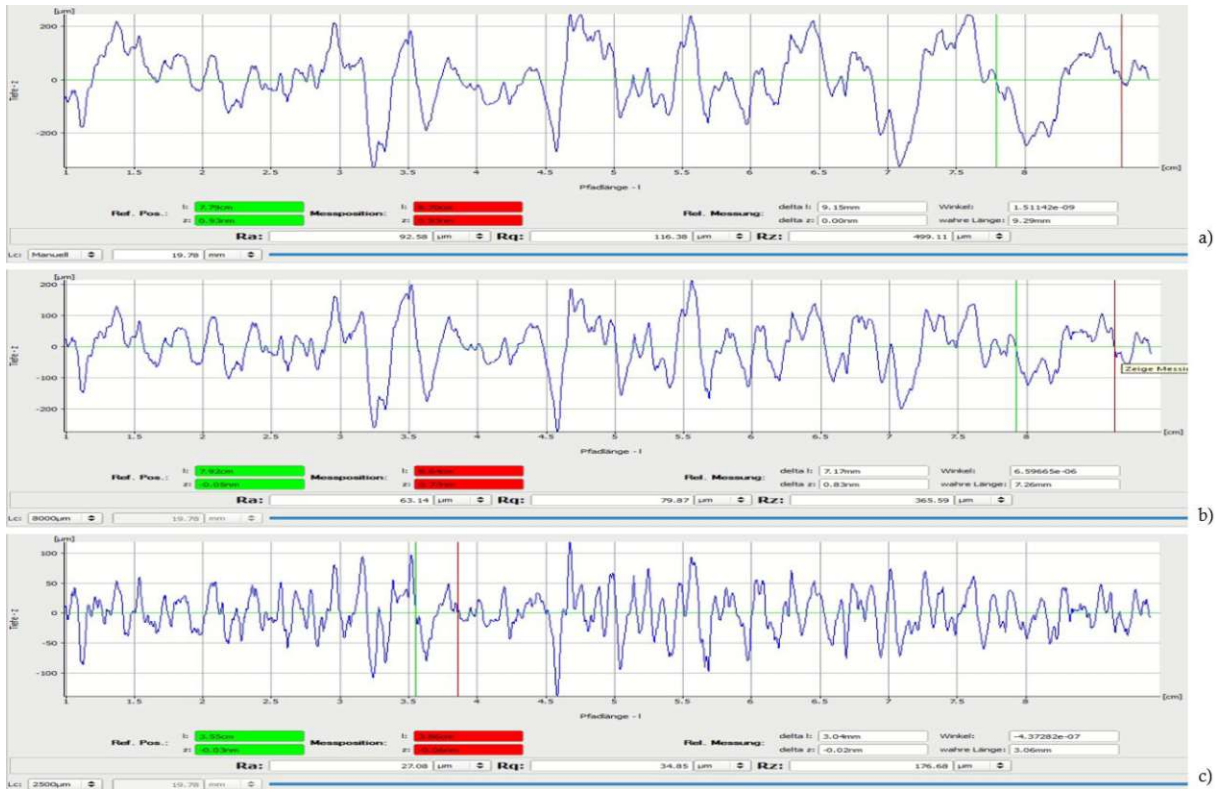
Figure 69: S_1 - Comparison of the sampling length lr for different cut-off wavelength λc – a) 19.78 mm, b) 8.0 mm and c) 2.5 mm

Results for the concrete surface taken with different lens focal lengths in two different attempts are presented and compared below.
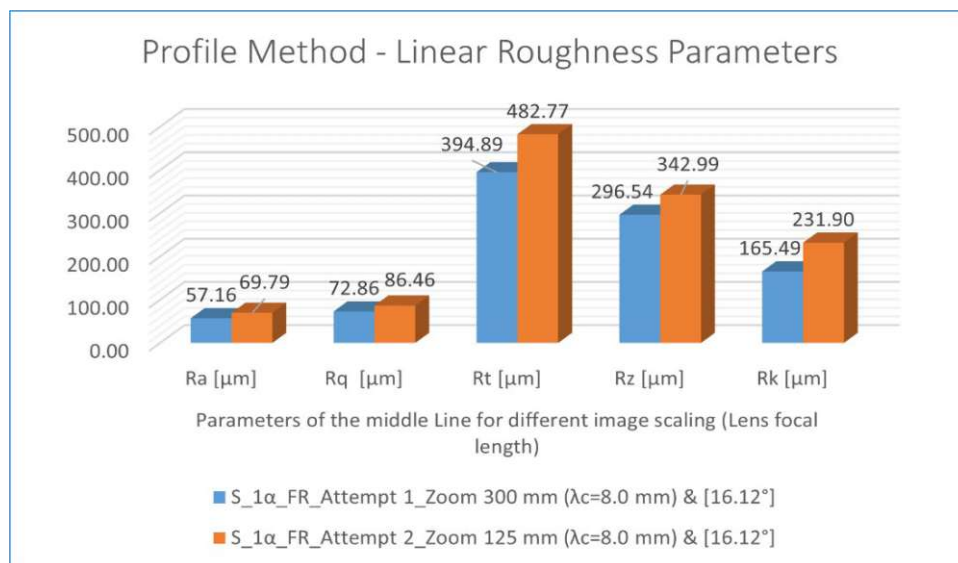
Figure 70: S_1 - Profile Roughness Parameters for different image scaling (Lens focal length)

The results of the parameter values for such an analysis vary depending on the type of concrete surface sample, as we will see in the following examples. However, in this case, the results of all the above parameters have shown a significant difference depending on the image scaling taken or the lens's focal length.

As the last case of the analysis of the profile roughness measurement module, I treated the obtained results of the currently known parameters as a function of the region of interest concerning the selected size of the concrete surface during the creation of the digital surface model for the same sample of the concrete surface, the same tilt angle, and the same cutoff wavelength λc:
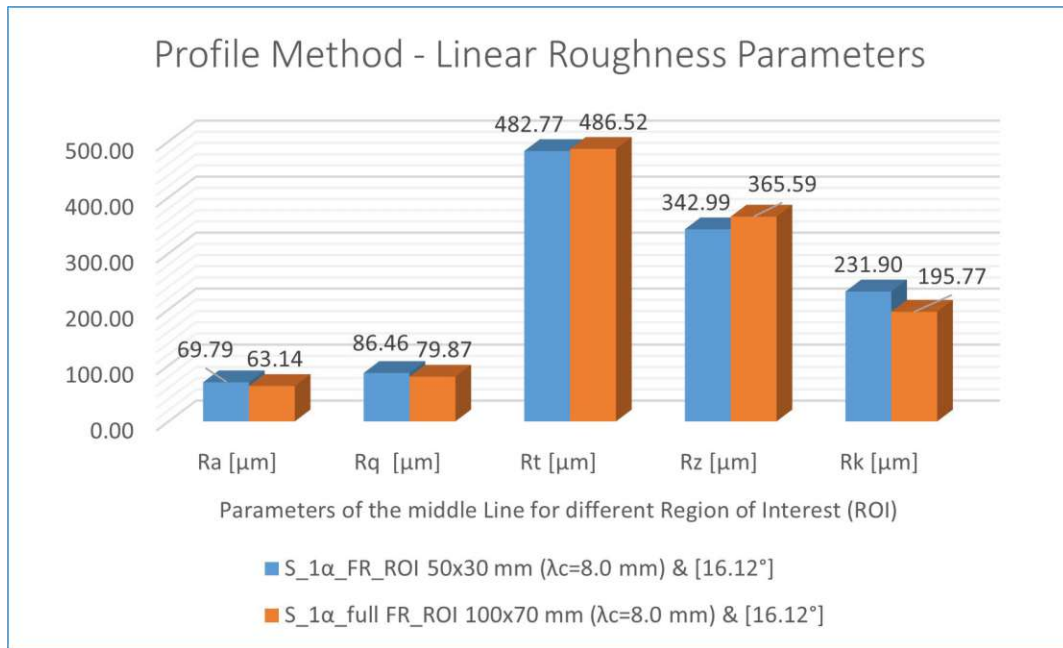
Figure 71: S_1 - Profile Roughness Parameters for different Region of Interest (ROI)

From the values of the above parameters Ra, Rq, Rt and Rz, we understand that almost each of them has a minimal difference. In contrast, only the value of the Rk parameter weighs a slightly more significant difference. The same situation is in almost all samples of the concrete surface, which I will present graphically below.

5.1.2 Surface 5: Foamed concrete

Also, for this sample of the concrete surface, as for surface 1, I processed and compared the parameters of the profile roughness modulus for the five influencing factors elaborated above, obtaining these results after creating the digital surface model and after the software calculations:

> For different Tilting Angles α, β and γ:
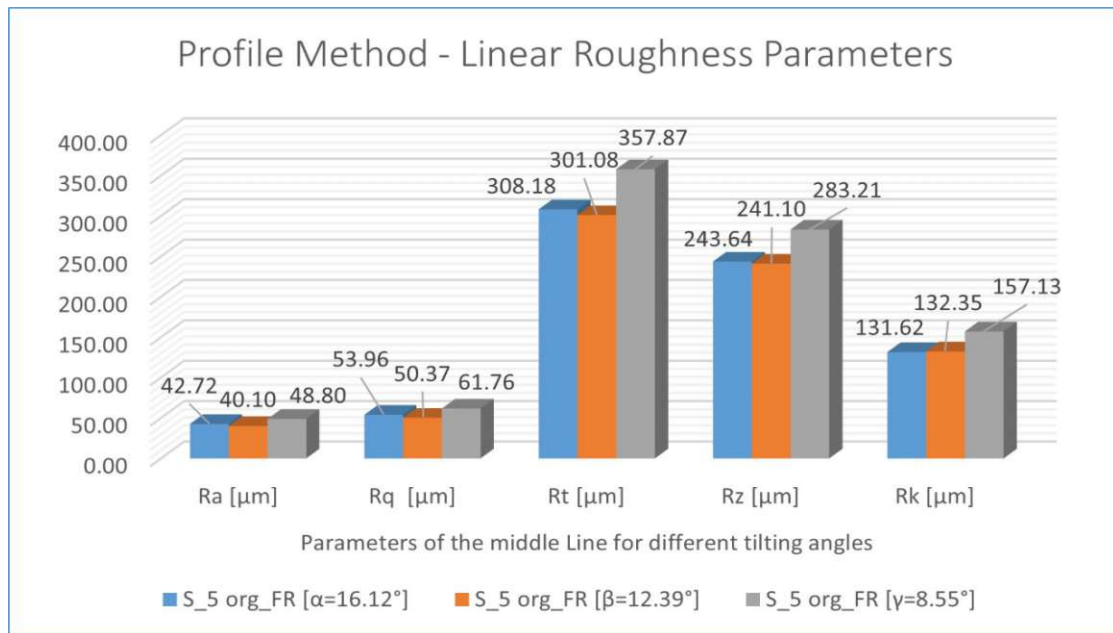
Figure 72: S_5 - Profile Roughness Parameters for different tilting angles

For this type of concrete surface, we note that the results for angles α and β are relatively the same for all parameters, while they change slightly for angle γ, albeit in small percentages, i.e., between 6 and 14%.

> For different Image Illumination, Shadow, and Saturation:
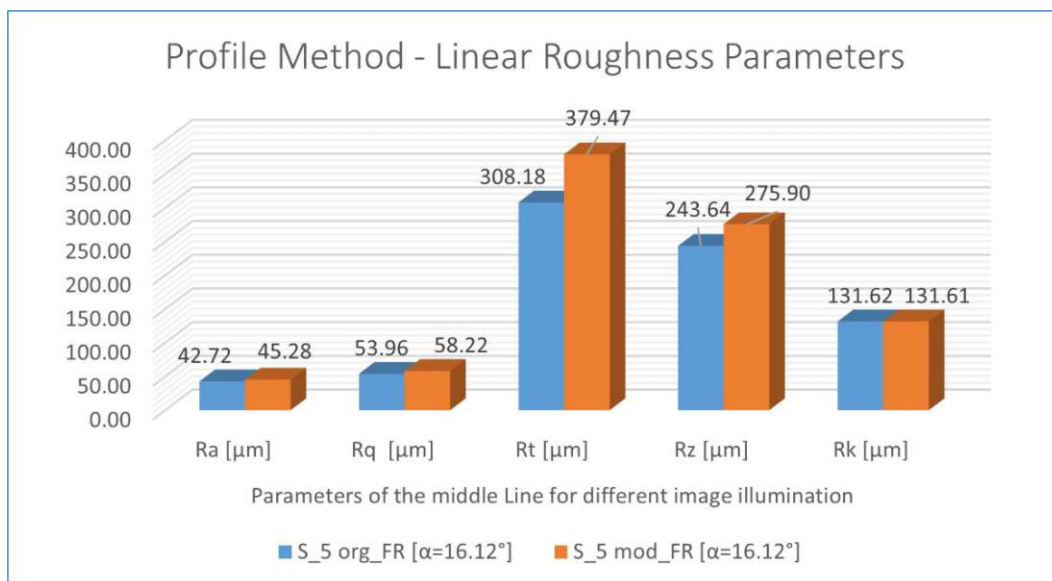
Figure 73: S_5 - Profile Roughness Parameters for different image illumination

The Figure 73 above shows very close values for the parameters Ra, Rq and Rk. In contrast, the values for the parameters Rt and Rz deviate by 23% and 13%, respectively, from the original state of the acquired images.

➢ For different Cut-off Wavelength λc_1, λc_2 and λc_3:
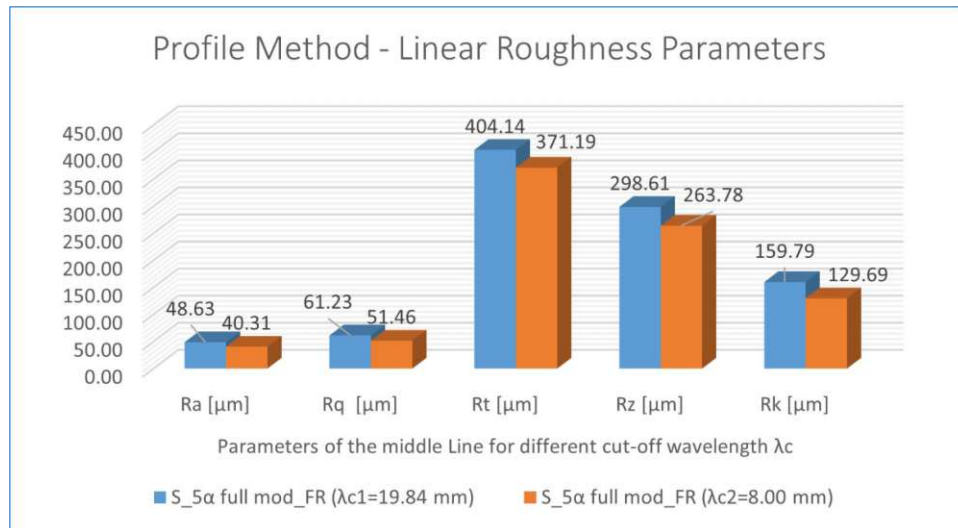
Figure 74: S_5 - Profile Roughness Parameters for different cutoff wavelength λc

In contrast to all the surfaces of the concrete specimens studied, for this type of surface, the difference in the results of all parameters as a function of the cutoff wavelength λc is much smaller and varies between 20 and 40%.

➢ For different Image Scaling (Lens focal Length) – Zoom 1 vs. Zoom 2:
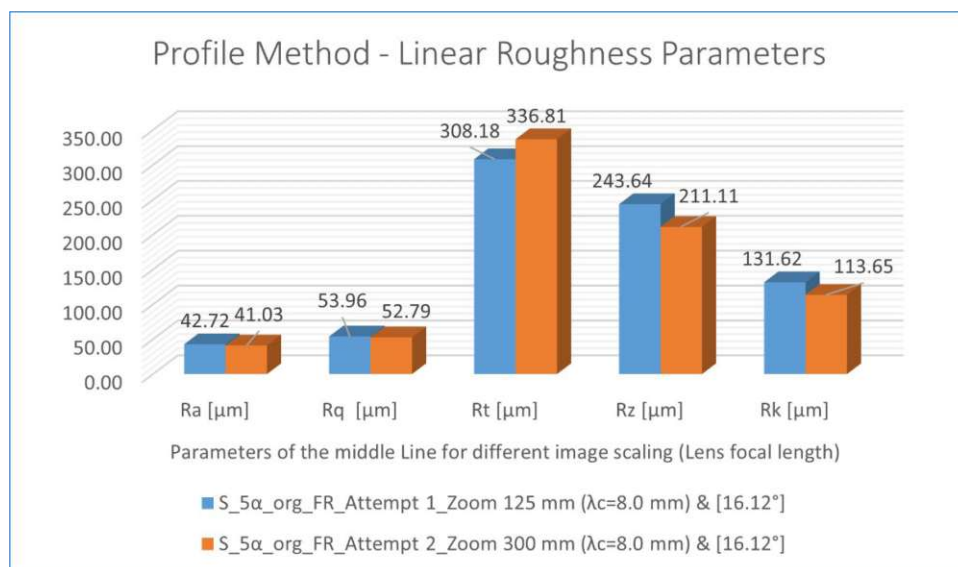
Figure 75: S_5 - Profile Roughness Parameters for different image scaling (Lens focal length)

For this type of influencing factor, the parameters Ra and Rq give almost the same results in this type of concrete surface, while Rt, Rz and Rk show variable results ranging from 10 to 16%.

➢ For different Region of Interest (ROI):
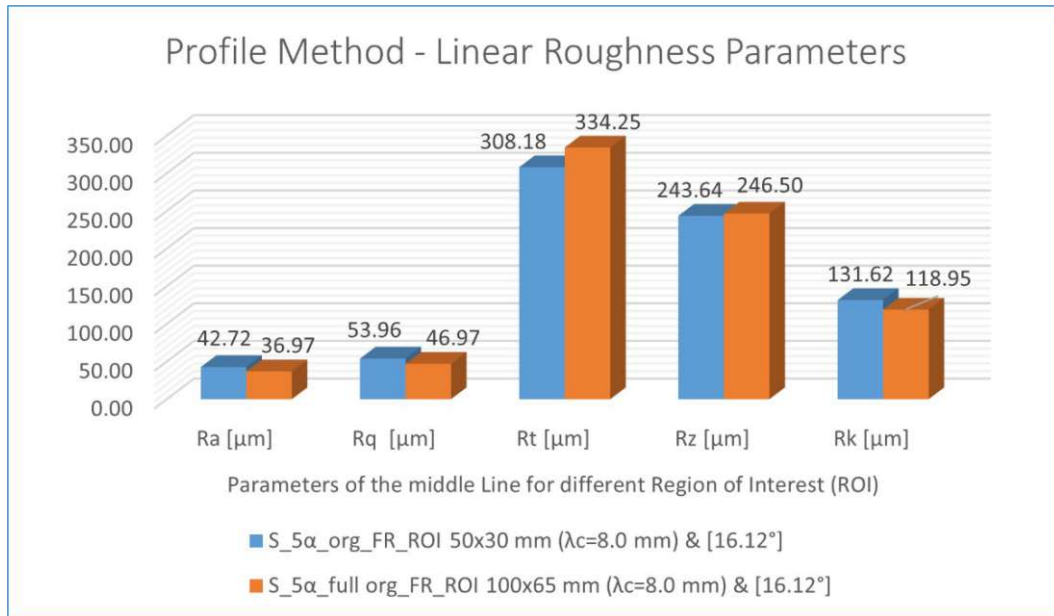
Figure 76: S_5 - Profile Roughness Parameters for different Region of Interest (ROI)

The results of the parameters for the different Regions of Interest for this type of concrete surface are also relatively close, with acceptable changes of 5-15%.

5.1.3 Surface 9: Concrete broom finish

The same as for surfaces 2 and 5, also for this type of concrete sample surface I took into consideration the five influencing factors for the calculation and comparison of the parameters of the profile roughness module, obtaining these results:

✓ For different Tilting Angles α, β and γ:
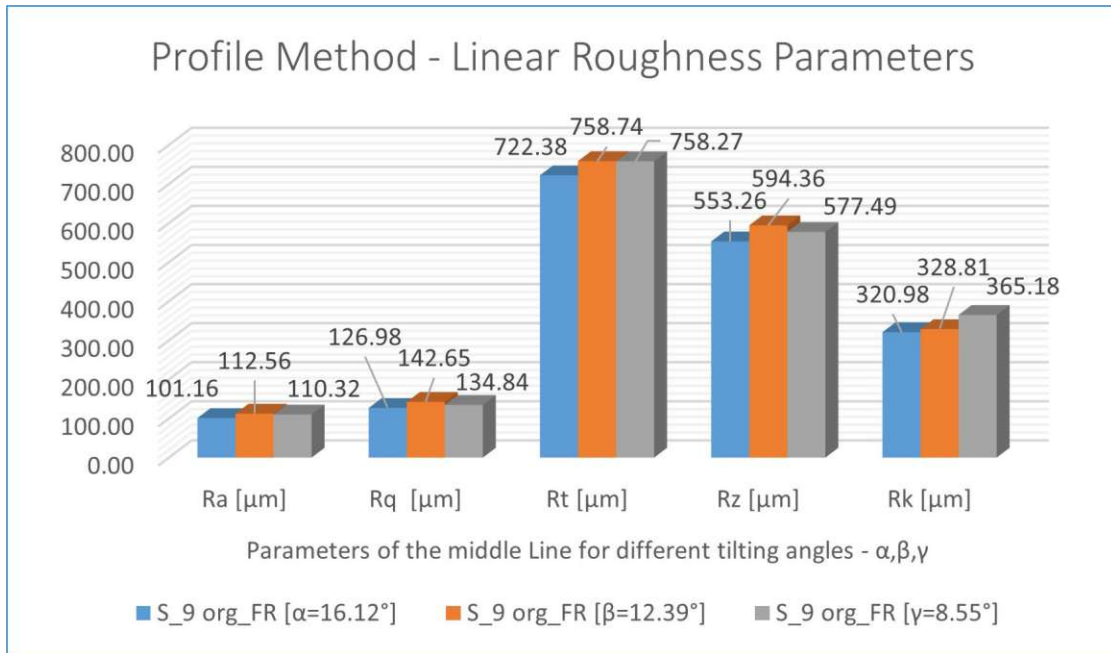
Figure 77: S_9 - Profile Roughness Parameters for different tilting angles

The obtained values of almost all parameters are slightly variable for angles β and γ, while for angle α the difference in the results is somewhat more pronounced but does not exceed the value of 15%.

✓ For different Image Illumination, Shadow, and Saturation:
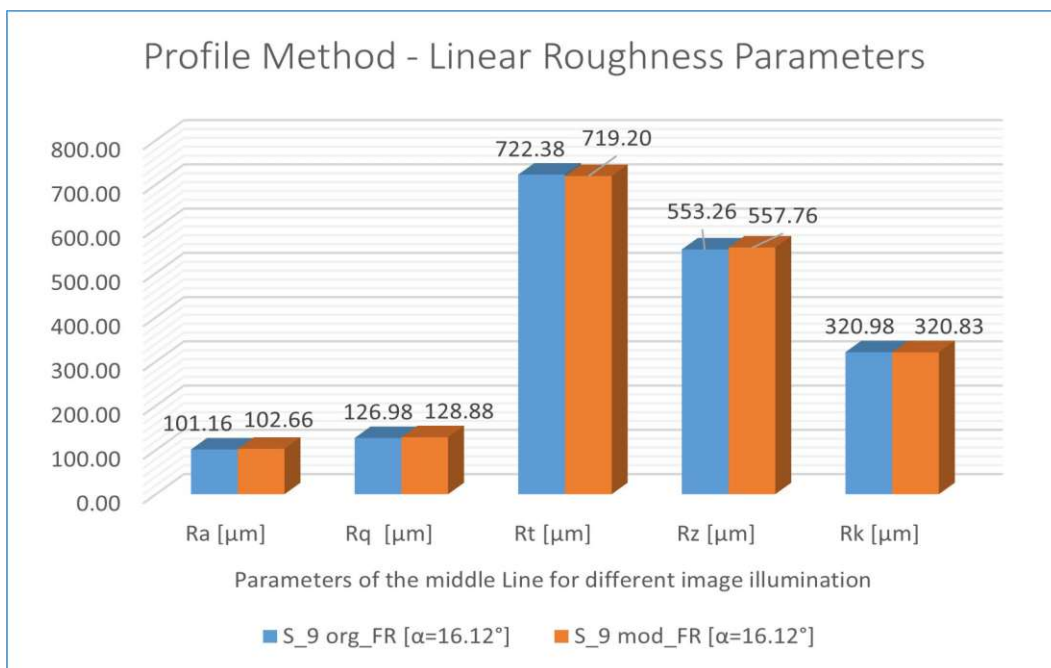
Figure 78: S_9 - Profile Roughness Parameters for different image illumination

In the context of this surface type, the results of the above parameters are almost identical for the original and modified Illumination, shadow, and saturation conditions.

✓ For different Cut-off Wavelength λc_1, and λc_3:
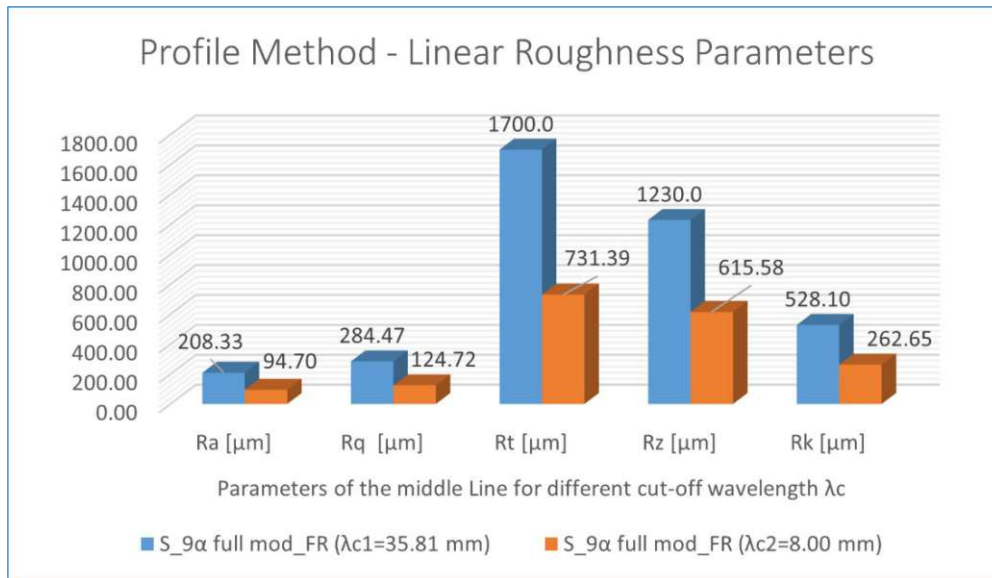
Figure 79: S_9 - Profile Roughness Parameters for different cutoff wavelength λc

As with almost all other surfaces elaborated, the difference in parameter results for different cutoff wavelengths λc is drastic, varying from 200 to 232% depending on the parameter.

✓ For different Image Scaling (Lens focal Length) – Zoom 1 vs. Zoom 2:
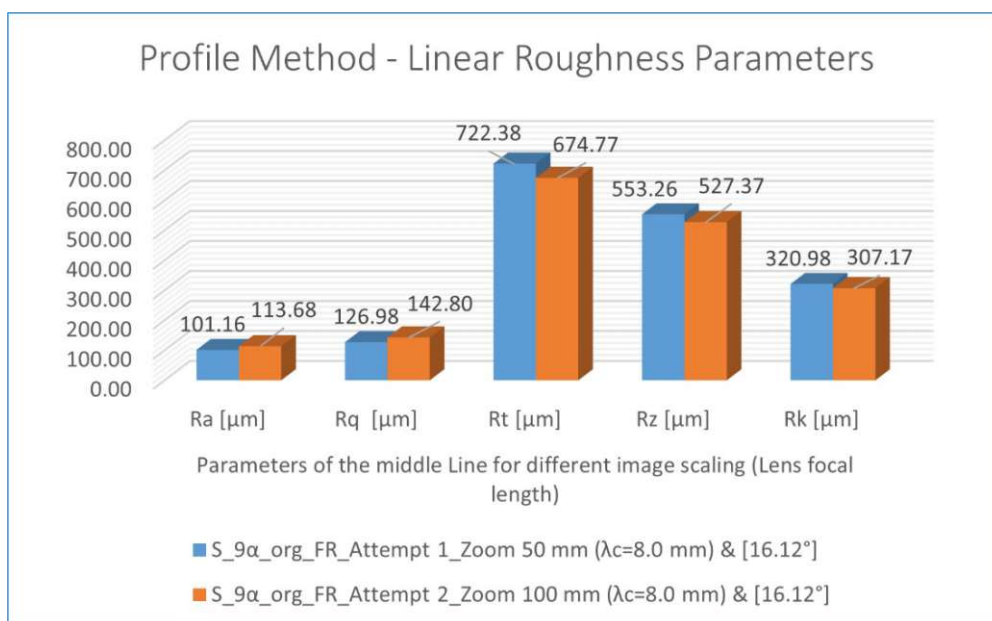
Figure 80: S_9 - Profile Roughness Parameters for different image scaling (Lens focal length)

The results of the analyzed parameter values for this surface type are close to each other for this influencing factor, except for the roughness depth parameter Rt.

✓ For different Region of Interest (ROI):
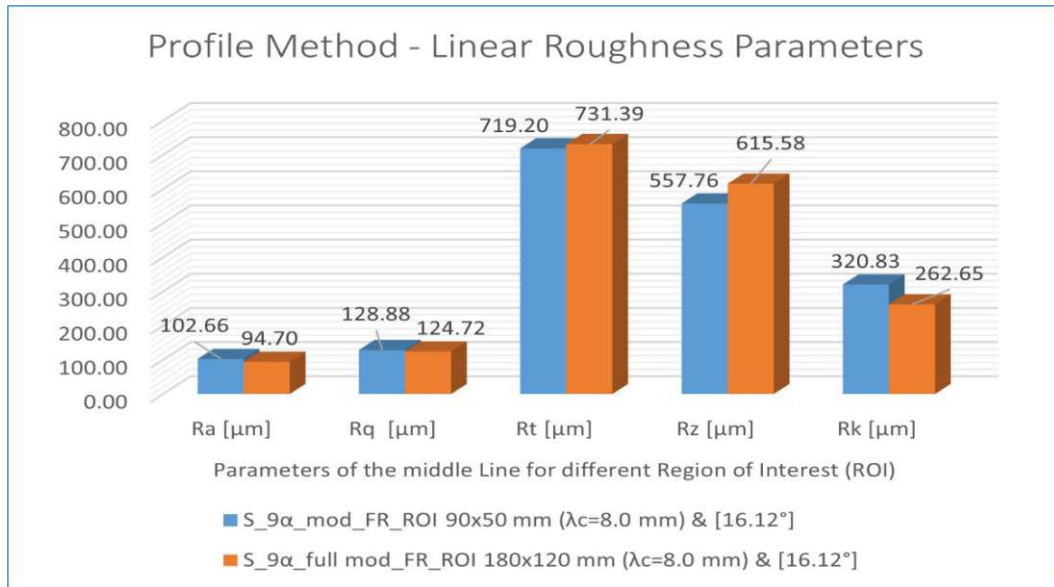
Figure 81: S_9 - Profile Roughness Parameters for different Region of Interest (ROI)

Within the Region of Interest, as an influencing factor for this type of concrete surface, we observe close results for the parameters Ra and Rq. At the same time, we have variable values for the parameters Rt, Rz and Rk, varying from 10-20%.

5.1.4 Surface 10: Precast smooth concrete (stone pavement)

For surface 10 of the concrete sample, I considered only these influencing factors with their respective results for the analysis of the roughness profiling module:

- For different Tilting Angles α, β and γ:
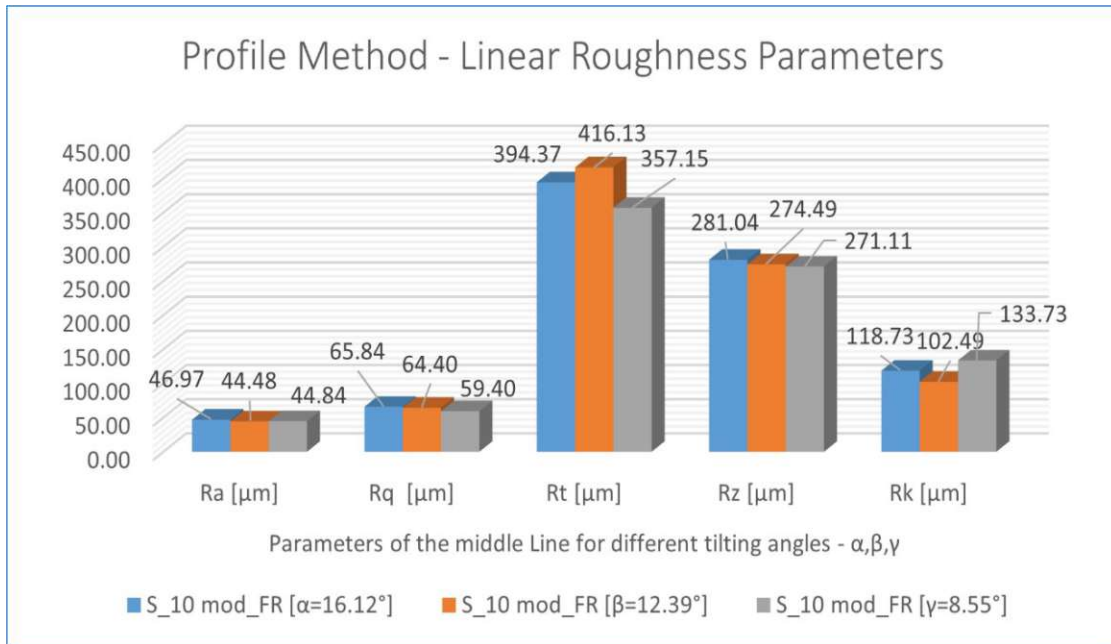
Figure 82: S_10 - Profile Roughness Parameters for different tilting angles

As in the case of surface 1, the values of the parameters Ra, Rq and Rz are almost the same for the type of concrete surface at different tilt angles, while for the parameters Rt and Rk the values of the results vary depending on the angle and the changes range from 17-31%.

- For different Image Illumination, Shadow, and Saturation:
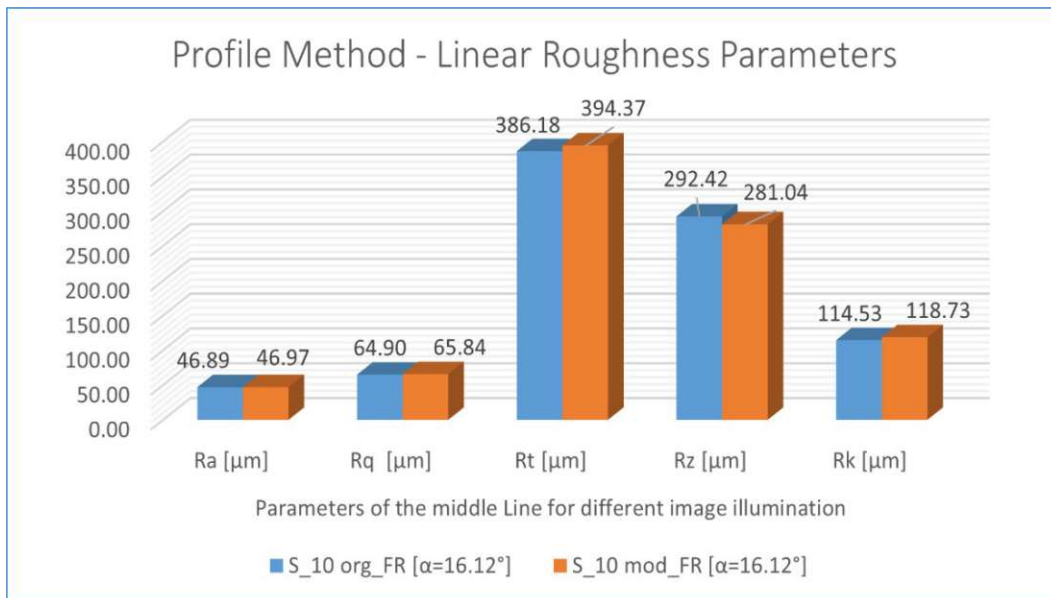
Figure 83: S_10 - Profile Roughness Parameters for different image illumination

From the above Figure 83, we can conclude that the values of almost all parameters are similar, with tiny and negligible changes. Thus, even with this type of concrete surface, the original or modified state of the acquired images does not lead to a change in the results.

- For different Image Scaling (Lens focal Length) – Zoom 1 vs. Zoom 2:
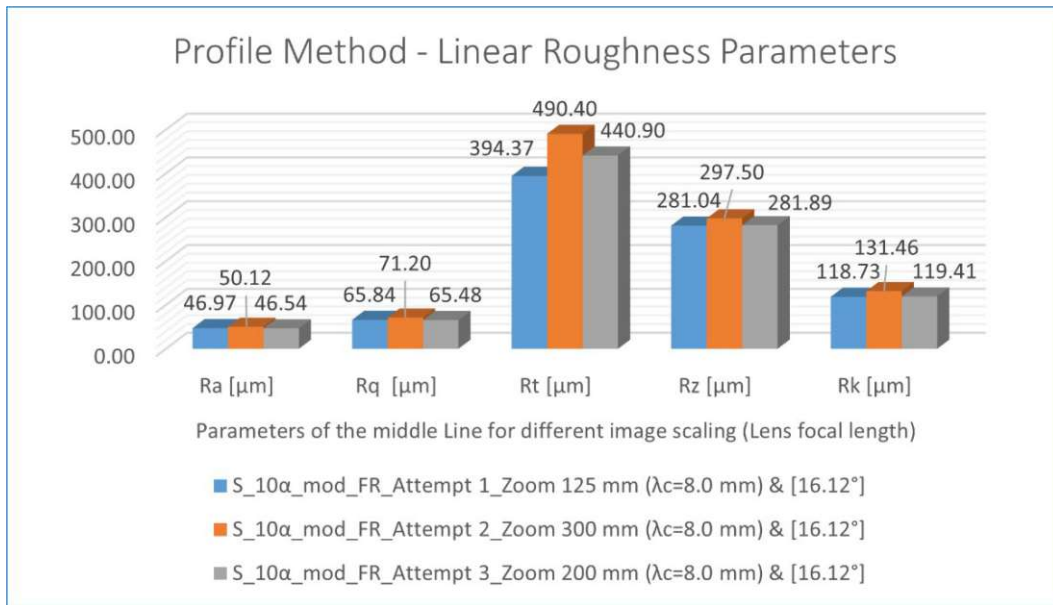
Figure 84: S_10 - Profile Roughness Parameters for different image scaling (Lens focal length)

Even for the image scaling obtained from different exposures with different lens focal lengths, all other parameters show similar values except for the parameter for the roughness depth Rt.

5.1.5 Surface 11: Precast concrete exterior staircase (rough-grained)

For the analysis of the roughness profile in the context of this surface, I treated only two of the influencing factors in the results of the parameters, where I consequently obtained these results:

o For different Tilting Angles α, β and γ:

86
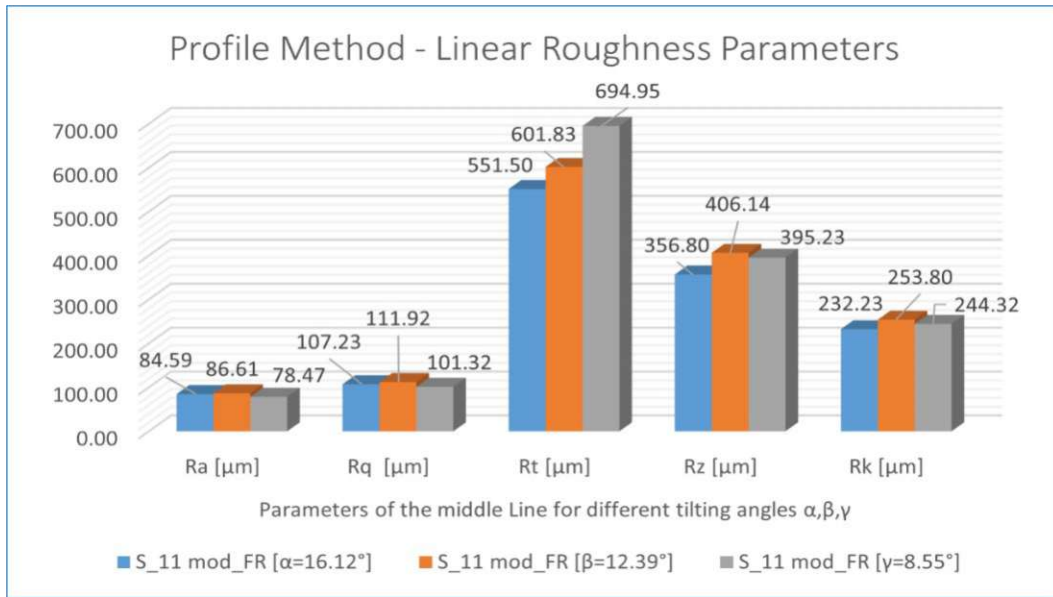
Figure 85: S_11 - Profile Roughness Parameters for different tilting angles

For this type of concrete surface, the most remarkable difference between the values obtained is observed for the parameter roughness Rt, with a change of about 26%. In contrast, for the other parameters, the changes in the values are about 10%.

o   For different Image Scaling (Lens focal Length) – Zoom 1 vs. Zoom 2:
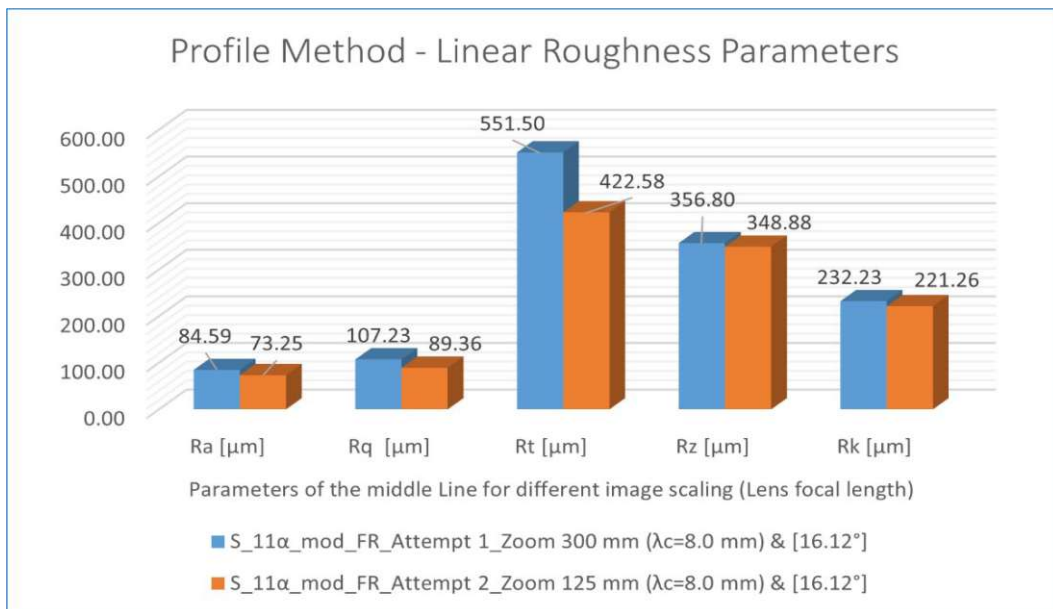
Figure 86: S_11 - Profile Roughness Parameters for different image scaling (Lens focal length)

Based on the values of the above parameters, there is a huge difference in the result for the parameter Rt, which exceeds 30%, then more minor differences for the parameters Ra and Rq. In contrast, the difference in the results is almost negligible for the parameters Rz and Rk.

5.1.6 Surface 12: Concrete sanded outside

As with Surface 11, I have addressed only two of the factors influencing profile roughness for concrete surfaces and have arrived at these relevant results:

- For different Tilting Angles α, β and γ:
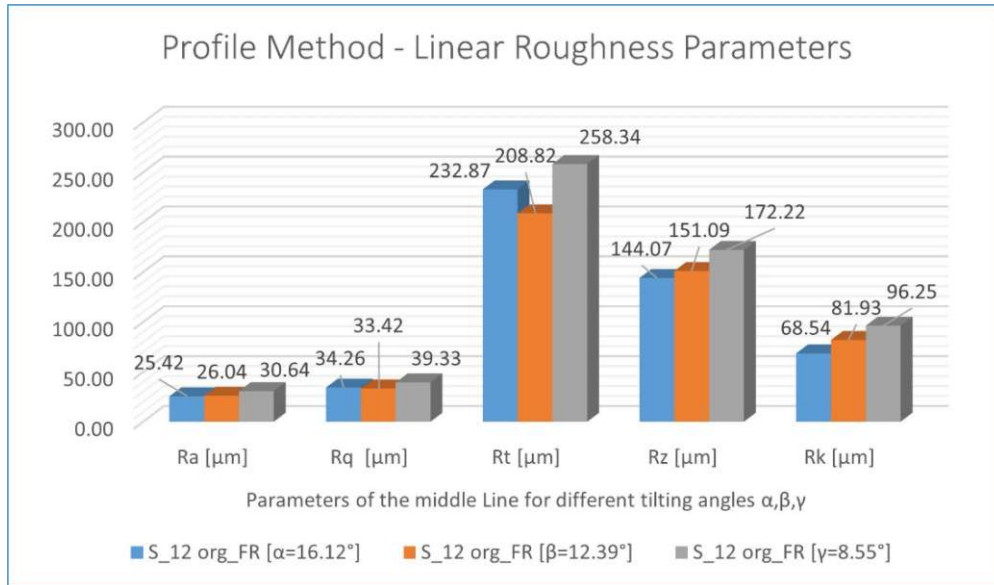
Figure 87: S_12 - Profile Roughness Parameters for different tilting angles

Since surface 12, like surface 5, is very flat, also in this case, the results for the parameters Rt, Rz, and Rk showed the most considerable differences compared to the results for the parameters Ra and Rq, which also makes the tilt angle an essential factor in the characterization of concrete surfaces, especially when the surfaces are very well leveled.

- For different Image Scaling (Lens focal Length) – Zoom 1 vs. Zoom 2:
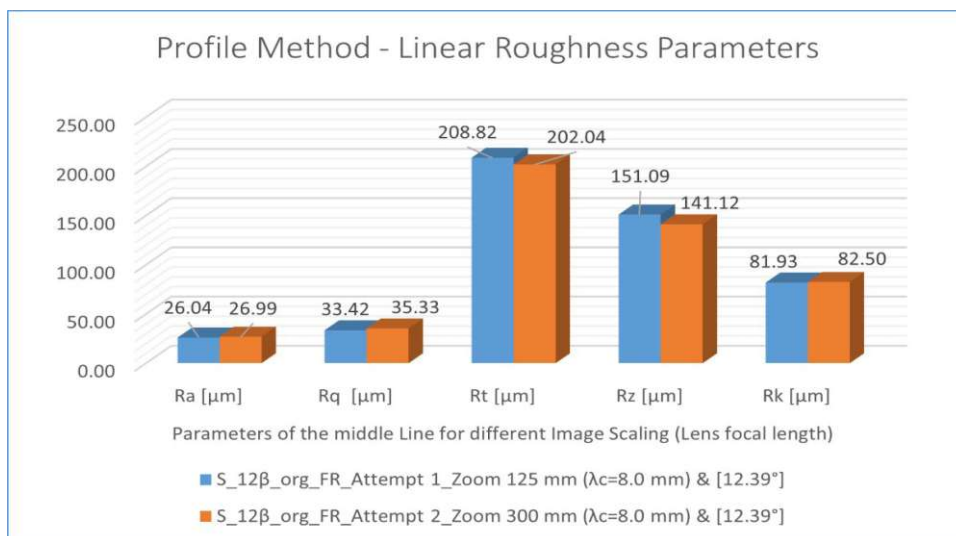
Figure 88: S_12 - Profile Roughness Parameters for different image scaling (Lens focal length)

The above results show that the results of all parameters for different image scaling are very similar for this type of concrete surface.

5.1.7 Surface 13: Plinth in-situ concrete, smoothed

Like surfaces 11 and 12, the influencing factors treated for this type of surface of the concrete sample are listed below, along with the obtained results of the parameters:

➕ For different Tilting Angles α, β and γ:
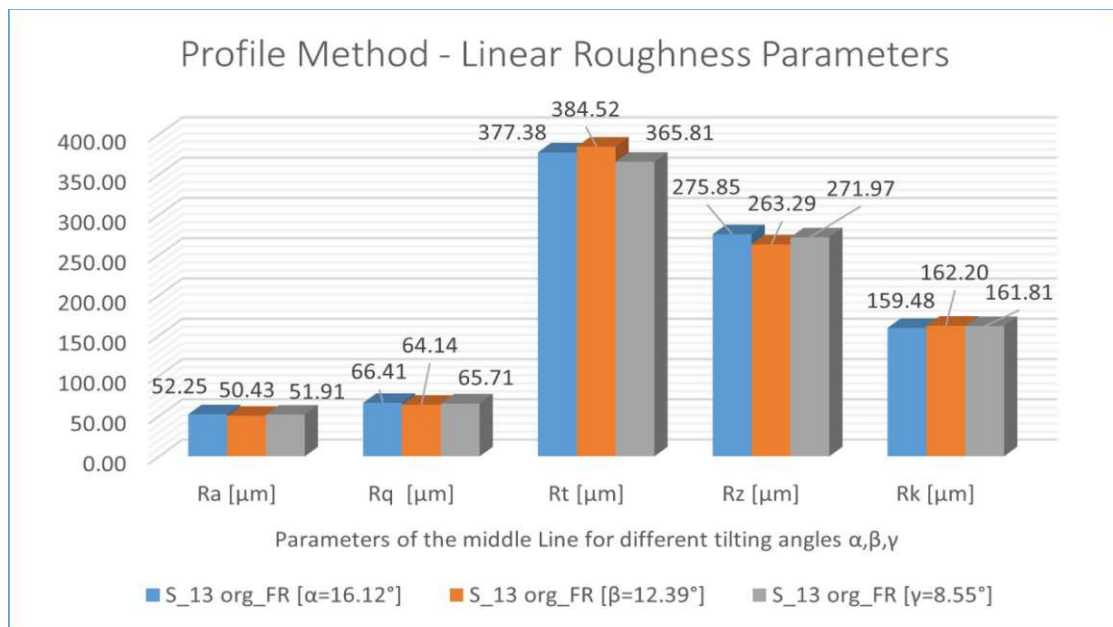
Figure 89: S_13 - Profile Roughness Parameters for different tilting angles

It is clearly observed that among all the analyzed parameters, there is a significant difference in the results for different tilt angles for this type of concrete surface.

➕ For different Image Scaling (Lens focal Length) – Zoom 1 vs. Zoom 2:
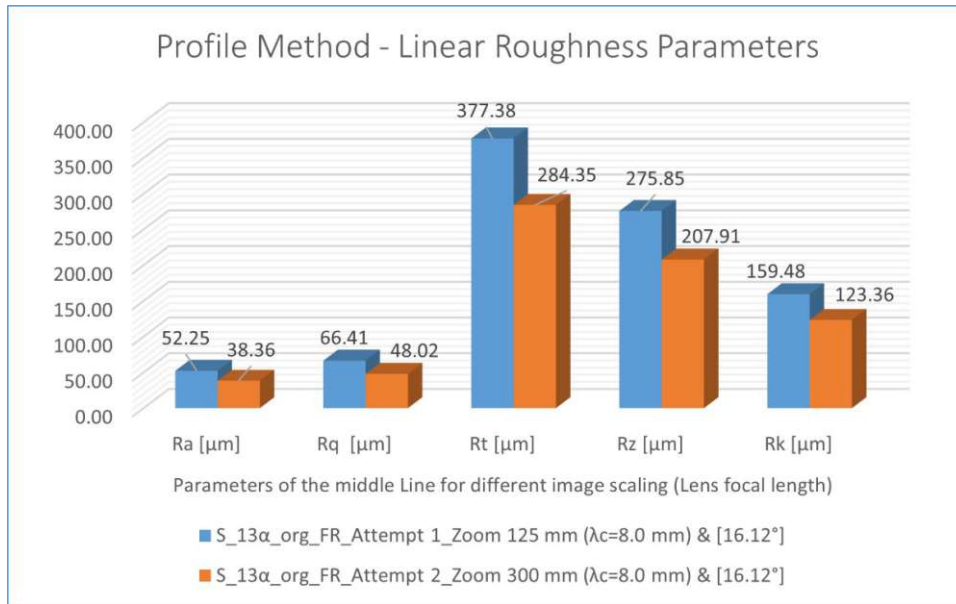
Figure 90: S_13 - Profile Roughness Parameters for different image scaling (Lens focal length)

With characteristics very similar to surface 1, this concrete surface also presents variable values of all analyzed parameters with a degree of change of 30-40%.

5.1.8 Surface 16: Concrete terrace slabs

Since this concrete surface served as tiles for the outdoor terrace, I considered it necessary to consider all possible influencing factors related to the parameters of profile roughness. In the following, I have elaborated on each of them and presented them in figures together with the obtained results:

❖ For different Tilting Angles α, β and γ:
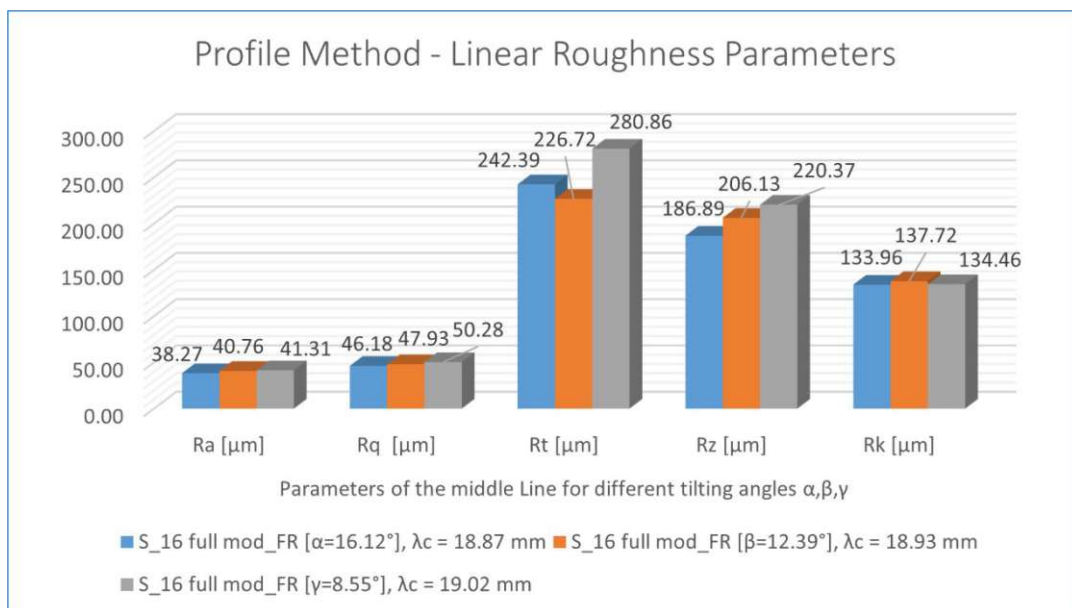
Figure 91: S_16 - Profile Roughness Parameters for different tilting angles

90

For different tilting angles, surface 16 gives almost the same values for the parameters Ra, Rq, and Rk. In contrast, the values for the parameters Rt and Rz vary significantly by up to 25%.

❖ For different Image Illumination, Shadow, and Saturation:
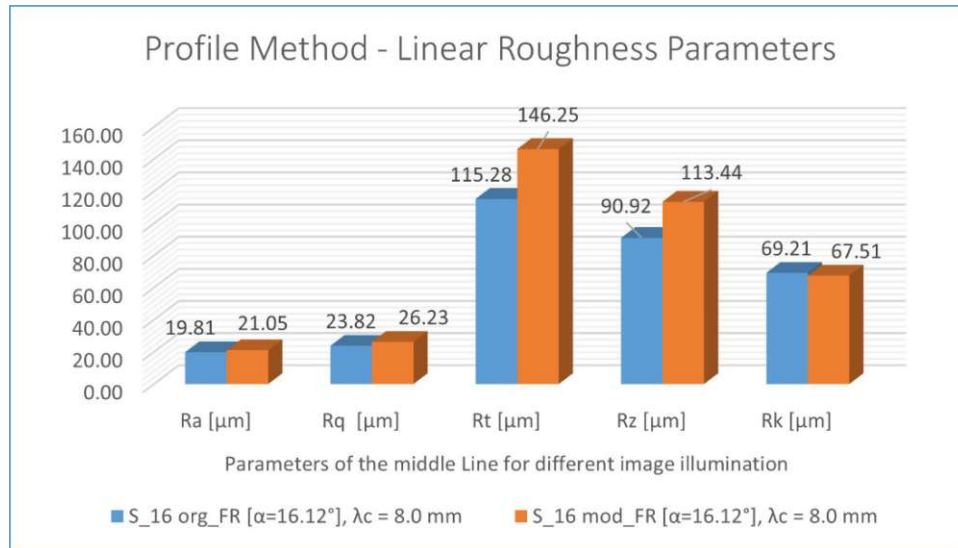
Figure 92: S_16 - Profile Roughness Parameters for different image illumination

Since this type of concrete slab is colored, the illumination, shading, and saturation factors from the original and the modified state of the image capture are more pronounced, at least for the parameters Rt and Rz, in the amount of 25-30%. In contrast, for the other parameters, the values are almost similar.

❖ For different Cut-off Wavelength λc_1, λc_2 and λc_3:
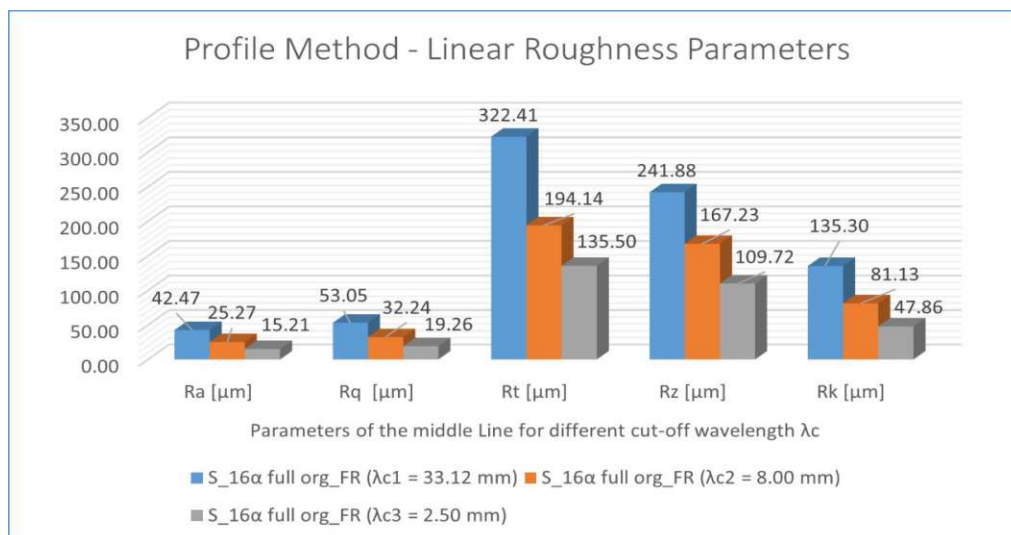
Figure 93: S_16 - Profile Roughness Parameters for different cutoff wavelength λc

As in the case of most of the surface types of the concrete specimens studied, the change in the cutoff wavelength λc also changes the values of each of the analyzed parameters in these terrace concrete tiles in the range of 220-285% as a function of the value of λc in an almost symmetrical manner. For this reason, I recommend that in similar investigations

on concrete surfaces, the value of λc should be adjusted to the size of the object under study to obtain optimal results.

❖ For different Image Scaling (Lens focal Length) – Zoom 1 vs. Zoom 2:
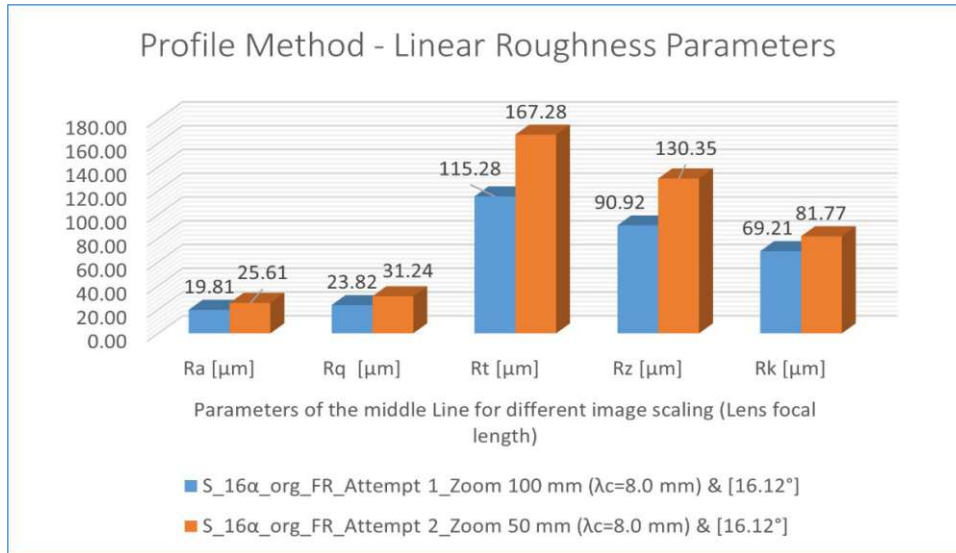
Figure 94: S_16 - Profile Roughness Parameters for different image scaling (Lens focal length)

Since the recorded surface from the first and second attempts shows an enormous difference, it was expected that the obtained results would also give variable values, especially for the parameters Rt and Rz, while the changes in the results for the parameters Ra, Rq, and Rk are within the same limits as for most other surfaces treated above.

❖ For different Region of Interest (ROI)
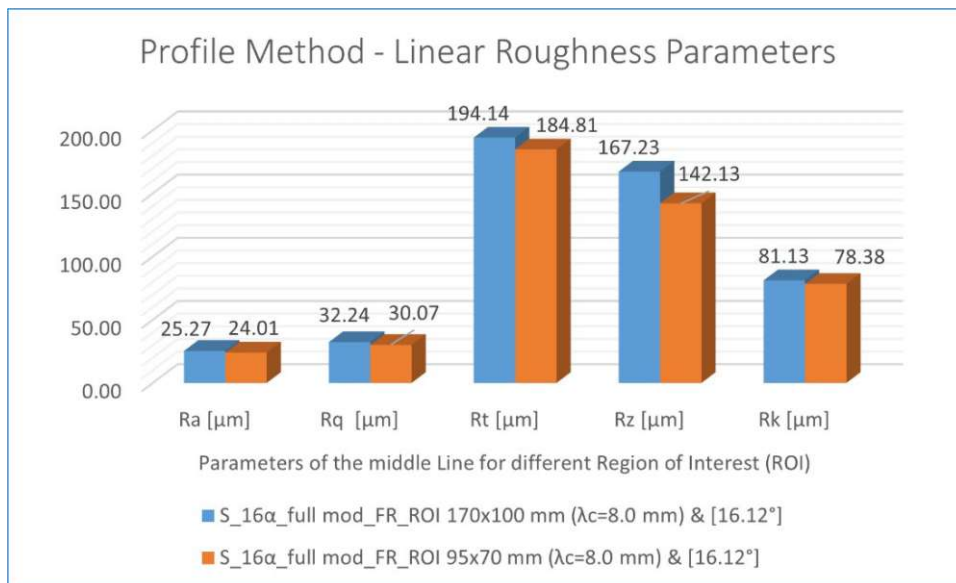
Figure 95: S_16 - Profile Roughness Parameters for different Region of Interest (ROI)

Analogous to the lens's focal length and for the Region of Interest, the result of the parameters changes in the same proportion, i.e., the parameters Rt and Rz vary slightly, while the parameters Ra, Rq, and Rk have almost identical values among themselves.

92

5.2 Results of the Texture Roughness Measurement Module

First, we give the dimensions of the measured and filtered surface for each of the concrete samples studied, to make the reading and comparison of the results as understandable as possible.

For the texture roughness measurements, as with the profile roughness measurements, we also evaluate the results calculated from the creation of the digital surface model for the same factors, although here we will focus somewhat more on the analysis of the histogram values and their significance, and the analysis of the BAC load curve values and their significance. We should also mention that the values of the parameters in this module are directly related to the shape or size of the surface selected for analysis, since the value of the cutting wavelength λc also depends on it. When manually changing this value, graphically displaying the roughness of the surface in a small frame, we can at least get an idea of whether the selected value is approximately the correct one. To illustrate the relationship between the cutoff wavelength and the surface roughness based on the obtained value of the depth, I will explain in the following examples the obtained values of a non-concrete surface whose roughness peaks I measured experimentally in the laboratory and presented in the above chapter.

I will also estimate that the values of the histogram setting vary within the analyzed surface of the same object depending on the size of the region of interest in the analysis. More specifically, I focused on describing the width of the histogram class for the surfaces of the treated examples as a function of the various factors mentioned above. Special attention was paid to the standard deviation and its comparison for different cases and the red and yellow lines of the histogram, respectively.

BAC compares the shape, depth, and parameter values of the ultimate load curve to determine if the required criterion of 40% is met.

Although the program calculates a vast number of surface roughness parameters during the creation of the digital surface model, I have focused only on the essential parameters, such as Sa, Sq, Sz, Sk, Smr1, Smr2.

In the following, the results from the creation of the digital surface model and the software calculation of the parameters of the surface roughness measurement module for the different samples of the concrete surfaces are processed, compared, and elaborated by the influencing factors mentioned below:

5.2.1 Results obtained within the analysis of the tilting angle α, β, γ:

To process, compare and analyze the parameters obtained from the texture roughness measurement module for different tilt angles, I will treat the surfaces of the following concrete samples:

- Surface 1: Shot-blasted concrete surface

In this analysis, three surfaces of the digital surface model with different tilting angles were examined. The surface from angle α had dimensions of 4.06 x 2.55 cm, with a true area of 10.78 cm² and a projected area of 10.28 cm². The surface from angle β had dimensions of

4.02 x 2.50 cm, with a true area of 10.66 cm^2 and a projected area of 10.01 cm^2. The surface from angle γ had dimensions 4.06 x 2.54 cm, with a true area of 10.96 cm^2 and a projected area of 10.23 cm^2. The cutoff wavelength λc is assumed to be 8.0 mm for all three angles.
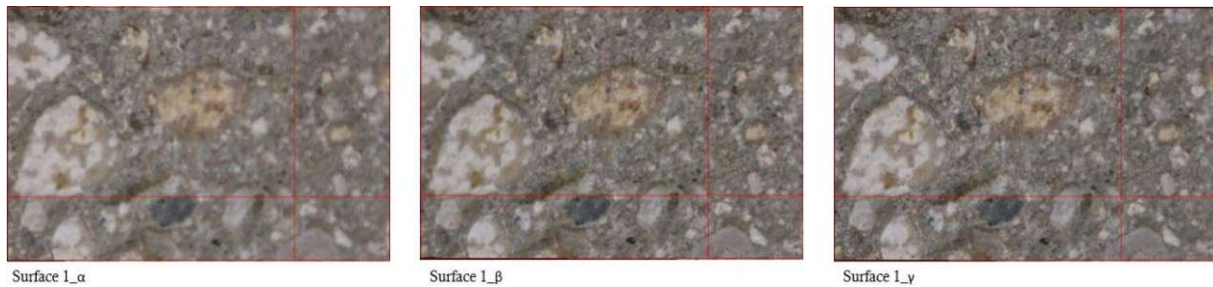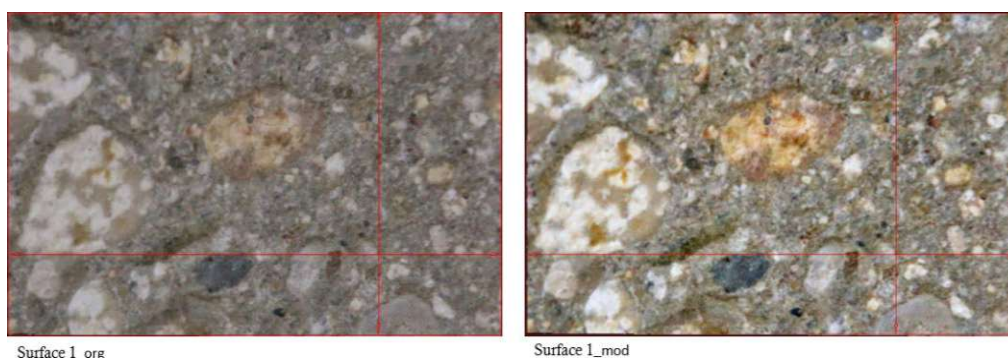

Figure 96: S_1 - Attempt 1 org FR for different tilting angles

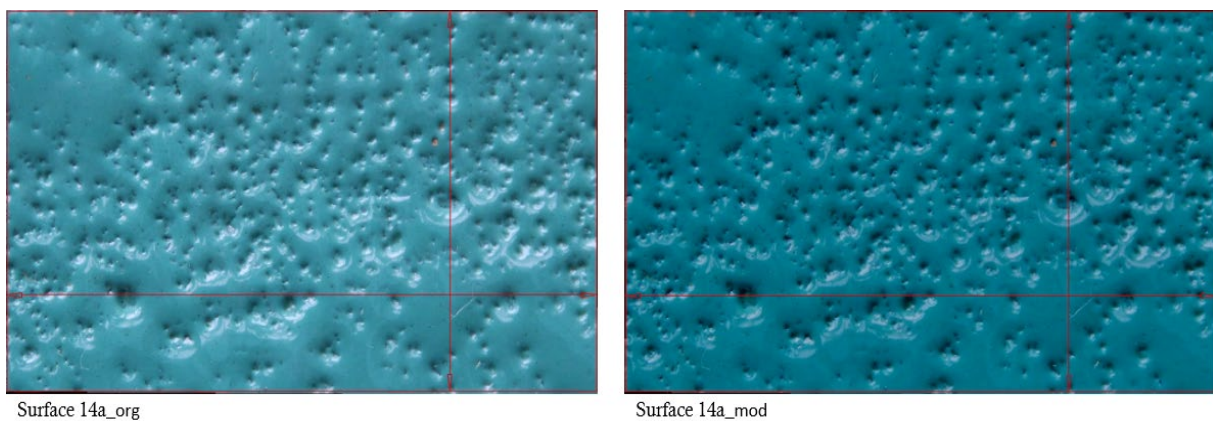The following parameter values were obtained from the software calculations:
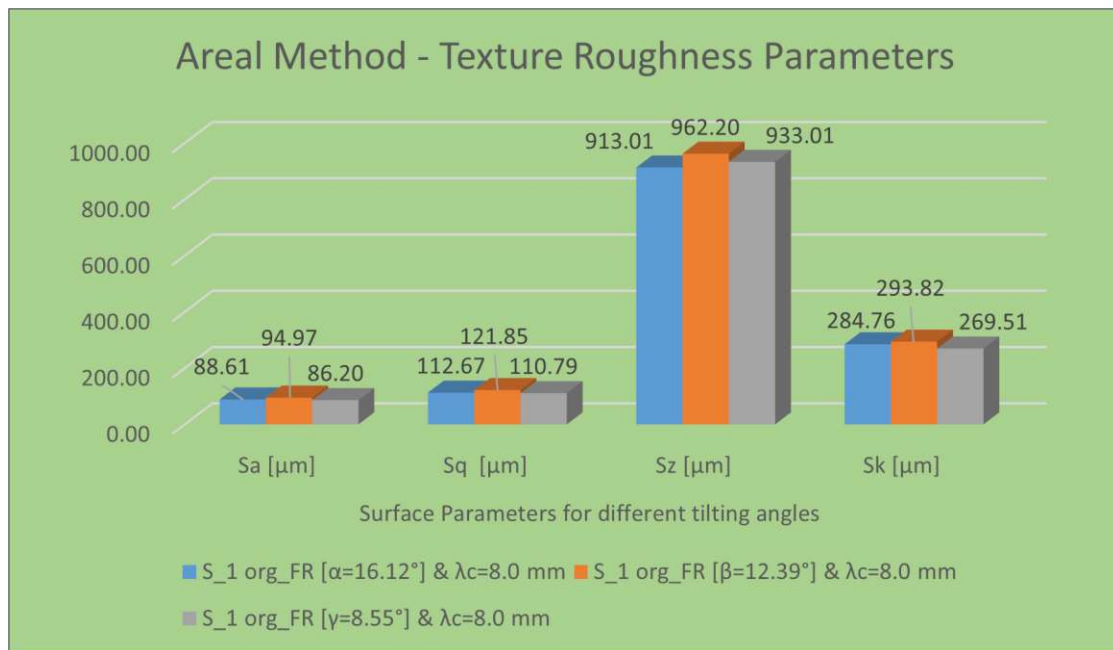
Figure 97: S_1 - Texture Roughness Parameters for different tilting angles

As can be seen from the Figure 97 above, the values of the surface roughness parameters are relatively similar, with very slight differences, which can also be seen from the approximate values of their standard deviations: 112.67 μm for angle α, 121.84 μm for angle β, and 110.79 μm for angle γ. Moreover, the class width of the Histogram is 8 μm in all three cases. The shapes and the maximum and minimum values of the histograms of these three cases for the surface texture also do not show such large differences. For the surface from angle α, the values are within a maximum of 425 μm and a minimum of -495 μm. For the surface from angle β, the values are between a maximum of 415 μm and a minimum of -510 μm. For the surface from angle γ, the values are within a maximum of 480 μm and a minimum of -455 μm.

The depth, shaping and values of Smr1 and Smr2 parameters associated with the strip width for all three load curves of the mentioned surfaces are shown in the following figures:
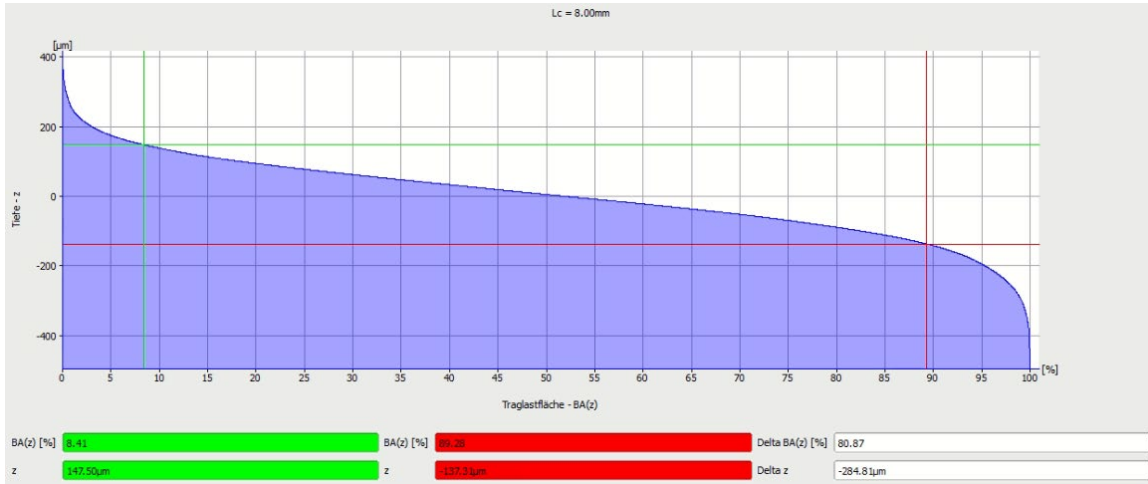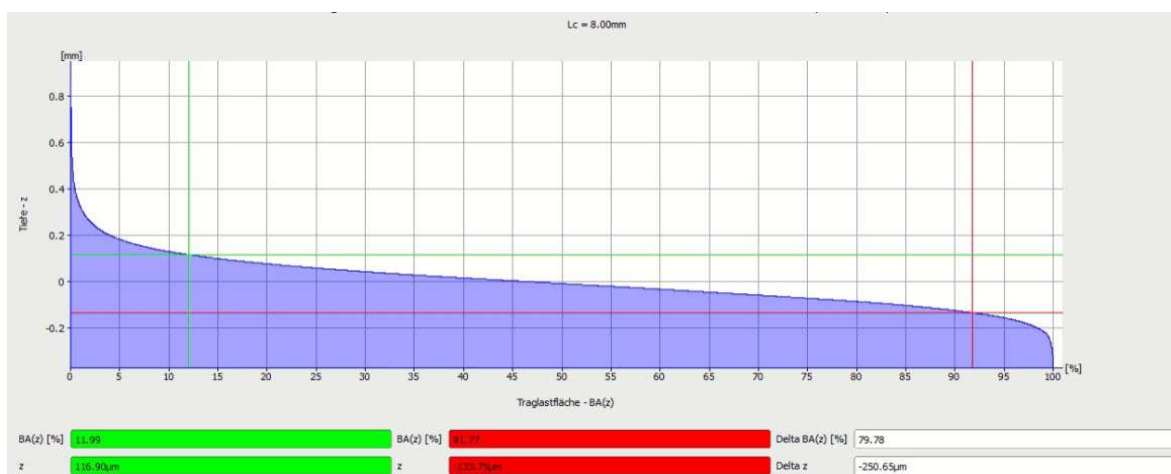
Figure 98: S_1 - Bearing Area Curve for angle α
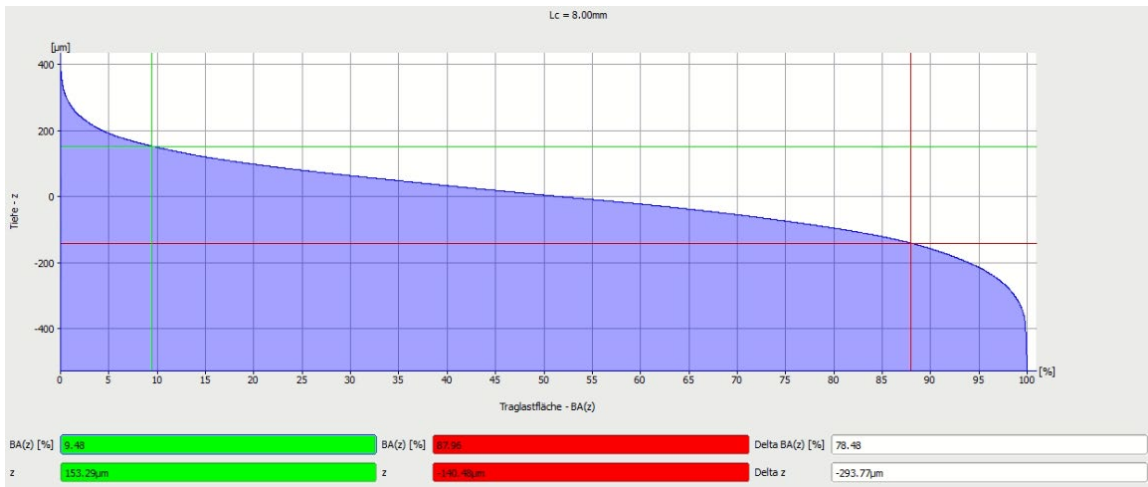
Figure 99: S_1 - Bearing Area Curve for angle β
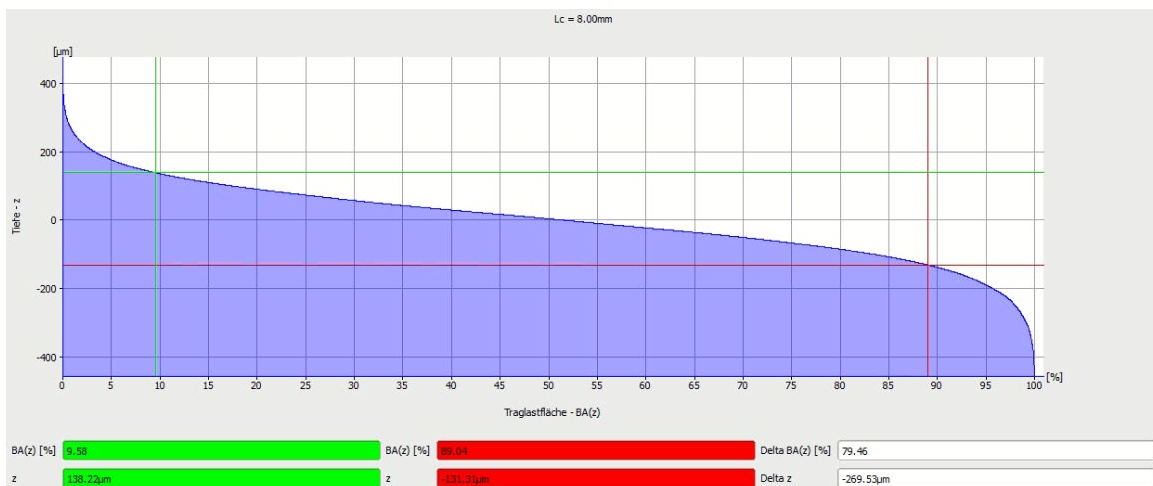
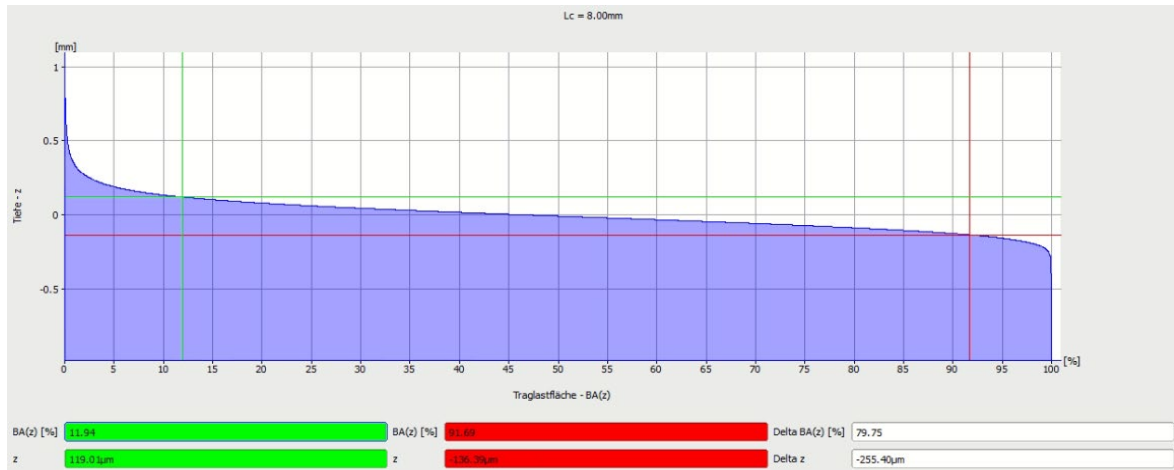*Figure 100: S_1 - Bearing Area Curve for angle γ*

The comparison of the above figures shows that the depth of the ultimate load curve is more significant in the case of angle β than in the other two cases, i.e., α and γ, due to the larger bandwidth.

- Surface 5: Foamed concrete

In this analysis, three surfaces of the digital surface model with different tilting angles were examined. The surface from angle α had dimensions of 5.02 x 2.99 cm, with a true area of 15.50 cm² and a projected area of 14.94 cm². The surface from angle β had dimensions of 4.98 x 2.94 cm, with a true area of 15.13 cm² and a projected area of 14.54 cm². The surface from angle γ had dimensions 4.99 x 2.97 cm, with a true area of 15.40 cm² and a projected area of 14.72 cm². The cutoff wavelength λc is also assumed to be approximately the same, respectively λc_α = 10.04 mm, λc_β = 9.96 mm and λc_γ = 9.97.
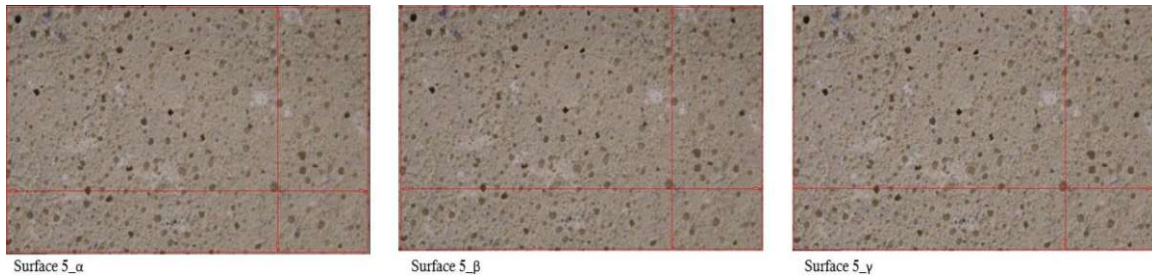
Figure 101: S_5 - Attempt 1 org FR for different tilting angles

The following parameter values were obtained from the software calculations:
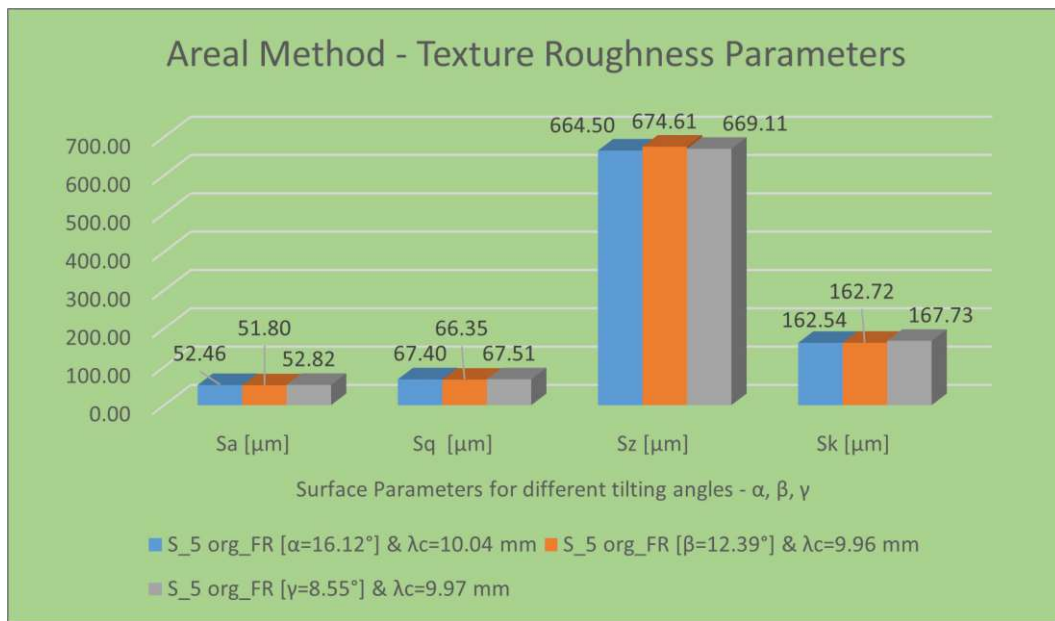
Figure 102: S_5 - Texture Roughness Parameters for different tilting angles

As can be seen from the Figure 102 above, the values of the surface roughness parameters are relatively similar, with very slight differences, which can also be seen from the approximate values of their standard deviations: 67.40 μm for angle α, 66.35 μm for angle β, and 67.51 μm for angle γ. Moreover, the class width of the Histogram is 5 μm in all three cases. The shapes and the maximum and minimum values of the histograms of these three cases for the surface texture also do not show such large differences. For the surface from angle α, the values are within a maximum of 320 μm and a minimum of -345 μm. For the surface from angle β, the values are between a maximum of 295 μm and a minimum of -

96

375 µm. For the surface from angle γ, the values are within a maximum of 325 µm and a minimum of -350 µm.

The depth, shaping and values of Smr1 and Smr2 parameters associated with the strip width for all three load curves of the mentioned surfaces are shown in the following figures:
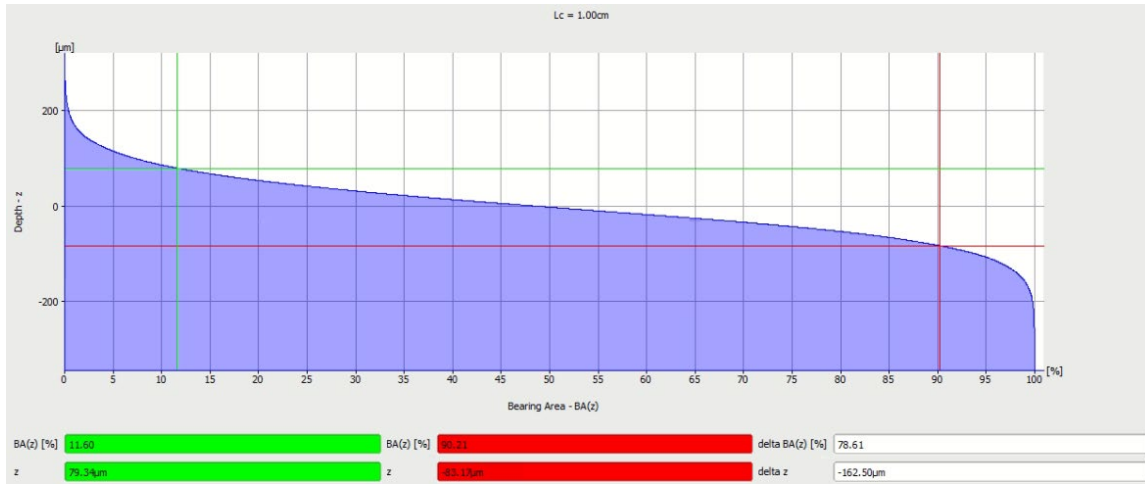
Figure 103: S_5 - Bearing Area Curve for angle α
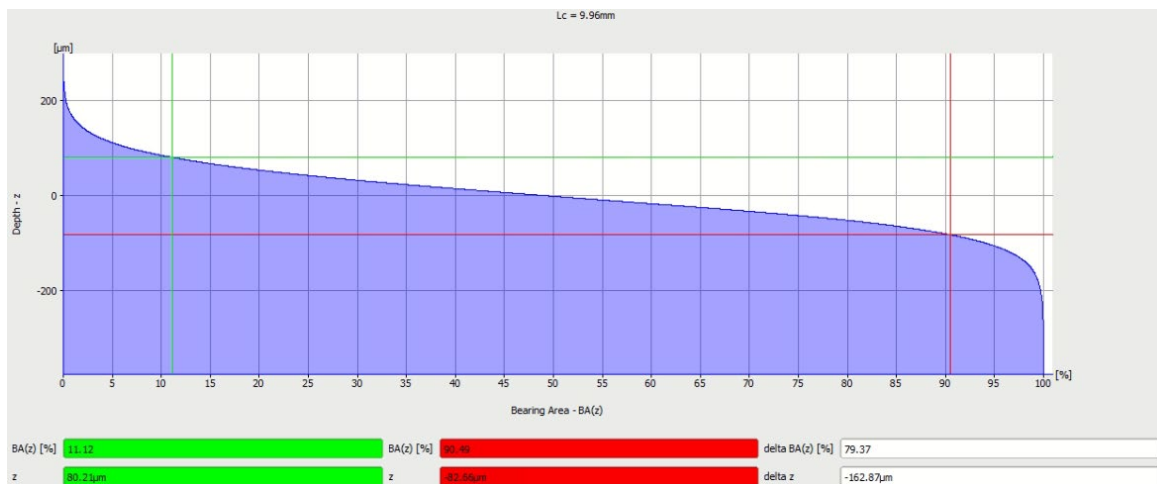
Figure 104: S_5 - Bearing Area Curve for angle β
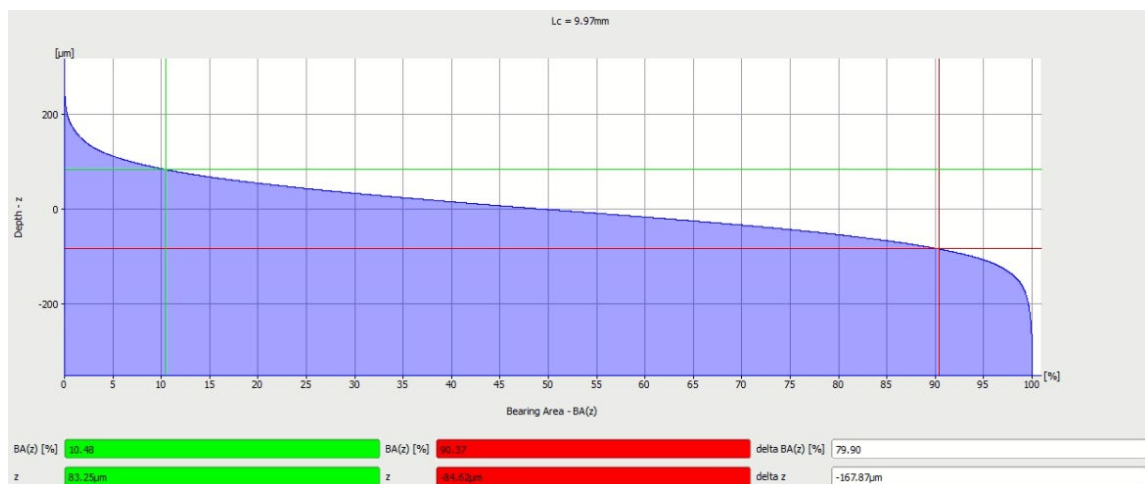
Figure 105: S_5 - Bearing Area Curve for angle γ

The comparison of the above figures shows that the depth of the ultimate load curve is more significant in the case of angle β than in the other two cases, i.e., α and γ, due to the smaller bandwidth in comparison with the case of the angle γ.

- Surface 16: Concrete terrace slabs

In this analysis, three surfaces of the digital surface model with different tilting angles were examined. The surface from angle α had dimensions of 4.14 x 2.55 cm, with a true area of 10.81 cm² and a projected area of 10.47 cm². The surface from angle β had dimensions of 4.02 x 2.47 cm, with a true area of 10.19 cm² and a projected area of 9.88 cm². The surface from angle γ had dimensions 4.01 x 2.51 cm, with a true area of 10.73 cm² and a projected area of 10.23 cm². The cutoff wavelength λc is assumed to be 8.0 mm for all three angles.


Surface 16_α   Surface 16_β   Surface 16_γ

Figure 106: Surface 16 - Attempt 1 mod FR for different tilting angles

The following parameter values were obtained from the software calculations:
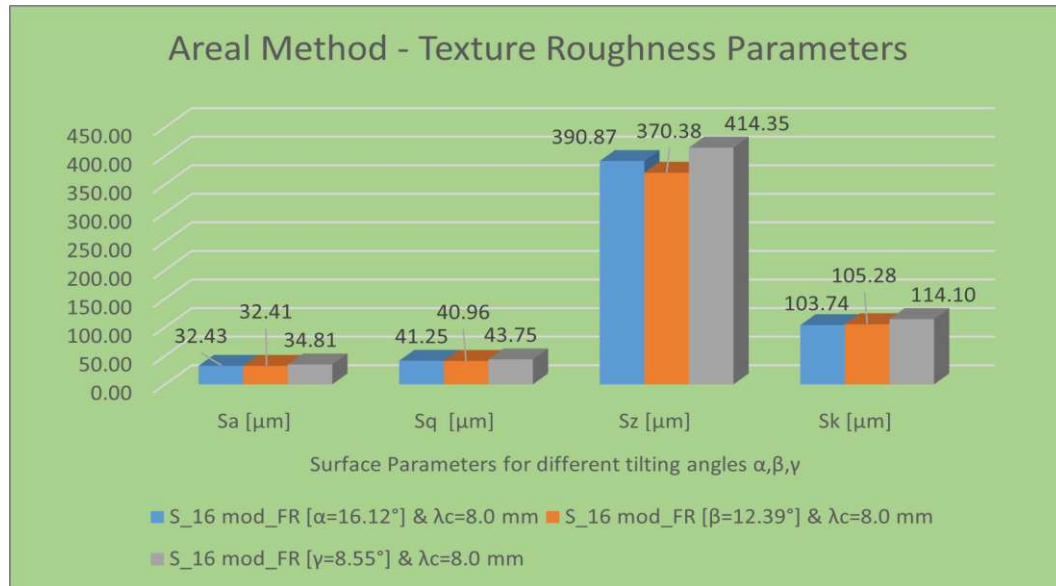
Figure 107: S_16 - Texture Roughness Parameters for different tilting angles

As can be seen from the Figure 107 above, the values of the surface roughness parameters are relatively similar, with very slight differences, which can also be seen from the approximate values of their standard deviations: 41.25 µm for angle α, 40.96 µm for angle β, and 73.75 µm for angle γ. Moreover, the class width of the Histogram is 3 µm in all three cases. The shapes and the maximum and minimum values of the histograms of these three cases for the surface texture also do not show such large differences. For the surface from angle α, the values are within a maximum of 225 µm and a minimum of -170 µm. For the

98

surface from angle β, the values are between a maximum of 215 μm and a minimum of -170 μm. For the surface from angle γ, the values are within a maximum of 195 μm and a minimum of -225 μm.

The depth, shaping and values of Smr1 and Smr2 parameters associated with the strip width for all three load curves of the mentioned surfaces are shown in the following figures:
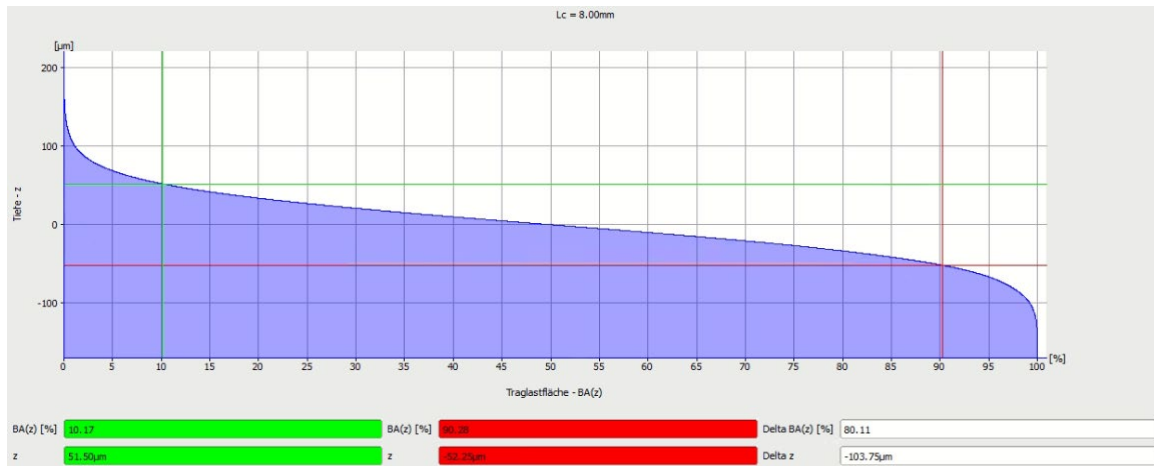
Figure 108: S_16 - Bearing Area Curve for angle α
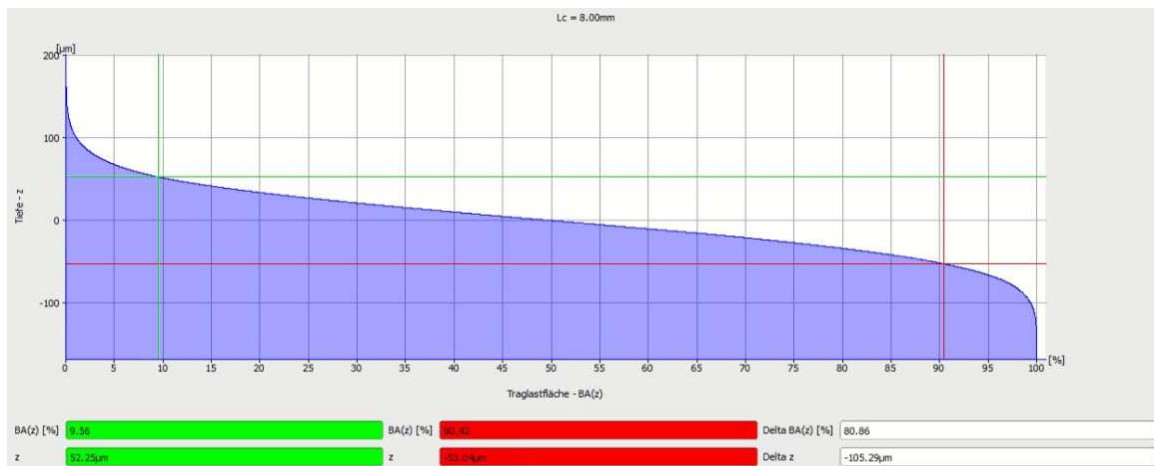
Figure 109: S_16 - Bearing Area Curve for angle β
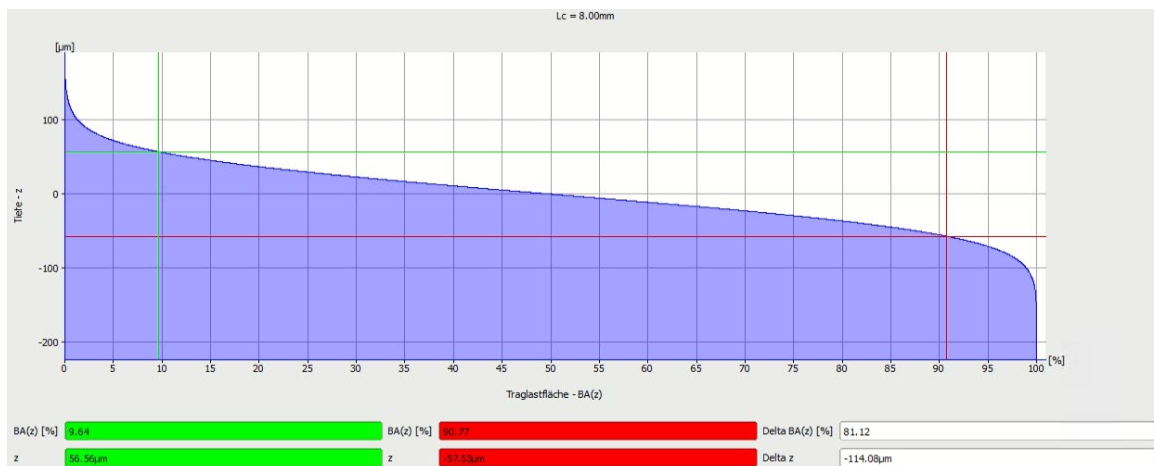
Figure 110: S_16 - Bearing Area Curve for angle γ

The comparison of the above figures shows that the depth of the ultimate load curve is more significant in the case of angle β than in the other two cases, i.e., α and γ, due to the larger bandwidth.

- Surface 20: LEGO plastic studded board above

Since it is not a concrete surface, the reason for using this type of surface for my thesis topic is directly related to the possibility of calibration and a clearer understanding of the roughness and volume parameters, in the absence of appropriate standards for surfaces made of concrete material. With the data from the practical measurement of the roughness depth Rt of this type of surface, through the comparison of the results, it is easier for us to understand which of the factors discussed in the study has the greatest influence on the values obtained for these parameters.

In this analysis, three surfaces of the digital surface model with different tilting angles were examined. The surface from angle α had dimensions of 5.98 x 3.10 cm, with a true area of 19.71 cm^2 and a projected area of 18.53 cm^2. The surface from angle β had dimensions of 5.97 x 3.40 cm, with a true area of 22.31 cm^2 and a projected area of 20.24 cm^2. The surface from angle γ had dimensions 6.00 x 3.18 cm, with a true area of 20.79 cm^2 and a projected area of 19.07 cm^2. The cutoff wavelength λc is assumed to be 8.0 mm for all three angles.

Surface 20_α   Surface 20_β   Surface 20_γ
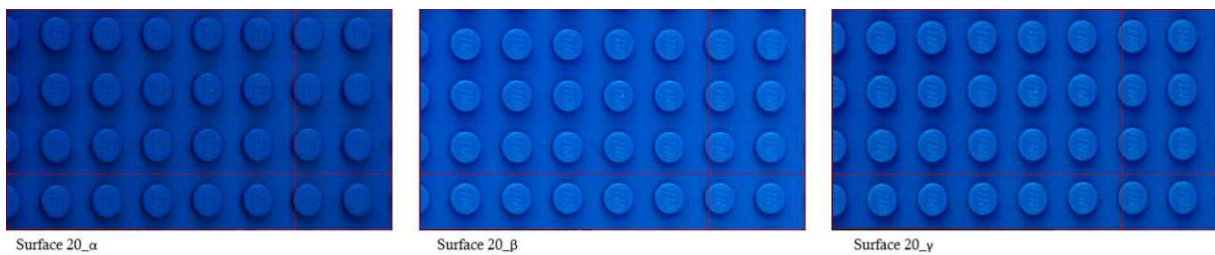
Figure 111: S_20_Attempt 1 full mod FR for different tilting angles

The following parameter values were obtained from the software calculations:
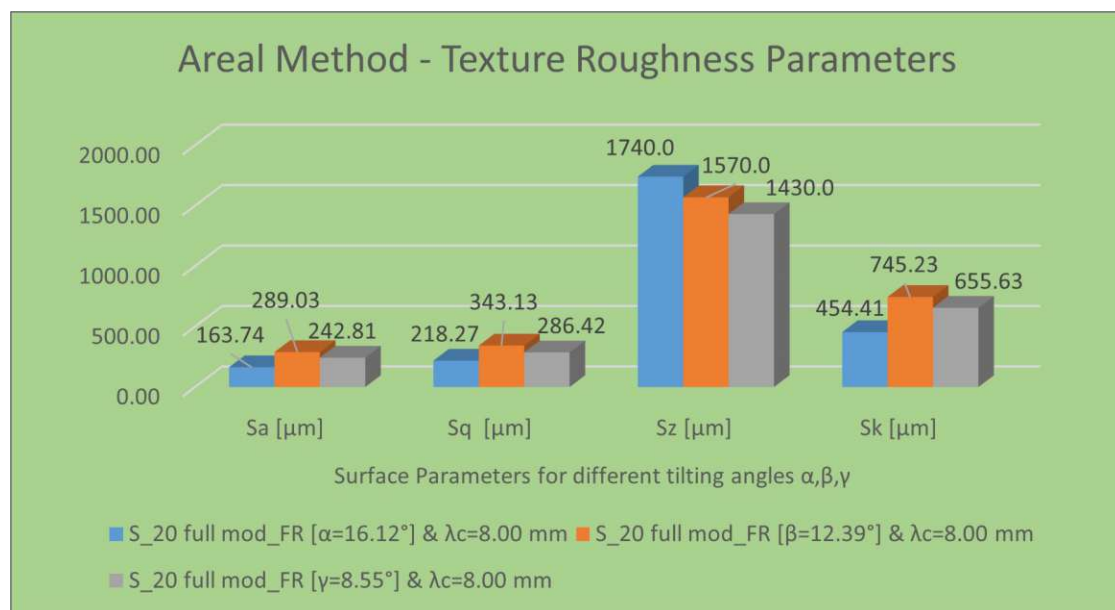
Figure 112: S_20 - Texture Roughness Parameters for different tilting angles

As can be seen from the Figure 112 above, the values of the surface roughness parameters change drastically, which can also be seen from the different values of their standard deviations: 0.22 mm for angle α, 0.34 mm for angle β, and 0.29 mm for angle γ. Moreover, even the class width of the Histogram changes from 0.02 mm for angles α and β, to 0.01 mm for angle γ. The shapes and the maximum and minimum values of the histograms of these three cases for the surface texture also do not show such a significant difference. For the surface from angle α, the values are within a maximum of 850 μm and a minimum of -890 μm. For the surface from angle β, the values are between a maximum of 890 μm and a minimum of -710 μm. For the surface from angle γ, the values are within a maximum of 830 μm and a minimum of -610 μm.

The depth, shaping and values of Smr1 and Smr2 parameters associated with the strip width for all three load curves of the mentioned surfaces are shown in the following figures:
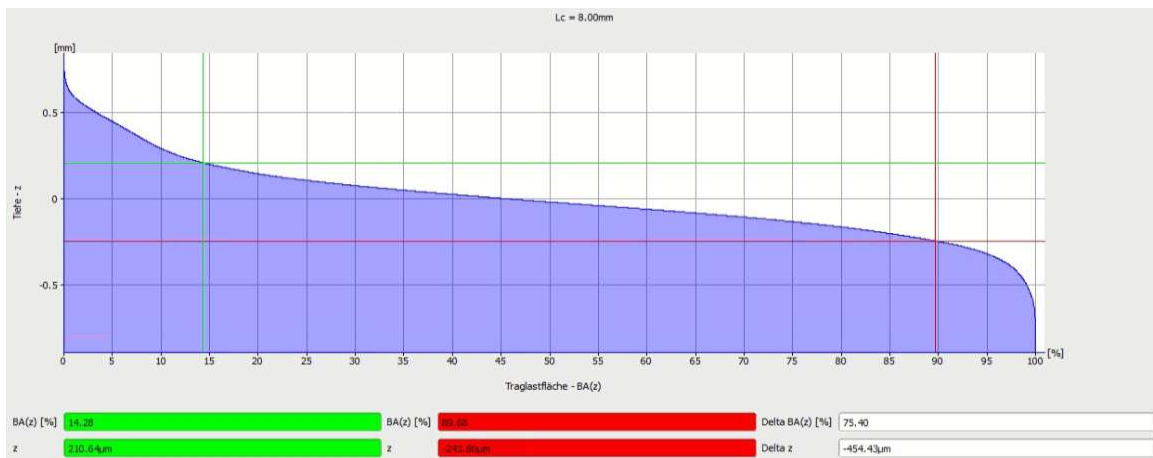
Figure 113: S_20 - Bearing Area Curve for angle α
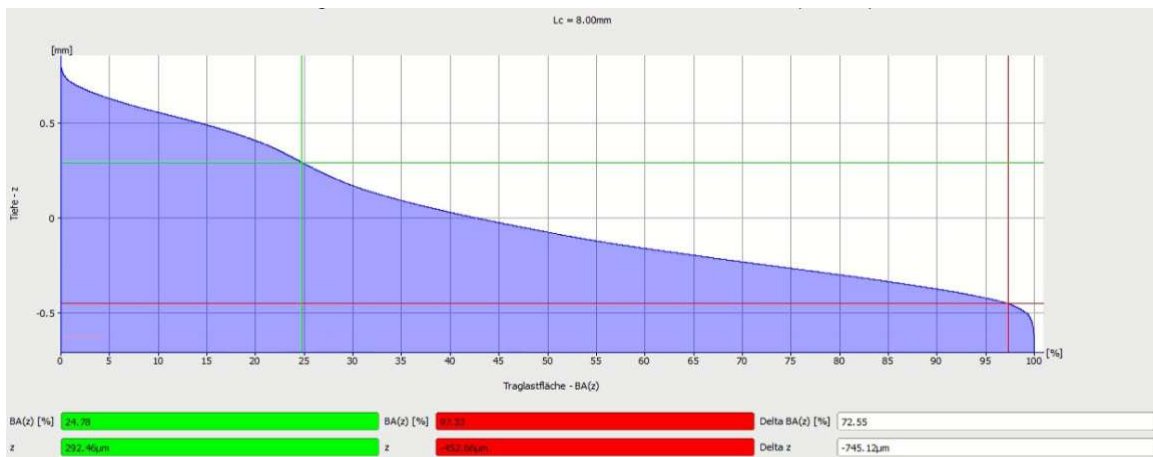
Figure 114: S_20 - Bearing Area Curve for angle β
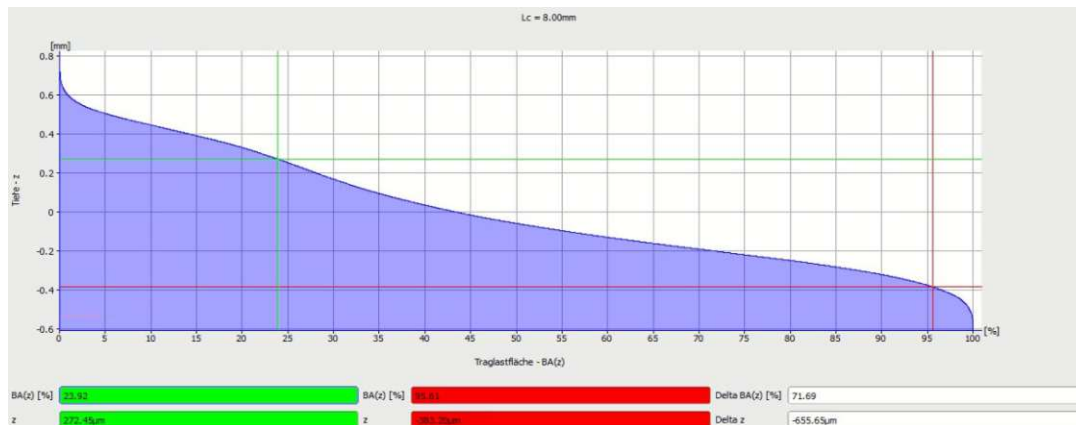
Figure 115: S_20 - Bearing Area Curve for angle γ

The comparison of the above figures shows that the depth of the ultimate load curve is more significant in the case of angle α than in the other two cases, i.e., β and γ, not only due to the smaller bandwidth but also because of the form closest to what the current literature proposes.

5.2.2 Results obtained within the analysis of the image illumination:

To process, compare and analyze the parameters obtained from the texture roughness measurement module for different image illumination, shadow, and saturation in the original and modified state of its acquisition, I will treat the surfaces of the following concrete samples:

➢ Surface 1: Shot-blasted concrete surface

In this analysis, two surfaces of the digital surface model with different illumination, shadow, and saturation for the original and the modified state of the captured stereo image pair were examined. The surface from the original state has dimensions of 4.02 x 2.50 cm, with a true area of 10.66 cm^2 and a projected area of 10.01 cm^2. The surface from the modified state has dimensions of 4.00 x 2.51 cm, with a true area of 10.75 cm^2 and a projected area of 9.98 cm^2. The cutoff wavelength λc is assumed to be 8.0 mm for both states.

Surface 1 org   Surface 1_mod

Figure 116: S_1 - Attempt 1 org FR vs. Attempt 1 mod FR

The following parameter values were obtained from the software calculations:
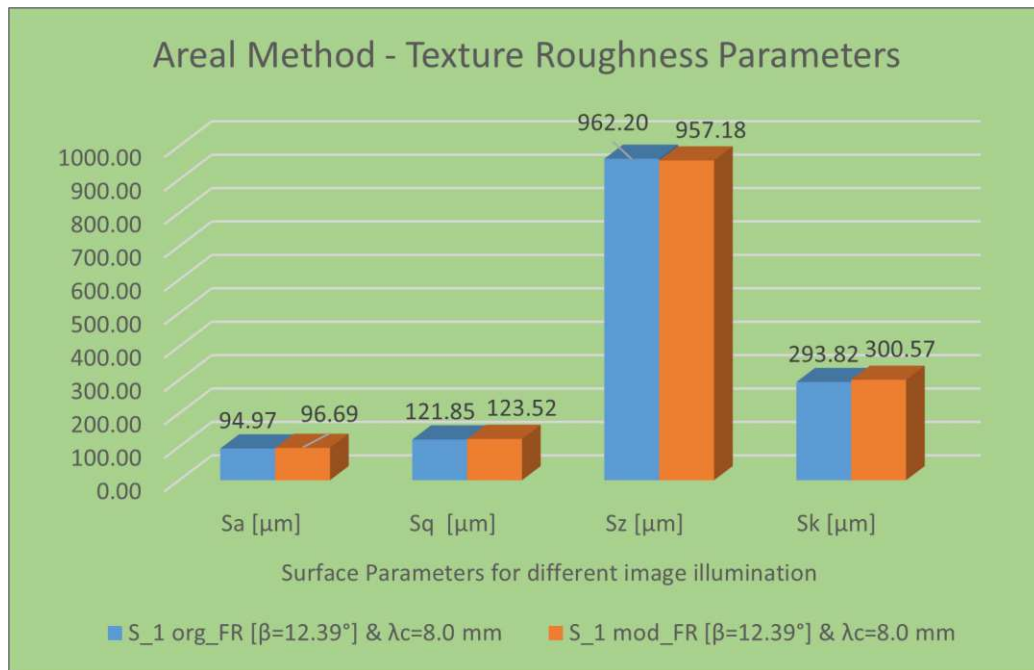
Figure 117: S_1 - Texture Roughness Parameters for different image illumination

As can be seen from the Figure 117 above, the values of the surface roughness parameters are significantly similar, with very slight differences, which can also be seen from the approximate values of their standard deviations: 121.84 μm for original state of illumination, and 123.47 μm for modified state of illumination. Moreover, the class width of the Histogram is 3 μm in all both cases. The shapes and the maximum and minimum values of the histograms of these two cases for the surface texture also shown such small differences. For the surface from original illumination, the values are within a maximum of 440 μm and a minimum of -528 μm. For the surface from modified illumination, the values are between a maximum of 444 μm and a minimum of -516 μm.

The depth, shaping and values of Smr1 and Smr2 parameters associated with the strip width for all three load curves of the mentioned surfaces are shown in the following figures:
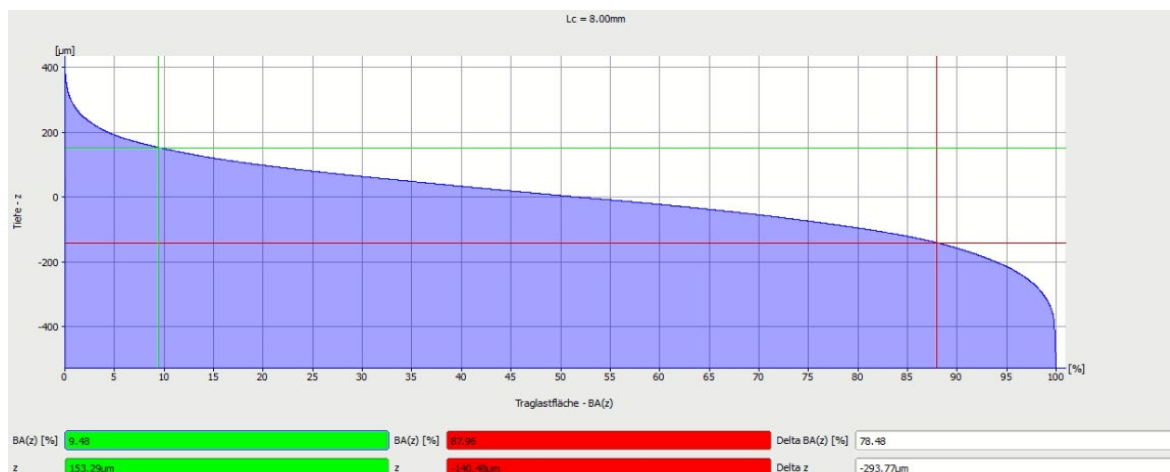
Figure 118: S_1 - Bearing Area Curve for original image illumination
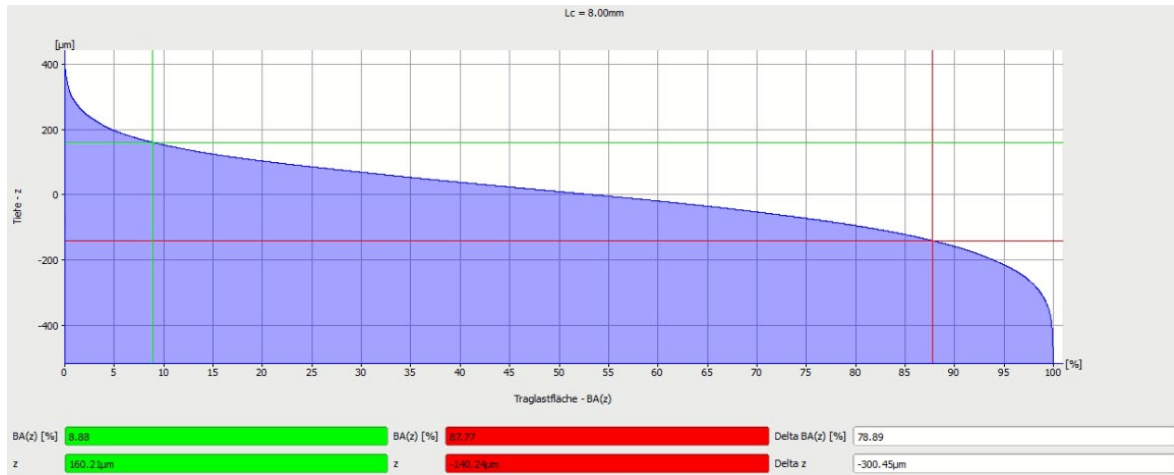
Figure 119: S_1 - Bearing Area Curve for modified image illumination

The comparison of the above figures shows that the depth of the ultimate load curve is almost identical in both cases due to the similar value of the bandwidth.

➢ Surface 14a: Synthetic resin coating OS11B

In this analysis, two surfaces of the digital surface model with different illumination, shadow, and saturation for the original and the modified state of the captured stereo image pair were examined. The surface from the original state has dimensions of 5.06 x 2.98 cm, with a true area of 15.78 cm^2 and a projected area of 15.01 cm^2. The surface from the modified state has dimensions of 5.03 x 2.96 cm, with a true area of 15.65 cm^2 and a projected area of 14.81 cm^2. The cutoff wavelength λc is assumed to be 8.0 mm for both states.

Figure 120: S_ 14a.II - Attempt 1 org FR vs. Attempt 1 mod FR

The following parameter values were obtained from the software calculations:
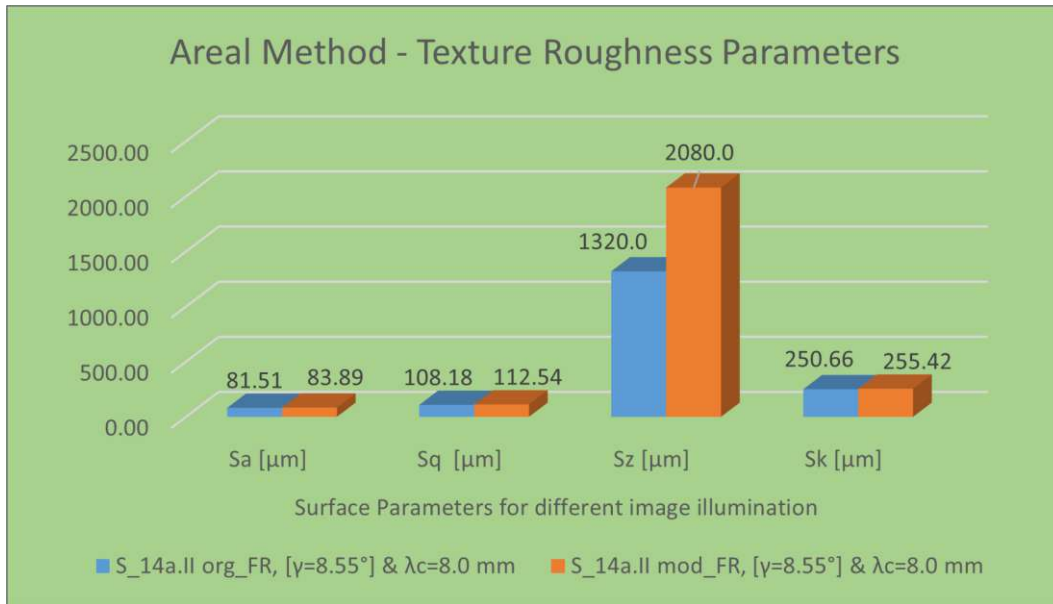
Figure 121: S_14a.II - Texture Roughness Parameters for different image illumination

As can be seen from the Figure 121 above, the values of the surface roughness parameters are significantly similar for Sa, Sq and Sk Parameters, until with significant differences for Sz parameter, despite the completely identical values of the standard deviations: 0.11 mm for original state of illumination, and 0.11 mm for modified state of illumination. However, even the class width of the Histogram is also changes from 17 to 13 μm for both cases. The shapes and the maximum and minimum values of the histograms of these two cases for the surface texture also shown a tremendous difference. For the surface from original illumination, the values are within a maximum of 980 μm and a minimum of -370 μm. For the surface from modified illumination, the values are between a maximum of 1140 μm and a minimum of -990 μm.

The depth, shaping and values of Smr1 and Smr2 parameters associated with the strip width for all three load curves of the mentioned surfaces are shown in the following figures:

Figure 122: S_14a.II - Bearing Area Curve for original image illumination

105

Figure 123: S_14a.II - Bearing Area Curve for modified image illumination

The comparison of the above figures shows that the depth of the ultimate load curve changes drastically in both cases despite to the approximately similar value of the bandwidth.

5.2.3 Results obtained within the analysis of the cutoff wavelength λc:

To process, compare and analyze the parameters obtained from the texture roughness measurement module for different values of the cutoff wavelength Lc within the same selected area, I will treat the surfaces of the following concrete samples:

✓ Surface 15: Synthetic resin coating OS11B

In this analysis, only one surfaces of the digital surface model with different cutoff wavelength λc_1, λc_2 and λc_3 were examined. This surface for all values of the cutoff wavelength λc_1, λc_2 and λc_3 had identical dimensions of 7.85 x 6.08 cm and value of a projected area of 47.59 cm^2, but it shows different values of a true area of 56.76 cm^2 for λc_1, 55.69 cm^2 for λc_2 and 52.09 cm^2 for λc_3. This surface is also modified in the context of the illumination.
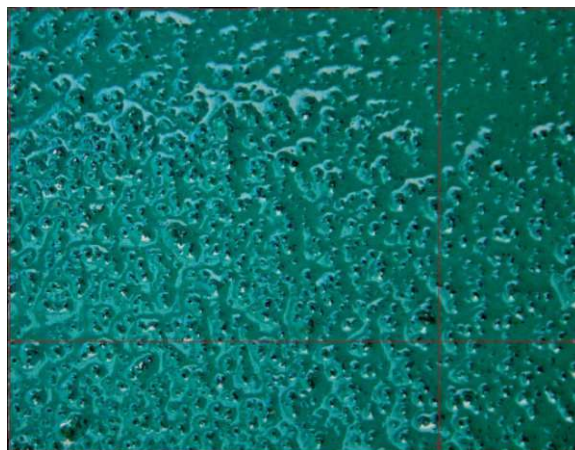
Figure 124: S_15. I - Attempt 1 full mod FR

106

The following parameter values were obtained from the software calculations:
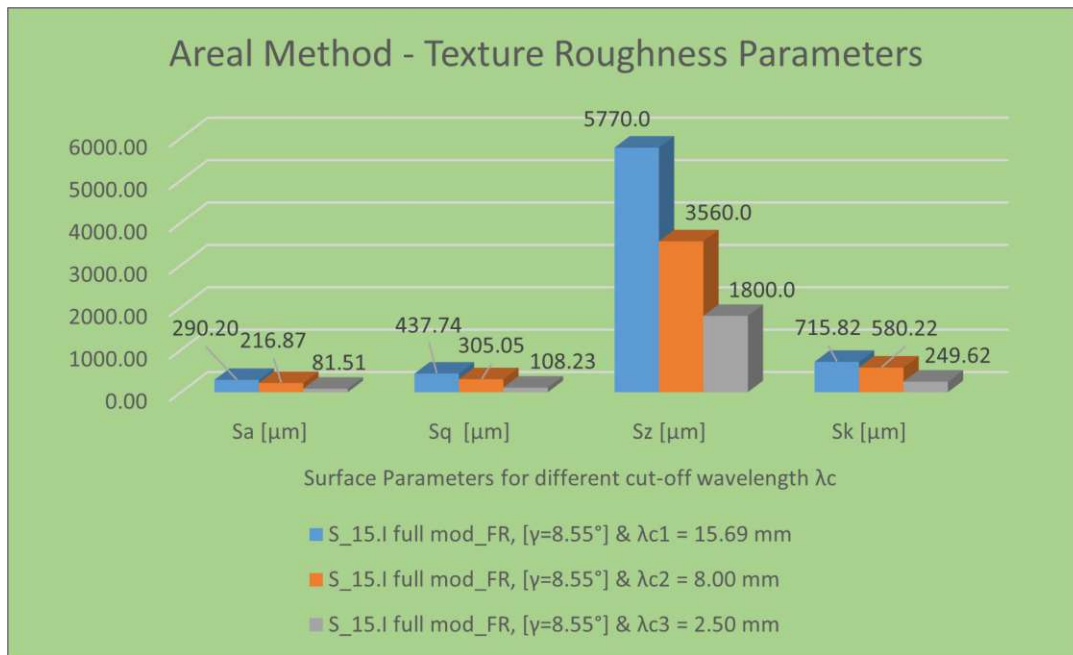
Figure 125: S_15. I - Texture Roughness Parameters for different cutoff wavelength λc

As can be seen from the Figure 125 above, the values of the surface roughness parameters change drastically from each other due to the entirely different values of the standard deviations and the class width of the Histogram. The shapes and the maximum and minimum values of the histograms of these three cases for the surface texture also showed a tremendous difference. For a better overview, I will give the following Figure 126:
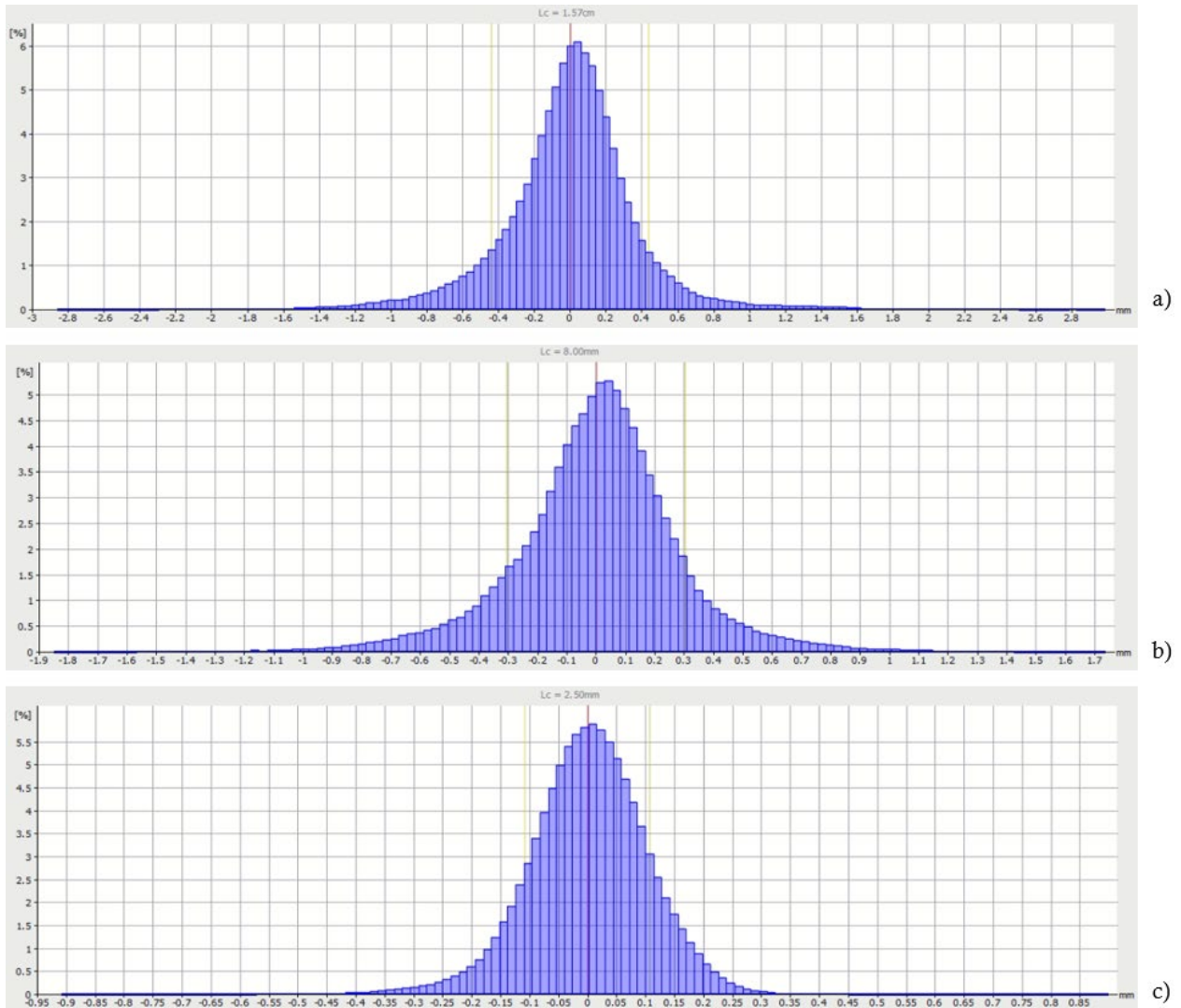
Figure 126: S_15. I - comparison of the cutoff wavelength - a) λc=15.7 mm, b) λc=8.0 mm and c) λc=2.5 mm

The Histogram for each of the cases shows a standard deviation as follows: for λc_1 = 15.69 mm, the value of Maximum is 2.98 mm, and the value of Minimum is -2.86 mm; for λc_2 = 8.00 mm, the value of Maximum is 1.73 mm and the value of Minimum reach -1.85 mm, for λc_3 = 2.50 mm the value of Maximum is 0.90 mm and the value of Minimum reach - 0.91 mm, what means a significant change in values for each of three cases.

5.2.4 Results obtained within the analysis of the Region of Interest:

To process, compare, and analyze the parameters obtained from the texture roughness measurement module for different selected Region of Interest within the same captured stereo pair images, realized within the same attempt, for the exact cutoff wavelength λc and the same tilt angle, I will treat the surfaces of the following concrete samples:

108

- Surface 14b: Synthetic resin coating OS11B

In this analysis, two surfaces of the digital surface model with different Region of Interest, and identical illumination, shadow and saturation within the same captured stereo image pair were examined. The surface from the smallest selection of the Region of Interest has dimensions of 5.06 x 3.04 cm, with a true area of 16.39 cm² and a projected area of 15.29 cm². The surface from the biggest selection of the Region of Interest has dimensions of 10.00 x 6.55 cm, with a true area of 70.17 cm² and a projected area of 65.31 cm². The cutoff wavelength λc is assumed to be 8.0 mm for both states.
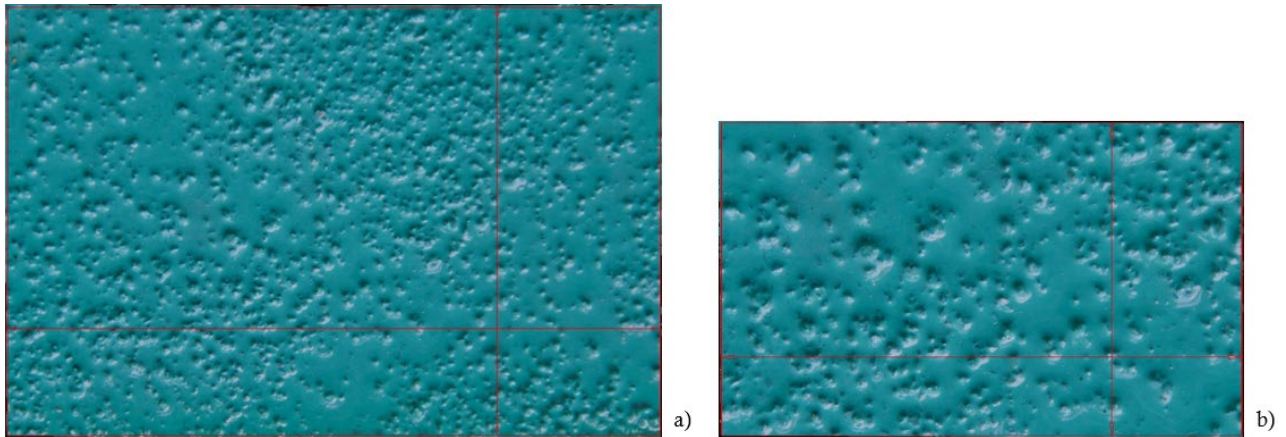
Figure 127: S_14b.I - a) Attempt 1 full mod FR, b) Attempt 1 mod FR

The following parameter values were obtained from the software calculations:
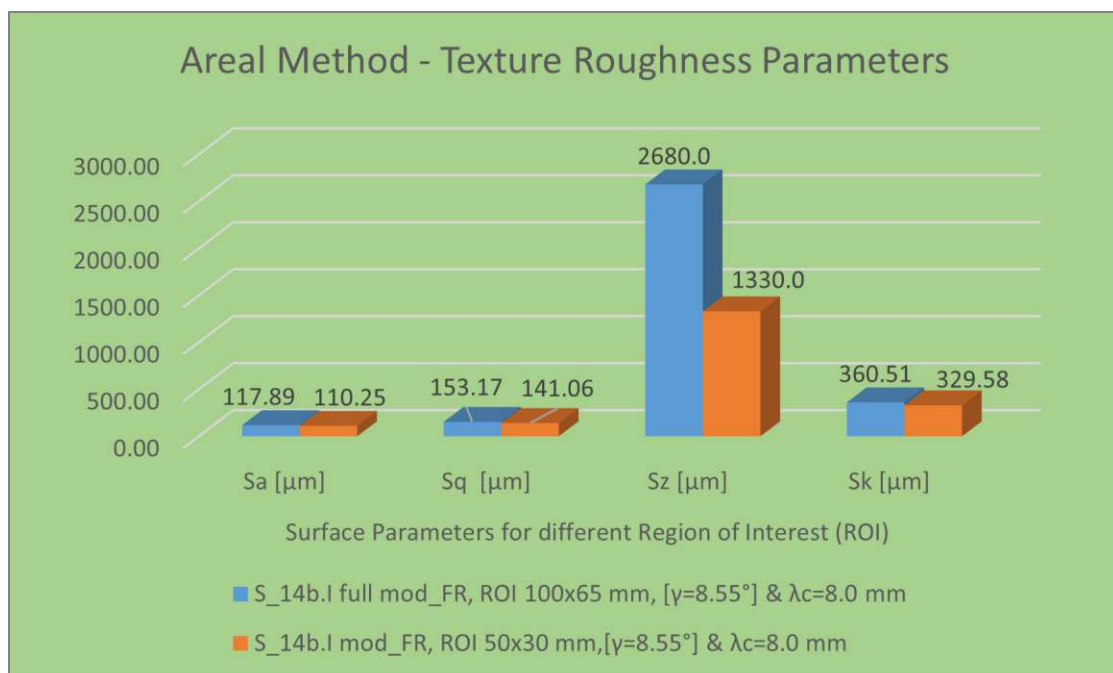
Figure 128: S_14b.I - Texture Roughness Parameters for different Region of Interest (ROI)

109

As can be seen from the above figure, the values of the surface roughness parameters are approximately similar for Sa, Sq and Sk Parameters, until with significant differences for Sz parameter, despite the nearly similar values of the standard deviations: 0.14 mm for smallest selection of the Region of the Interest, and 0.15 mm for biggest selection of the Region of Interest. However, even the class width of the Histogram is also changes from 14 to 24 μm for both cases. The shapes and the maximum and minimum values of the histograms of these two cases for the surface texture also shown a tremendous difference. For the smallest part of the Region of Interest, the values are within a maximum of 820 μm and a minimum of -530 μm. For the the biggest part of the Region of Interest, the values are between a maximum of 1210 μm and a minimum of -1480 μm. For a better understanding of the influence of the Region of Interest, I will represent the Histogram of the digital surface model with the following Figure 129:
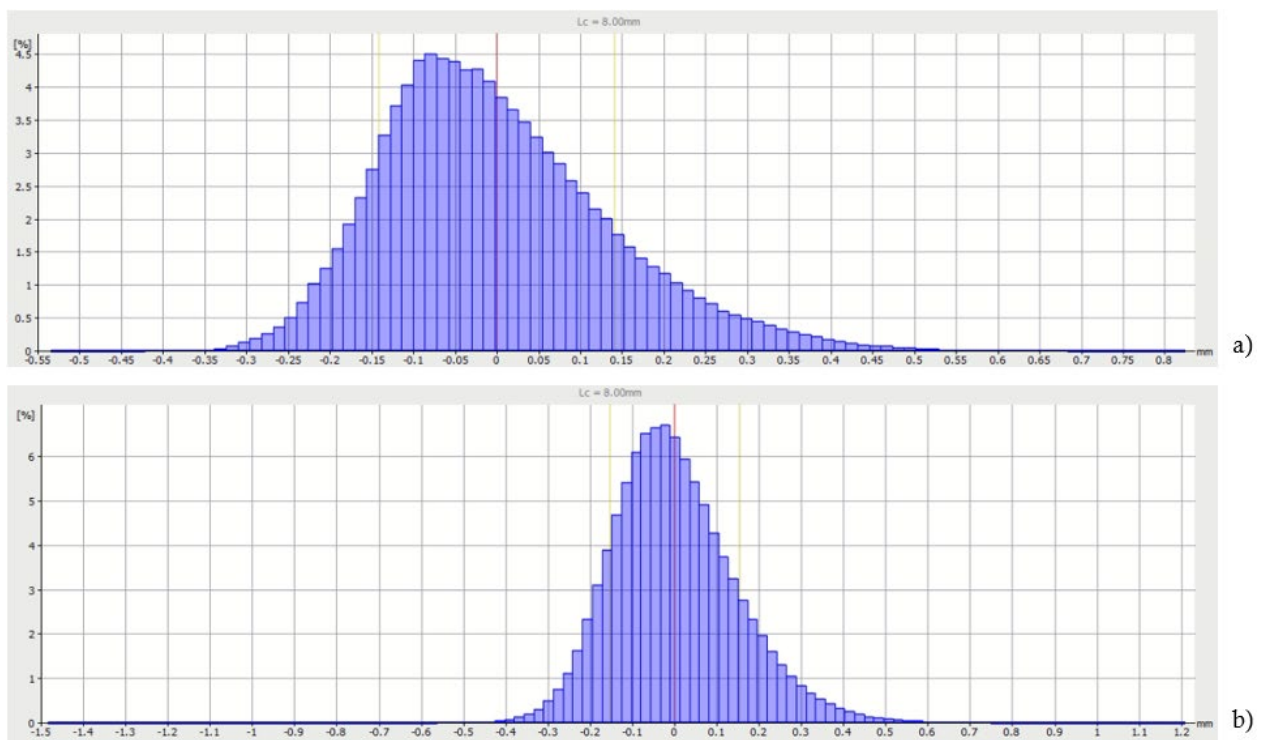
Figure 129: S_14b.I - comparison of different Region of Interest - a) small ROI, b) big ROI

5.3 Results of the Volume Measurement Module

In the context of volume measurements, after selecting the size, respectively the desired dimensions of the surface for measurement, the software after the measures, automatically gives us the calculated values of the volume between the ISO surface and that of the object as upper and lower surface, initially through the film soap mode. Still, I manually changed the modes in the top cover, bottom cover and cutting plane, to compare the results between them and draw conclusions about the accuracy of each of these modes.

In the following examples, I will show the ISO surface on the surface of the object as well as the acquired values of the volumes depending on these surfaces.

110

As for the two surfaces made of non-concrete materials, which are part of this study only for reasons of calibration and the possibility of measuring their volume practically in the laboratory, I considered it more convenient to start precisely with surfaces 18 and 20 for the measurements of the parameters. From here, it will be easier to understand which of the modes the software offers to calculate the volume is more likely to be accurate, so in future scientific work, researchers will focus on this direction. For each of the four factors influencing the volume parameters that I have presented below, I will examine at least two surfaces of the concrete specimens so that all my research is included.

5.3.1 Results obtained within the analysis of the Region of Interest:

> ➢ Surface 20: LEGO plastic studded board below

In the framework of the Volume Measurements Module within the analysis of the Region of the Interest, I have used the same tilting angle β = 12.39° and the same image illumination. For the smallest part of the Region of Interest, a Surface with dimensions from 3.19 x 2.38 cm, depth d = 1.95 mm was selected. According to this selection has Mex an ISO Projected Area from 7.63 cm^2 and projected Volume from 1.488 cm^3 calculated. For the biggest part of the Region of Interest, a Surface with dimensions from 4.44 x 3.06 cm, depth d = 2.01 mm was selected. According to this selection has MeX an ISO Projected Area from 13.60 cm^2 and projected Volume from 2.734 cm^3 calculated. From the comparison of this two selected Areas, the Software has obtained following results of volume parameters, presented in the figures below, according to the modes of volume measurement:
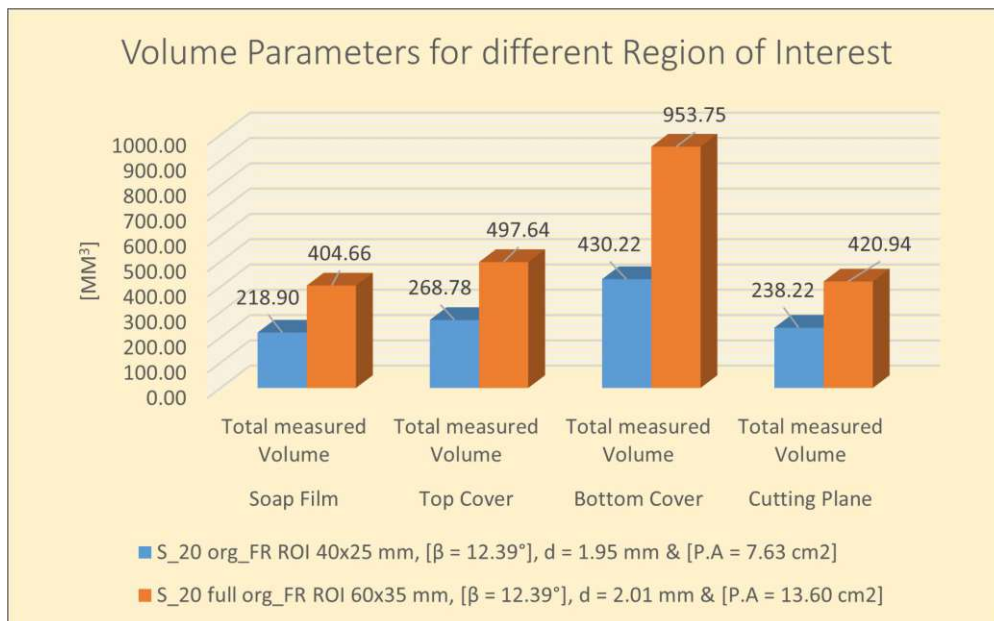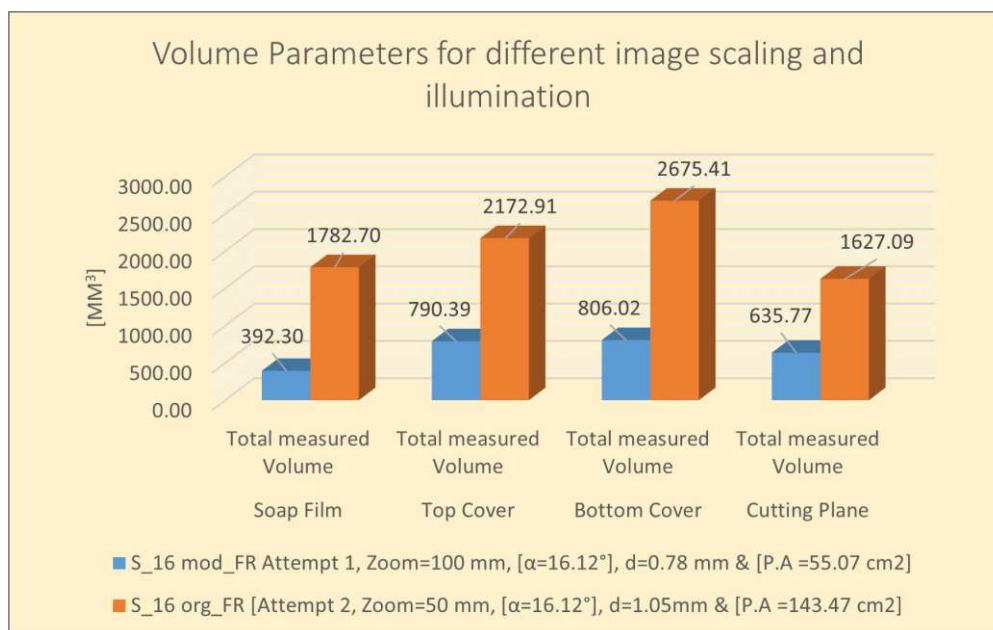

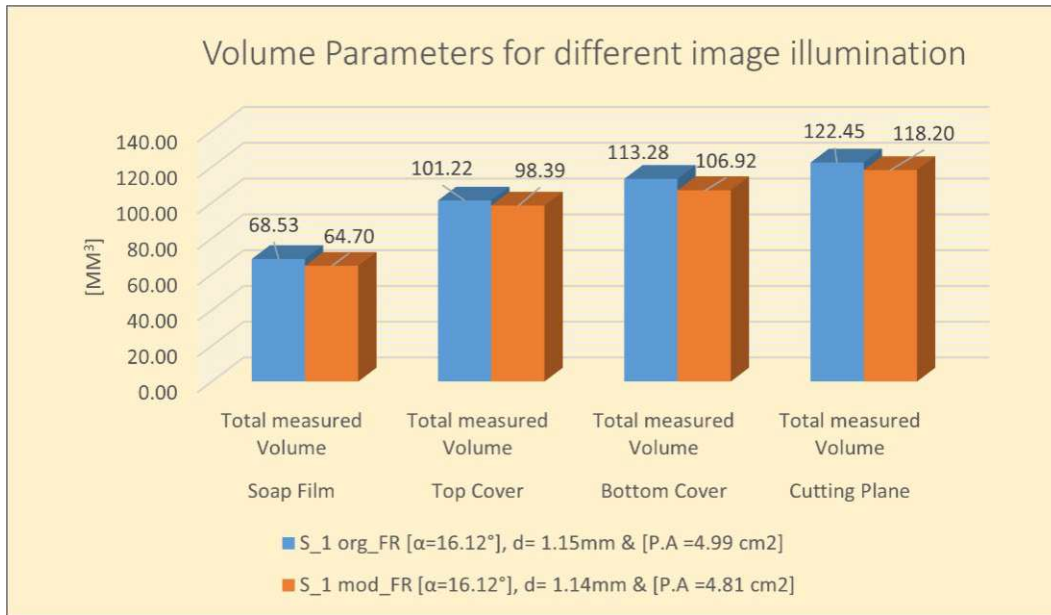*Figure 130: S_20 - Total measured Volume in mm^3 for different Region of Interest*
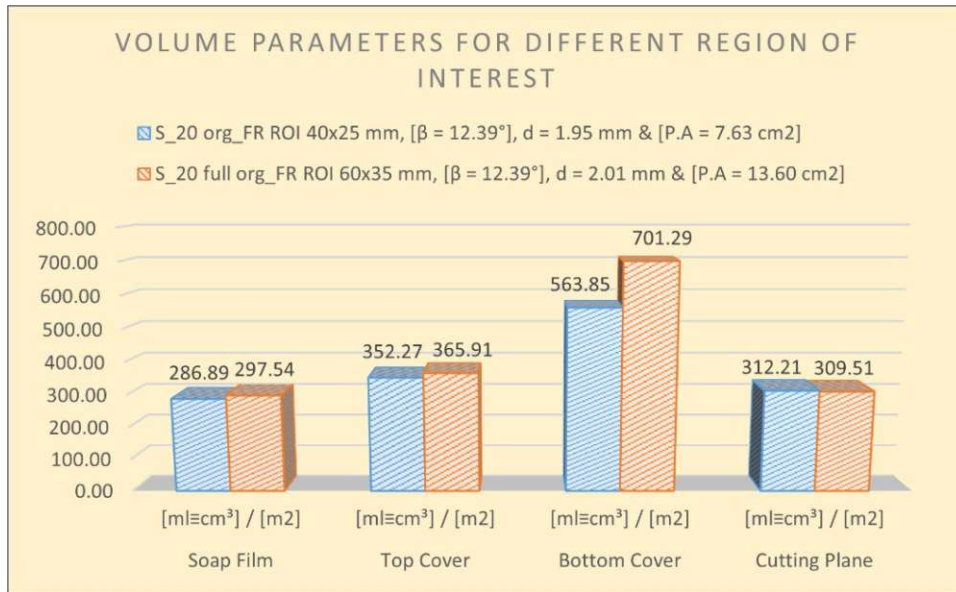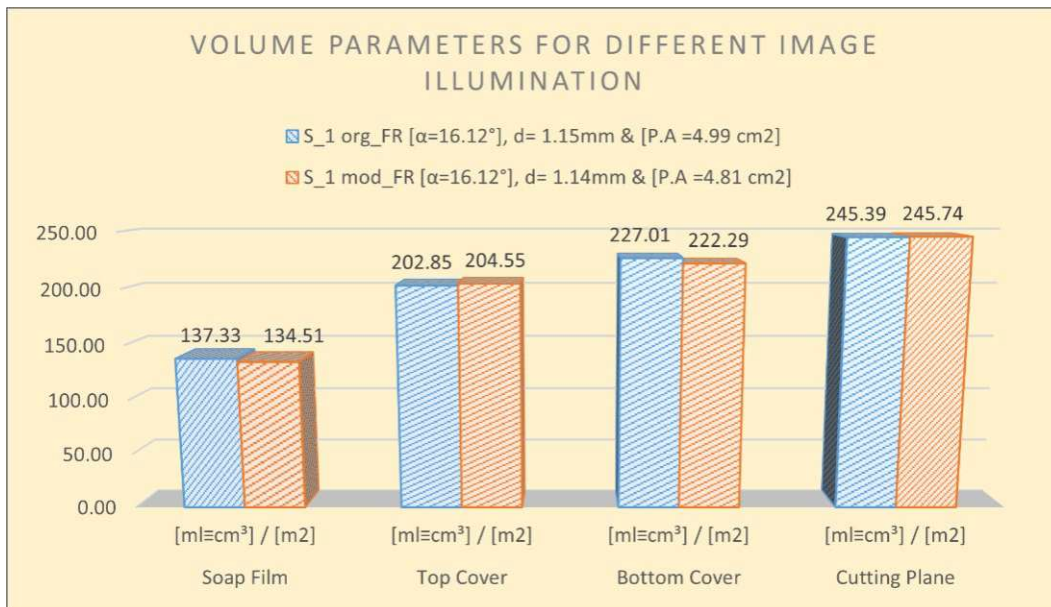
Figure 131: S_20 - Volume Parameters in cm³/1000 cm³ for different Region of Interests

Figure 130 shows the values of the total measured volume above and below the ISO surface for each of the four modes for two different areas of interest for surface 20. In contrast, Figure 131 shows the volume values on cm³ obtained concerning the projected Area per 1000 cm² on the selected surface for these measurements.

If we compare the results obtained from the software calculation with those obtained from the practical measurement in the laboratory, we have the following:

a. According to **practical measures**, measured Volume pro Area = **311,80 cm³/1000 cm²**

b. According to **Soap Film mode**, measured Volume pro Area varies between **286,89** and **297,54 cm³/1000 cm²**

c. According to **Top Cover mode**, measured Volume pro Area varies between **352,27** and **365,91 cm³/1000 cm²**, which means not big difference in results,

d. According to **Bottom Cover mode**, measured Volume pro Area varies between **563,85** and **701,29 cm³/1000 cm²**, which means drastic changes in results,

e. According to **Cutting Plane mode**, measured Volume pro Area varies between **312,21** and **309,51 cm³/1000 cm²**, which is approximately the same result as that from practical measurement.

From the comparison of these values, it can be seen that of the three automatic modes, the soap film mode is most approximated for samples of surfaces with great depth, such as the LEGO plastic plate with dimples. Conversely, the manual cutting plane mode can obtain the most accurate results.

➤ Surface 18: Wooden floorboards grooved

In the framework of the Volume Measurements Module within the analysis of the Region of the Interest, I have used the same tilting angle γ = 8.55° and the same image illumination. For the smallest part of the Region of Interest, a Surface with dimensions from 3.55 x 2.46

cm, depth d = 1.93 mm was selected. According to this selection has Mex an ISO Projected Area from 8.70 cm² and projected Volume from 1.633 cm³ calculated. For the biggest part of the Region of Interest, a Surface with dimensions from 7.28 x 4.92 cm, depth d = 1.95 mm was selected. According to this selection has MeX an ISO Projected Area from 34.97 cm² and projected Volume from 7.2 cm³ calculated. From the comparison of this two selected Areas, the Software has obtained following results of volume parameters, presented in the figures below, according to the modes of volume measurement:
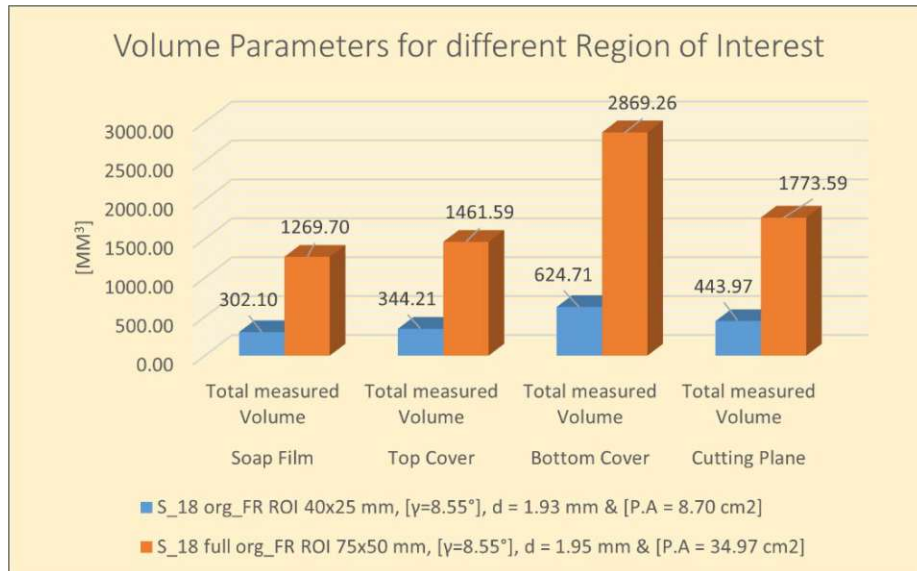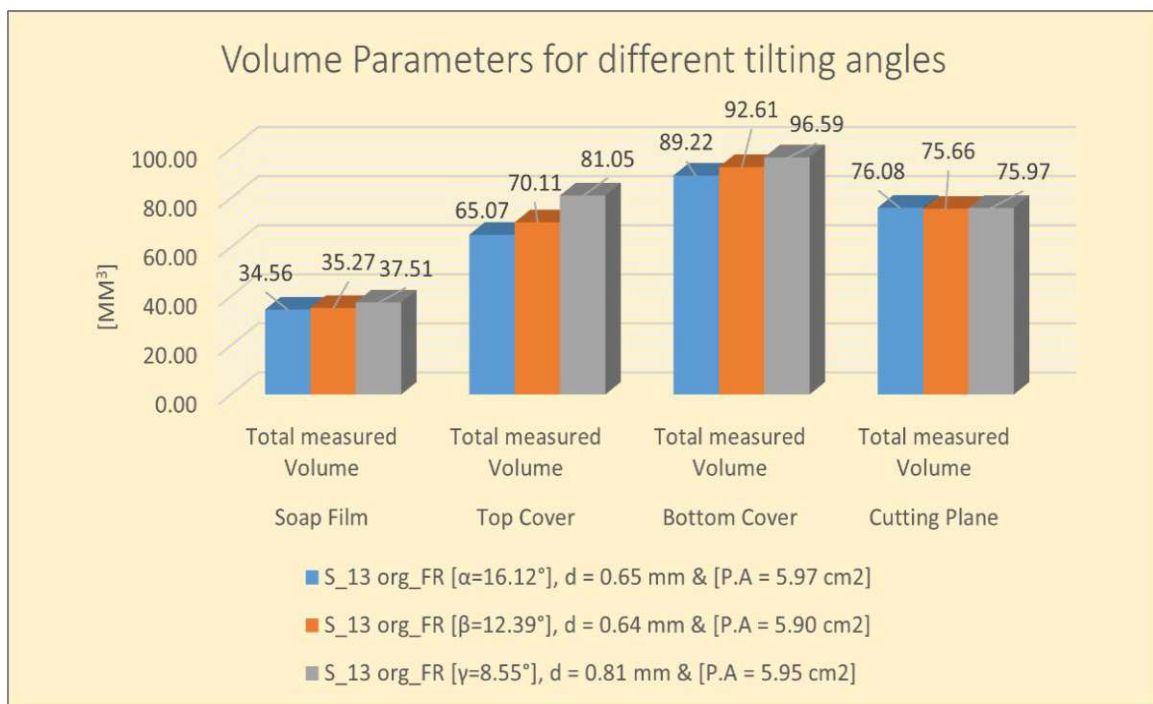

Figure 132: S_18 - Total measured Volume in mm³ for different Region of Interest
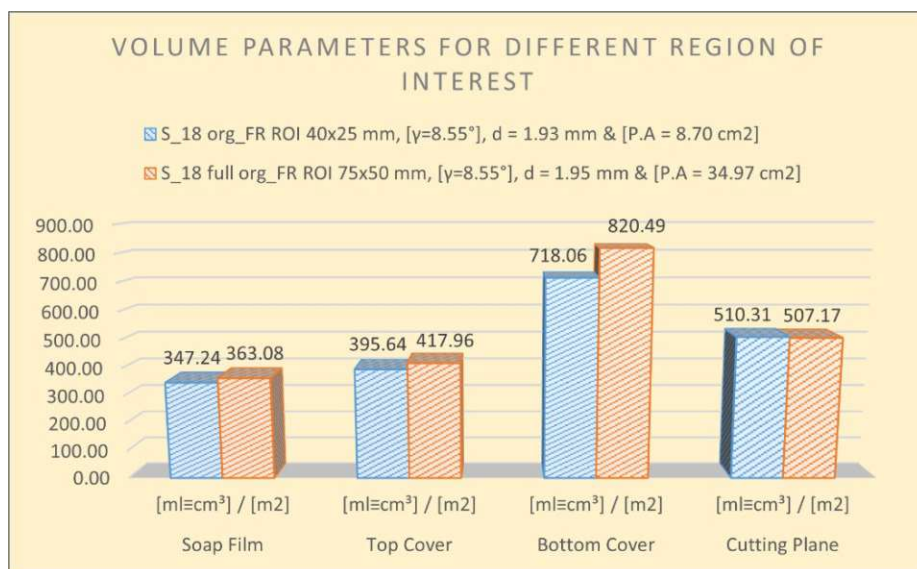
Figure 133: S_18 - Volume Parameters in cm³/1000 cm³ for different Region of Interests

Figure 132 shows the values of the total measured volume above and below the ISO surface for each of the four modes for two different areas of interest for surface 20. In contrast, Figure 133 shows the volume values on cm3 obtained concerning the projected Area per 1000 cm2 on the selected surface for these measurements.

113

If we compare the results obtained from the software calculation with those obtained from the practical measurement in the laboratory, we have the following:

a. According to **practical measures**, measured Volume pro Area = **506,70 cm^3/1000 cm^2**

b. According to **Soap Film mode**, measured Volume pro Area varies between **347,24** and **363,08 cm^3/1000 cm^2**, which means not big difference in results,

c. According to **Top Cover mode**, measured Volume pro Area varies between **395,64** and **417,96 cm^3/1000 cm^2**, which means still big difference in results,

d. According to **Bottom Cover mode**, measured Volume pro Area varies between **718,06** and **820,49 cm^3/1000 cm^2**, which means drastic changes in results,

e. According to **Cutting Plane mode**, measured Volume pro Area varies between **510,31** and **507,17 cm^3/1000 cm^2**, which is approximately the same result as that from practical measurement.

According to the results of the calculated Volumes from three automatic modes, Soap Film, Top Cover and Bottom Cover, we note that none of these measurements is precise enough to serve as a reference point for surfaces with grooves for similar scientific studies. Therefore, although measuring the volume is the most tedious and takes the most time, it is possible to obtain more accurate results with the Cutting plane. In the following Volume measurements of different samples of concrete surfaces, I will just compare the results between modes for different influencing factors.

➤ Surface 1: Shot-blasted concrete surface

In the framework of the Volume Measurements Module within the analysis of the Region of the Interest, I have used the same tilting angle α = 16.12° and the same image illumination. For the smallest part of the Region of Interest, a Surface with dimensions from 2.68 x 1.82 cm, depth d = 1.27 mm was selected. According to this selection has Mex an ISO Projected Area from 4.87 cm^2 and projected Volume from 0.618 cm^3 calculated. For the biggest part of the Region of Interest, a Surface with dimensions from 9.55 x 6.38 cm, depth d = 2.34 mm was selected. According to this selection has MeX an ISO Projected Area from 61.0 cm^2 and projected Volume from 14.274 cm^3 calculated. From the comparison of this two selected Areas, the Software has obtained following results of volume parameters, presented in the figures below, according to the modes of volume measurement:
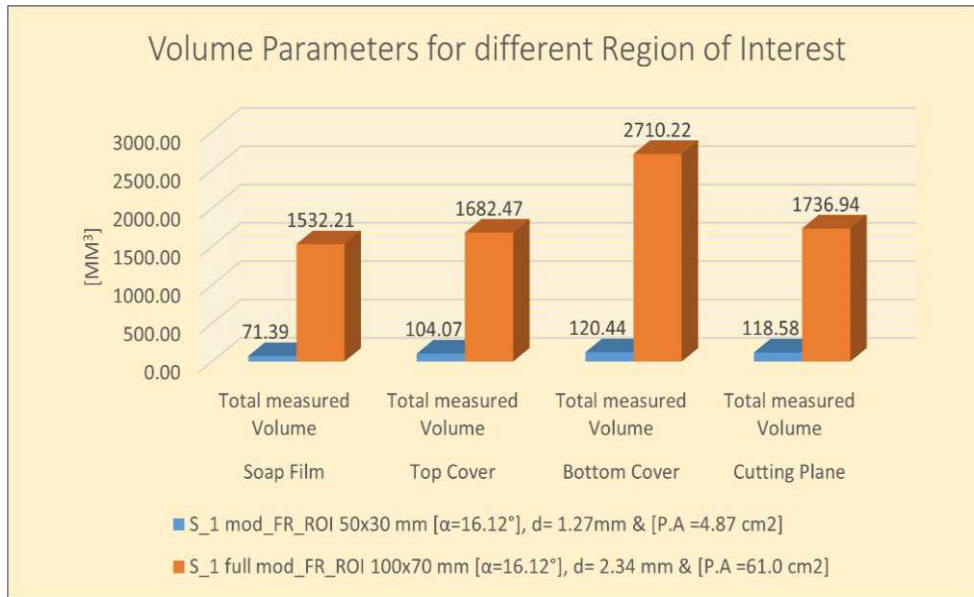
Figure 134: S_1 - Total measured Volume in mm³ for different Region of Interest
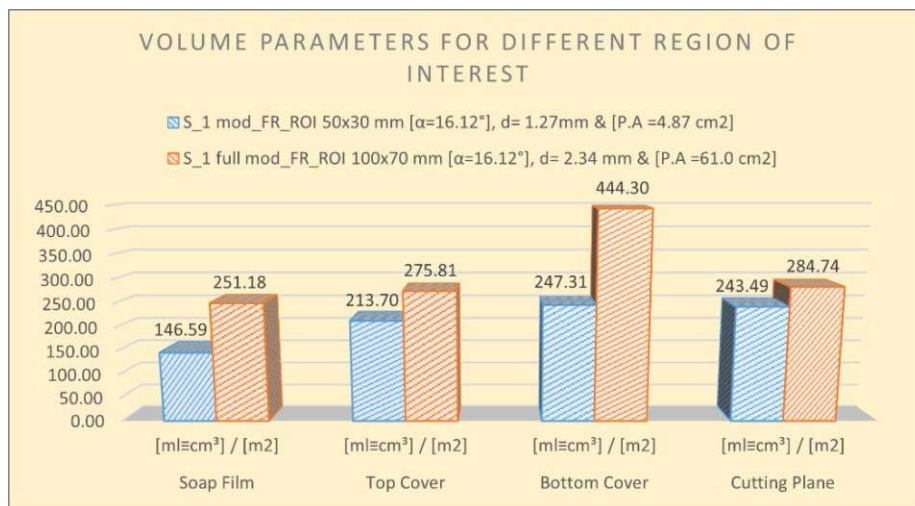
Figure 135: S_1 - Volume Parameters in cm³/1000 cm³ for different Region of Interests

According to the result in the Figure 135 above, only Top Cover and Cutting Plane modes shown tiny changes between two Regions of Interest, until at the two other modes results changes drastically, which means that the size of the selected Region it is crucial for obtaining exact results.

➤ Surface 9: Concrete broom finish

In the framework of the Volume Measurements Module within the analysis of the Region of the Interest, I have used the same tilting angle $\alpha = 16.12°$ and the same image illumination. For the smallest part of the Region of Interest, a Surface with dimensions from 3.00 x 2.22 cm, depth $d = 3.69$ mm was selected. According to this selection has Mex an ISO Projected Area from 6.65 cm² and projected Volume from 2.454 cm³ calculated. For the biggest part of the Region of Interest, a Surface with dimensions from 14.20 x 8.12

115

cm, depth d = 6.40 mm was selected. According to this selection has MeX an ISO Projected Area from 115.09 cm² and projected Volume from 73.658 cm³ calculated. From the comparison of this two selected Areas, the Software has obtained following results of volume parameters, presented in the figures below, according to the modes of volume measurement:
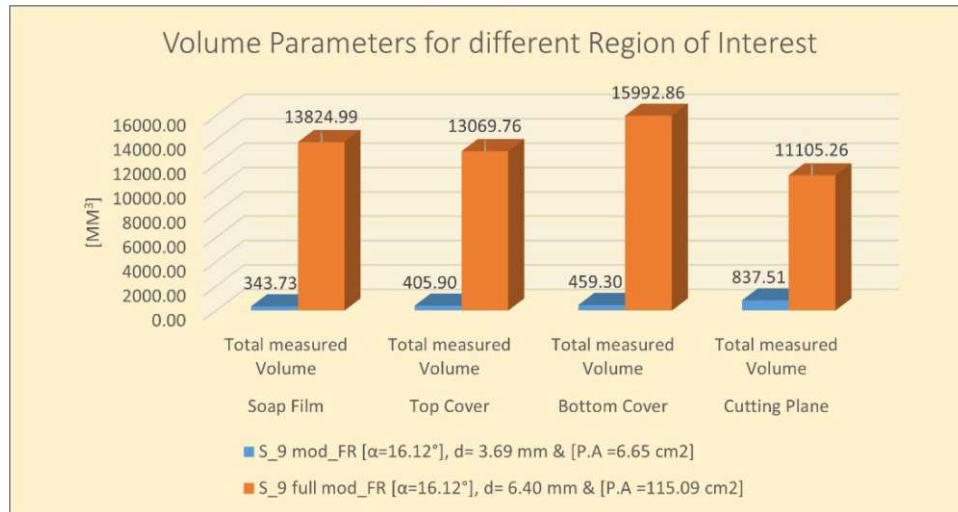
Figure 136: S_9 - Total measured Volume in mm³ for different Region of Interest
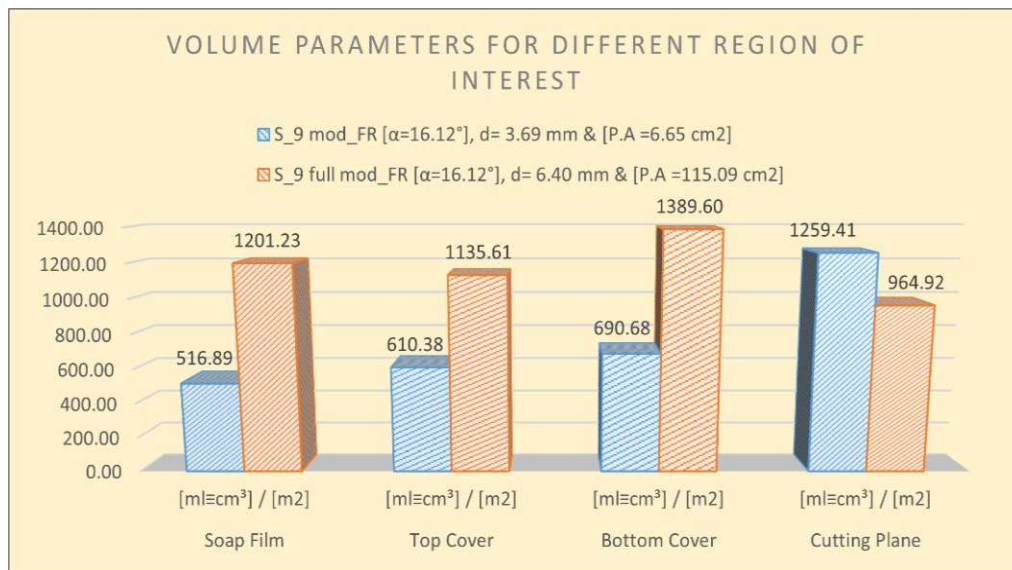
Figure 137: S_9 - Volume Parameters in cm³/1000 cm³ for different Region of Interests

By comparing results from the Figure 137 above, only Cutting Plane modes shown average changes between two Regions of Interest, until at all three other modes results changes drastically, which means that the size of the selected Region it is crucial for obtaining exact results.

5.3.2 Results obtained within the analysis of the image scaling (Lens focal length):

✓ Surface 10: Precast smooth concrete (stone pavement)

In the framework of the Volume Measurements Module within the analysis of the Image Scaling using different Lens focal Lengths in three individual attempts, I have used the same tilting angle α = 16.12° and the same image illumination. From Attempt 1 a Surface with dimensions from 2.99 x 1.86 cm, depth d = 0.85 mm was selected. According to this selection has Mex an ISO Projected Area from 5.57 cm^2 and projected Volume from 0.476 cm^3 calculated. From Attempt 2 a Surface with dimensions from 3.06 x 1.72 cm, depth d = 0.90 mm was selected. According to this selection has Mex an ISO Projected Area from 5.26 cm^2 and projected Volume from 0.474 cm^3 calculated. From Attempt 3 a Surface with dimensions from 3.00 x 1.75 cm, depth d = 0.97 mm was selected. According to this selection has Mex an ISO Projected Area from 5.25 cm^2 and projected Volume from 0.510 cm^3 calculated. From the comparison of those three selected Areas, the Software has obtained following results of volume parameters, presented in the figures below, according to the modes of volume measurement:
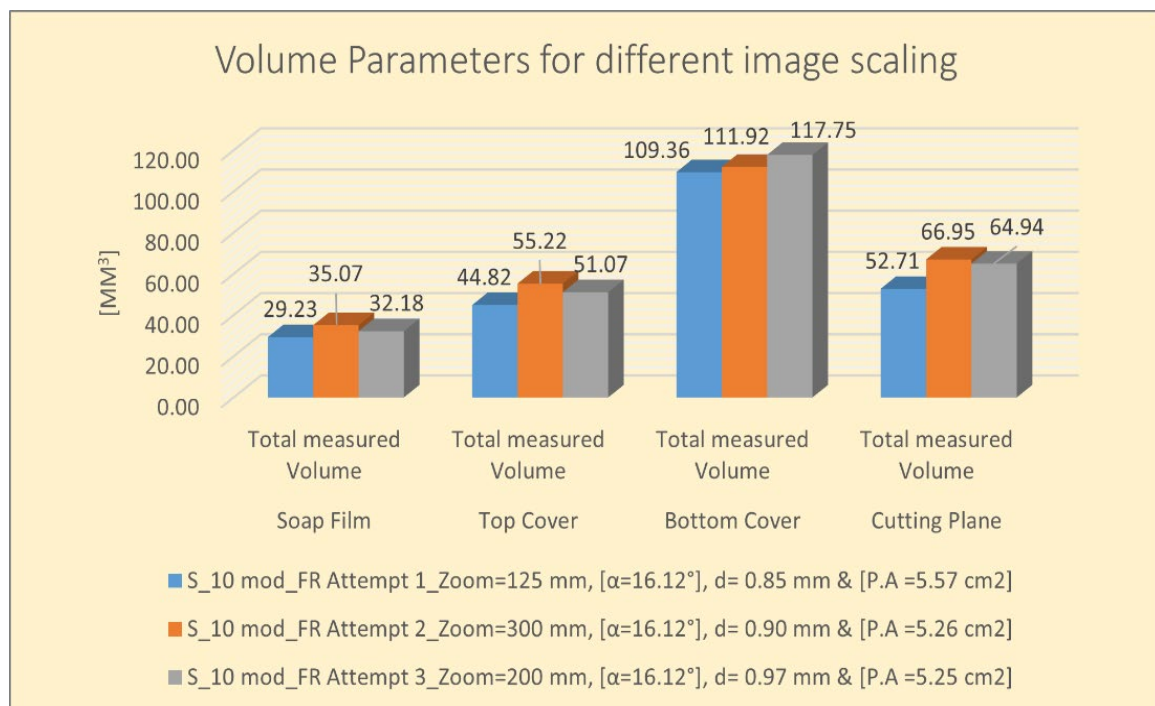
Figure 138: S_10 - Total measured Volume in mm³ for different image scaling (Lens focal length)
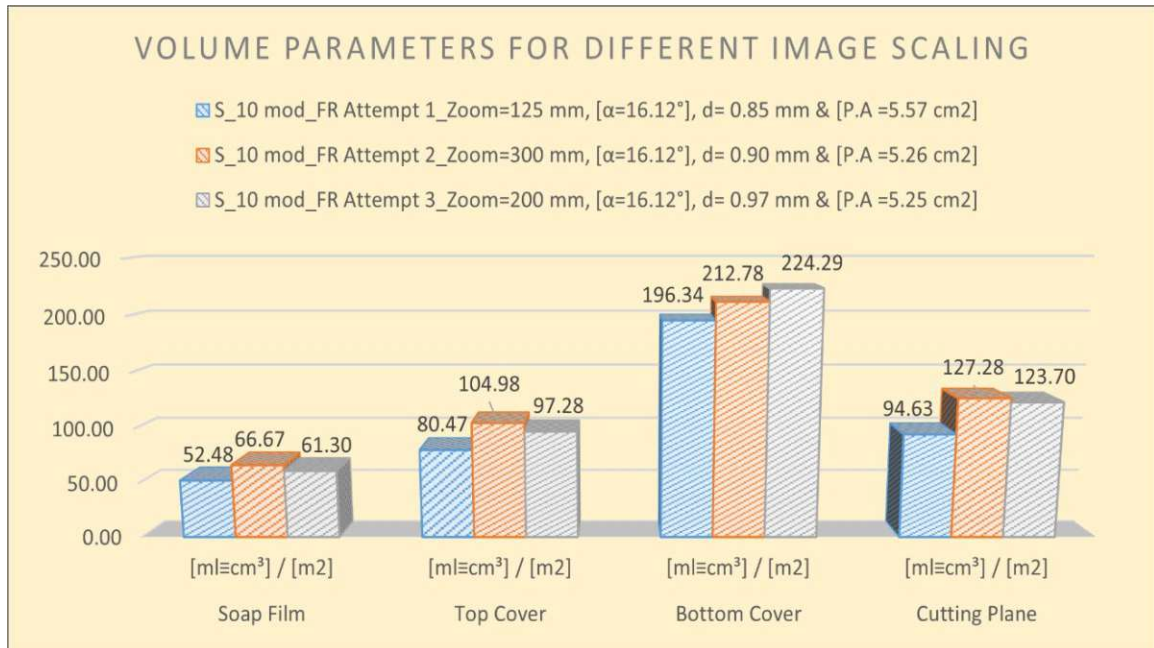
Figure 139: S_10 - Volume Parameters in cm³/1000 cm³ for different image scaling (Lens focal length)

Obtained results for three out to four modes in the figure above shows us, that as smaller the focal length of the Lens it is, the less precise will be the results in the framework of the volume measurements. That makes the mode Bottom Cover less useful in comparation with the other three modes.

✓ Surface 11: Precast concrete exterior staircase (rough-grained)

In the framework of the Volume Measurements Module within the analysis of the Image Scaling using different Lens focal Lengths in two individual attempts, I have used the same tilting angle α = 16.12° and the same image illumination. From Attempt 1 a Surface with dimensions from 3.01 x 1.68 cm, depth d = 1.45 mm was selected. According to this selection has Mex an ISO Projected Area from 5.07 cm² and projected Volume from 0.735 cm³ calculated. From Attempt 2 a Surface with dimensions from 3.00 x 1.67 cm, depth d = 1.42 mm was selected. According to this selection has Mex an ISO Projected Area from 5.01 cm² and projected Volume from 0.711 cm³ calculated. From the comparison of those two selected Areas, the Software has obtained following results of volume parameters, presented in the figures below, according to the modes of volume measurement:
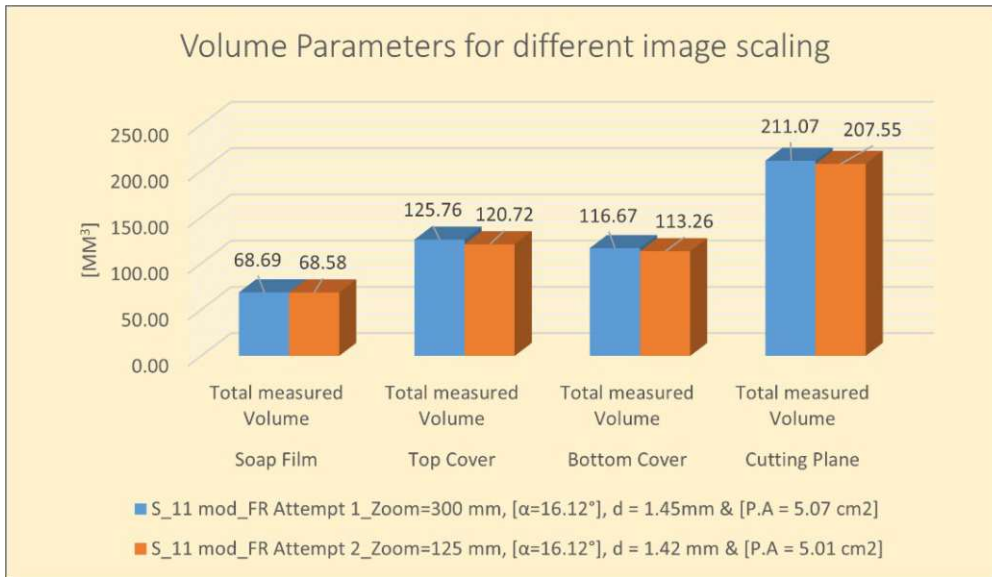
Figure 140: S_11 - Total measured Volume in mm³ for different image scaling (Lens focal length)
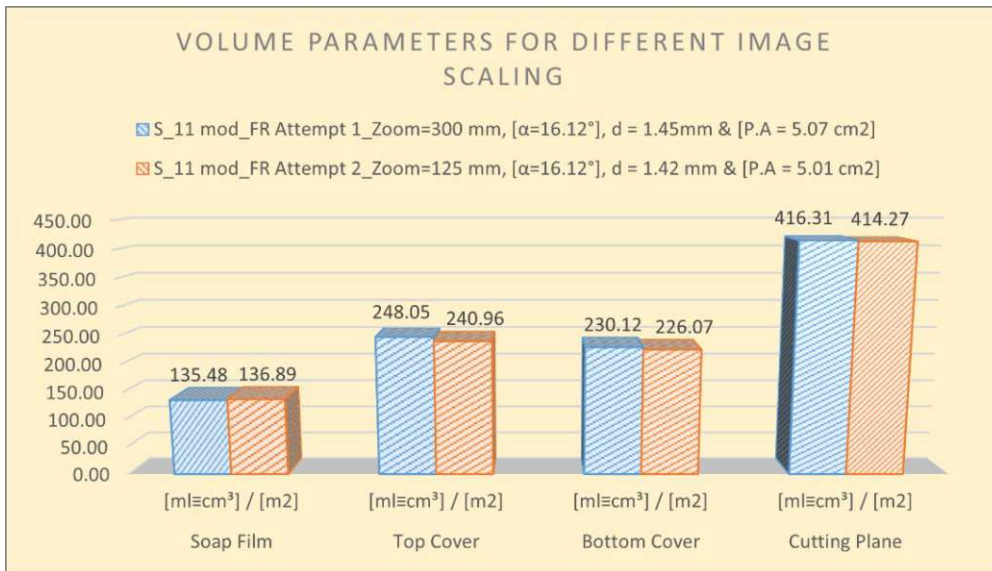
Figure 141: S_11 - Volume Parameters in cm³/1000 cm³ for different image scaling (Lens focal length)

As can be seen from the volume measurement results above, the results for this type of surface are almost identical within the same mode, with extremely small differences.

✓ Surface 12: Concrete sanded outside

In the framework of the Volume Measurements Module within the analysis of the Image Scaling using different Lens focal Lengths in two individual attempts, I have used the same tilting angle α = 16.12° and the same image illumination. From Attempt 1 a Surface with dimensions from 3.00 x 1.58 cm, depth d = 0.43 mm was selected. According to this selection has Mex an ISO Projected Area from 4.74 cm² and projected Volume from 0.203 cm³ calculated. From Attempt 2 a Surface with dimensions from 2.98 x 1.54 cm, depth d

119

= 0.46 mm was selected. According to this selection has Mex an ISO Projected Area from 4.57 cm² and projected Volume from 0.210 cm³ calculated. From the comparison of those two selected Areas, the Software has obtained following results of volume parameters, presented in the figures below, according to the modes of volume measurement:
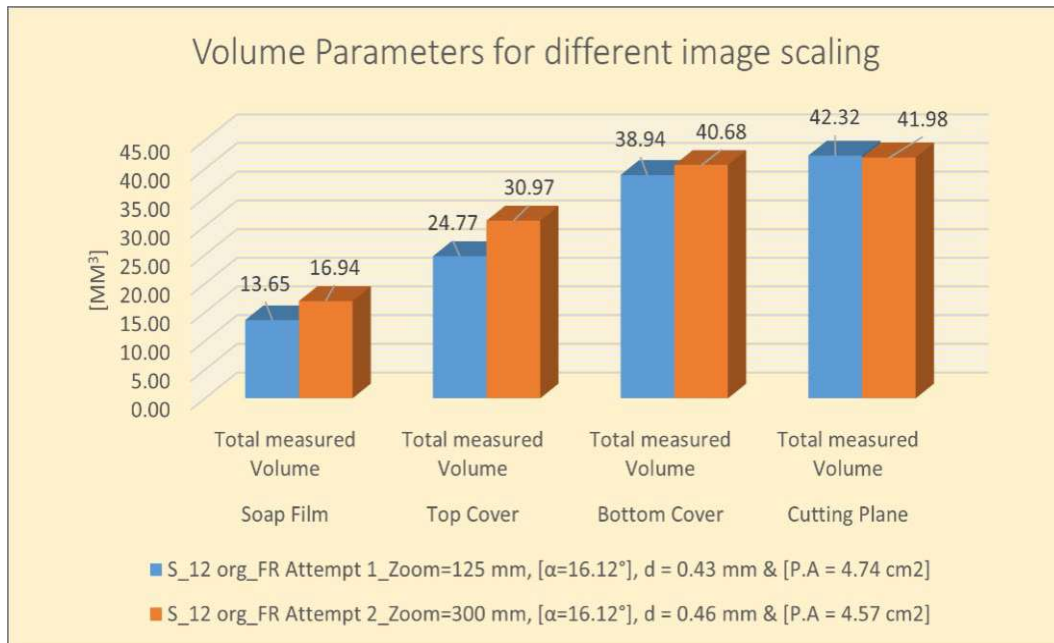
Figure 142: S_12 - Total measured Volume in mm³ for different image scaling (Lens focal length)
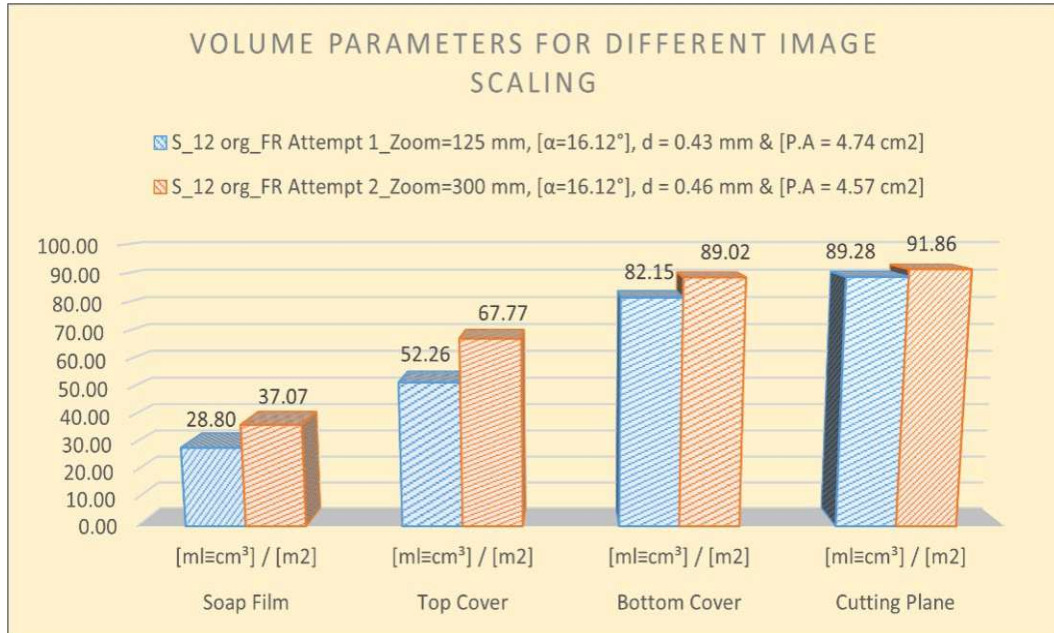
Figure 143: S_12 - Volume Parameters in cm³/1000 cm³ for different image scaling (Lens focal length)

In contrast to the results for surface 11, the measured volume values for each of the three automatic modes differ relatively more for this type of surface compared to the manual mode, that of the Cutting Plane.

5.3.3 Results obtained within the analysis of the image illumination:

- Surface 16: Concrete terrace slabs

For Volume Measurements Module within the analysis of the Image Illumination, shadow, and saturation in original and modified state of the captured stereo pair images, in the context of this sample of the concrete surface I've used different Lens focal Lengths in two different attempts, while the tilting angle α = 16.12° it remains unchanged. For original illumination form Attempt 1, a Surface with dimensions from 8.91 x 6.35 cm, depth d = 0.78 mm was selected. According to this selection has Mex an ISO Projected Area from 55.07 cm^2 and projected Volume from 4.295 cm^3 calculated. For modified illumination form Attempt 2, a Surface with dimensions from 16.00 x 8.98 cm, depth d = 1.05 mm was selected. According to this selection has Mex an ISO Projected Area from 143.47 cm^2 and projected Volume from 15.064 cm^3 calculated. From the comparison of those two selected Areas, the Software has obtained following results of volume parameters, presented in the figures below, according to the modes of volume measurement:

Figure 144: S_16 - Total measured Volume in mm^3 for different image illumination and scaling
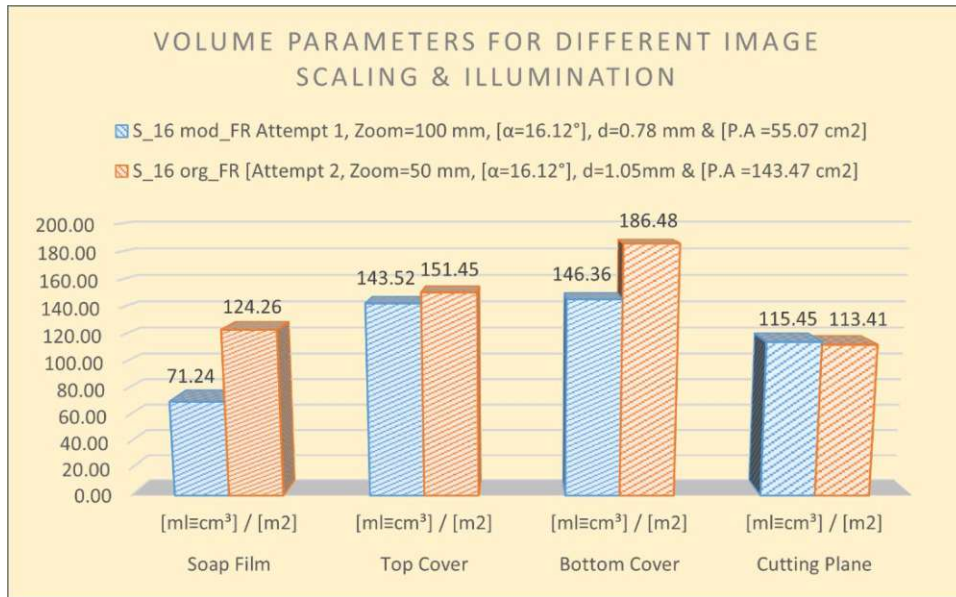
Figure 145: S_16 - Volume Parameters in cm³/1000 cm³ for different image illumination and scaling

The results of these volume measurements again show almost the same results as for the top cover, with the only difference being that the top cover results are slightly closer.

- Surface 1: Shot-blasted concrete surface

For Volume Measurements Module within the analysis of the Image Illumination, shadow, and saturation in original and modified state of the captured stereo pair images, in the context of this sample of the concrete surface I've used identic tilting angle α = 16.12°. For original illumination, shadow, and saturation, a Surface with dimensions from 2.70 x 1.85 cm, depth d = 1.15 mm was selected. According to this selection has Mex an ISO Projected Area from 4.99 cm^2 and projected Volume from 0.574 cm^3 calculated. For modified illumination form Attempt 2, a Surface with dimensions from 2.67 x 1.80 cm, depth d = 1.14 mm was selected. According to this selection has Mex an ISO Projected Area from 4.81 cm^2 and projected Volume from 0.548 cm^3 calculated. From the comparison of those two selected Areas, the Software has obtained following results of volume parameters, presented in the figures below, according to the modes of volume measurement:

Figure 146: S_1 - Total measured Volume in mm³ for different image illumination

Figure 147: S_1 - Volume Parameters in cm³/1000 cm³ for different image illumination

From the results obtained and shown in the figure above, it is clear that the results for the four modes are almost unchanged in the cases where the volume measurement is performed based only on the original or modified illumination conditions. This means that for most types of concrete surfaces, illumination based on the criteria recommended by the software does not deviate and leads to identical results.

5.3.4 Results obtained within the analysis of the tilting angle α, β, γ:

- Surface 13: Plinth in-situ concrete, smoothed

For Volume Measurements Module within the analysis of this influencing factor, I've used three different tilting angle α = 16.12°, β = 12.39° and γ = 8.55° with identical illumination, shadow, and saturation conditions. For the first tilting angle α, a surface with dimensions from 3.02 x 1.98 cm, depth d = 0.65 mm was selected. According to this selection has MeX an ISO Projected Area from 5.97 cm^2 and projected Volume from 0.390 cm^3 calculated. For the second tilting angle β, a Surface with dimensions from 3.01 x 1.96 cm, depth d = 0.64 mm was selected. According to this selection has MeX an ISO Projected Area from 5.90 cm^2 and projected Volume from 0.379 cm^3 calculated. For the third tilting angle γ, a Surface with dimensions from 3.00 x 1.98 cm, depth d = 0.81 mm was selected. According to this selection has MeX an ISO Projected Area from 5.95 cm^2 and projected Volume from 0.484 cm^3 calculated. From the comparison of those three selected Areas, the software has obtained following results of volume parameters, presented in the figures below, according to the modes of volume measurement:

Figure 148: S_13 - Total measured Volume in mm3 for different tilting angle α, β, and γ
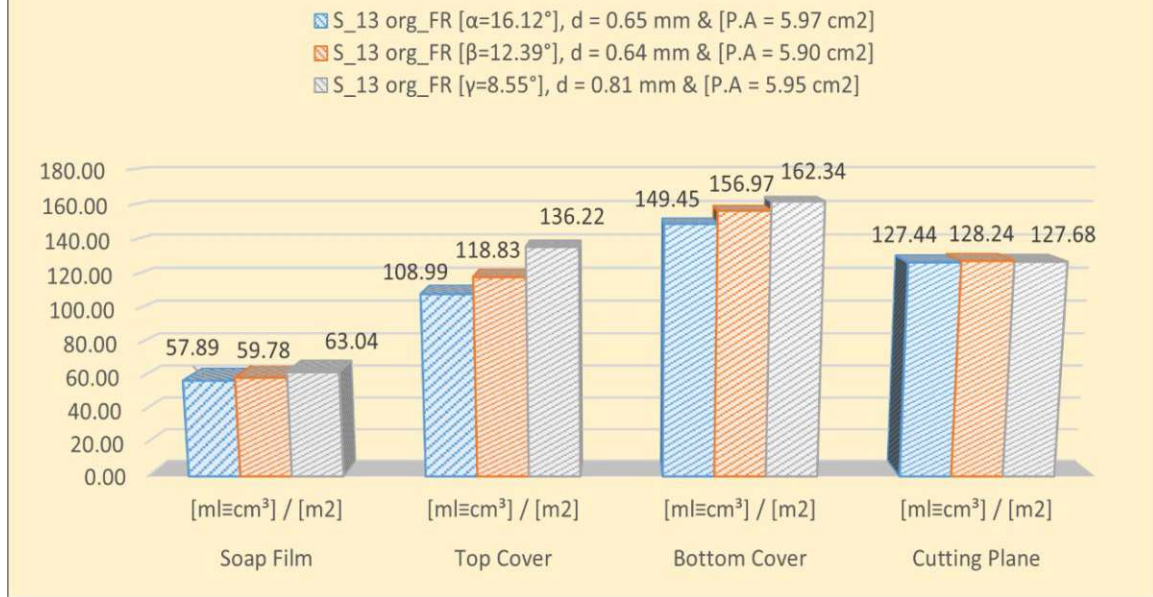
Figure 149: S_13 - Volume Parameters in cm3/1000 cm3 for different tilting angle α, ß, and γ

Although the results of the volume measurements differ considerably between the different modes, the results at different tilt angles within the same mode are very close for the Soap Film and Cutting Plane modes. At the same time, they vary for the Top and Bottom Cover modes depending on the tilting angle.

- Surface 9: Concrete broom finish

For Volume Measurements Module within the analysis of this influencing factor, I've used three different tilting angle α = 16.12°, β = 12.39° and γ = 8.55° with identical modified illumination, shadow, and saturation conditions. For the first tilting angle α, a Surface with dimensions from 3.00 x 2.22 cm, depth d = 3.69 mm was selected. According to this selection has MeX an ISO Projected Area from 6.65 cm² and projected Volume from 2.454 cm³ calculated. For the second tilting angle β, a Surface with dimensions from 3.00 x 2.22 cm, depth d = 3.60 mm was selected. According to this selection has MeX an ISO Projected Area from 6.66 cm² and projected Volume from 2.398 cm³ calculated. For the third tilting angle γ, a Surface with dimensions from 3.00 x 2.17 cm, depth d = 3.57 mm was selected. According to this selection has MeX an ISO Projected Area from 6.52 cm² and projected Volume from 2.328 cm³ calculated. From the comparison of those three selected Areas, the Software has obtained following results of volume parameters, presented in the figures below, according to the modes of volume measurement:
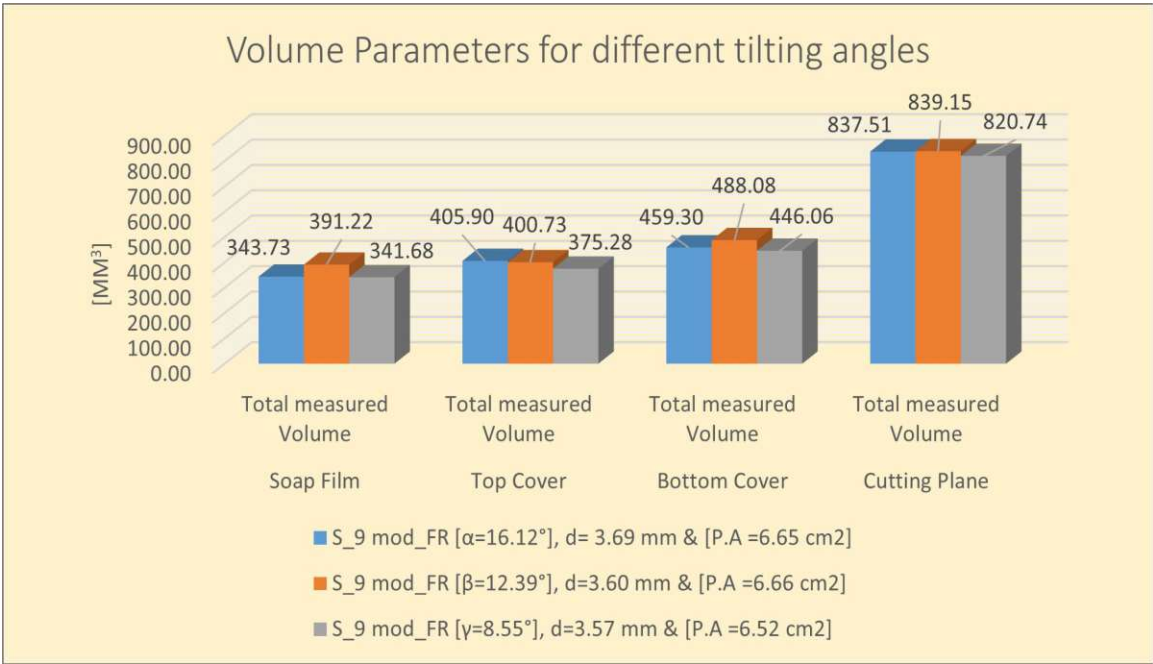
Figure 150: S_9 - Total measured Volume in mm3 for different tilting angle α, β, and γ
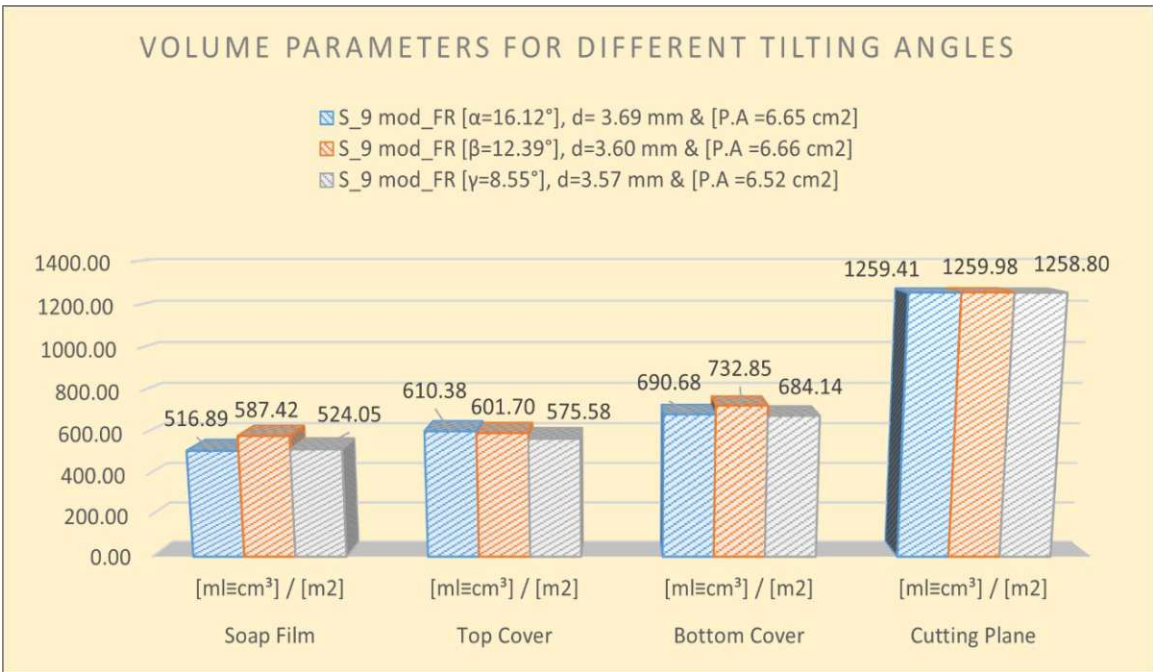
Figure 151: S_9 - Volume Parameters in cm3/1000 cm3 for different tilting angle α, β, and γ

Under this type of concrete surface, the results obtained from the software calculation for the volume measurements, increase depending on the type of mode, while the changes in the results within the modes are small for the three automatic modes, until the manual mode, so that in Cutting Plane, the results obtained are completely identical and without any change.

6. Conclusion and summary

To successfully apply the stereoscopic method for the characterization of surfaces, both concrete and other building materials, for specific study purposes, I can conclude from my research and experimental work presented and summarized in this paper that a crucial and necessary step is the accurate application of the photogrammetric method for planar registration at different tilt angles of stereo image pairs, which is very necessary for the three-dimensional generation of the digital surface model (DSM).

Before proceeding to the practical phase of image acquisition and then to the software calculation, any researcher must define and elaborate on the parameters of the surface and volume to determine the roughness of the surface. For the cases where the definition and elaboration of the roughness of the profile are necessary, it should be noted that in their framework, we distinguish the primary profile, roughness, and waviness. The roughness profile itself also consists of vertical, horizontal, and mixed parameters. A common criterion for both surface and profile roughness is the applicability of a minimum slope of 40% for the Bearing Area Curve (BAC).

Of course, during this process of taking two-dimensional images, particular emphasis should be given to the uniformity of illumination of the surface that will be photographed because this also affects the sharpness and clarity of the images, this significant factor in the creation of the digital surface model (DSM) and the calculation of the necessary parameters. To perform the photogrammetric method, various working tools are needed, such as: Single-lens reflex (SLR) camera with high image capture quality, lenses with different focal lengths, a device for changing the camera position, and tools for measuring the projection distance, the sampling distance, and the horizontal tilt distance, from which the tilt angle is also determined.

After capturing the stereo image pairs, we create the digital surface model (DSM) using the MeX software. For this purpose, the two acquired images are uploaded to the Stereo Creator. In this case, after completing the calibration data and selecting the region of interest, the program creates the required three-dimensional image model by overlaying the images. In the next step, profile, surface, and volume analysis are possible.

To compare the results of the roughness and volume of the surfaces and to get a clear overview of the accuracy of the parameters obtained from the software calculation, I have treated in this work, in addition to the samples of the concrete surfaces, two samples of other surfaces, one of wood and one of plastic. I have compared the results obtained for the roughness depth and its volume with those obtained from practical measurements in the laboratory.

By comparing and evaluating the results of the profile roughness measurement module, the following can be determined:

1. The most considerable difference between the values of all parameters of the roughness profile for all investigated surfaces is found for different cutoff wavelengths λc.
2. The closest values of profile roughness parameters for most of the studied surfaces are obtained for the illumination of the recorded surface, either from the original state or after its modification, except for surfaces 5 and 16, which are very flat.

3. Within the analysis of the parameters for the tilting angle, I note that their values depend on the type of concrete surface, while the parameters Rt and Rk show the most remarkable tendency to change.

4. Analyzing the influence factor related to the scaling of the image by the focal length of the lens, which was realized by two or three different individual attempts, I conclude that, except for Surface 12, where the values of all parameters remained almost unchanged, the difference in the results of nearly all parameters was significant in the other examined surface samples.

5. The different selection of the Region of Interest (ROI) for the same stereo image pair also has a tiny effect on the change in the values of the profile parameters, except for the parameters Rz and Rk, and only for some of the surfaces studied.

Therefore, depending on the size of the object under examination, attention should be paid especially to the change in the value of the cutoff wavelength λc, as well as to the scaling of the image at different focal lengths of the lens, as this is directly related to the quality of the acquired images.

By comparing and evaluating the results of the texture roughness measurement module, the following can be determined:

(1) After knowing the values for the thickness as well as the depth of the surface roughness of the plastic board from the practical measurement in the laboratory and comparing them with the values from the software calculations, it was much easier for me to determine which influencing factors had a significant impact in determining the roughness of the surface. Therefore, I concluded that for the surface in question, the results closest to those obtained from practical measurements were obtained for the largest tilting angle, the illumination in the original state, and the largest selected area of the region of interest. I had to approximate the value of the cutoff wavelength λc until I found the most accurate value.

(2) In the other studied samples of concrete surfaces, except for surface 13, the values of surface roughness parameters show minimal changes regardless of the tilting angle.

(3) Even for the original or modified state of the image illumination, the values of the surface roughness parameters remain within the range of acceptable changes except for the glossy-colored areas 14a and 15.

(4) Since in the analysis of surface roughness, the calculation of parameters is performed for the entire selected range, it is natural that the most remarkable changes in the results are given by the difference in the value of the cut wavelength λc, which was also proved by the results obtained for almost all the studied samples of concrete surfaces.

(5) Within the analysis of the parameters of surface roughness for the selected size of the region of interest, from the results obtained, I note that for some of the surfaces, we have a drastic change in the value of the parameter Sz. In contrast, on other surfaces, the values of the parameters either do not change significantly or all the parameters change, as is the case with surface 13.

Since there are no existing regulations or standards specifying the analysis of volume measurements and the determination of their parameters, I used the data obtained practically in the laboratory from volume measurements for two samples of non-concrete surfaces. As a result, the volume obtained for the surface under study was compared with the values measured in the three automatic modes until I made some approximations in manual mode until I found results almost identical to those of the practical measurements. Based on the significant differences in the compared practical and software results for all three automatic modes such as Soap Film, Top Cover and Bottom Cover, I can conclude that none of them can be considered good when it comes to volume measurements of selected ISO surfaces obtained from the creation of the digital surface model (DSM) after registering the images with the stereoscopic method.

In summary, I can say that photogrammetric investigations for characterizing concrete surfaces provide valuable results if suitable parameters are considered.

References

[1] A.W. Momber, R.-R. Schulz, Handbuch der Oberflächenbearbeitung Beton: Bearbeitung - Eigenschaften - Prüfung, Basel - Boston - Berlin: Birkhäuser Verlag, 2006, p. 19.

[2] A.W. Momber, R.-R. Schulz, Handbuch der Oberflächenbearbeitung Beton: Bearbeitung - Eigenschaften - Prüfung, Basel - Boston - Berlin: Birkhäuser Verlag, 2006, p. 20.

[3] M. Peyerl, *Bruchmechanische und stereoskopische Charakterisierung von Interfaces zementgebundener Werkstoffe,* Wien: Technische Universität, Dissertation, 2012, p. 50.

[4] A.W. Momber, R.-R. Schulz, Handbuch der Oberflächenbearbeitung Beton: Bearbeitung - Eigenschaften - Prüfung, Basel - Boston - Berlin: Birkhäuser Verlag, 2006, p. 451.

[5] *DIN 4760: Gestaltabweichungen: Begriffe - Ordnungssystem,* Berlin: Deutches Institut für Normung, 1982, p. 1.

[6] A.W. Momber, R.-R. Schulz, Handbuch der Oberflächenbearbeitung Beton: Bearbeitung - Eigenschaften - Prüfung, Basel - Boston - Berlin: Birkhäuser Verlag, 2006, p. 455.

[7] *DIN 4760: Gestaltabweichungen: Begriffe - Ordnungssystem,* Berlin: Deutches Institut für Normung, 1982, p. 2.

[8] *DIN EN ISO 8785:1999-10: Oberflächenunvollkommenheiten: Begriffe, Definitionen und Kenngröße,* Berlin: Deutsches Institut für Normung, 1999, p. 3.

[9] *DIN EN ISO 8785:1999-10: Oberflächenunvollkommenheiten: Begriffe, Definitionen und Kenngröße,* Berlin: Deutches Institut für Normung, 1999, p. 2.

[10] A.W. Momber, R.-R. Schulz, Handbuch der Oberflächenbearbeitung Beton: Bearbeitung - Eigenschaften - Prüfung, Basel - Boston - Berlin: Birkhäuser Verlag, 2006, p. 453.

[11] *DIN EN ISO 8785:1999-10: Oberflächenunvollkommenheiten: Begriffe, Definitionen und Kenngröße,* Berlin: Deutsches Institut für Normung, 1999, pp. 3-6.

[12] C. Zeiss, „Oberflächenparameter," Carl Zeiss Industrielle Messtechnik GmbH, 8 2016. [Online]. Available: http://pages.zeiss.com/rs/896-XMS-794/images/DE_60_050_004I_Oberflaeche_A0.pdf. [Zugriff am 01 03 2021].

[13] *ISO 3274:1996 - Surface texture: Profile method - Nominal characteristics of contact (stylus) instruments,* Geneva: International Standard, 1996, p. 2.

[14] *DIN EN ISO 4287:2010-07: Oberflächenbeschaffenheit: Tastschnittverfahren - Benennungen - Definitionen und Kenngrößen der Oberflächenbeschaffenheit,* Berlin: Deutsches Institut für Normung, 2010, p. 7.

[15] *DIN EN ISO 4287:2010-07: Oberflächenbeschaffenheit: Tastschnittverfahren - Benennungen - Definitionen und Kenngrößen der Oberflächenbeschaffenheit,* Berlin: Deutches Institut für Normung, 2010, p. 8.

[16] *DIN EN ISO 4287:2010-07: Oberflächenbeschaffenheit: Tastschnittverfahren - Benennungen - Definitionen und Kenngrößen der Oberflächenbeschaffenheit,* Berlin: Deutches Institut für Normung, 2010, p. 6.

[17] *DIN EN ISO 4287:2010-07: Oberflächenbeschaffenheit: Tastschnittverfahren - Benennungen - Definitionen und Kenngrößen der Oberflächenbeschaffenheit,* Berlin: Deutches Institut für Normung, 2010, p. 9.

[18] Jenoptik, „Rauheitsmesssysteme von Jenoptik – Oberflächenkenngrößen in der Praxis," JENOPTIK Industrial Metrology Germany GmbH, 1 2016. [Online]. Available: https://www.pruefmittel24.com/documents/9305-PosterOberflaechenkenngroessen.pdf. [Zugriff am 3 3 2021].

[19] *DIN EN ISO 4287:2010-07: Oberflächenbeschaffenheit: Tastschnittverfahren - Benennungen - Definitionen und Kenngrößen der Oberflächenbeschaffenheit,* Berlin: Deutches Institut für Normung, 2010, p. 10.

[20] *DIN EN ISO 4287:2010-07: Oberflächenbeschaffenheit: Tastschnittverfahren - Benennungen - Definitionen und Kenngrößen der Oberflächenbeschaffenheit,* Berlin: Deutches Institut für Normung, 2010, p. 11.

[21] S. Jung, *Oberflächenbeurteilung - Rauheitsmessung,* Stuttgart: Universität Stuttgart: Institut für Maschinenelemente, 2012, p. 2.

[22] M. Peyerl, *Bruchmechanische und stereoskopische Charakterisierung von Interfaces zementgebundener Werkstoffe,* Wien: Technische Universität: Dissertation, 2012, p. 54.

[23] *DIN EN ISO 4287:2010-07: Oberflächenbeschaffenheit: Tastschnittverfahren - Benennungen - Definitionen und Kenngrößen der Oberflächenbeschaffenheit,* Berlin: Deutches Institut für Normung, 2010, p. 15.

[24] A.W. Momber, R.-R. Schulz, Handbuch der Oberflächenbearbeitung Beton: Bearbeitung - Eigenschaften - Prüfung, Basel - Boston - Berlin: Birkhäuser Verrlag, 2006, p. 20.

[25] A.W. Momber, R.-R. Schulz, Handbuch der Oberflächenbearbeitung Beton: Bearbeitung - Eigenschaften - Prüfung, Basel - Boston - Berlin: Birkhäuser Verlag, 2006, p. 22.

[26] *DIN EN ISO 4288:1998-04: Oberflächenbeschaffenheit: Tastschnittverfahren - Regeln und Verfahren für die Beurteilung der Oberflächenbeschaffenheit,* Berlin: Deutsches Institut für Normung, 1998, p. 7.

[27] *DIN EN ISO 4287:2010-07: Oberflächenbeschaffenheit: Tastschnittverfahren - Benennungen - Definitionen und Kenngrößen der Oberflächenbeschaffenheit,* Berlin: Deutches Institut für Normung, 2010, p. 12.

[28] *DIN EN ISO 4287:2010-07: Oberflächenbeschaffenheit: Tastschnittverfahren - Benennungen - Definitionen und Kenngrößen der Oberflächenbeschaffenheit,* Berlin: Deutches Institut für Normung, 2010, p. 13.

[29] *DIN EN ISO 4287:2010-07: Oberflächenbeschaffenheit: Tastschnittverfahren - Benennungen - Definitionen und Kenngrößen der Oberflächenbeschaffenheit,* Berlin: Deutches Institut für Normung, 2010, p. 14.

[30] A.W. Momber, R.-R. Schulz, Handbuch der Oberflächenbearbeitung Beton: Bearbeitung - Eigenschaften - Prüfung, Basel - Boston - Berlin: Birkhäuser Verlag, 2006, p. 460.

[31] G. Mahr, „Perthometer Oberflächen-Kenngrößen," Beuth Verlag GmbH, Berlin, 1999.

[32] *DIN EN ISO 4287:2010-07: Oberflächenbeschaffenheit: Tastschnittverfahren - Benennungen - Definitionen und Kenngrößen der Oberflächenbeschaffenheit,* Berlin: Deutches Institut für Normung, 2010, p. 16.

[33] *DIN EN ISO 4287:2010-07: Oberflächenbeschaffenheit: Tastschnittverfahren - Benennungen - Definitionen und Kenngrößen der Oberflächenbeschaffenheit,* Berlin: Deutches Institut für Normung, 2010, p. 18.

[34] *DIN EN ISO 4287:2010-07: Oberflächenbeschaffenheit: Tastschnittverfahren - Benennungen - Definitionen und Kenngrößen der Oberflächenbeschaffenheit,* Berlin: Deutches Institut für Normung, 2010, p. 19.

[35] *DIN EN ISO 13565-2:1998-04: Oberflächenbeschaffenheit: Tastschnittverfahren: Oberflächen mit plateauartigen funktionsrelevanten Eigenschaften: Teil 2: Beschreibung der Höhe mittels linearer Darstellung der Materialanteilkurve,* Berlin: Deutsches Institut für Normung, 1998, p. 2.

[36] *DIN EN ISO 13565-2:1998-04: Oberflächenbeschaffenheit: Tastschnittverfahren: Oberflächen mit plateauartigen funktionsrelevanten Eigenschaften: Teil 2: Beschreibung der Höhe mittels linearer Darstellung der Materialanteilkurve,* Berlin: Deutches Institut für Normung, 1998, p. 3.

[37] *DIN EN ISO 13565-2:1998-04: Oberflächenbeschaffenheit: Tastschnittverfahren: Oberflächen mit plateauartigen funktionsrelevanten Eigenschaften: Teil 2: Beschreibung der Höhe mittels linearer Darstellung der Materialanteilkurve,* Berlin: Deutches Institut für Normung, 1998, p. 4.

[38] *DIN EN ISO 13565-3:2000-08: Oberflächenbeschaffenheit: Tastschnittverfahren; Oberflächen mit plateauartigen funktionsrelevanten Eigenschaften: Teil 3: Beschreibung der Höhe von Oberflächen mit der Wahrscheinlichkeitsdichtekurve,* Berlin: Deutches Institut für Normung, 2000, p. 2.

[39] *DIN EN ISO 13565-3:2000-08; Oberflächenbeschaffenheit: Tastschnittverfahren; Oberflächen mit plateauartigen funktionsrelevanten Eigenschaften; Teil 3: Beschreibung der Höhe von Oberflächen mit der Wahrscheinlichkeitsdichtekurve,* Berlin: Deutches Institut für Normung, 2000, p. 3.

[40] *DIN EN ISO 13565-3:2000-08; Oberflächenbeschaffenheit: Tastschnittverfahren; Oberflächen mit plateauartigen funktionsrelevanten Eigenschaften; Teil 3: Beschreibung der Höhe von Oberflächen mit der Wahrscheinlichkeitsdichtekurve,* Berlin: Deutches Institut für Normung, 2000, p. 4.

[41] M. Peyerl, *Bruchmechanische und stereoskopische Charakterisierung von Interfaces zementgebundener Werkstoffe,* Wien: Technische Universität: Dissertation, 2012, p. 58.

[42] M. Peyerl, *Bruchmechanische und stereoskopische Charakterisierung von Interfaces zementgebundener Werkstoffe,* Wien: Technische Universität: Dissertation, 2012, p. 59.

[43] *Handbook of the Software MeX: Version 6.2.1,* Graz: Alicona Imaging GmbH, 2018, p. 73.

[44] *Handbook of the Software MeX: Version 6.2.1,* Graz: Alicona Imaging GmbH, 2018, p. 74.

[45] *Handbook of the Software MeX: Version 6.2.1,* Graz: Alicona Imaging GmbH, 2018, p. 76.

[46] *Handbook of the Software MeX: Version 6.2.1,* Graz: Alicona Imaging GmbH, 2018, p. 77.

[47] *Handbook of the Software MeX: Version 6.2.1,* Graz: Alicona Imaging GmbH, 2018, p. 78.

[48] *DIN EN ISO 4288:1998-04: Oberflächenbeschaffenheit: Tastschnittverfahren - Regeln und Verfahren für die Beurteilung der Oberflächenbeschaffenheit,* Berlin: Deutches Institut für Normung, 1998, p. 5.

[49] *DIN EN ISO 4288:1998-04: Oberflächenbeschaffenheit: Tastschnittverfahren - Regeln und Verfahren für die Beurteilung der Oberflächenbeschaffenheit,* Berlin: Deutches Institut für Normung, 1998, p. 4.

[50] *DIN EN ISO 4288:1998-04: Oberflächenbeschaffenheit: Tastschnittverfahren - Regeln und Verfahren für die Beurteilung der Oberflächenbeschaffenheit,* Berlin: Deutches Institut für Normung, 1998, p. 6.

[51] *DIN EN ISO 4288:1998-04: Oberflächenbeschaffenheit: Tastschnittverfahren - Regeln und Verfahren für die Beurteilung der Oberflächenbeschaffenheit,* Berlin: Deutches Institut für Normung, 1998, p. 8.

[52] R.-R. Schulz, *Rautiefenmessung an Betonoberflächen,* Frankfurt: University of Applied Sciences: Vorlesung, pp. 21-23.

[53] A.W. Momber, R.-R. Schulz, Handbuch der Oberflächenbearbeitung Beton: Bearbeitung - Eigenschaften - Prüfung, Basel - Boston - Berlin: Birkhäuser Verlag, 2006, p. 482.

[54] A.W. Momber, R.-R. Schulz, Handbuch der Oberflächenbearbeitung Beton: Bearbeitung - Eigenschaften - Prüfung, Basel - Boston - Berlin: Birkhäuser Verlag, 2006, p. 481.

[55] A.W. Momber, R.-R. Schulz, Handbuch der Oberflächenbearbeitung Beton: Bearbeitung - Eigenschaften - Prüfung, Basel - Boston - Berlin: Birkhäuser Verlag, 2006, p. 483.

[56] A.W. Momber, R.-R. Schulz, Handbuch der Oberflächenbearbeitung Beton: Bearbeitung - Eigenschaften - Prüfung, Basel - Boston - Berlin: Birkhäuser Verlag, 2006, p. 471.

[57] A.W. Momber, R.-R. Schulz, Handbuch der Oberflächenbearbeitung Beton: Bearbeitung - Eigenschaften - Prüfung, Basel - Boston - Berlin: Birkhäuser Verlag, 2006, p. 472.

[58] A.W. Momber, R.-R. Schulz, Handbuch der Oberflächenbearbeitung Beton: Bearbeitung - Eigenschaften - Prüfung, Basel - Boston - Berlin: Birkhäuser Verlag, 2006, p. 473.

[59] C. Heipke, *Photogrammetrie und Fernurkunfung - eine Einführung,* 1st Hrsg., Hannover: Springer Spektrum Verlag, 2017, p. 9.

[60] Norbert Pfeifer, Camillo Ressl, *Grundzüge der Photogrammetrie,* D. f. G. u. Geoinformation, Hrsg., Wien: Technische Universität Wien, 2020, p. 7.

[61] Norbert Pfeifer, Camillo Ressl, *Grundzüge der Photogrammetrie,* D. f. G. u. Geoinformation, Hrsg., WIen: Technische Universität Wien, 2020, pp. 7-8.

[62] N. D'Amico, *Photogrammetric Techniques for Evaluation and Analysis of Concrete Structures and Specimens,* Lowell, Massachusetts: University of Massachusetts: Master Thesis, 2017, p. 23.

[63] Norbert Pfeifer, Camillo Ressl, *Grundzüge der Photogrammetrie,* D. f. G. u. Geoinformation, Hrsg., Wien: Technische Universität Wien, 2020, p. 9.

[64] A. Spitzer, *Verwendung von Spiegeln zur vollständigen photogrammetrischen Oberflächenrekonstruktion von schwer zugänglichen Objekten,* Wien: Technische Universität Wien: Diplomarbeit, 2009, pp. 18-19.

[65] M. Peyerl, *Bruchmechanische und stereoskopische Charakterisierung von Interfaces zementgebundener Werkstoffe,* Wien: Technische Universität: Dissertation, 2012, p. 65.

[66] M. Peyerl, *Bruchmechanische und stereoskopische Charakterisierung von Interfaces zementgebundener Werkstoffe,* Wien: Technische Universität: Dissertation, 2012, p. 66.

[67] J. Böhm, *Charakterisierung der Struktur von Putzoberflächen mittels Photogrammetrie,* Wien: FH Campus Wien: Masterarbeit, 2021, p. 30.

[68] *Handbook of the Software MeX: Version 6.2.1,* Graz: Alicona Imaging GmbH, 2018, p. 12.

[69] *Handbook of the Software MeX: Version 6.2.1,* Graz: Alicona Imaging GmbH, 2018, p. 9.

[70] *Handbook of the Software MeX: Version 6.2.1,* Graz: Alicona Imaging GmbH, 2018, p. 17.

[71] *Handbook of the Software MeX: Version 6.2.1,* Graz: Alicona Imaging GmbH, 2018, p. 13.

[72] *Handbook of the Software MeX: Version 6.2.1,* Graz: Alicona Imaging GmbH, 2018, p. 20.

[73] *Handbook of the Software MeX: Version 6.2.1,* Graz: Alicona Imaging GmbH, 2018, p. 11.

[74] *Handbook of the Software MeX: Version 6.2.1,* Graz: Alicona Imaging GmbH, 2018, pp. 13-14.

[75] *Handbook of the Software MeX: Version 6.2.1,* Graz: Alicona Imaging GmbH, 2018, p. 117.

[76] M. Peyerl, *Bruchmechanische und stereoskopische Charakterisierung von Interfaces zementgebundener Werkstoffe,* Wien: Technische Universität: Dissertation, 2012, p. 69.

[77] *Handbook of the Software MeX: Version 6.2.1,* Graz: Alicona Imaging GmbH, 2018, p. 115.

[78] M. Peyerl, *Bruchmechanische und stereoskopische Charakterisierung von Interfaces zementgebundener Werkstoffe,* Wien: Technische Universität: Dissertation, 2012, p. 61.

[79] M. Peyerl, *Bruchmechanische und stereoskopische Charakterisierung von Interfaces zementgebundener Werkstoffe,* Wien: Technische Universität: Dissertation, 2012, p. 67.

[80] N. Jerabek, *Anwendung und Methodik digitaler Photogrammetrie im Arbeitsprozess,* Wien: Technische Universität: Diplomarbeit, 2015, p. 113.

[81] *Handbook of the Software MeX: Version 6.2.1,* Graz: Alicona Imaging GmbH, 2018, p. 55.

[82] *Handbook of the Software MeX: Version 6.2.1,* Graz: Alicona Imaging GmbH, 2018, p. 68.

List of Figures

List of Tables

Appendix A

Results of Parameters from the Texture Roughness Parameters:

A 1 - S_1 Texture Roughness Parameters for different cutoff wavelength λc

*A 2 - S_1 Texture Roughness Parameters for different Region of Interest (ROI)*

*A 3 - S_5 Texture Roughness Parameters for different image illumination*
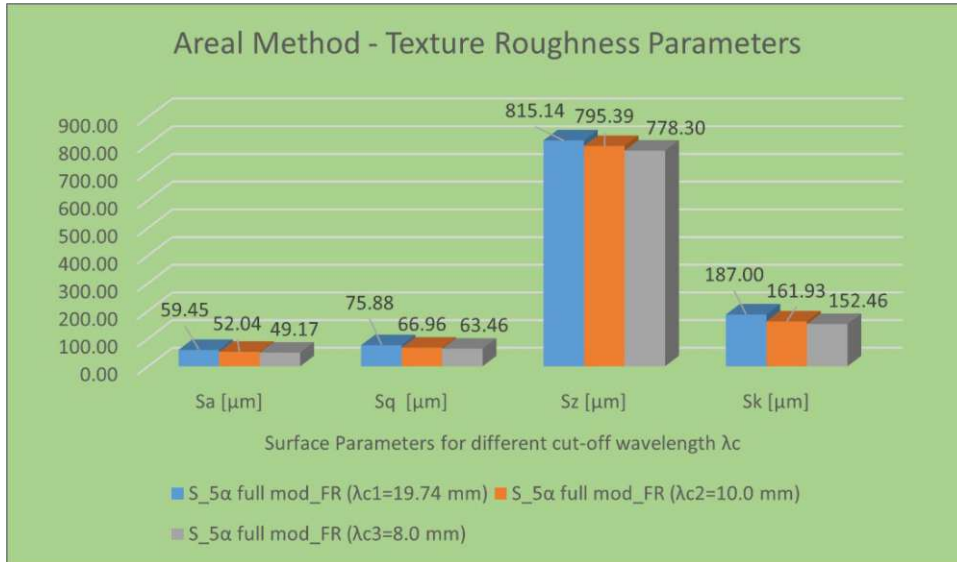
*A 4 - S_5 Texture Roughness Parameters for different cutoff wavelength λc*
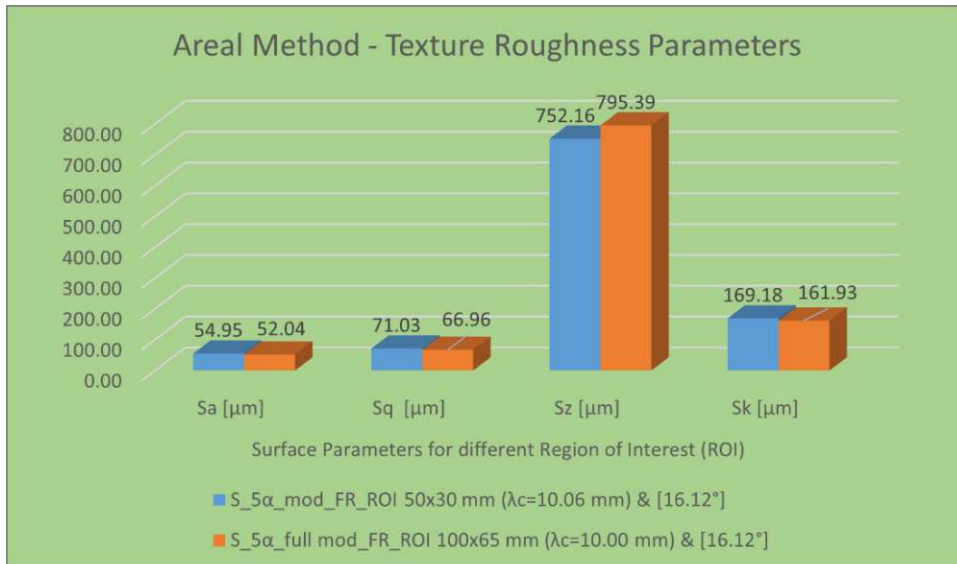
A 5 - S_5 Texture Roughness Parameters for different Region of Interest (ROI)
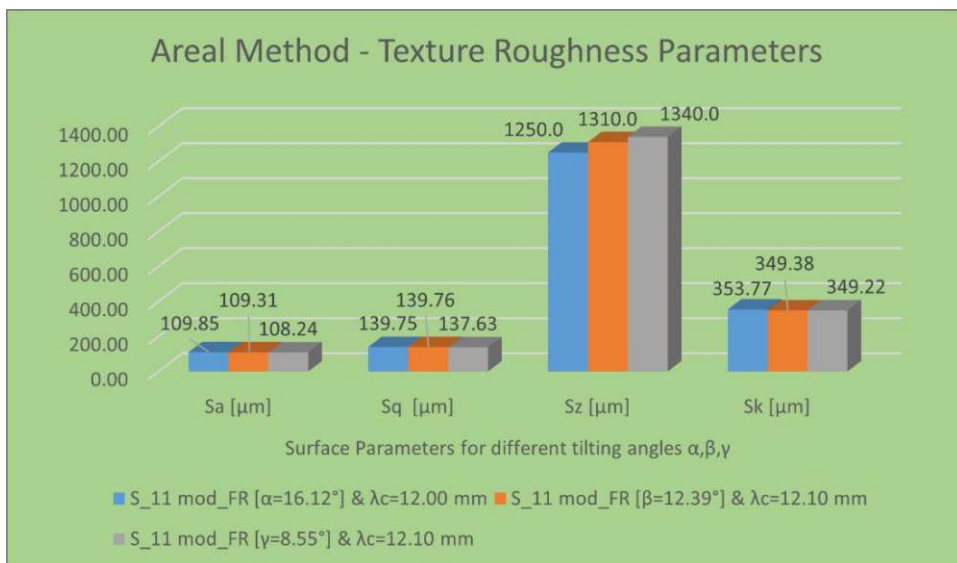
A 6 - S_11 Texture Roughness Parameters for different tilting angles α, β, γ
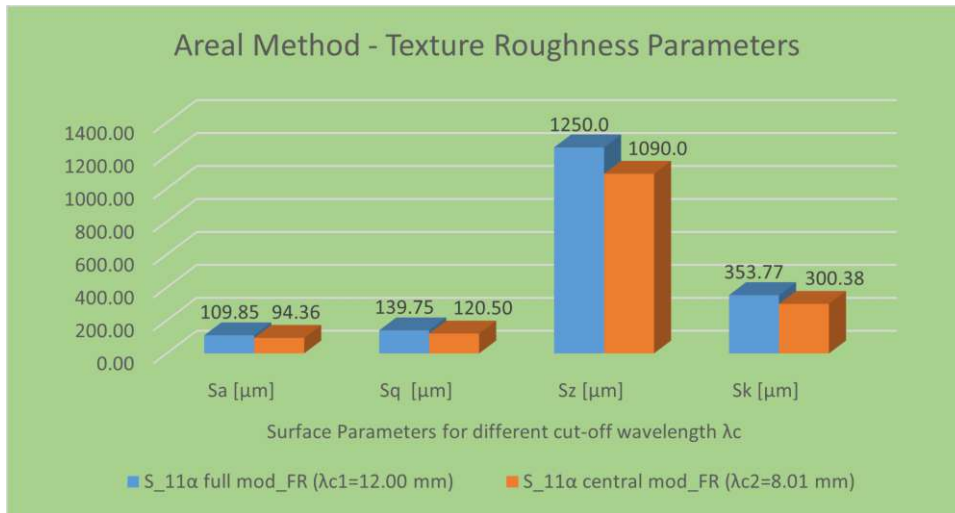
A 7 - S_11 Texture Roughness Parameters for different cutoff wavelength λc
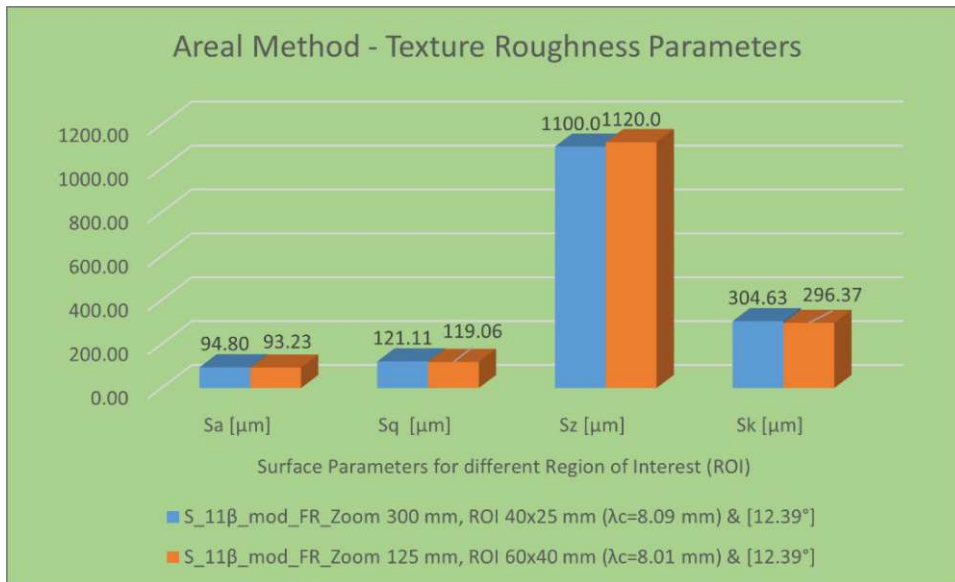
A 8 - S_11 Texture Roughness Parameters for different Region of Interest (ROI)
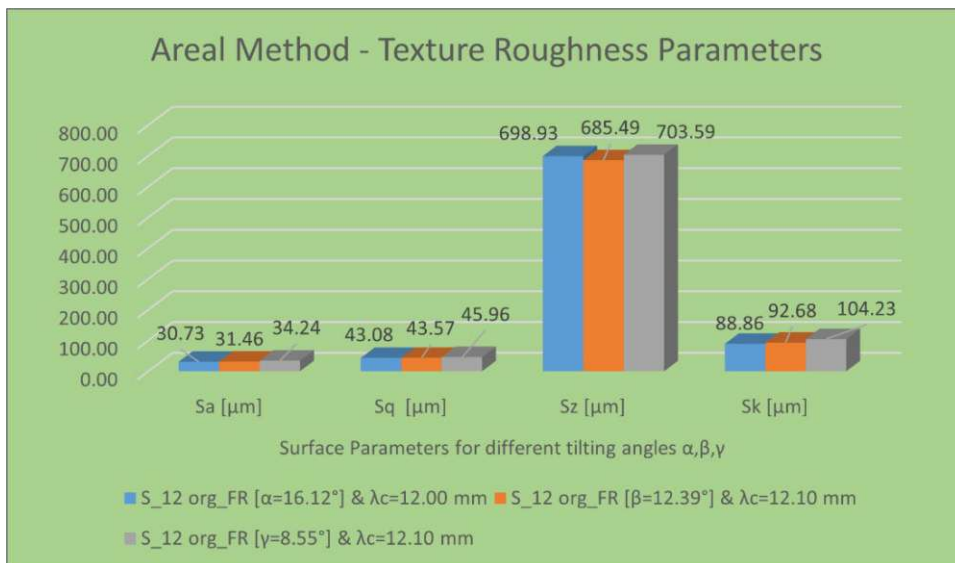
A 9 - S_12 Texture Roughness Parameters for different tilting angles α, β, γ
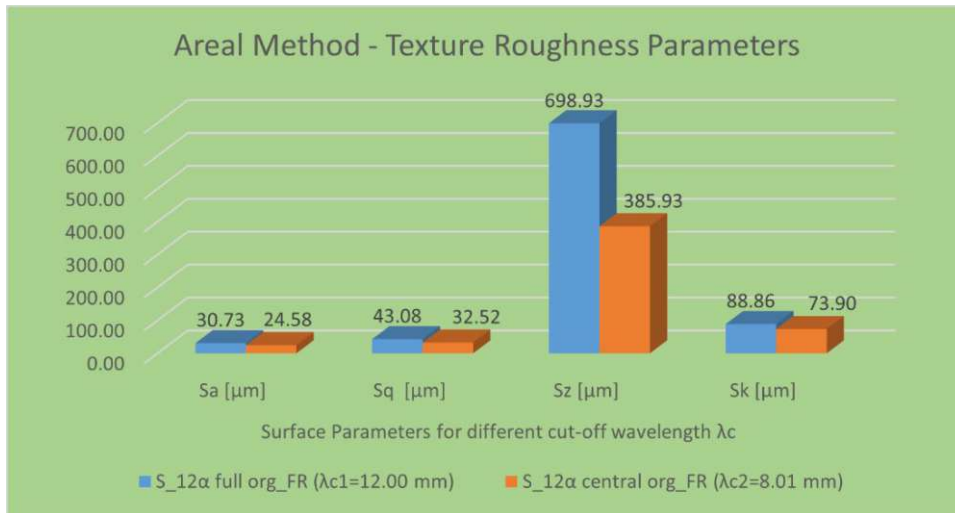
A 10 - S_12 Texture Roughness Parameters for different cutoff wavelength λc
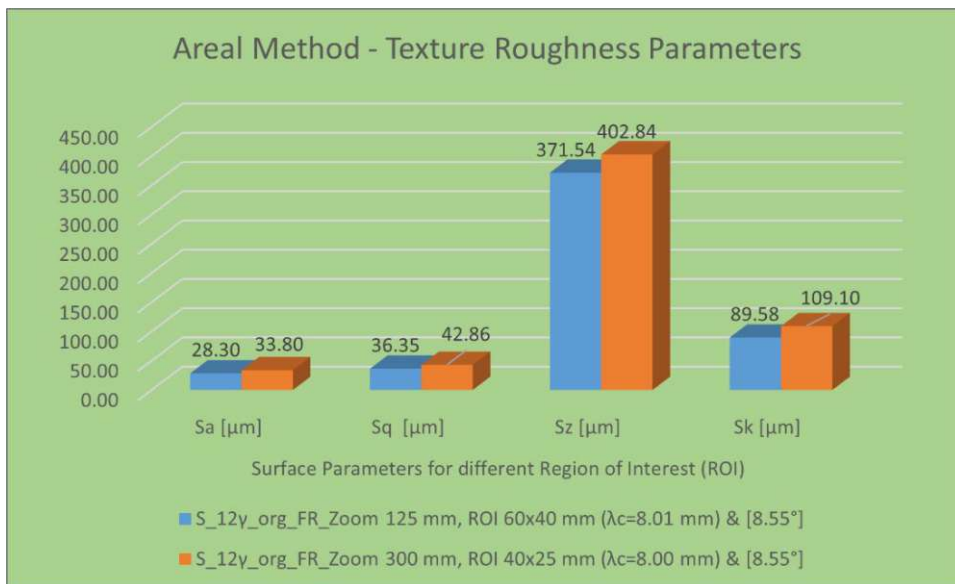
A 11 - S_12 Texture Roughness Parameters for different Region of Interest (ROI)
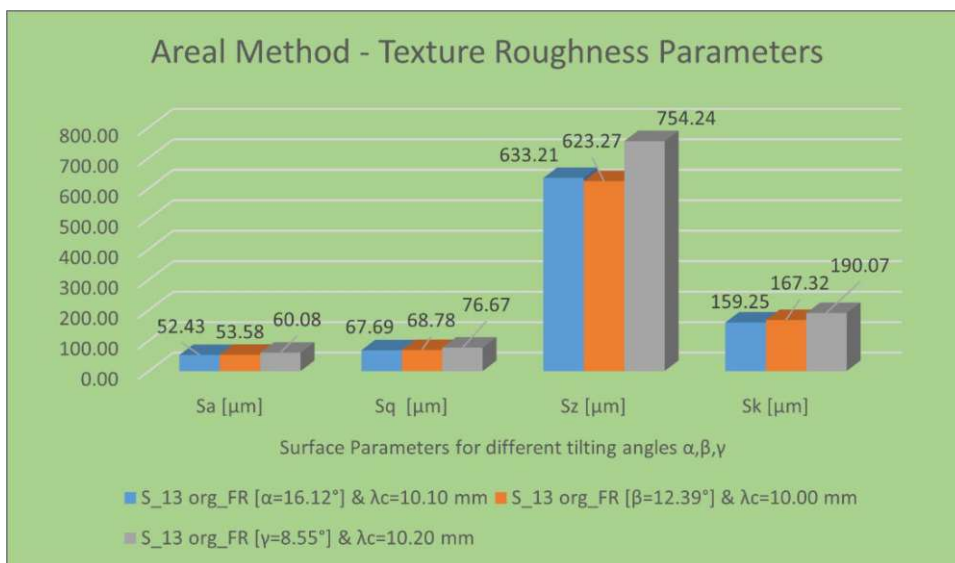
A 12 - S_13 Texture Roughness Parameters for different tilting angles α, β, γ
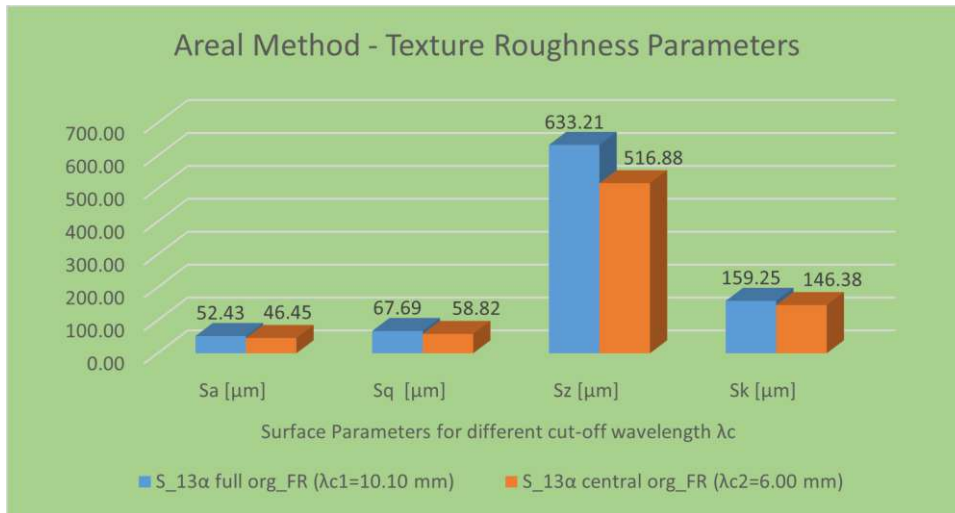
A 13 - S_13 Texture Roughness Parameters for different cutoff wavelength λc
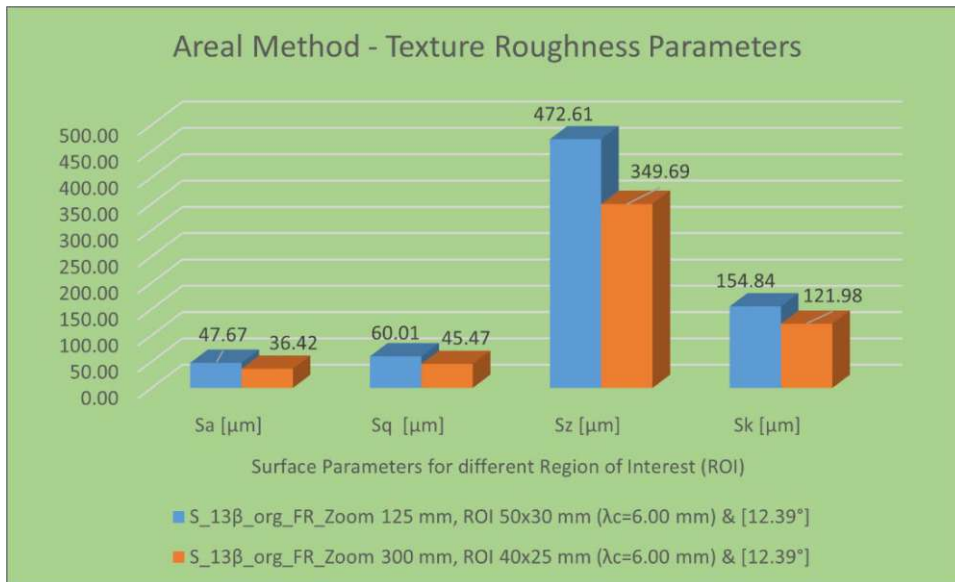
A 14 - S_13 Texture Roughness Parameters for different Region of Interest (ROI)
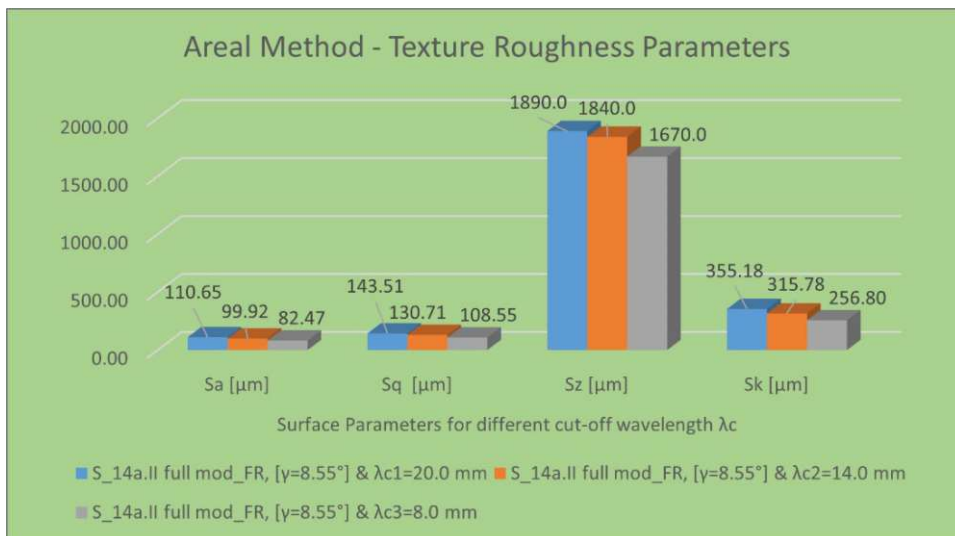
A 15 - S_14a.II Texture Roughness Parameters for different cutoff wavelength λc
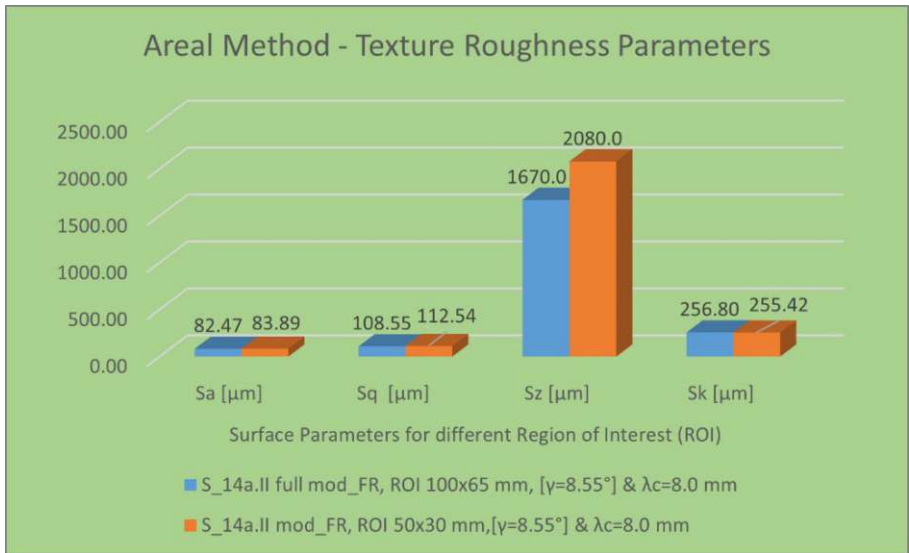
A 16 - S_14a.II Texture Roughness Parameters for different Region of Interest (ROI)
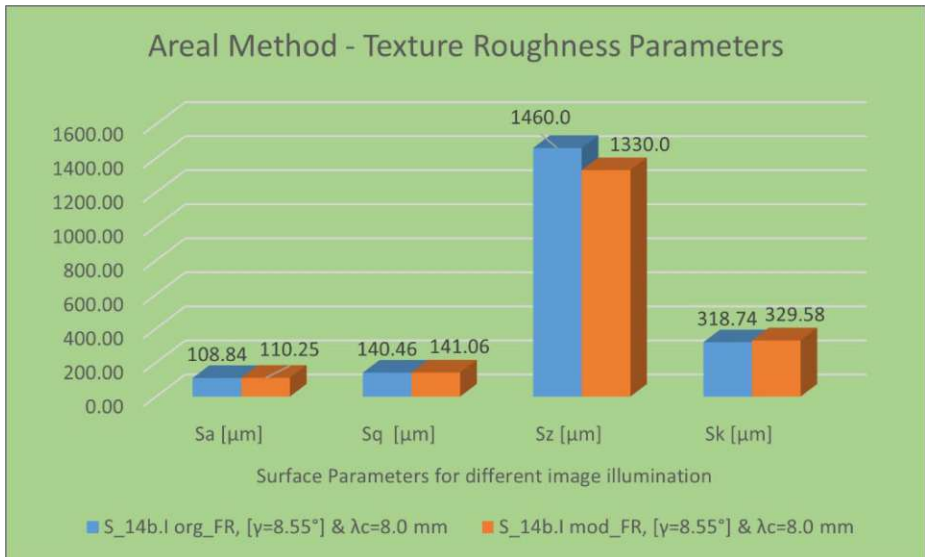
A 17 - S_14b.I Texture Roughness Parameters for different image illumination
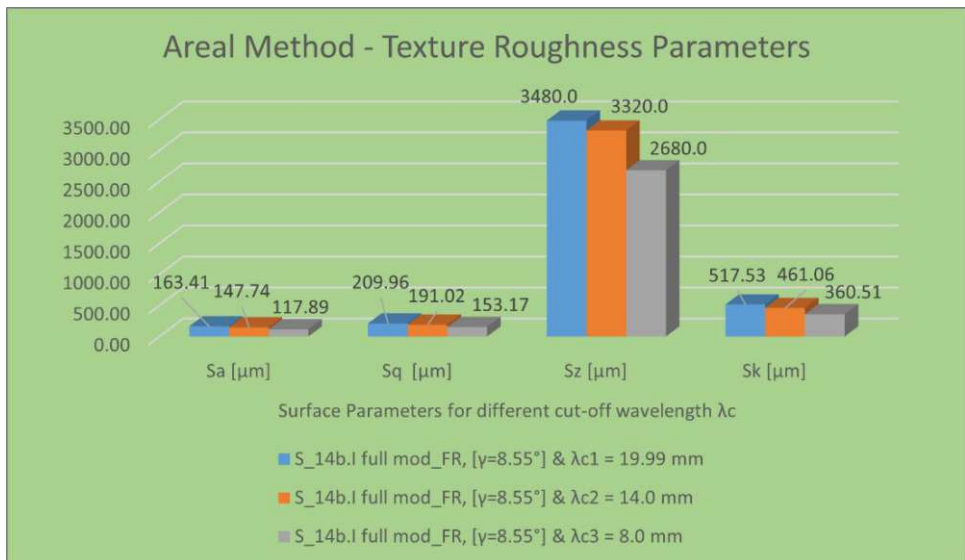
A 18 - S_14b.I Texture Roughness Parameters for different cutoff wavelength λc
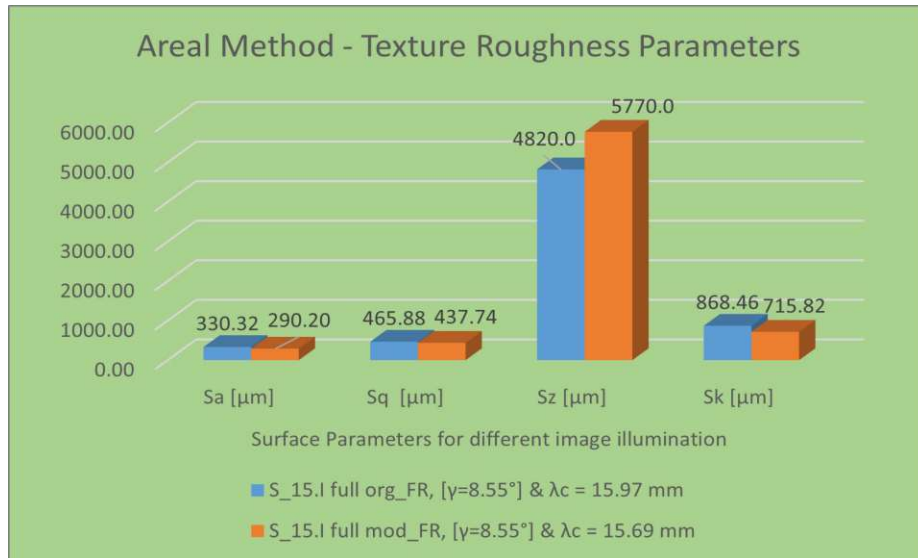
A 19 - S_15.I Texture Roughness Parameters for different image illumination
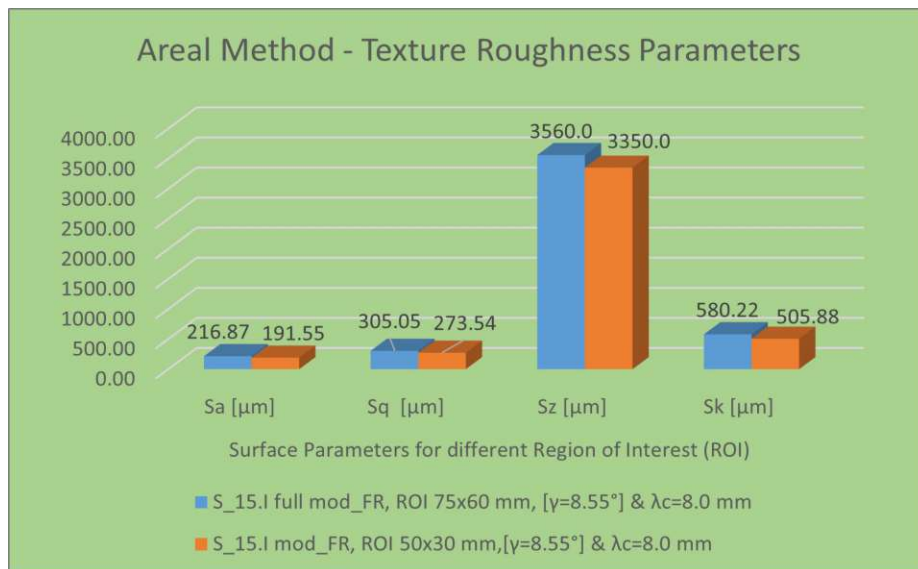
A 20 - S_15.I Texture Roughness Parameters for different Region of Interest (ROI)
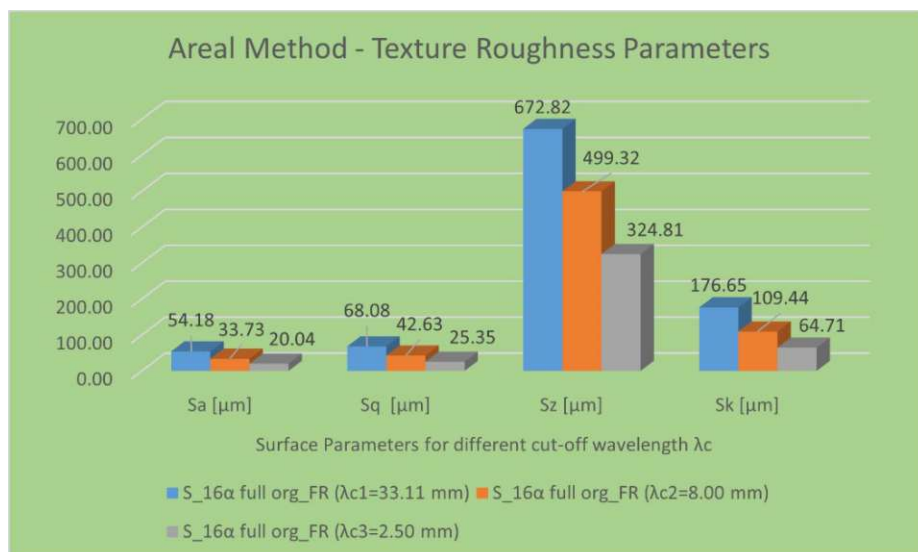
A 21 - S_16 Texture Roughness Parameters for different cutoff wavelength λc

147
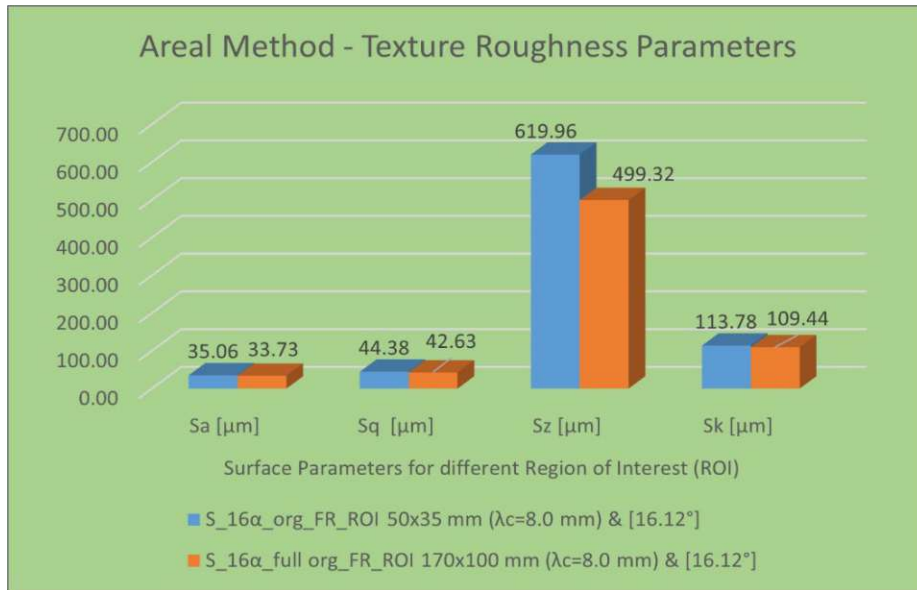
A 22 - S_16 Texture Roughness Parameters for different Region of Interest (ROI)
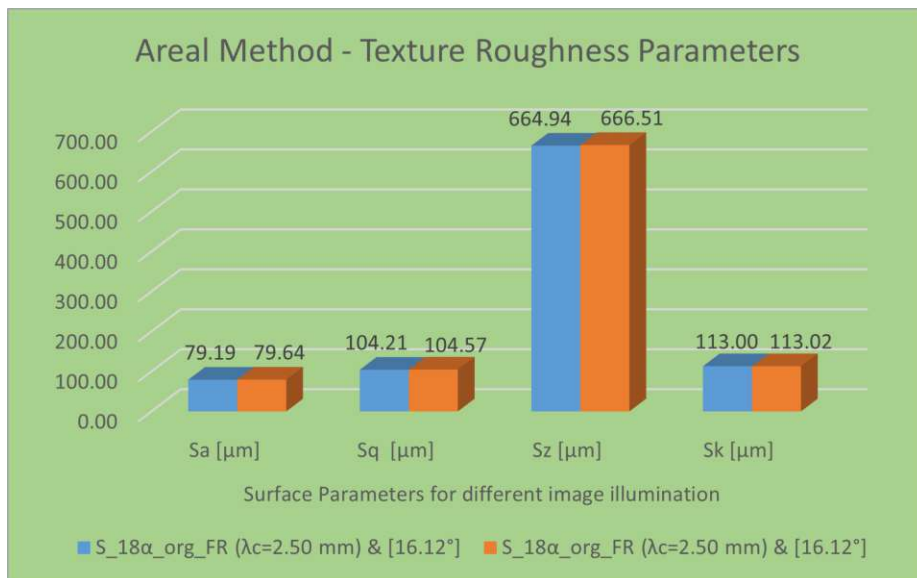
A 23 - S_18 Texture Roughness Parameters for different image illumination
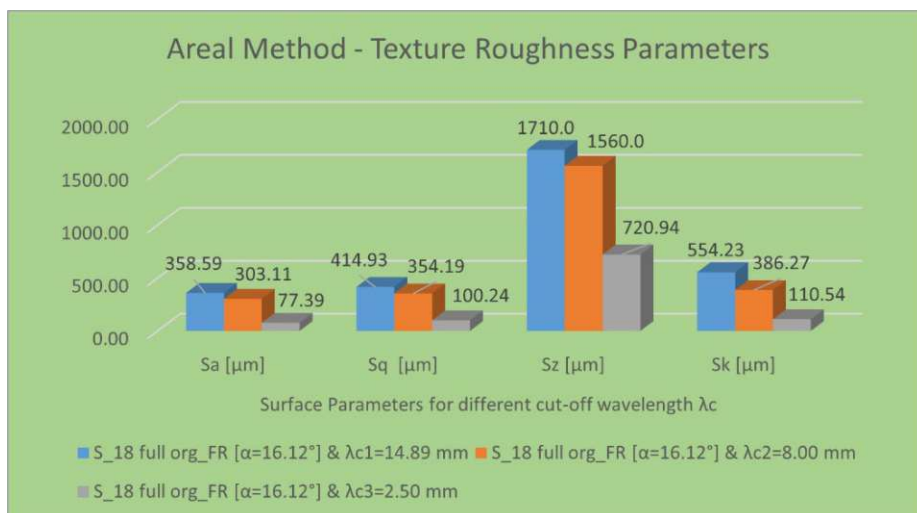
A 24 - S_18 Texture Roughness Parameters for different cutoff wavelength λc

148
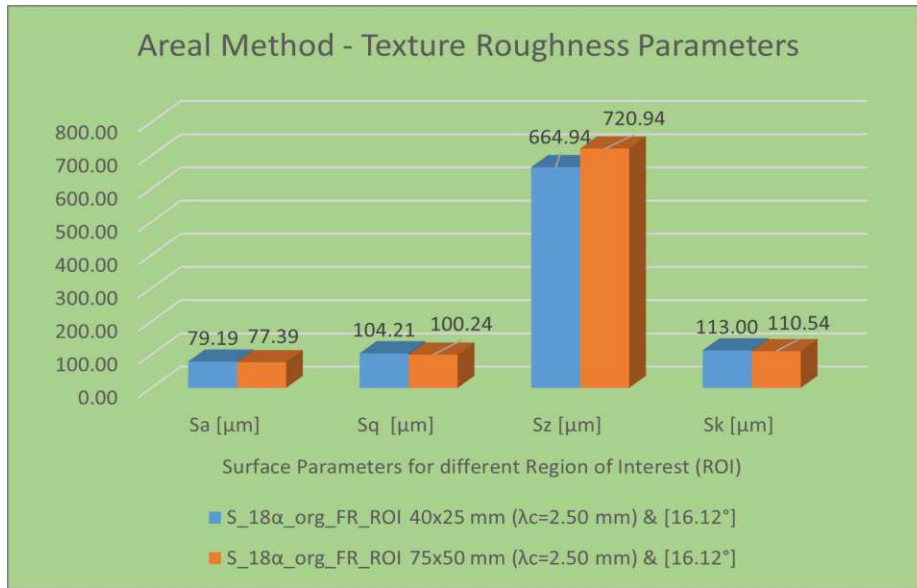
A 25 - S_18 Texture Roughness Parameters for different Region of Interest (ROI)
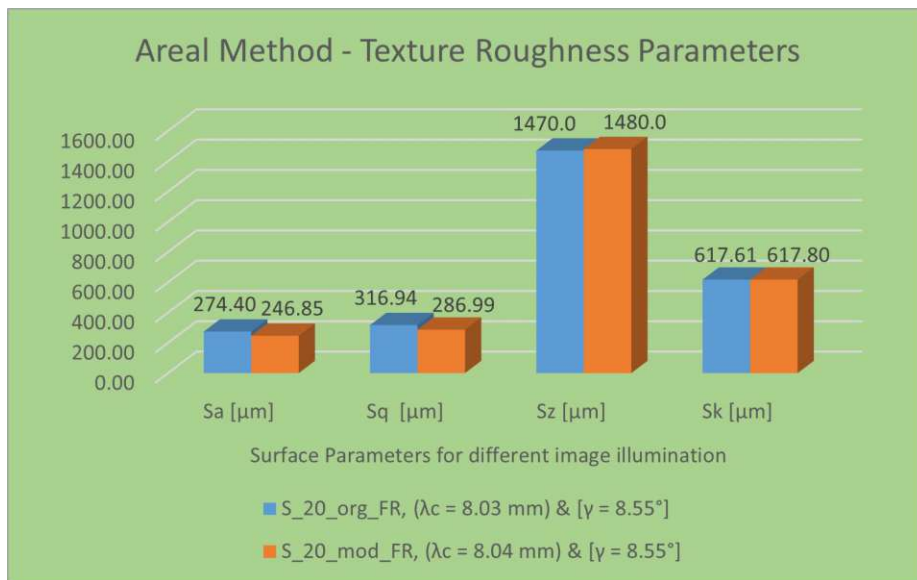
A 26 - S_20 Texture Roughness Parameters for different image illumination
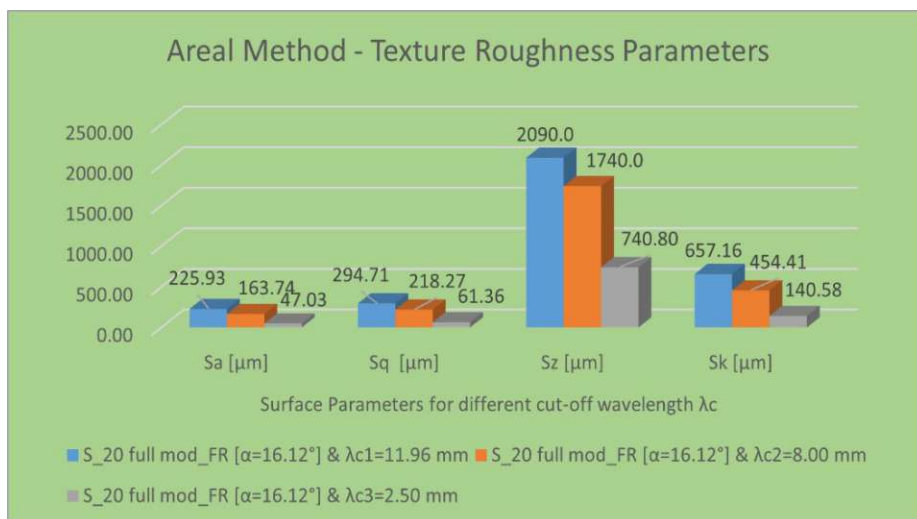
A 27 - S_20 Texture Roughness Parameters for different cutoff wavelength λc

Appendix B
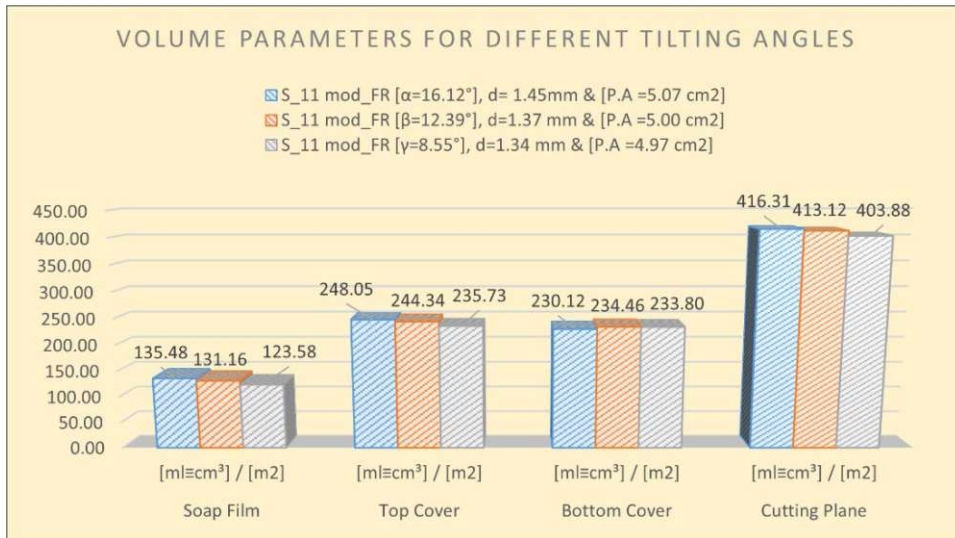
Results of Volume Measurements for different Modes:
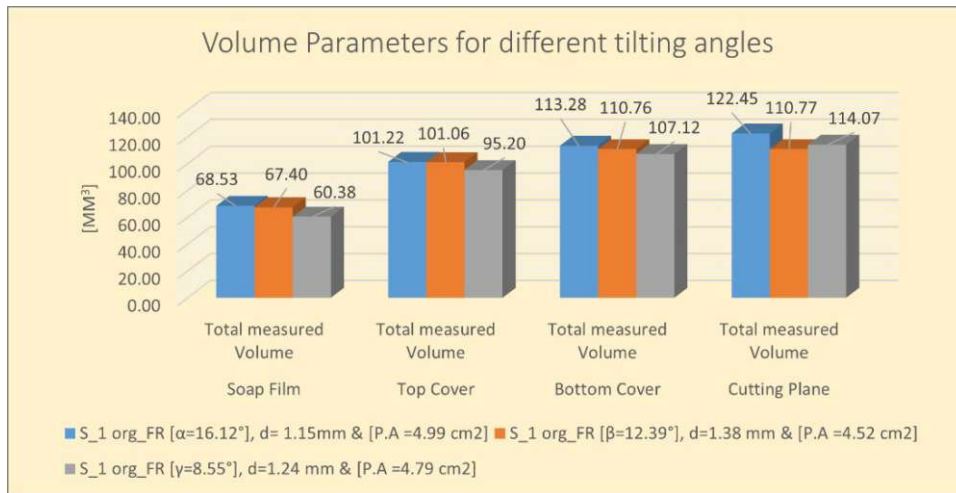
B 1 - S_1 - Total measured Volume in mm3 for different tilting angle α, β, and γ
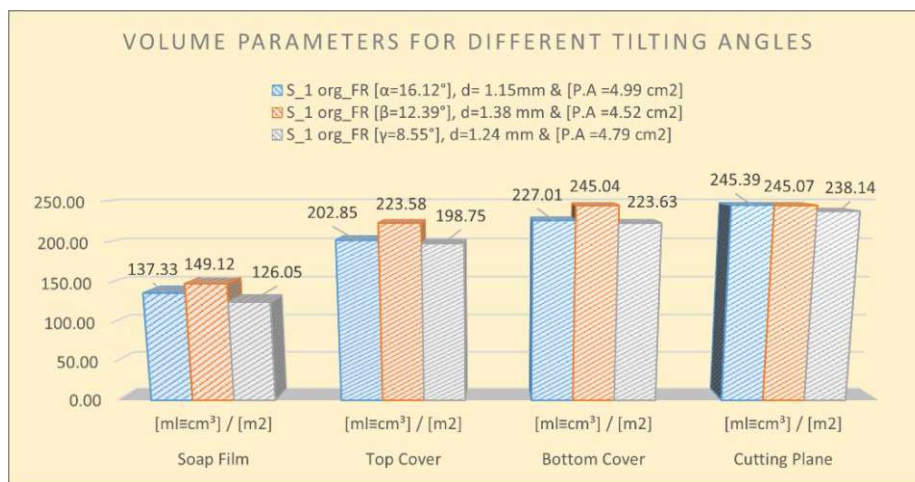
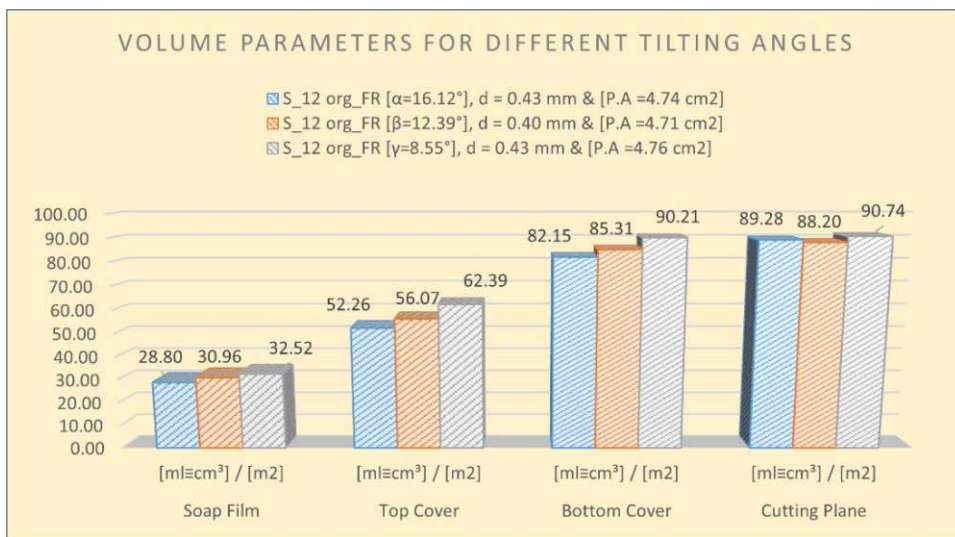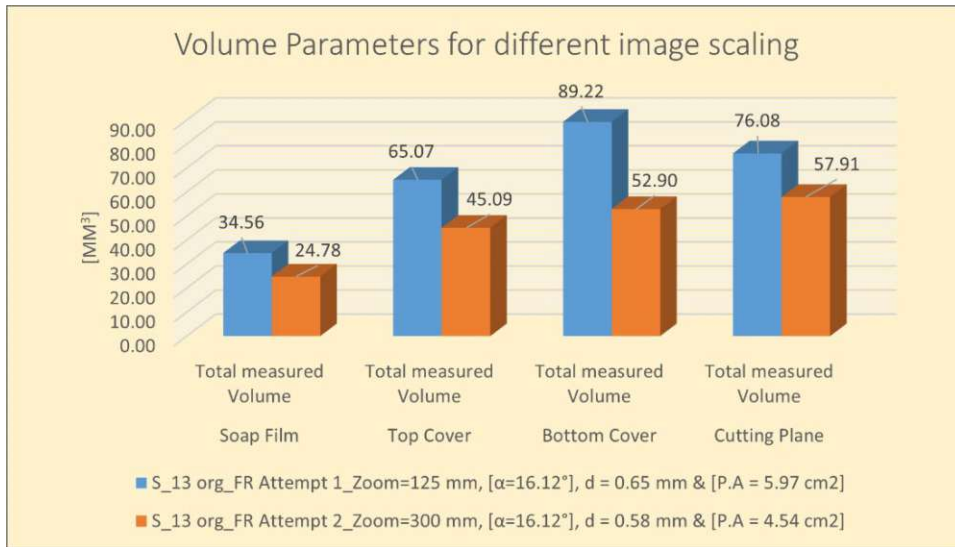*B 2 - S_1 - Volume Parameters in cm3/1000 cm3 for different tilting angle α, β, and γ*
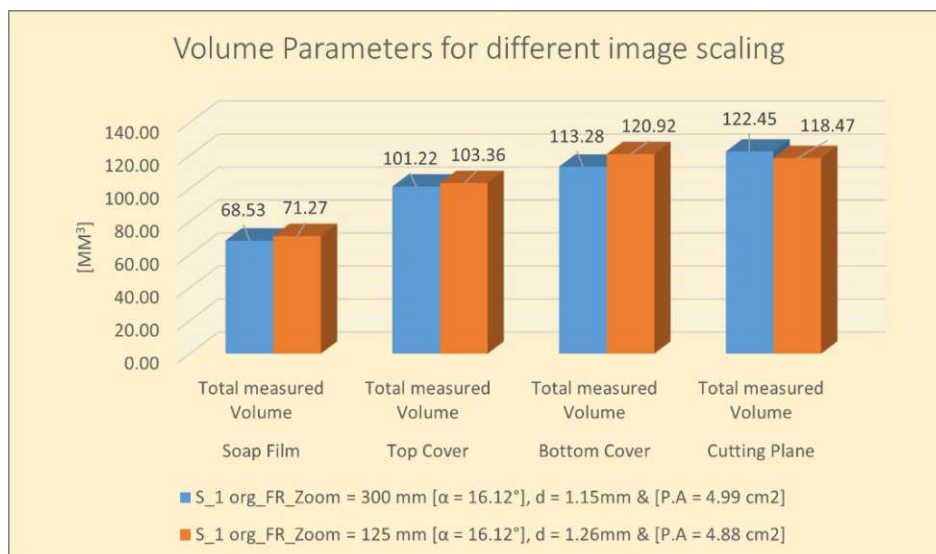
B 3 - S_1 - Total measured Volume in mm3 for different image scaling (Lens focal length)
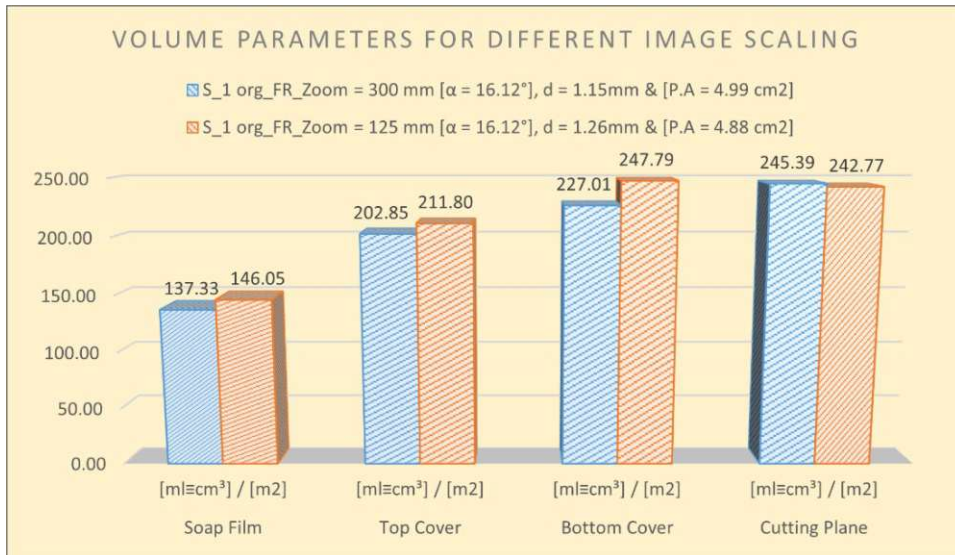
B 4 - S_1 - Volume Parameters in cm3/1000 cm3 for different image scaling (Lens focal length)
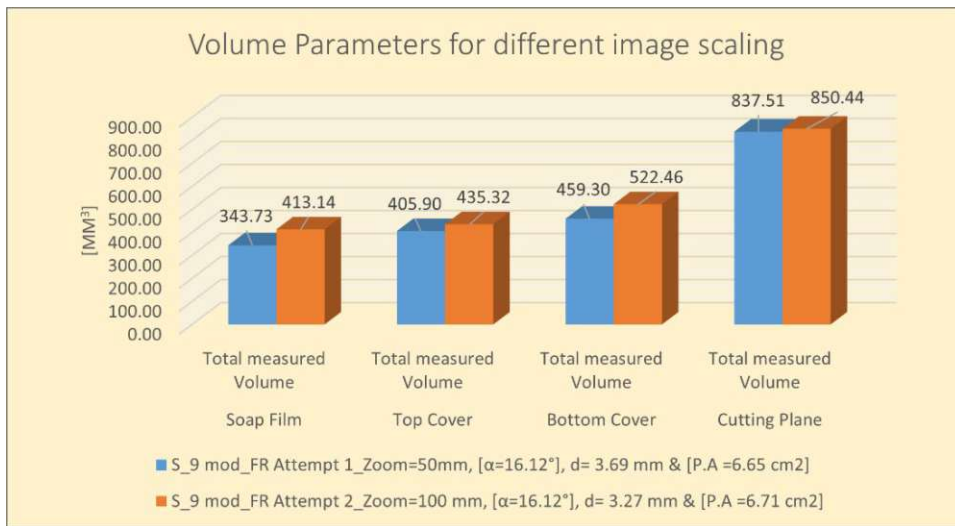
B 5 - S_9 - Total measured Volume in mm3 for different image scaling (Lens focal length)
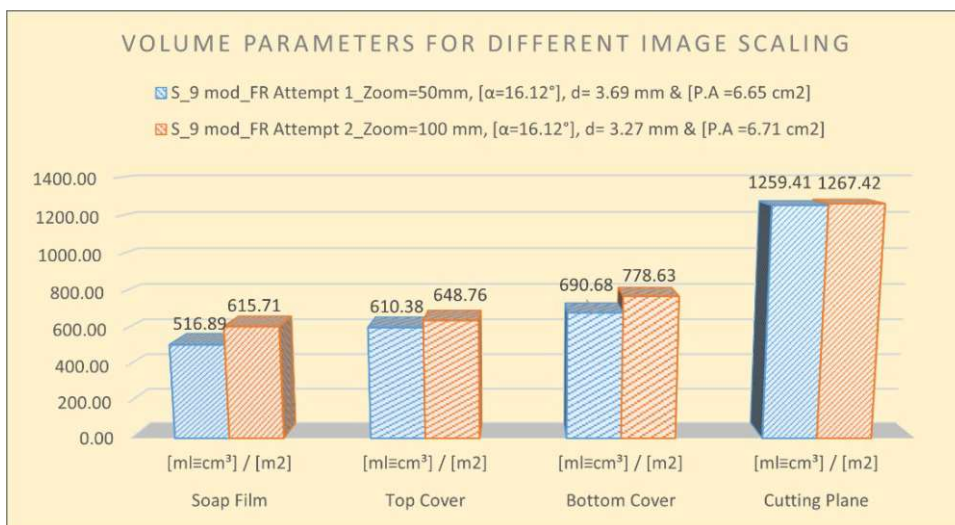
B 6 - S_9 - Volume Parameters in cm3/1000 cm3 for different image scaling (Lens focal length)
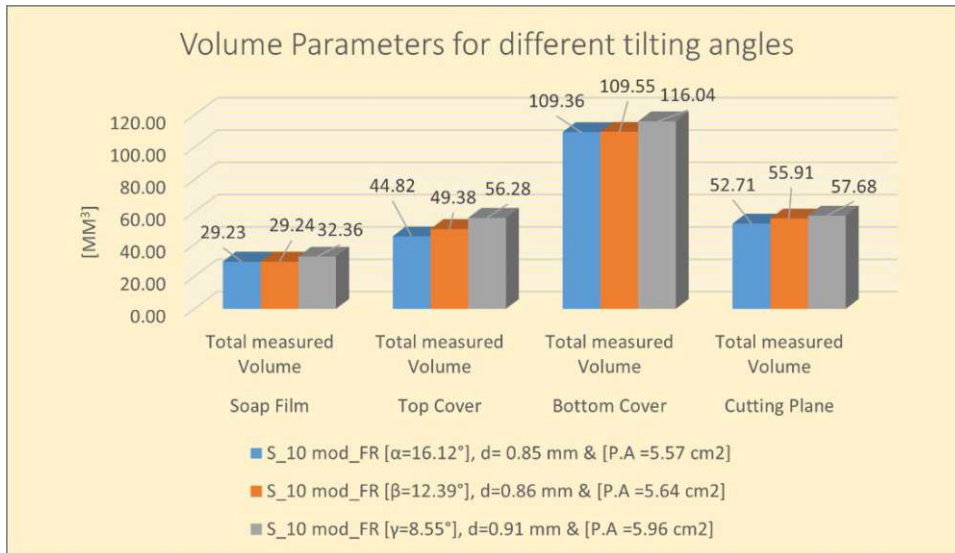
B 7 - S_10 - Total measured Volume in mm3 for different tilting angle α, β, and γ
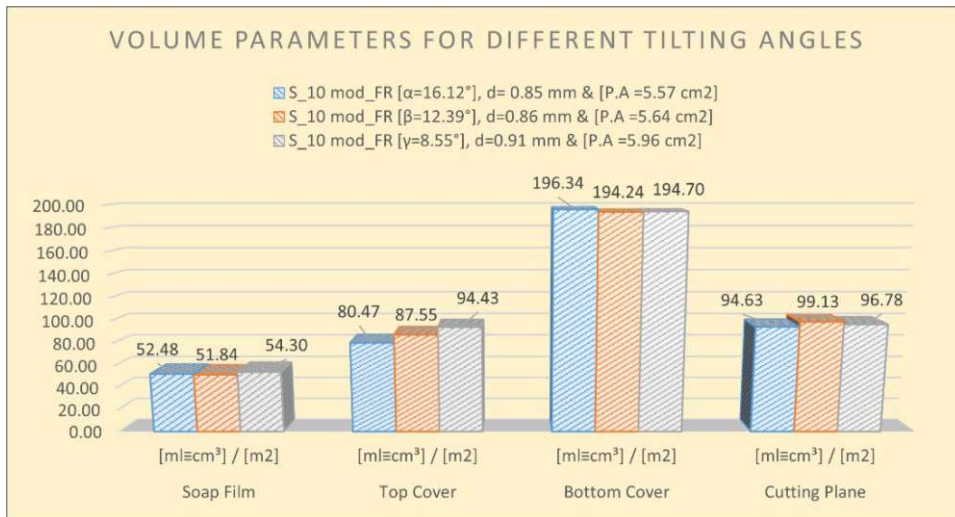
B 8 - S_10 - Volume Parameters in cm3/1000 cm3 for different tilting angle α, β, and γ
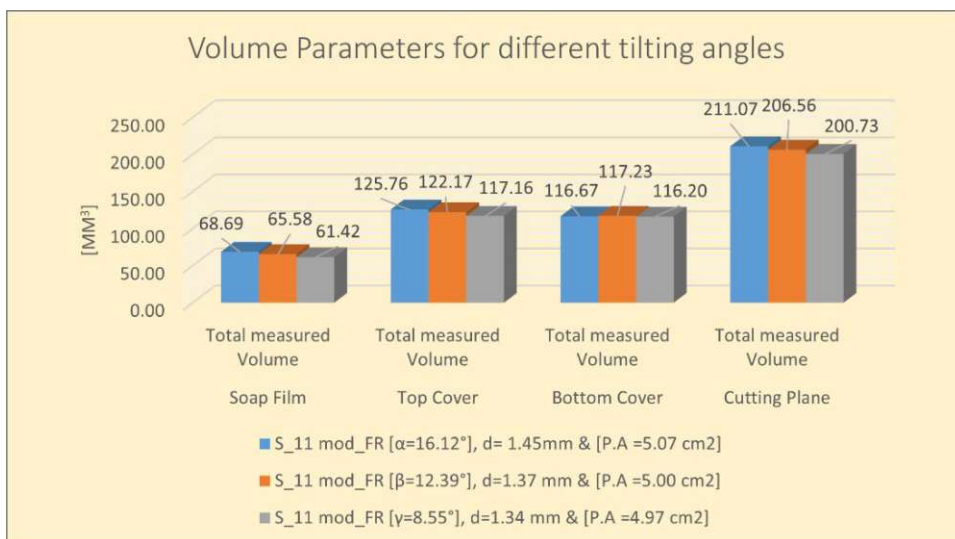
B 9 - S_11 - Total measured Volume in mm3 for different tilting angle α, β, and γ

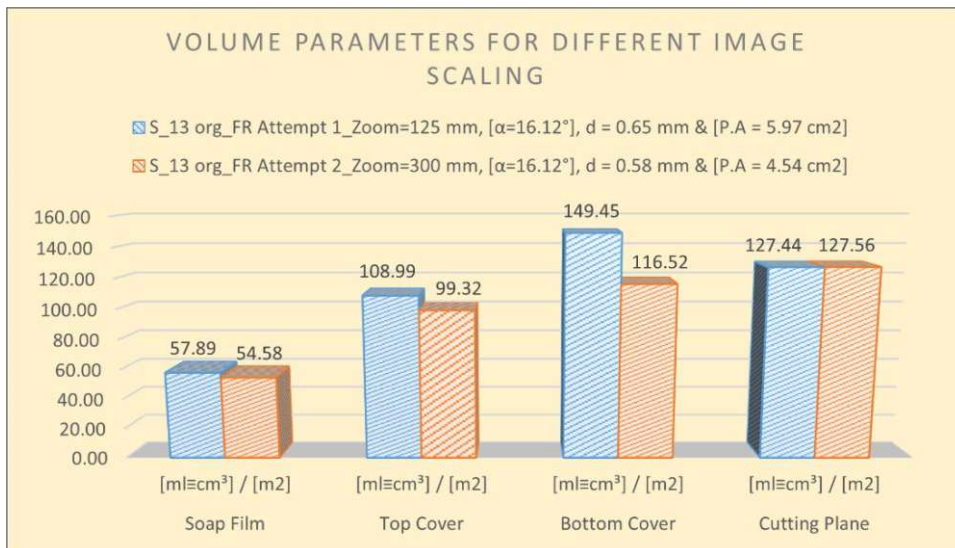*B 10 - S_11 - Volume Parameters in cm3/1000 cm3 for different tilting angle α, ß, and γ*
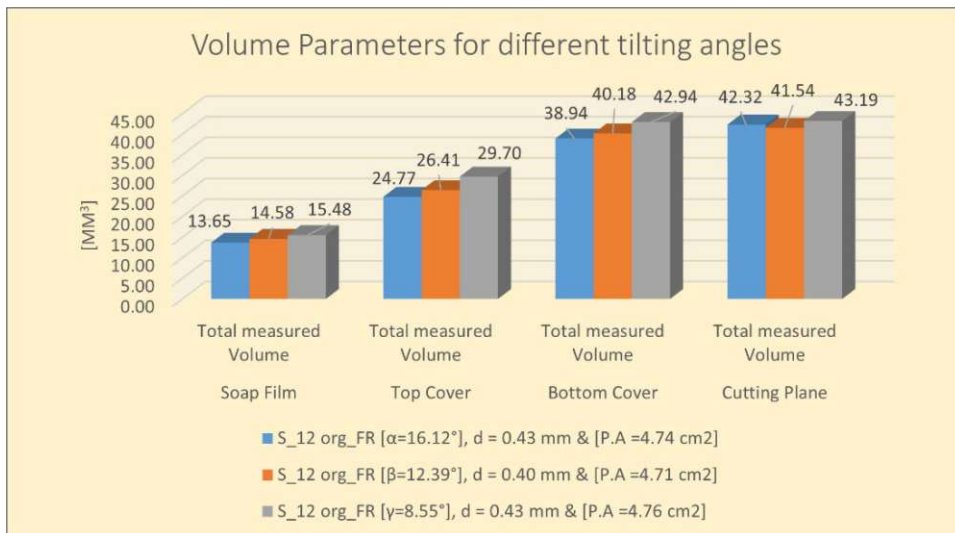
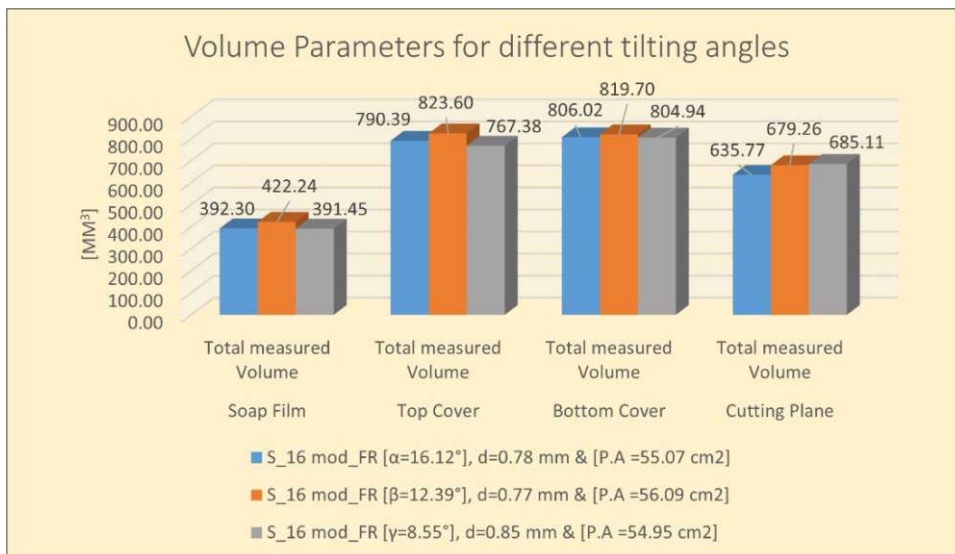*B 11 - S_12 - Total measured Volume in mm3 for different tilting angle α, ß, and γ*

B 12 - S_12 - Volume Parameters in cm3/1000 cm3 for different tilting angle α, ß, and γ
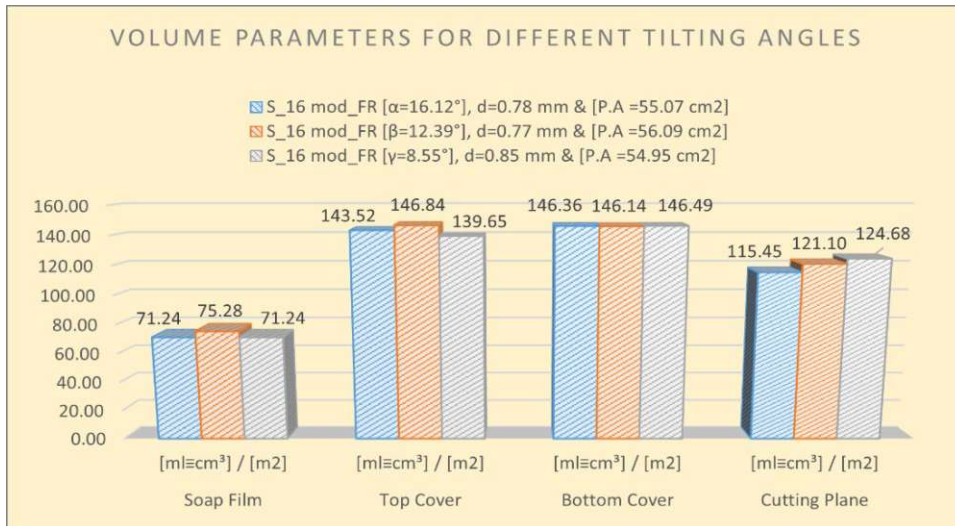
B 13 - S_13 - Total measured Volume in mm3 for different image scaling (Lens focal length)
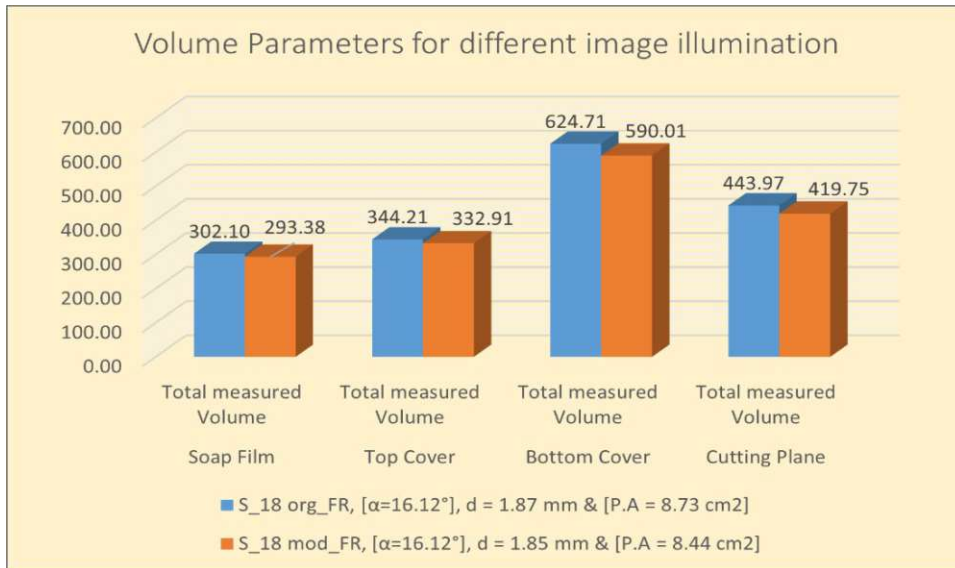

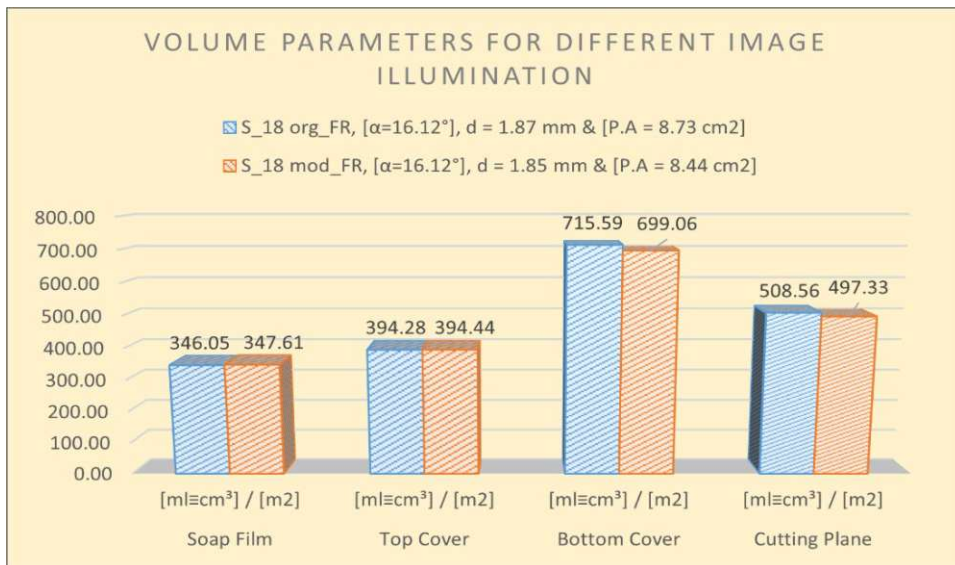*B 14 - S_13 - Volume Parameters in cm3/1000 cm3 for different image scaling (Lens focal length)*

B 15 - S_16 - Total measured Volume in mm3 for different tilting angle α, β, and γ

B 16 - S_16 - Volume Parameters in cm3/1000 cm3 for different tilting angle α, β, and γ

B 17 - S_18 - Total measured Volume in mm3 for different image illumination

B 18 - S_18 - Volume Parameters in cm3/1000 cm3 for different image illumination